Vol. 94 No. 2 December 1, 1977
Completing Vol. 94

ISSN 0003-2670

ANALYTICA CHIMICA ACTA

International journal devoted to all branches of analytical chemistry

ELSEVIER SCIENTIFIC PUBLISHING COMPANY

ANALYTICA CHIMICA ACTA

International journal devoted to all branches of analytical chemistry
Revue internationale consacrée à tous les domaines de la chimie analytique
Internationale Zeitschrift für alle Gebiete der analytischen Chemie

PUBLICATION SCHEDULE FOR 1977 (incorporating the section on Computer Techniques and Optimization).

	J	F	M	A	M	J	J	A	S	O	N	D
Analytica Chimica Acta	88/1	88/2	89/1	89/2	90	91/1	91/2	92/1	92/2	93	94/1	94/2
Section on Computer Techniques and Optimization									95/ 1+2			95/3+4

Scope. *Analytica Chimica Acta* publishes original papers, short communications, and reviews dealing with every aspect of modern chemical analysis, both fundamental and applied. The section on *Computer Techniques and Optimization* is devoted to new developments in chemical analysis by the application of computer techniques and by interdisciplinary approaches, including statistics, systems theory and operation research.

Submission of Papers. Manuscripts (three copies) should be submitted to:
for *Analytica Chimica Acta*: Dr. A.M.G. Macdonald, Department of Chemistry, The University, P.O. Box 363, Birmingham B15 2TT, England.
for the section on *Computer Techniques and Optimization*: Dr. J.T. Clerc, Laboratorium für Organische Chemie, Swiss Federal Institute of Technology, Universitätstrasse 16, CH-8092 Zürich, Switzerland.

Information for Authors. Papers in English, French and German are published. There are no page charges. Manuscripts should conform in layout and style to the papers published in this Volume. Authors should consult Vol. 93, p. 379 for detailed information. Reprints of this information are available from the Editors or from: Elsevier Editorial Services Ltd., Mayfield House, 256 Banbury Road, Oxford OX2 7DE (Great Britain).

Reprints. Fifty reprints will be supplied free of charge. Additional reprints (minimum 100) can be ordered. An order form containing price quotations will be sent to the authors together with the proofs of their article.

Advertisements. Advertisement rates are available from the publisher.

Subscriptions. Subscriptions should be sent to: Elsevier Scientific Publishing Company, P.O. Box 211, Amsterdam, The Netherlands. The section on *Computer Techniques and Optimization* can be subscribed to separately.

Publication. *Analytica Chimica Acta* (including the section on *Computer Techniques and Optimization*) appears in 8 volumes in 1977. The subscription for 1977 (Vols. 88–95) is Dfl. 920.00 plus Dfl. 112.00 (postage) (Total approx. US $ 420.95). The subscription for the *Computer Techniques and Optimization* section only (Vol. 95) is Dfl. 115.00 plus Dfl. 14.00 (postage) (Total approx. US $ 52.75). Journals are sent automatically by air mail to the U.S.A. and Canada at no extra cost and to Japan, Australia and New Zealand for a small additional postal charge. All earlier volumes (Vols. 1–87) are available at Dfl. 115.- (plus postage).

Claims for issues not received should be made within three months of publication of the issue, otherwise they cannot be honoured free of charge.

Printed in The Netherlands

Liquid Chromatography under Pressure – HPLC

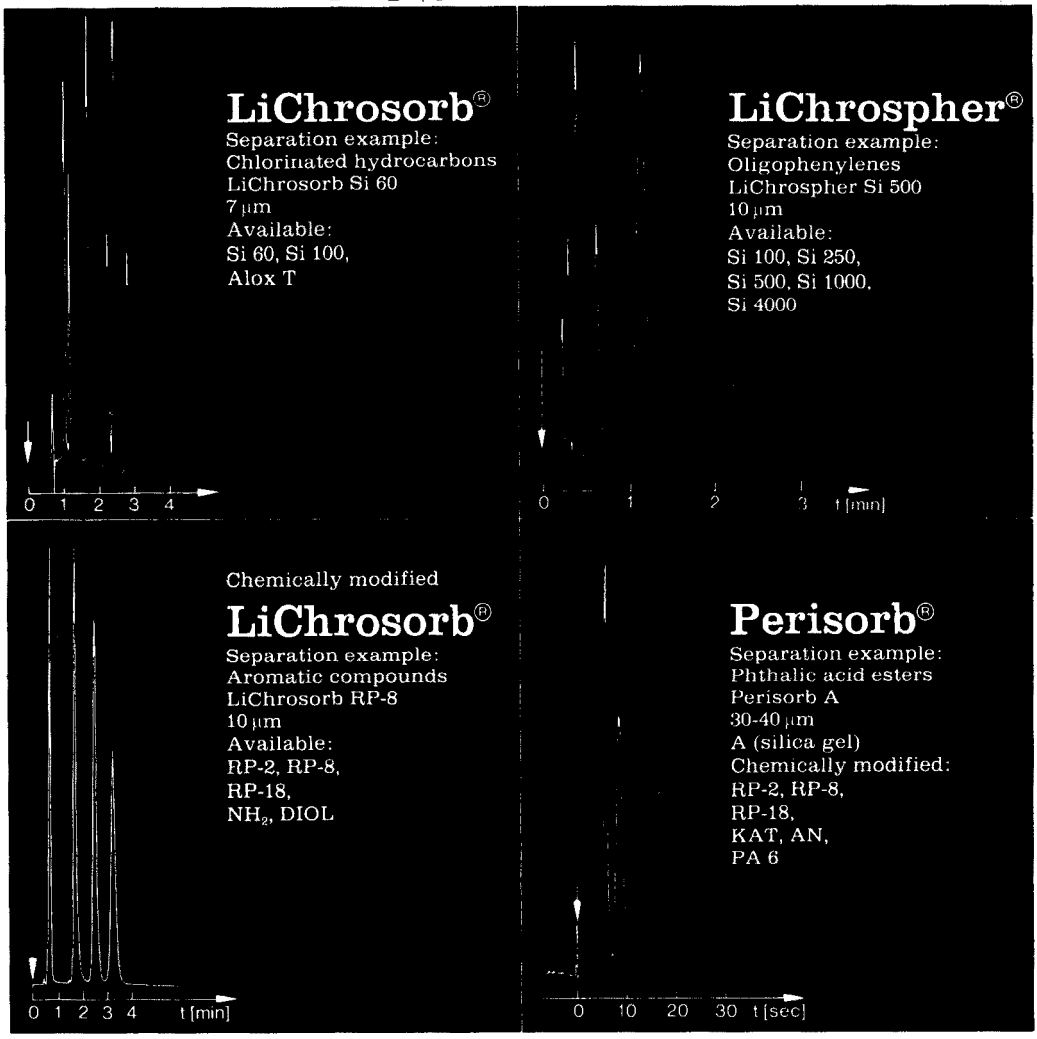

397 f-EÜ

LiChrosorb® through and through porous, irregular particles:
(1) about 30 µm, for dry filling;
(2) fine particles (5, 7, 10 µm), to be introduced into the column by a suspension method.

LiChrospher® spherical particles, through and through porous.
Perisorb® supports with a porous surface, with an about 1–2 µm chromatographically active layer around a glass core, spherical (30-40 µm).

Please send for Data sheets and Examples of application series.

E. Merck, Darmstadt, Federal Republic of Germany

Analytica Chimica Acta, 94 (1977) 225—236

PRECONCENTRATION OF TRACE ELEMENTS BY PARTIAL DISSOLUTION OF THE MATRIX—MULTIELEMENT PRECONCENTRATION FROM MANGANESE

E. JACKWERTH*, J. MESSERSCHMIDT and R. HÖHN

Institut für Spektrochemie und angewandte Spektroskopie, Bunsen-Kirchhoff-Str. 11, 4600 Dortmund 1, (Federal Republic of Germany)

(Received 24th May 1977)

SUMMARY

Trace elements such as Ag, Au, Bi, Cd, Co, Cu, Fe, Ga, In, Ni, Pb, Pd and Tl, can be preconcentrated with recoveries of better than 95% from high-purity manganese if the sample is coated with a thin layer of mercury before its dissolution in HCl to a small residue. For determination of the trace elements, the residue is completely dissolved in aqua regia. After separation of the mercury by reductive precipitation, Bi, Cd, Co, Cu, Fe, Ga, In, Ni, Pb, and Tl are determined by flame a.a.s. ('injection method'). Ag, Au and Pd are determined in the mercury-containing solution. The relative standard deviation was usually about 5%; Cu, Fe and Pb were proved to be inhomogeneously distributed in the sample (electrolytically produced manganese), and so the standard deviations were considerably greater. The detection limits for the different elements were between 0.6 and 0.004 ppm, depending on the sensitivity of their a.a.s. determination. The theoretical basis of this preconcentration method and its applicability to multielement analysis of different high-purity metals are discussed.

When high-purity metals are analysed, the determination of trace elements at extremely low concentrations in the sample is often satisfactory only after separation and preconcentration. For this purpose, distribution methods are frequently applied, the different reactions of traces and matrix element with suitable complexing agents being exploited. Successful application of preconcentration methods becomes particularly difficult if traces and matrix form very similar compounds. This is well known for the transition elements and their reactions with most of the common chelating group reagents. For such separations of traces and matrix, the most helpful methods are those which utilize chemical or physical properties that are quite different from their chemical complex behaviour, e.g. differences in volatility or solubility of suitable compounds etc. Alternatively, for the analysis of some special materials, procedures involving partial dissolution of the matrix can be used. Here the different electrochemical behaviours of the components in metallic samples are utilized for their separation.

The method is based on the following principle: a mixture of metals with the particles in electric contact can be considered to behave as an alloy-electrode

when it is dipped into an electrolyte solution. The most electronegative component of the metallic mixture determines the potential of the whole sample [1]. When an acid is used as electrolyte, only this component will be dissolved. When this metal has been completely removed from the mixture, the metal next in the electrochemical series then controls the potential and will be attacked by the acid. By interrupting the dissolution process at an appropriate point, the different elements in the sample can be separated.

The possibility of separating metals in this way has been applied for many centuries. For instance, the Roman Emperors made use of the method to falsify the value of coins [2]. Thus, silver denarii coined during the reign of Septimius Severus (A.D. 192—211) have only a plating of pure silver, the remaining material consisting of an alloy with a high content of copper [3, 4]. As is now known, prior to mintage the raw metal was treated with acid, i.e. the copper was extracted from the surface of the copper—silver alloy leaving the silver which, when coined, not only feigned a high fineness but also protected the coins from corrosion [4]. Jewellery and objets d'art of inferior value made of silver alloys with high copper contents, have also been treated by this procedure ("blanching") since classical times.

GENERAL CONSIDERATIONS

Dissolution of a metal in acid is a redox process. According to the Nernst equation, the potential E_M of a metallic sample (standard potential E_M^0; activity a_M of the metal in the sample) dipped into a solution of its ions (activity $a_M{}^{n+}$ of the n-valent ions in the solution) is

$$E_M = E_M^0 + (R\ T/n\ F)\ \ln\ (a_M{}^{n+}/a_M) \qquad (1)$$

For pure metals, $a_M = 1$ by definition.

In a system of various metals (mixtures, alloys), a_M, and therefore E_M, depend on the composition of the metallic phase; non-ideally pure metals together with their metallic impurities must also be considered as systems of that kind. According to the evaluation of the pertinent equilibria, the potential of metals contaminated with trace elements is, as a rule, determined solely by the most electronegative component. Therefore, in the reaction of acid with an electronegative metal, only the matrix is first dissolved; traces nobler than the matrix remain on the surface of the sample. Applications of this procedure have given, for example, a considerable improvement in the spectrochemical detection of a series of elements in zinc metal [5]. The first analytically useful preconcentration of trace elements prior to their determination in high-purity metals involved the liquid metals mercury and gallium [6, 7], whereas with solid metal samples the application failed. In view of this, two cases must be considered.

1. The traces adhere firmly to the dissolving metal. During the dissolution, an impermeable layer of nobler trace elements is formed on the surface of the sample. No further material from inside the sample will permeate this layer,

because the diffusion rates are small in solid phases [8]. In the surface area, the activity a_M of the matrix metal decreases permanently, and accordingly, the potential E_M increases. Henceforth, it depends on the acid used whether the traces are also dissolved, or whether the process of dissolution ceases.

2. The traces accumulate only as porous aggregates on the sample residue. In this situation, the acid can still permeate the layer and continue its reaction with the matrix metal. The dissolution process is, of course, unhindered, but the particles of the trace layer may break off from the sample. As soon as such particles are disconnected from electric contact with the electronegative matrix, they may be dissolved by the acid. In this case, too, complete or reproducible preconcentration of trace elements is difficult to achieve.

These considerations indicate that a useful separation of traces and matrix with solid samples by partial dissolution of the sample is possible only if (a) the traces adhere to the residue, and (b) the matrix material can be transported from inside the sample to its surface. These contrary postulates can be realized quite simply by amalgamation of the sample before its dissolution. A liquid metallic phase is thus formed at the surface, through which the matrix is transported and wherein the traces remain.

The possibility of separation by successive dissolution of an amalgamated metallic sample can be demonstrated simply. For example, from a mixture of 1.3 g Zn, 0.01 g Cd and 0.01 g Pb, which is amalgamated with 0.5 g Hg, zinc as the most electronegative component is first dissolved with HCl; cadmium is not attacked until all the zinc has dissolved, and lead dissolves only after the sample is completely free from cadmium (Fig. 1). The potential of the sample always increases abruptly when the residual amount of a component has been dissolved by the acid. To formulate this relation between the composition of an amalgam and its potential, Jangg and Kirchmayr [9, 10] deduced a modified Nernst equation. On addition of mercury to a metal M, the potential E_M of the metal changes to that of the amalgam

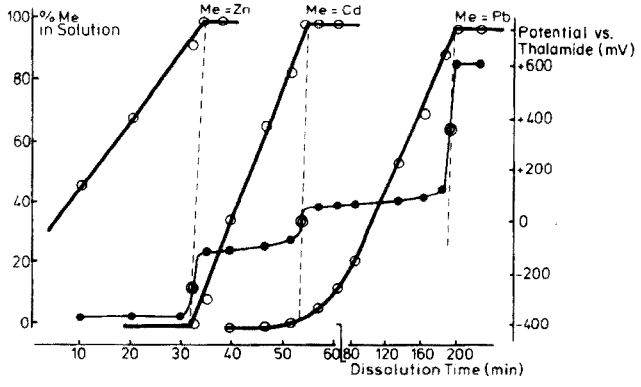

Fig. 1. Dissolution behaviour and potential course of a Zn—Cd—Pb—Hg mixture in HCl. The sample contained 1300 mg Zn, 10 mg Pb, 10 mg Cd and 500 mg Hg. For dissolution, the sample was treated with 100 ml of 37% HCl at 90°C.

$$E_{MA} = E_M^0 - \frac{\Delta G^0}{n F} + \frac{R T}{n F} \ln \frac{a_{M^{n+}} a^*_{MA} a^{*y}_{Hg}}{a_{MA}} \quad (2)$$

where E_{MA} is the potential of the amalgam MA; E_M^0 the standard potential of the amalgam-forming metal M; ΔG^0 the Gibb's free energy of the compound or mixed crystal MHg_y; $a_{M^{n+}}$ the activity of the metal ions M^{n+} in solution; a_{MA} the activity of the metal M in the amalgam; a^*_{MA} and a^*_{Hg} are, respectively, the activity of metal M and the activity of mercury when the amalgam is saturated with M; and y is the ratio of the atomic numbers Hg : M in MHg_y.

As in the Nernst equation for pure metals, bonding parameters and the activities of mercury and the metal dissolved in mercury are valid. However, in most cases, concentrations can adequately replace activities [9].

If the metal M and the mercury do not form a compound or mixed crystal in the amalgam, then $\Delta G^0 = 0$ and $\lim_{y \to 0} a^y_{Hg} = 1$. Moreover, for an amalgam saturated with M, $a_{MA} = a^*_{MA}$. Therefore, eqn. (2) simplifies to

$$E_{MA} = E_M^0 + (RT/nF) \ln a_{M^{n+}} \quad (3)$$

This corresponds to eqn. (1) for pure metals and states that an amalgam saturated with M has the same potential as the pure metal M.

If a compound is formed, the potential E_{MA} shifts to more positive values because for most intermetallic compounds with mercury, ΔG^0 is negative. The potential E_{MA} of unsaturated amalgams is also more positive than that of the pure metal E_M; when the metal activity a_{MA} is decreased by an order of magnitude, the potential E_{MA} increases by $59/n$ mV (25°C).

The validity of eqn. (2) has been proved by Jangg and Kirchmayr in investigations with numerous amalgams over large concentration ranges [9]. However, the equation is not valid for the electrochemical behaviour of very dilute amalgams: according to several reports, the amalgam-forming metal is potential-deciding only above a definite concentration in mercury [9—12]. This minimum concentration — different for the various metals — amounts to 10^{-3}—10^{-5}% (w/w) at room temperature. Traces and matrix can therefore be separated from each other only to a certain extent. Strictly, the process of dissolution must be interrupted when the potential of the amalgam begins to increase because of the decrease of the matrix metal concentration, i.e. at a concentration of at least about 10^{-3}% of the matrix in mercury. If the sample is dissolved beyond that concentration, the more electropositive traces may also be lost. In fact, the threshold concentration is even higher because of the inhomogeneous distribution of the matrix within the whole amalgam: the concentration gradient from inside the sample to its surface caused by the continuous dissolution of the matrix metal must be considered. Therefore, a complete separation of traces and matrix cannot be achieved, yet quantitative preconcentration of traces in the residue of samples is possible.

The dependence of amalgam potential on metal concentration limits the field of application to certain elements, i.e. such metals influence the electrochemical behaviour of amalgams, the solubility of which in mercury is above the limit mentioned. Accordingly, Jangg classifies amalgam-forming metals into two groups [10]: (a) a group of electroactive elements with solubilities exceeding 10^{-3}% (w/w) in mercury (Ag, Al, Au, Ba, Bi, Ca, Cd, Cs, Cu, In, K, Li, Mg, Mn, Na, Pb, Rb, Sn, Sr, Tl and Zn); and (b) a group of electroinactive elements with solubilities of less than 10^{-3}% (w/w) in mercury (Ce, Co, Cr, Fe, Ga, La, Nd, Ni, Pr, Pt, Sb, Sm, Th, Ti, U and Zr). Only elements of group (a) contribute to the chemical reactivity of their amalgam; with elements of group (b) mercury alone forces the reactions [10]. This means that only elements from group (a) can be used as matrix material in analysis; those of group (b) are not suitable. Furthermore, metals of group (b) are often lost as trace elements during partial dissolution because they may be suspended in mercury as solid particles. In most cases, the particles are stripped of their coating and dissolved by oxidizing acids [14]. Though partial dissolution is limited in its application, the method has some important advantages over other separation techniques. First, the trace elements are preconcentrated solely by dissolution of the amalgamated sample; expensive additional separation steps are unnecessary. Secondly, except for the acid and mercury, which are readily obtained in high-purity grade, no additional reagents are required in the preconcentration process, so that blank values can be kept very low. Thirdly, synthetic reference samples for examination and calibration can easily be prepared.

The practicability of this method has been tested for the analysis of several pure metals; the trace recoveries obtained are listed in Table 1. Detailed procedures for trace preconcentration and determination are given in the references cited. In this paper the analysis of high-purity manganese is described; the method of partial dissolution of the matrix is used for preconcentration of traces of Ag, Au, Bi, Cd, Co, Cu, Fe, Ga, In, Ni, Pb, Pd and Tl.

PRECONCENTRATION OF TRACE ELEMENTS FROM MANGANESE METAL BY PARTIAL DISSOLUTION OF THE AMALGAMATED MATRIX

Sample and pretreatment

With its standard potential $E^0_{Mn^{2+}/Mn} = -1.05$ V, manganese is one of the most electronegative heavy metals known. The number of nobler trace metals suitable for preconcentration is therefore relatively large. Thus the method of partial dissolution of the matrix seems to be most useful for multielement preconcentration from manganese. Manganese dissolves only slightly in mercury: at 20°C the solubility is about 0.002% (w/w) and increases to about 0.03% at 100°C [13, 19]. Manganese and mercury form the compound Mn_2Hg_5 which decomposes above 95°C to MnHg and Hg [13]. The Mn—Hg compound is easily segregated from the saturated amalgam [20].

TABLE 1

Trace recoveries for preconcentration from high-purity metals by partial dissolution of the matrix

Trace element	Standard potential (V)	Matrix metal								
		Al	Mn	Zn	Cd	In	Tl	Sn	Pb	Bi
Al	−1.66									
Mn	−1.05									
Zn	−0.76	>95	~40							
Ga	−0.52	>95	>95	>80						
Cd	−0.40	>95	>95	>95						
In	−0.34	>95	>95	>95	95					
Tl	−0.33	>95	>95	>95	—					
Co	−0.27	—	>95	>95	>95	>95	~60			
Ni	−0.23	—	>95	>95	>95	>95	~60			
Sn	−0.14	~80	~80	>95	>95	95				
Pb	−0.13	>95	>95	>95	>95	>95	~90			
Fe	−0.04	—	>95	~40	>95	>95	~60			
Bi	+0.23	95	>95	>95	>95	>95	>95	90	>95	
Cu	+0.34	—	>95	90	>95	>95	>95	75	>95	—
Ag	+0.79	—	<95	>95	>95	>95	>95	95	>95	>95
Pd	+0.83	—	>95	>95	>95	>95	>95	90	>95	>95
Au	+1.42	—	>95	>95	>95	>95	>95	93	>95	>95
Literature		[15]		[16]	[17]	[18]	[18]	[18]	[18]	[18]

The sample material used was electrolytically produced metal in the form of brittle, platelet-like flakes about 2-mm thick (99.9% Mn, Riedel de Haen, Seelze, Germany, Art. No. 13258). This material does not amalgamate spontaneously in contact with mercury, even when the surface is etched with dilute acid. However, when the two metals are contacted in an ultrasonic bath in the presence of dilute HCl, complete coating of the sample material is easy. With this treatment mercury forms a dark dispersion of very small droplets, most of which coat the surface of the manganese flakes immediately. Subsequent heating of the acid solution to boiling makes the residual mercury coagulate and deposit on the flakes. A homogeneous adhesive coat of amalgam is obtained and the acid phase of the suspension becomes completely clear.

Preparation of calibration samples

During the process of partial dissolution of amalgamated samples of manganese in HCl, the behaviour of the traces Ag, Au, Bi, Cd, Co, Cu, Fe, Ga, In, Ni, Pb, Pd, Tl and Zn was investigated. As most of these elements could not be detected in the sample material used, even after preconcentration, calibration samples with the trace contents listed in Table 2 were prepared. For this purpose, traces were precipitated from hydrochloric acid solution by cementation on previously amalgamated manganese samples; Ag was added in the form of its amalgam. To force precipitation, the solution was heated

TABLE 2

Results for the trace analysis of electrolytically produced manganese

Trace element	Calibration range (ppm)	Recovery (%)	R.s.d.		Detection limit (3σ) (ppm)
			$s/\bar{x}$ (N = 10)	Trace content of the sample (ppm)	
Au	0.13—1.5	>95	0.058	0.25	0.05
Ag	0.1—10	>95	0.050	0.27	0.008
Bi	0.5—5	>95	0.058	0.95	0.1
Cd	0.01—0.3	>95	0.022	0.06	0.004
Co	0.1—1	>95	0.047	0.27	0.04[b]
Cr	0.25—3	<5			
Cu	0.4—3	>95	0.39[a]	0.30	0.008[b]
Fe	1.3—15	>95	0.21[a]	1.6	0.02[b]
Ga	1.3—15	>95	0.084	2.4	0.6
In	0.5—7.5	>95	0.052	0.88	0.3
Ni	1.0—7.5	>95	0.090	1.0	0.02[b]
Pb	0.2—3.0	>95	0.35[a]	0.16	0.03[b]
Pd	0.13—1.5	>95	0.041	0.25	0.1
Pt	0.13—1.5	~30			
Sn	1—5	~80			
Tl	0.1—7.5	>95	0.022	0.98	0.04
Zn	0.13—1.5	~40			

[a]Inhomogeneous sample material (see text).
[b]Calculated from the fluctuations of a.a.s. background.

to boiling, and HCl was added until hydrogen was generated. The amount of trace precipitation was checked by analysing the acid phase.

The utility of the samples thus prepared for calibration of the preconcentration method was tested extensively. It was shown that it is unimportant whether the traces are actually in the amalgam when the dissolution starts — as in the calibration samples — or reach the amalgam during the dissolution, as in real sample material.

The recovery achieved by preconcentration for all the elements investigated was determined by comparative analyses of trace concentrates and standard solutions. For this purpose, manganese samples with increasing trace contents were prepared as described; the added elements were preconcentrated and determined by the recommended procedure (see below). Simultaneously, the analytical signals of standard solutions containing equal trace additives were measured. The recovery of preconcentration for each element was calculated from the quotient of the slopes of the corresponding calibration lines.

Investigations on partial dissolution of manganese

The relatively small solubility of manganese in mercury and the formation of intermetallic compounds influence the dissolution of amalgamated

manganese samples in many respects. When samples are dissolved at room temperature in 3—6 M HCl, the surface is rapidly stripped of its mercury coating and the sample is dissolved in a violent reaction, usually at the exposed spots. When the dissolution is done at the boiling point of the acid, this stripping is avoided, possibly because of the higher solubility of manganese in the amalgam phase, and the dissolution process is much smoother.

The dissolution process is rather strange. Initially, the amalgamated samples dissolve rapidly in the boiling hydrochloric acid; the rate of dissolution stops. On further treatment of the sample with acid, the potential residue of more than 50 mg is still very large. Thereafter the sample behaves as a passivated metal. When the potential of the dissolving samples is measured, there is a sudden increase in potential of about 120 mV when the dissolution stops. On further treatment of the sample with acid, the potential increases slowly to the value of pure mercury, which is reached when the residual manganese is finally dissolved from the amalgam.

Additional investigations showed that the beginning of the sudden decrease in reaction rate and the quantity of manganese then remaining in the residue, depend strongly on the quantity, concentration and temperature of the acid used for the dissolution of the samples. The higher the temperature and quantity of HCl, the later the reaction rate begins to decrease, and the smaller is the amount of manganese in the residue. The interrupted dissolution process can, however, be restarted by addition of stronger HCl. To keep the reaction rate constant during the whole dissolution, it is advisable to use dilute HCl (3 M) first, followed by more concentrated acid (maximum 7 M HCl).

The influence of temperature is more complicated: when the temperature is increased, the reaction becomes more violent, but near boiling point there is then a decrease in reaction. In these experiments, the manganese samples (1 g) were amalgamated with 120 mg of mercury. When the manganese weights were increased to 10 g with 120 mg of mercury, the effects observed disappeared.

The studies so far do not suffice for reliable interpretation of the behaviour of amalgamated manganese during dissolution in hydrochloric acid. Yet, the formation of several Mn—Hg compounds appears to be of some importance. Particularly, a temperature of 95°C — as reported [13] for the transformation of Mn_2Hg_5 to MnHg — and the passivation of samples at temperatures near the boiling point of the acid, indicate such correlations.

Trace preconcentration

Depending on the purity of the sample used, most metals are detectable — if at all — only after strong preconcentration. To obtain low detection limits, it was necessary to transfer the preconcentrated elements into a small volume of solution. For determination, the 'injection method', a variation of flame atomic absorption spectrometry, was used [21, 22]. In this method, aliquot parts (50—100 μl) of the solution of trace metals produce analytical

signals which scarcely differ in height from those obtained by conventional flame a.a.s. Thus, even for a sequential determination of many different elements, the total volume of the measured solution could be limited to a few millilitres.

Preliminary tests had shown that high amounts of manganese and mercury remaining in the sample residue interfered with the trace determination by non-specific absorption and diminution of the trace signals. Therefore, care was taken to ensure that manganese was dissolved out of the amalgam to a residual amount not exceeding 5—10 mg; mercury was eliminated from the trace concentrate by a simple separation step. For the concentrate, the total volume of 2.0 ml chosen sufficed for the determination of more than 10 elements sequentially without difficulty.

The nature of the preconcentration technique and the special behaviour of manganese require particular attention to some points of the operating conditions. Quantitative preconcentration of trace elements can be expected only if all particles of the sample are kept in electrical contact throughout the dissolution process. Parts of the sample or trace particles reaching the surface which are separated from the dissolving matrix by too violent a reaction become reactive themselves and are attacked by the acid. Losses of trace constituents are then unavoidable. Therefore, the weighed sample should preferably consist of one piece only or at the most 2—3. Powdered sample material is not suitable. Furthermore, the dissolution rate must be limited by selection of an acid concentration which ensures that particles of the sample are not stripped off. Yet it is difficult to define the most suitable acidity, because the violence of reaction depends on the content and kind of impurities in the sample. Working conditions divergent from those recommended here may be necessary in some cases. The concentration of acid and temperature must be high enough to allow the dissolution to proceed continuously and rapidly; otherwise, the amalgam phase may be stripped from the sample — as described above — or the potential may increase to values at which traces normally more electropositive than manganese can be dissolved. Therefore, in the recommended procedure, the hydrochloric acid is preheated to about 70°C before addition to the sample.

Results

Table 2 shows the results obtained for the preconcentration of traces from electrolytically produced manganese metal. The data for recovery are valid for the calibration ranges mentioned. Samples differing greatly from those used here should be analysed by this method only after recoveries have been checked.

For the determination of the relative standard deviation $s_r = s/\bar{x}$, 10 samples of manganese were analysed. The cementation procedure (see above) was used to adjust the trace contents of most of the elements to the values given in Table 2. The abnormally high values of the standard deviation for the determination of Cu, Fe and Pb are caused by inhomogeneous distribution of the elements in the sample (see below).

The limit of detection (3σ) was calculated from the fluctuations of the element signals by analysing 25 manganese samples without any addition of traces. For Co, Cu, Fe, Ni and Pb, of which relatively high contents were present in the manganese used, the background fluctuations of flame a.a.s. near the analytical signals were used for calculation. In these cases the detection limits listed can be regarded only as estimated values.

EXPERIMENTAL

Amalgamation of samples

Manganese (10.0 g; not more than 3 pieces of approximately the same size) is added to 120 mg of mercury and 5 ml of water in a 25-ml glass beaker, which is then placed in an ultrasonic bath. On addition of 0.5 ml of 37% HCl, the manganese becomes covered with a layer of mercury. The mixture is heated to boiling whereupon the residual mercury is deposited on the manganese, and the acid phase becomes clear. If necessary, a further 0.5-ml portion of HCl is added.

Partial dissolution of samples

The amalgamated sample is added to 50 ml of boiling 3 M HCl (150-ml glass beaker). When the initial rapid reaction becomes slower, the solution is decanted and replaced by fresh acid preheated to about 70°C. If necessary, more concentrated acid must be used (see above). The preconcentration is stopped when the residue still contains 5—10 mg of manganese. This final phase of reaction is indicated by the disappearance of the initial edged shape of the residue and by formation of a mercury drop.

Separation of mercury from the residue

The sample residue is washed free of chloride with water, and dissolved in 1 ml of 65% HNO_3 and 0.5 ml of water (50-ml PTFE beaker). The solution is evaporated to 0.5 ml, and then 10 ml of water and 2 ml of 98% formic acid are added. When the solution is boiled, the mercury separates and flows together to drops. After evaporation to 1—2 ml, 1 ml of 37% HCl is added and evaporation is continued to about 0.5 ml. By pipet, the solution is quantitatively transferred to a 2-ml volumetric flask and diluted to the mark with water. This solution is used for the determinations of Bi, Cd, Co, Cu, Fe, Ga, In, Ni, Pb and Tl. Together with mercury, the traces of Au and Pd are co-precipitated quantitatively whereas Ag is partially lost. To obtain complete reduction of silver, ascorbic acid must be used as precipitant for the noble metals and for mercury. However, the a.a.s. determination of some trace elements in the acid phase may be affected by surplus ascorbic acid and its oxidation products.

Dissolution of mercury for the determination of Ag, Au and Pd

After the solution of less noble trace elements has been decanted, the remaining mercury is dissolved in a mixture of 0.5 ml of 65% HNO_3 and 1.5 ml of 37% HCl (with the same PTFE beaker for dissolution). The solution is evaporated nearly to dryness, and the residue is dissolved in 0.5 ml of 65% HNO_3. By pipet, the solution is quantitatively transferred to a 2-ml volumetric flask and diluted to the mark with water. Au and Pd are determined in this solution.

Trace determination by the 'injection method' of flame a.a.s.

A Varian model 1000 atomic absorption spectrometer equipped with a background compensator and a recorder (T02N1-H, Rikadenki Electronics) was used. The electronegative group of trace elements is determined with an air—acetylene flame. For the determination of noble metals, the air—hydrogen flame is necessary because of the relatively high amounts of mercury; otherwise explosive mercury acetylide may be formed within the nebulizer system. For the determination of each element, 50-μl aliquots are injected with a piston microlitre pipet into a small plastic funnel connected to the nebulizer by a short piece of tubing. The pulse-like analytical signals are recorded. Details of this method have already been published [21, 22].

INVESTIGATIONS ON HOMOGENEITY OF SAMPLE MATERIAL

The data for standard deviations listed in Table 2 show that the values for Cu, Fe and Pb are worse by about one order of magnitude than the values for the other trace elements. Cu, Fe and Pb are present as relatively large impurities in the samples used. As there is no reason to assume that these elements might behave unlike the others, the homogeneity of the sample material was tested. The investigations were carried out together with another method for trace preconcentration from manganese, which — in contrast to the method described here — allows the analysis of powdered material. As the results have already been reported [23], only a summary is given below.

It was shown that the fluctuations of the analytical values decreased by about an order of magnitude when — instead of electrolytically produced manganese flakes — 10-g samples were taken from material which had been powdered in amounts of about 500 g before analysis. For direct application of uncrushed metal flakes, over 100 g must be used for each analysis before the contribution of inhomogeneity to the total standard deviation can be neglected. Accordingly, there is no doubt that the abnormally high values of the standard deviation for Cu, Fe and Pb (Table 2) can be attributed to inhomogeneous distribution of those traces in the sample material.

REFERENCES

1 G. Kortüm, Lehrbuch der Elektrochemie, Weinheim 1972, Verlag Chemie.
2 S. Bolin, State and Currency in the Roman Empire to A.D. 300, Stockholm, 1958, Almquist and Wiksell.
3 R. Klockenkämper, Z. Anal. Chem., in press.
4 H. J. Kellner and W. Specht, Feingehalt und Gewicht des römischen Denars, in: Jahrbuch für Numismatik und Geldgeschichte, 11 (1961) 43, Kallmünz, Verlag Michael Cassleben.
5 W. Seith and J. Herrmann, Spectrochim. Acta, 1 (1941) 548.
6 E. Jackwerth and A. Kulok, Z. Anal. Chem., 257 (1971) 28.
7 E. Jackwerth and J. Messerschmidt, Anal. Chim. Acta, 87 (1976) 341.
8 W. Jost, Diffusion in Solids, Liquids, Gases, Academic Press, New York, 1960.
9 G. Jangg and H. Kirchmayr, Z. Chem., 3 (1963) 47.
10 G. Jangg, Metall (Berlin), 19 (1965) 442.
11 G. Tammann and J. Hinnüber, Z. Anorg. Allg. Chem., 160 (1927) 249.
12 T. Erdey-Grúz and A. Vázsonyi-Zihaly, Z. Phys. Chem. A177, (1936) 292.
13 G. Jangg and H. Bach, Quecksilber und Amalgammetallurgie, in: G. Eger, Handbuch der technischen Elektrochemie, Teil 1, 2. Aufl., Leipzig 1961, Akad.Verlagsgesellschaft.
14 G. Jangg and H. Jedlicka, Electrochim. Acta, 13 (1968) 671.
15 R. Höhn and E. Jackwerth, Spectrochim. Acta, 29B (1974) 225.
16 E. Jackwerth, E. Döring, J. Lohmar and G. Schwark, Z. Anal. Chem., 260 (1972) 177.
17 R. Höhn and E. Jackwerth, Z. Anal. Chem., 282 (1976) 21.
18 R. Höhn, Doctoral Thesis, Ruhr-Universität, Bochum, 1975.
19 M. Kozlowski and O. Songina, Separation by Liquid Amalgams, in: Wilson and Wilson's Comprehensive Analytical Chemistry, Vol. III, Elsevier, Amsterdam, 1975.
20 Ullmanns Encyclopädie der technischen Chemie, 3. Aufl., Bd. 12, München-Berlin 1960, Verlag Urban and Schwarzenberg.
21 E. Sebastiani, K. Ohls and R. Riemer, Anal. Chem., 264 (1973) 105.
22 H. Berndt and E. Jackwerth, Spectrochim. Acta, 30B (1975) 169.
23 H. Berndt, E. Jackwerth and M. Kimura, Anal. Chim. Acta, in press.

Analytica Chimica Acta, 94 (1977) 237–244

CHEMICAL ANALYSIS OF MANGANESE NODULES
Part III. Determination of Thallium, Molybdenum and Vanadium after Anion-Exchange Separation

J. KORKISCH* and I. STEFFAN

Institute for Analytical Chemistry, Analysis of Nuclear Raw Materials Division, University of Vienna, Währingerstrasse 38, A-1090 Vienna (Austria)

G. ARRHENIUS

University of California, Scripps Institution of Oceanography, Geological Research Division, La Jolla, California 92037 (U.S.A.)

(Received 13th June 1977)

SUMMARY

A method is described for the determination of thallium, molybdenum and vanadium in manganese nodules. After dissolution of the sample in a mixture of perchloric and hydrofluoric acids, thallium and molybdenum are adsorbed on the strongly basic anion-exchange resin Dowex 1 (chloride form) from 6 M hydrochloric acid containing bromine. Molybdenum is eluted with 2 M perchloric acid–1 M hydrochloric acid and determined by a.a.s. with a nitrous oxide—acetylene flame. Thallium is eluted with an aqueous solution of sulphur dioxide and, after evaporation of the eluate, this element is determined by a.a.s. with an air—acetylene flame. The same method is used for the assay of vanadium in the 6 M hydrochloric acid effluent. The method was used successfully for the determination of thallium, molybdenum and vanadium at the ppm level in numerous samples of nodules from the Pacific Ocean and Lake Michigan.

For the determination of thallium, molybdenum and vanadium in manganese nodules, spectrographic methods have been used [1—6]; analytical techniques based on atomic-absorption spectrometry, following the removal of interfering main constituents, have not been described in the literature. The present paper reports a method for the atomic-absorption determination of thallium, molybdenum and vanadium after their separation by anion exchange.

EXPERIMENTAL

Solutions and reagents

Ion-exchange resin. The strongly basic anion-exchanger Dowex 1-X8 (Bio-Rad AG1-X8; 100-200 mesh; chloride form) was used. Slurry the resin (4 g) with a few ml of 1 M hydrochloric acid; after ca. 30 min, pour into an ion-exchange column filled with the same acid. Subsequently pretreat the resin as mentioned in the Procedure.

Standard solutions. From aliquots of stock solutions containing 100 μg of Tl(I), Mo(VI) and V(V) per ml of 6 M hydrochloric acid, prepare dilute standard solutions of the elements in 6 M hydrochloric acid.

1:1 Sulphurous acid. Dilute an aqueous 5--6% solution of SO_2 with an equal volume of water.

2 M Perchloric acid—1 M hydrochloric acid. Mix 200 ml of perchloric acid (70%) with 100 ml of concentrated hydrochloric acid and dilute to 1200 ml with water.

Apparatus

The Teflon "bombs" used for the dissolution of the samples have been described previously [7].

The separations of thallium, molybdenum and vanadium were done in ion-exchange columns of the type and dimensions described earlier [8].

A Perkin-Elmer atomic-absorption spectrophotometer 303 (equipped with a Hitachi Perkin-Elmer Recorder connected to a read-out accessory) was used with the following instrumental settings.

Grating:	Ultraviolet (Tl, Mo and V)
Wavelength:	276.8 nm (Tl), 313.3 nm (Mo) and 318.4 nm (V)
Scale expansion:	Up to 10 × (Tl, Mo, and V)
Slit:	5(3 mm; 2-nm band pass) (Tl) and 4(1 mm; 0.7-nm band pass) (Mo and V)
Source:	Hollow-cathode lamps (Tl, Mo and V)
Lamp current:	20 mA (Tl), 38 mA (Mo) and 40 mA (V)
Burner:	Standard burner head (Tl) and N_2O-burner (Mo and V)
Acetylene pressure:	8 psig; 7.0 on flow-meter (arbitrary scale) (Tl) and 13 on flow-meter (arbitrary scale) (Mo and V)
Nitrous oxide pressure:	30 psig; 5.5—6 on flow meter (arbitrary scale) (Mo and V)
Air-pressure:	30 psig; 9.0 on flow meter (arbitrary scale) (Tl)
Noise suppression:	Up to 4 (Tl, Mo and V)

When the measurements are carried out in 6 M hydrochloric acid, the following sensitivities for 1% absorption are obtained: Tl = 0.85 ppm; Mo = 0.52 ppm; and V = 1.30 ppm.

Procedure

Dissolution of samples. Dry the manganese nodule sample at 110°C for 2 d. Dissolve 1 g by the procedure described previously [7]. Dilute the final filtrate with 6 M hydrochloric acid to 100 ml (sample solution).

Ion-exchange separation

Dilute 10 ml of the sample solution with 15 ml of 6 M hydrochloric acid, add 0.25 ml of saturated bromine water and immediately afterwards pass the mixture through an ion-exchange column containing 4 g of the anion exchanger (pretreated with 100 ml of 6 M hydrochloric acid to which 1.0 ml of saturated bromine water was added) at a flow-rate which corresponds to the back-pressure of the resin bed (about 0.7 ml min^{-1}). Subsequently, wash

the resin bed with 20 ml of 6 M hydrochloric acid containing 0.2 ml of saturated bromine water, and combine this effluent with that obtained when the sample solution was passed. (These combined effluents contain the vanadium). Elute molybdenum and some co-adsorbed elements with 200 ml of 2 M perchloric acid—1 M hydrochloric acid (molybdenum eluate). Subsequently elute thallium with 200 ml of 1:1 sulphurous acid (thallium eluate).

Determination of vanadium

Evaporate the combined effluents containing the vanadium to dryness on a steam bath, dissolve the residue in 5 ml of 6 M hydrochloric acid, add 1 to 2 drops of hydrogen peroxide solution (30%) and evaporate to dryness again. Dissolve the residue in 10 ml of 6 M hydrochloric acid containing 4 mg of aluminium [9] and aspirate the solution into the nitrous oxide—acetylene flame. Construct calibration curves by aspirating suitable standard solutions of vanadium before and after each batch of samples.

Determination of molybdenum

Evaporate the molybdenum eluate to dryness under an infrared lamp, dissolve the residue in 5 ml of 6 M hydrochloric acid, add 1—2 drops of hydrogen peroxide solution (30%), evaporate to dryness on a steam-bath, and proceed as described for vanadium.

Determination of thallium

Evaporate the thallium eluate on a steam-bath, dilute the residual 1—2 drops of sulphuric acid with 5 ml of 6 M hydrochloric acid, add 1—2 drops of hydrogen peroxide solution (30%) and heat on the steam bath until effervescence ceases. Dilute the solution to 10 ml with 6 M hydrochloric acid and carry out the atomic-absorption measurements with an air—acetylene flame.

RESULTS AND DISCUSSION

Ion-exchange separations

On the anion-exchange column, thallium(III) is very strongly retained as the anionic chloride complex (K_d = 7100); vanadium is not adsorbed from the 6 M hydrochloric acid containing bromine but passes into the effluent quantitatively, together with all the other elements which do not form anionic complexes under these conditions. Completely adsorbed, together with the thallium, are molybdenum (K_d = 350), uranium (K_d = 283) [7], iron(III) and zinc.

Elemental bromine must be present in the sorption solution as well as in the 6 M hydrochloric acid wash solution to ensure that thallium is in the trivalent state; thallium(I) is not retained by the anion-exchange resin from hydrochloric acid media [10]. Cobalt and copper, which are adsorbed to

some extent as well as residual vanadium, are completely removed from the resin bed by the 6 M hydrochloric acid wash solution containing bromine.

The elution of adsorbed molybdenum is best performed with the 2 M perchloric acid—1 M hydrochloric acid mixture, which is a very efficient eluent for molybdenum [11]. During this elution of molybdenum, thallium is not co-eluted, but remains strongly adsorbed on the resin from which it is eluted subsequently with sulphurous acid, which reduces thallium to the readily eluted monovalent oxidation state.

Addition of hydrogen peroxide to the residues obtained after evaporation of the eluates and effluents greatly facilitates the dissolution of vanadium, molybdenum and thallium, which are then determined by atomic-absorption measurements (see Procedure).

APPLICATION TO MANGANESE NODULES

Thallium

Table 1 gives the results obtained when this procedure was applied to the analysis of 10 separate 1-g portions of the same manganese nodule sample. Comparison of the results for thallium in column A with those of columns B and C shows that direct a.a.s. gives results for this element which are invariably higher by an average of about 16.6% than those measured after application

TABLE 1

Results of thallium, molybdenum and vanadium determinations in the manganese nodule sample 112 DK 20[a]
(A = Results obtained by direct a.a.s. of the elements in the 6 M hydrochloric acid sample solutions. B = Results obtained after application of the procedure. C = As under B, but after deduction of 100 μg Tl, 500 μg Mo, and 400 μg V added to the samples before their dissolution.)

Thallium (ppm)			Molybdenum (ppm)			Vanadium (ppm)		
A	B	C	A	B	C	A	B	C
180	156	160	427	404	412	528	510	527
187	156	161	430	404	395	535	516	530
183	158	158	430	404	412	537	516	519
185	161	159	436	410	412	530	518	527
185	159	153	434	404	412	517	518	521
180	157	150	435	398	410	510	515	513
186	159	163	430	394	415	530	512	543
187	159	159	432	410	417	540	525	554
184	157	158	433	403	401	530	528	528
185	157	160	429	403	406	535	539	554
184.2[b]	157.9[b]	158.1[b]	431.3[b]	403.4[b]	409.2[b]	529.2[b]	519.7[b]	531.6[b]

[a]Metallgesellschaft AG, Frankfurt, West Germany. This sample contains 22.1% and 13.6% of manganese and iron, respectively.
[b]Arithmetic mean.

of the anion-exchange separation procedure. This was found to result from interferences in the a.a.s. measurements caused by the presence of iron and, to some extent, by manganese. For the interference by iron in the measurement of thallium, there was evidence of a considerable increase in the thallium absorption with increasing iron concentration and/or decreasing thallium content of the samples. Thus, the difference between the thallium values of columns A and B of the Lake Michigan nodule (see Table 2) is not in the 11.9—25.8% range as it is for the marine nodules, but is greater than 300% because of its extremely high iron and relatively low thallium contents.

Comparison of the thallium results listed in columns B and C of Table 1 shows that the added amounts of thallium (100 $\mu g\ g^{-1}$ nodule sample) were recovered quantitatively in all cases, i.e. thallium is not lost during the separation and evaporation procedures.

The thallium content not only varies considerably between that obtained for the Lake Michigan nodule and that of the marine nodules (see Table 2) but also with varying location in the oceans. For 5 manganese nodule samples from the Indian Ocean, Campbell Plateau, Blake Plateau, Gulf of Aden, and Loch Fyne, thallium concentrations of 21.77 ppm, 131 ppm, 199.8 ppm, 29.8 ppm, and 1.85 ppm, respectively, were found by Glasby [4].

The average thallium content of 133 ppm (see Table 3), which is the result of thallium determinations in 112 nodule samples analysed by the described procedure, falls in the same average range found by other investigators [12—16] and is close to the world ocean average content (129 ppm) of thallium in ferromanganese oxide deposits [17]. In the same samples thallium

TABLE 2

Results of determinations of thallium, molybdenum and vanadium in manganese nodules from the Pacific Ocean and Lake Michigan
(A = Results obtained by direct a.a.s. of the elements in 6 M hydrochloric acid sample solutions. B = Results obtained by application of the procedure.)

Sample	Thallium (ppm)		Molybdenum (ppm)		Vanadium (ppm)	
	A	B	A	B	A	B
MR-8	298	264	454	440	513	495
MR-9	224	197	542	511	531	541
MR-15	222	185	580	556	479	474
MR-16A	226	202	592	576	493	494
MR-26	209	182	504	486	519	514
AMPH 85P	176	146	364	340	647	637
RC 12-87, 25 cm.	166	132	263	248	488	471
RC 13-70, Mgr. Nod. Top	143	125	292	282	376	362
7 TOW-129D crust	307	263	503	499	636	630
Lake Michigan nodule[a]	28	<7	8	7	193	196

[a]This sample contained 1.7% and 25.6% of manganese and iron, respectively.

TABLE 3

Average contents of thallium in various groups of ferromanganese oxide deposits

Ocean	Average thallium content (ppm)	Reference
Pacific Ocean	133	This paper
Pacific Ocean	100	[12]
Pacific Ocean	194	[13]
Atlantic Ocean	77	[13—15]
Indian Ocean	100	[13, 15, 16]

was also determined by direct a.a.s. in the 6 M hydrochloric acid sample solutions, giving results which were ca. 12—25% higher because of spectral interferences caused by the presence of iron. In this case considerably higher average thallium contents were obtained for the 112 samples analysed.

In comparison with ferromanganese deposits in the world's oceans, the crustal abundance of thallium is only 0.45 ppm [18] so that thallium is very much enriched in manganese nodules (factor, 286.66) if the world ocean average content (129 ppm) is taken as the basis for the calculation. This is the largest enrichment factor so far found for an element when this kind of comparison is made. Very high enrichment in nodules is also shown by molybdenum (factor, 274.66) but vanadium is much less enriched (factor, 4.13).

Thallium is also one of the elements most enriched in manganese nodules compared with other marine sediments [3]; the latter contain approximately 1 ppm of thallium.

Thallium in nodules has some geochemical features in common with cobalt [14], although statistical correlations between these elements, or between thallium and either iron or manganese, have not been observed in this laboratory or by other investigators [17].

Molybdenum and vanadium

Tables 1 and 2 give the results obtained with the described procedure. Comparison of the results for molybdenum in columns A, B and C shows that the added amounts of molybdenum were recovered quantitatively (compare columns B and C) but that the direct atomic-absorption determination gave molybdenum contents higher than those measured after use of the anion-exchange separation procedure (compare columns A with B and C). These higher values were caused by spectral interferences from the presence of manganese and other constituents in the 6 M hydrochloric acid sample solutions.

In contrast to molybdenum, interferences were not observed in the determinations of vanadium, which gave virtually the same results before and after the anion-exchange separation (compare columns A of Tables 1 and 2 with columns B and C); the added amounts of vanadium were

TABLE 4

Molybdenum and vanadium contents of marine nodules (A = Number of samples analysed)

Ranges found				Reference
A	Molybdenum (ppm)	A	Vanadium (ppm)	
112	23—1056	70	270—934	This paper
141	50—710	—	210—1100	[1]
112	178—900	—	—	[19]
98	93—800	98	100—930	[20]
58	50—900	58	190—1000	[21]
55	120—640	26	170—740	[22]
32	7—710	29	34—560	[23]
27	2—717	—	—	[24]
15	66—533	15	50—448	[25]
13	190—1100	13	320—850	[14]
12	50—500	10	500—800	[26]
10	10—600	10	110—190	[27]
8	200—390	8	850—1600	[28]
5	490—910	6	340—900	[2]
5	182—510	—	—	[29]
—	—	26	260—480	[30]
1	500	1	300	[31]
1	2000	1	730	[32]
1	466	—	—	[33]
—	—	1	50	[34]

recovered quantitatively, as for molybdenum (compare columns B and C, Table 1).

The procedure described was used to determine molybdenum and vanadium in 112 and 70 manganese nodule samples, respectively. The results obtained fall in the range found for other nodules by other investigators (see Table 4) [1, 2, 14, 19—34]. Similar results, not cited in Table 4, are reported by Willis [24] (300—1000 ppm Mo), Kerl [35] (90—800 ppm Mo, and 100—900 ppm V) and Glasby [5] (182 samples from the Western Flanks of the Carlsberg Ridge, Indian Ocean gave mean values for molybdenum and vanadium of 434 ppm and 820 ppm, respectively).

In connection with the low molybdenum content found in the Lake Michigan nodule (see Table 2), other investigators [36] report that nodules from this lake contain, on average, 52 ppm of molybdenum.

Further geochemical discussions of the results shown in Tables 1—4 will be presented at a later date.

This research was sponsored in part by the Fonds zur Förderung der wissenschaftlichen Forschung, Vienna, Austria. Samples were supplied by Lamont-Doherty Geological Observatory, M. B. Fisk at the Scripps Institution

of Oceanography, and the Lake Michigan sample by Dr. David Edgington (Argonne National Laboratory). Generous support from these sources is gratefully acknowledged.

REFERENCES

1 J. L. Mero, The mineral resources of the sea, Elsevier, New York, 1965, p. 312.
2 G. P. Glasby, J. S. Tooms and J. R. Cann, Deep Sea Res., 18 (1971) 1179.
3 G. P. Glasby, Naturwissenschaften, 62 (1975) 133.
4 G. P. Glasby, Mar. Chem., 1 (1972—73) 105.
5 G. P. Glasby, in D. R. Horn (Ed.), Ferromanganese Deposits on the Ocean Floor, National Science Foundation, Washington, D.C., 1972, pp. 293.
6 G. P. Glasby, H. Bäcker and M. A. Meylan, Erzmetall, 28 (1975) 340.
7 J. Korkisch, I. Steffan, G. Arrhenius, M. Fisk and J. Frazer, Anal. Chim. Acta, 90 (1977) 151 (Part 2).
8 W. Koch and J. Korkisch, Mikrochim. Acta, (1972) 687.
9 J. Korkisch and H. Gross, Talanta, 20 (1973) 1153.
10 J. Korkisch, Modern Methods for the Separation of Rarer Metal Ions, Pergamon Press, Oxford, 1969.
11 J. Korkisch, L. Gödl and H. Gross, Talanta, 22 (1975) 669.
12 J. P. Riley and P. Sinhaseni, J. Mar. Res., 17 (1958) 466.
13 L. H. Ahrens, J. P. Willis and C. O. Oosthuizen, Geochim. Cosmochim. Acta, 31 (1967) 2169.
14 J. P. Willis and L. H. Ahrens, Geochim. Cosmochim. Acta, 26 (1962) 751.
15 R. C. Harriss, J. H. Crocket and M. Stainton, Geochim. Cosmochim. Acta, 32 (1968) 1049.
16 R. C. Harriss, Nature, 219 (1968) 54.
17 D. S. Cronan, in J. P. Riley and R. Chester (Eds.), Chemical Oceanography, 2nd edn. Vol. 5, Academic Press, 1976, p. 240.
18 S. R. Taylor, Geochim. Cosmochim. Acta, 28 (1964) 1273.
19 W. Raab, Papers from a conference on ferromanganese deposits on the ocean floor. IDOE-NSF. D. R. Horn (Ed.), 1972, 31—49.
20 D. S. Cronan and J. S. Tooms, Deep Sea Res., 14 (1967) 239.
21 H. W. Menard, E. D. Goldberg and H. E. Hawkes, Scripps Institution of Oceanography, unpublished data.
22 D. S. Cronan and J. S. Tooms, Deep Sea Res., 16 (1969) 355.
23 N. M. Strakhov, L. Y. Shterenberg and V. O. Kalinenko, Acad. Sci. U.S.S.R., Geological Institute, 185 (1968) 76.
24 J. P. Willis, M.Sc. Thesis, Department of Geochemistry, University of Cape Town, South Africa, June 1970.
25 P. L. Bezrukov and P. F. Andruschenko, Int. Geol. Rev., 15(3) (1973) 342.
26 C. P. Summerhayes, N.Z. J. Geol. Geophys., 10(6) (1967) 1372.
27 B. Winterhalter, Geotek. Julk., (1966), 69.
28 F. Aumento, D. E. Lawrence and A. G. Plant, Geol. Surv. Can., Paper 68-32, 1968.
29 C. P. Summerhayes and J. P. Willis, Joint Geol. Surv. Univ. Cape Town Mar. Geol. Progr. Tech. Rep., 5 (1973) 121.
30 L. A. Rancitelli and R. W. Perkins, Inter-University program of reasearch on ferromanganese deposits of the ocean floor, Phase I Report, 1—5 (1973).
31 J. Ostwald and F. W. Frazer, Miner. Deposita, 8 (1973) 303.
32 R. S. Diets, Calif. J. Mines Geol., 51 (1955) 209.
33 E. V. Grill, J. W. Murray and R. D. MacDonald, Nature, 219 (1968) 358.
34 E. D. Goldberg and G. O. S. Arrhenius, Geochim. Cosmochim. Acta, 13 (1958) 153.
35 J. F. Kerl, Erzmetall, 23 (1970) 1.
36 R. Rossmann, E. Callender and C. J. Bowser, 24th IGC, 1972, Section 10, pages 336—341.

Analytica Chimica Acta, 94 (1977) 245—256

INVESTIGATIONS OF REACTIONS INVOLVED IN FLAMELESS ATOMIC ABSORPTION PROCEDURES
Part VI. A Study of some Factors Influencing the Determination of Lead in Sulphate Matrices

K. JOHANSSON, W. FRECH and A. CEDERGREN

Department of Analytical Chemistry, University of Umeå, S-901 87 Umeå (Sweden)

(Received 27th June 1977)

SUMMARY

The degree of interference from various sulphates in the determination of lead by flameless a.a.s. is high (e.g. the decrease in the signal from lead is 10% for 2 nanomol of sodium sulphate) and decreases in the order sodium ≥ potassium ≥ calcium ≥ magnesium. The interference from magnesium sulphate can be eliminated by ashing the sample at 870 ± 10°C. Results obtained from high-temperature equilibrium calculations show that gaseous lead sulphide is responsible for the interferences in the presence of sodium sulphate. Theoretical conditions for the formation of gaseous lead sulphide are outlined. The influence of carbon on the reactions involved was investigated by use of standard graphite as well as glassy carbon tubes; the results are compared with those found theoretically. In the presence of a tenfold excess of lanthanum(III), the recovery of lead is higher than 90% for all the sulphates investigated, at least up to an amount of 0.2 μmol. The addition of oxygen as well as hydrogen to the inert gas decreases the interference from sodium sulphate, in accordance with the theoretical predictions.

Few papers deal with the interferences from sulphate salts in the determination of lead by graphite furnace atomic absorption spectrometry (a.a.s.). Barnard and Fishman [1] observed a decreased sensitivity for lead in the presence of nanomole amounts of sodium sulphate. Dolinšek and Štupar [2] reported that interferences caused by magnesium and sodium sulphates could be minimized by the addition of EDTA to the sample solution; in 1 mM sodium sulphate solution the lead signal was depressed by 74%; if EDTA was added, the relative absorbance was somewhat increased. Hodges [3] proposed the use of orthophosphoric acid to remove the sulphates present in urine as sulphuric acid during the drying and ashing of samples. High non-specific absorbance was obtained by this matrix modification. By adding ammonium molybdate to the sample solution the non-specific absorbance could be decreased to a level small enough to allow compensation. Too few results were reported for the usefulness of orthophosphoric acid in suppressing the interferences caused by various sulphate salts to be assessed. Anderssen [4] studied the effect of lanthanum(III) on the signal from lead in sodium sulphate solutions; in solutions 0.4% in lanthanum(III), lead was completely

recovered up to a concentration of 0.06% of sulphate. The lanthanum added was supposed to form lanthanum sulphide which is stable (in vacuum) up to 2400 K. The effect of lanthanum on other sulphates was not investigated. Recently, Thompson et al. [5] reported a positive effect of lanthanum(III) in the determination of lead in non-saline waters containing calcium, sodium, magnesium, and sulphate (0.3—3 mM). No comparison with the sensitivity obtained in a pure aqueous solution was given.

To summarize, a general investigation of the interferences from sulphates in the determination of lead has not been made. The purpose of this paper is (i) to determine the extent of the interferences caused by various sulphate salts, (ii) to study the nature of the interferences, and (iii) to study methods by which the interferences can be minimized. As in the previous parts of this series [6—10] most of the experimental results are correlated with high-temperature equilibrium calculations.

EXPERIMENTAL

Instrumentation

A Perkin-Elmer HGA 2100 graphite furnace connected to a research spectrophotometer was used as described earlier [10]. The instrumental parameters are given in Table 1.

Reagents and materials

Suprapure sulphuric and nitric acids (Hopkin and Williams) were used. All other chemicals were of p.a. grade (Merck). Glassy carbon (Tokai, Lux Ore and Chemical, Inc., Tokyo, Japan) tubes manufactured in this department were used in some experiments; in all others, standard graphite tubes (Perkin-Elmer) were used.

TABLE 1

Instrumental parameters for the graphite furnace atomic absorption determination

	Time (s)	Temp (°C)		
Drying	45	90	Wavelength (nm)	283.3
Ashing	55	varying	Slit width (μm)	150
Atomization	6	1500	Metal lamp current (mA)	6
Cleaning	3	2650	Hydrogen lamp current (mA)	20
			Sample volume (μl)	20[a]
			Argon flow (l min^{-1})	
			internal	0.25[a]
			external	1

[a]Gas stop used.

Separate sulphur interference studies

The single effect of sulphur was studied by means of carbon disulphide; 20 ng of lead as nitrate and 10 μl of carbon disulphide were pipetted successively into the furnace with a drying step in between. After additional drying for 20 s at 90°C, the inert gas flow was interrupted and the tube was heated at a rate of 44° C/s up to 1400° C. The temperature of a standard graphite tube was monitored by a photosensitive diode, the signal of which was registered on a chart recorder. Simultaneously, the absorbance for lead was measured. For comparison, the experiments were repeated without the addition of carbon disulphide.

Preparation of gas mixtures

The procedure described in Part V [10] was followed in preparing oxygen—argon as well as hydrogen—argon gas mixtures. For the investigations with oxygen the gas-stop function was not used. The experiments with hydrogen were performed with gas stop of argon during atomization, but with a continuing hydrogen flow of 12 ml min^{-1}.

Determination of sulphur liberated from the graphite tube during heating

Coulometric determinations of the amount of sulphur liberated from the tubes during heating were made for standard graphite and glassy carbon tubes. A 10 mM sulphate solution (20 μl) was transferred to a graphite tube and dried at 80°C. The graphite tube to be studied was then placed in a quartz tube (see Fig. 1) inserted into an electrically heated oven provided with a thermoelement connected to a thermoregulator. A schematic diagram of the experimental arrangement is shown in Fig. 1. The gas stream was bubbled through the sample compartment of a coulometric cell. Determinations of sulphur dioxide were made with electrically generated iodine [7] while the determinations of hydrogen sulphide were performed with

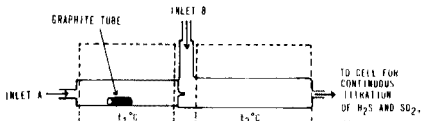

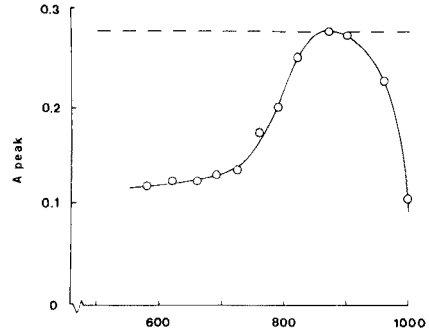

Fig. 1. Schematic experimental arrangement for the coulometric determination of sulphur.

Fig. 2. Peak absorbance values for 10 mM $MgSO_4$ containing lead (0.1 μg ml^{-1}) as a function of ashing temperature. The extrapolated line corresponds to a 1 mM nitric acid solution.

generated silver ions in a sodium carbonate electrolyte at pH 11. Sulphur dioxide as well as hydrogen sulphide were titrated continuously as described earlier [7, 11]. The following combinations of gas flows were used; (i) inlet A, 180 ml min^{-1} of Ar; inlet B, closed; t_2 = 300°C for determination of hydrogen sulphide, and (ii) inlet A, 180 ml min^{-1} of Ar; inlet B, 2 ml min^{-1} of O_2; t_2 = 1100°C for total determination of sulphur (by conversion to sulphur dioxide).

High-temperature equilibrium calculations

High-temperature equilibrium calculations were performed as described in Part I [6]. The amounts of elements left in the graphite tube after drying a sample of 20 μl of 10 mM sodium sulphate are shown in Table 2, which also gives the amounts used in the calculations. The main components in the condensed and gaseous phases are shown in Table 3.

RESULTS AND DISCUSSION

Interferences from various sulphates

Table 4 summarizes the recovery of lead obtained for various types of sulphate; the interferences are most severe for sodium and potassium sulphates. Even amounts of sodium sulphate as low as 2 nanomol decreased

TABLE 2

Estimated amounts of elements after drying 20 μl of 10 mM of sodium sulphate at 90°C, and amounts used in the calculations

Element standard state	Estimated amount after drying (μmol)	Amount used in the calculations (μmol)
Na	0.4	varying
Pb	5×10^{-5}	5×10^{-5}
S_2	0.1	varying
H_2	0.4[a]	varying
O_2	0.6[b]	varying
Ar	2	2
C	—	varying

[a]Originating from the water adsorbed on the graphite [7].
[b]0.2 μmol originating from the water adsorbed.

TABLE 3

Compounds considered to be the main reaction products in the gaseous and condensed phases

Gaseous	Ar, CH_4, CO, CO_2, COS, CS, CS_2, H, H_2, HO, H_2O, H_2S, HS, Na, O, O_2, Pb, Pb_2, PbO, PbS, S, S_2, SO, SO_2
Condensed	C, Na_2O, Na_2S, Na_2CO_3, Na_2SO_4, Pb, PbO, PbS

TABLE 4

Relative peak absorbance (%) for 20-μl of lead solution (0.04 μg ml^{-1}) in various concentrations of sulphates
(The results are referred to lead in aqueous solution. Ashing temperature, 620°C.)

Conc. (mM)	Na_2SO_4	K_2SO_4	$MgSO_4$[a]	$CaSO_4$	H_2SO_4
0.1	90 ± 3.3	89 ± 1.2	100 ± 1.2	100 ± 1.2	—
0.5	42 ± 2.0	57 ± 2.3	94 ± 1.1	81 ± 1.1	—
5	26 ± 2.2	33 ± 1.2	79 ± 1.1	42 ± 2.4	100 ± 1
50	—	—	45 ± 2.4	35 ± 4.8	100 ± 1

[a]Lead can be recovered completely by ashing the samples at 870 ± 10°C.

the signal for lead significantly, in agreement with previous results [1]. For amounts of sodium sulphate larger than ca. 1 μmol, the non-specific absorbance obtained (0.65 absorbance units) was too high to establish the level of the specific absorbance. For each sulphate investigated, the ashing temperature was 620°C. Except for magnesium sulphate this temperature was ideal. The ashing curve for magnesium sulphate is shown in Fig. 2. The dotted line shows the sensitivity for lead obtained in a pure water solution. As can be seen, the interferences caused by magnesium sulphate can be eliminated by ashing at 870 ± 10°C.

Nature of the interferences

Figure 3 shows the absorbance for lead obtained with standard graphite and glassy carbon tubes in the presence of carbon disulphide (B,C). For comparison, the signal without carbon disulphide added, using standard graphite (A), is shown. The atomization interval of lead is not changed in the presence of carbon disulphide, but the signal for lead is depressed. Compared with standard graphite, the extent of the interference is considerably enhanced for glassy carbon tubes. The results indicate that lead, in the form of gaseous lead sulphide, is lost. As indicated by earlier experiments [10] with carbon disulphide, the reaction rate between carbon and this compound is dependent on the structure of the graphite. This means that a high partial pressure of sulphur is expected in the rather inert glassy carbon tube.

Adams and Kirkbright [12] showed that gaseous sulphur was generated during the atomization of potassium sulphate in a graphite furnace atomizer; 0.1 μmol of potassium sulphate gave rise to a partial pressure of sulphur of ca. 5×10^{-4} atm (calculated value at 1900°C) as estimated by the authors. This high value indicates that the partial pressure of sulphur during the atomization of lead will be sufficient for the formation of gaseous lead sulphide (considering the value of the equilibrium constant).

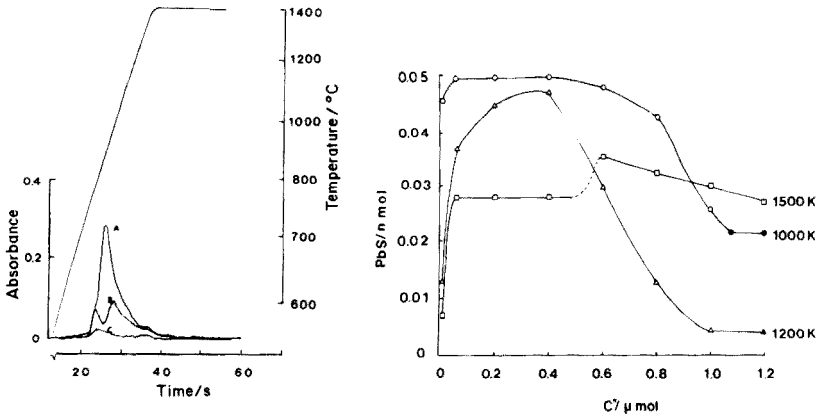

Fig. 3. Absorbance obtained for 20 ng of lead as a function of temperature. The upper curve shows the output signal from the photosensitive diode, referred to the right-hand scale. (A) Absorbance, without carbon disulphide added, for a standard graphite tube, (B) with 10 μl of carbon disulphide added, (C) glassy carbon with 10 μl of carbon disulphide added.

Fig. 4. The formation of gaseous lead sulphide at equilibrium and a total pressure of 1 atm at various temperatures as a function of the input amounts of carbon. The input amounts (μmol) were: H_2 = 0.4, O_2 = 0.6, S_2 = 0.1, Na = 0.4, Ar = 2 and Pb = 5 × 10^{-5}. The filled symbols represent calculations in which solid carbon is present at equilibrium.

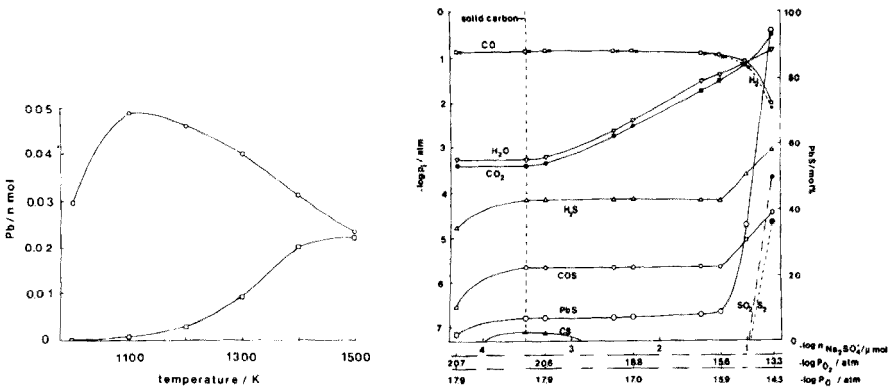

Fig. 5. The formation of gaseous lead as a function of temperature for input amounts of carbon equal to 1.3 μmol, upper curve, (solid carbon present at equilibrium) and 0.4 μmol (no solid carbon present at equilibrium) respectively. The input amount of sodium sulphate was 0.2 μmol.

Fig. 6. The distribution of gaseous sulphur compounds and other gaseous main reaction products as a function of the input amounts of sodium sulphate for C = 0.4 μmol. The temperature was 1200 K.

High-temperature equilibrium calculations

Conditions for the formation of gaseous lead sulphide in a sodium sulphate matrix are given in Figs. 4—6. The effect of a variation in the temperature as well as in the input amount of carbon is demonstrated in Fig. 4. The amount of carbon was varied to simulate an incomplete reaction between carbon and sodium sulphate. Figure 4 includes calculations for which solid carbon is present at equilibrium, i.e., the sulphate has reacted completely with carbon. Generally, the formation of gaseous lead sulphide is smallest for either a large deficit or an excess of carbon. Gaseous lead is the main lead substance present with gaseous lead sulphide in the calculations represented in Fig. 4. The fraction of gaseous lead sulphide formed depends primarily on the partial pressure of sulphur; the equilibria involved are discussed below.

A survey of the effect of temperature on the formation of gaseous lead atoms is shown for two input amounts of carbon in Fig. 5. The upper curve represents calculations for which solid carbon was present at equilibrium. This curve shows that a maximum in the formation of gaseous lead is obtained at about 1100 K. At this temperature the probability of obtaining an equilibrium state is low for uncatalyzed reactions with regard to the carbon—sulphate system. This implies that interferences are always to be expected. The lower curve simulates the influence of temperature, assuming an incomplete reaction between carbon and the sulphate. The shape of the curve indicates that the recovery of gaseous lead should theoretically be increased by means of the heating rate of the atomization device.

The distribution of the main compounds in the gaseous phase are shown in Fig. 6 for various input amounts of sodium sulphate. Since the input amount of carbon was held constant at 0.4 μmol, solid carbon was always present for input amounts of sodium sulphate less than 0.3 nmol. Figure 6 shows that the partial pressure of sulphur is greatly increased for the highest input amounts of sodium sulphate. This can be explained by the decrease in the partial pressure of hydrogen (as a consequence of the increase in the partial pressure of oxygen) so that the partial pressure of sulphur is increased according to the reaction $H_2(g) + \frac{1}{2}S_2(g) \Leftrightarrow H_2S(g)$. Figure 6 also shows that significant amounts of gaseous lead sulphide are formed in the presence of as little as 0.1 nmol of sodium sulphate. The distribution of sulphur compounds in the condensed phase is shown in Fig. 7 as a function of input amounts of carbon. Sodium carbonate is not included in Fig. 7 but is also present for input amounts of carbon less than 0.8 μmol. The maximum amount of sodium carbonate formed is 3 nmol.

Determination of total sulphur and hydrogen sulphide liberated from the graphite tubes

To investigate the role of various conditions of the graphite in the formation of gaseous lead sulphide, the reaction between glassy carbon, as

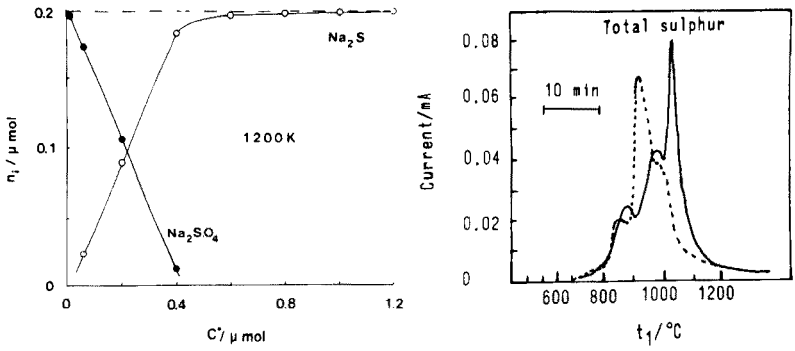

Fig. 7. The distribution of sodium sulphide and sodium sulphate at 1200 K as a function of various input amounts of carbon. The input amounts used correspond to 0.2 μmol of sodium sulphate.

Fig. 8. Recorded coulometric determination of total sulphur liberated from glassy carbon (dotted line) and standard graphite tubes as a function of temperature (t_1 °C).

well as standard graphite, and sodium sulphate was studied by measuring sulphur-containing reaction products. Figure 8 shows the total amount of sulphur liberated from the respective tubes as a function of temperature. The recovery of sulphur for standard graphite was 85% when the temperature of the furnace was maintained at 1200°C for 5 min, compared with 75% for glassy carbon. The curve shows that small amounts of sulphur were still liberated when the experiment was interrupted. Figure 9 shows the amount of hydrogen sulphide formed as a function of temperature for the two types of graphite; hydrogen sulphide is formed at lower temperatures (900°C) in the glassy carbon tube than with standard graphite (1000°C). With glassy carbon, the main sulphur compound formed in the interval 700—850°C was sulphur dioxide as determined coulometrically (iodine system, inlet B closed) in separate experiments. The corresponding interval for standard graphite was 700—950°C.

The results given in the preceding paragraph show that for temperatures lower than 850°C the system is far from a true equilibrium state since at these temperatures the amount of sulphur dioxide found experimentally was three orders of magnitude larger than that theoretically predicted.

Figure 10 compares the theoretically calculated amounts of hydrogen sulphide formed and the integrated amounts found experimentally. To simulate what happens in glassy carbon and standard graphite tubes, the input amounts of carbon used in the high-temperature calculations were 0.4 and 1.3 μmol, respectively. The upper curves show the formation of hydrogen sulphide, in glassy carbon as well as standard graphite tubes provided with 0.2 μmol of sodium sulphate, as a function of temperature. The theoretical curves in the temperature interval 1100—1200 K show that, for the higher input amounts of carbon, much less hydrogen sulphide will be formed. The experimental results can therefore be explained by the

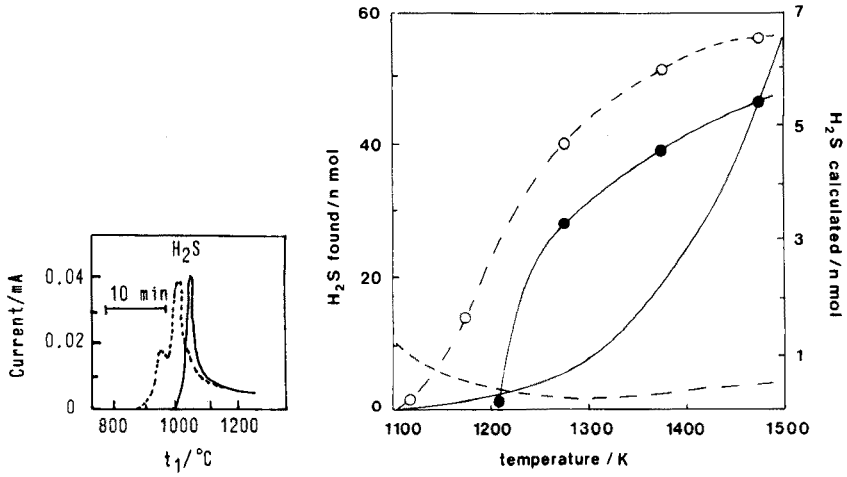

Fig. 9. Recorded coulometric determination of hydrogen sulphide liberated from glassy carbon (dotted line) and standard graphite tubes as a function of temperature (t_1 °C).

Fig. 10. Comparison between theoretical and experimental results with regard to the formation of hydrogen sulphide as a function of temperature. The upper curve (dotted line) shows the amounts of hydrogen sulphide released from a glassy carbon tube and should be compared with the calculated values indicated by the lower curve (dotted line, input amount of carbon = 0.4 μmol). The filled dots represent the amount of hydrogen sulphide released from a standard graphite tube and should be compared with the solid curve (input amount of carbon = 1.3 μmol). The input amount of sodium sulphate used in the calculations corresponds to 0.2 μmol of sodium sulphate, equivalent to the amount used in the experiments.

calculations; in the experiments there is a continuous removal of hydrogen sulphide, while the theoretical results represent conditions corresponding to a closed reactor. This explains the difference between the left and right hand scales in Fig. 10. The results given in Fig. 10 indicate that: (i) the glassy carbon and standard graphite systems approach a true equilibrium state for temperatures of ca. 1200 K; (ii) it is relevant to simulate what happens in glassy carbon and standard graphite by varying the input amount of carbon. The effects of various input amounts of carbon on the formation of gaseous lead sulphide is complicated but can be illustrated by the curve for 1200 K shown in Fig. 4. When the effects on the formation of gaseous lead sulphide of two different input amounts of carbon are compared, the formation of lead sulphide is larger for 0.2 μmol of carbon than for 0.8 μmol. In contrast, the formation of gaseous lead sulphide is larger for 0.4 μmol of carbon than for 0.2 μmol. Experiments showed that the magnitude of the interferences depended on the condition of the graphite tubes. For sodium sulphate, the interferences are larger in glassy carbon than in standard graphite.

Minimization of the interferences

The following attempts were made to minimize the interferences: (i) removal of the sulphate matrix by ashing, (ii) matrix modification, including the addition of lanthanum nitrate, (iii) use of auxiliary gases either to remove the sulphate during ashing or to minimize the formation of gaseous sulphur during atomization. The results were as follows. (i) Except for magnesium sulphate, the interferences from the various sulphates studied could not be overcome by ashing. (ii) Table 5 shows the effect of a tenfold excess of lanthanum(III) on various 10 mM sulphate solutions. The recovery of lead, as related to the signal obtained in pure aqueous solutions, was considerably increased as a result of this matrix modification. For lower concentrations of sulphate, the recovery was higher. Coulometric experiments showed that, in the presence of an excess of lanthanum(III), sulphur could not be detected during heating (up to 1200°C) of the graphite tubes containing sulphate solutions of sodium, potassium, and magnesium, respectively. These results indicate the formation of a stable lanthanum—sulphur compound. (iii) The use of hydrogen was insufficient to remove the sulphates at temperatures lower than 790°C, as determined coulometrically. Except for magnesium sulphate, lead is lost at this temperature.

Table 6 shows that the addition of oxygen as well as hydrogen during atomization significantly increased the signal for lead in a sodium sulphate matrix. To investigate the effects of oxygen, glassy carbon had to be used since this rather inert material permits fairly high partial pressures of oxygen within the tube. The observed effect of oxygen can be understood by considering the theoretical results given in Fig. 4; for small amounts of carbon, which can be considered to be equivalent to the presence of more oxygen, the formation of gaseous lead sulphide decreases. For zero input of carbon, the partial pressure of oxygen in a sodium sulphate matrix will exceed 10^{-7} atm at 1200 K; this results in the formation of extremely small amounts of gaseous lead sulphide. However, for such high partial pressures of oxygen, interferences from the formation of gaseous lead oxide are expected, according to equilibrium calculations [8].

The effect of hydrogen on the interferences from sodium sulphate was investigated for glassy carbon as well as standard graphite. Table 6 shows

TABLE 5

The effect of a tenfold excess of lanthanum(III) (equivalents) on the relative peak absorbance for 20 μl of lead solution (0.1 μg ml^{-1}) in various sulphate salts (10 mM) (The results are referred to values obtained for lead in aqueous solution. Ashing temperature, 620°C.)

	Recovery, %			
	Na_2SO_4	K_2SO_4	$MgSO_4$	$CaSO_4$
Without La added	31 ± 2.4	25 ± 1.5	38 ± 2.8	46 ± 3.5
La added	92 ± 3.3	92 ± 3.3	96 ± 1.4	96 ± 2.5

TABLE 6

Peak absorbance obtained for 20 μl of lead (0.2 μg ml^{-1}) in sodium sulphate solutions (The inner flow with respect to argon and argon gas mixtures was 54 ml min^{-1} each.)

A peak					
Glassy carbon,[a] 1 mM Na_2SO_4		Glassy carbon, 5 mM Na_2SO_4		Standard graphite, 5 mM Na_2SO_4	
Ar only	2 vol % O_2 in Ar	Ar only	10 vol % H_2 in Ar	Ar only	10 vol % H_2 in Ar
0.094 ±0.0055 $n = 5$	0.135 ±0.0045 $n = 5$	0.186 ±0.0096 $n = 8$	0.223 ±0.0092 $n = 8$	0.179 ±0.0066 $n = 8$	0.265 ±0.0152 $n = 8$

[a]Gas stop not used.

that the addition of hydrogen increased the signal for lead in a sodium sulphate matrix significantly for both types of graphite. However, lead could not be completely recovered compared with a pure aqueous solution. With regard to the effect of hydrogen on the formation of gaseous lead sulphide, these results are in accordance with those discussed theoretically under the section "High-temperature equilibrium calculations". Separate calculations showed that, even at high partial pressures of hydrogen, significant amounts of gaseous lead sulphide were formed.

CONCLUSIONS

Several parameters govern the formation of gaseous lead in sulphate matrices, e.g. the nature of graphite affects both the reaction rates in the carbon/sulphur system and the amount of hydrogen generated within the tube [7]. Consequently, large variations with regard to sulphate interferences are to be expected in graphite atomizers. Therefore materials permitting a better control of the atmosphere in the atomizers than graphite might improve the sensitivity as well as the reproducibility of lead determinations in sulphate matrices.

The authors thank Dr. G. Eriksson for valuable discussions.

REFERENCES

1 W. M. Barnard and M. J. Fishman, At. Absorpt. Newsl., 12 (1973) 118.
2 F. Dolinšek and J. Štupar, Analyst (London), 98 (1973) 841.
3 D. J. Hodges, Analyst (London), 102 (1977) 66.
4 A. Andersson, At. Absorpt. Newsl., 15 (1976) 71.
5 K. C. Thompson, K. Wagstaff and K. C. Wheatstone, Analyst (London), 102 (1977) 310.
6 W. Frech and A. Cedergren, Anal. Chim. Acta, 82 (1976) 83.

7 W. Frech and A. Cedergren, Anal. Chim. Acta, 82 (1976) 93.
8 W. Frech and A. Cedergren, Anal. Chim. Acta, 88 (1977) 57.
9 J-Å. Persson, W. Frech and A. Cedergren, Anal. Chim. Acta, 92 (1977) 85.
10 J-Å. Persson, W. Frech and A. Cedergren, Anal. Chim. Acta, 92 (1977) 95.
11 A. Cedergren, A. Wikby and K. Bergner, Anal. Chem., 47 (1975) 100.
12 M. J. Adams and G. F. Kirkbright, Can. J. Spectrosc., 21 (1976) 127.

Analytica Chimica Acta, 94 (1977) 257—268

THE GROUP EXTRACTION OF NOBLE METALS WITH *S*-(1-DECYL)-*N,N'*-DIPHENYLISOTHIOURONIUM BROMIDE AND THEIR DETERMINATION IN THE ORGANIC EXTRACT BY ATOMIC-ABSORPTION SPECTROMETRY

E. A. JONES, A. WARSHAWSKY[§], K. DIXON, D. J. NICOLAS[≠] and T. W. STEELE*

National Institute for Metallurgy, Randburg 2125 (South Africa)

(Received 10th June 1977)

SUMMARY

The distribution coefficients are given for the noble metals and associated base metals between *S*-(1-decyl)-*N,N'*-diphenylisothiouronium (DDTU) in diisobutyl ketone and aqueous solutions containing varying molarities of hydrochloric acid. DDTU is a satisfactory reagent for the extraction of noble metals as a group from most of the associated base metals. Base metals such as iron(III), tin(II), and selenium(IV), which are co-extracted, can be removed from the organic phase by washing with 0.1 M hydrochloric acid; this affects only the recovery of iridium. Although the noble metals cannot be recovered from the organic phase by back-extraction, direct measurement in the organic phase is possible in the presence of zinc dibenzyldithiocarbamate added as a releasing agent. The final solution for analysis contains 6 mg of additive per 10 ml of solution.

The determination of the noble metals by atomic-absorption spectrometry is seriously affected by interferences from the sodium and sulphate ions present in solutions for analysis. These elements are removed, somewhat tediously, by ion exchange and precipitation. Group separations unaffected by sodium and sulphate would facilitate analysis for the noble metals.

The use of isothioureapolystyrene [1, 2] for group separations of noble metals on a decagram scale prompted the development of a liquid analogue of the polymer, which it was hoped would provide a group separation of noble metals from base metals, fast extraction and phase separations, and the possibility of removing any extracted base metals by back-washing. If these criteria were fulfilled, a method for direct determination of the noble metals in the organic extract would be necessary. Preliminary tests indicated that uranium, which can be used [3, 4] as a releasing agent in aqueous media, is not likely to be effective in organic media.

Several isothiouronium compounds were prepared according to the following schemes for aromatic (1), and aliphatic (2) types.

[§] Present address: The Weizmann Institute of Science, Rehovot, Israel.

[≠] Present address: Johannesburg Consolidated Investment Research Laboratories, South Africa.

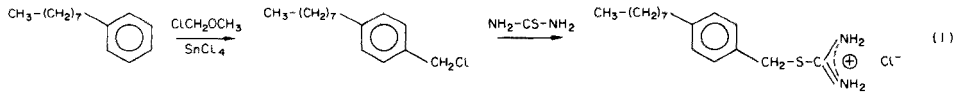

(1)

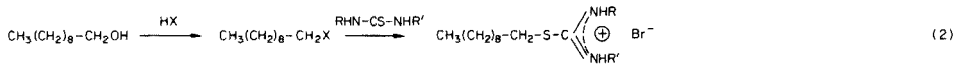

(2)

where R and R′ may be represented by the combinations (a) R = H and R′ = H, (b) R = C_6H_5 and R′ = C_6H_5, and (c) R = C_6H_5 and R′ = t-C_4H_9, and where X = Cl, Br.

The substituted thiourea compounds were prepared by the following two methods:

Symmetrical: $2RNH_2 + CS_2 + S \rightarrow$ RHN-CS-NHR

Others: R-NCS + R′NH_2 → RNH-CS-NHR′

Of the compounds mentioned (some of which have been described as fungicides [5], *S*-(1-decyl)-*N,N′*-diphenylisothiouronium (DDTU, compound 2b) was selected for further study after preliminary experiments.

In this paper, the analytical possibilities of this compound are evaluated with particular reference to group separation of the noble metals and their direct determination by atomic-absorption spectrometry especially from media containing sulphate ions.

EXPERIMENTAL

Preparation of DDTU and its solubility in organic media

The reagent DDTU was prepared by the reaction, at reflux temperature for 6 h, of 11.6 g of n-decyl bromide with 11.4 g of *N,N′*-diphenylthiourea (Fluka) in a 500-ml flask connected to a double-jacketed condenser in 12 ml of 98% ethanol. The product was transferred to a beaker and the solvent was evaporated, the residue being dissolved in 75 ml of carbon tetrachloride, treated with activated charcoal (0.1 g), stirred, and filtered through a Whatman No. 542 filter paper. The carbon tetrachloride was evaporated, and the residue dissolved in 100 ml of chloroform. The solution was again filtered and the solvent was then evaporated off. The resultant DDTU was a viscous liquid having a mass of about 16 g.

DDTU is freely soluble in a wide range of organic media, namely, acetone, methanol, ethanol, dioxane, diisobutyl ketone (DIBK), methyl isobutyl ketone (MIBK), trichlorethylene, carbon tetrachloride, chloroform, benzene, and toluene. Since, ultimately, the possibilities of analysis for the extracted

noble metals by atomic-absorption spectrometry were to be considered, the choice of diluent was limited to solvents that could be flamed directly (i.e., the alcohols and ketones) and to those that either would not extract the base metals, or would do so only to a small extent. DIBK was chosen as being the diluent most suitable for the purpose.

Standard solutions

Standard solutions for the noble metals were prepared as described by Mallett et al. [6], and those for the base metals from the metal chlorides or oxides.

Equilibrium conditions for extraction

Before the determination of the equilibrium distribution coefficients (D) of the noble and base metals, some preliminary investigations were necessary to establish the rate of reaction between DDTU and the noble metals, and the optimum concentration of reagent.

For the determination of equilibrium conditions for extraction, a standard noble-metal solution (10 ml) containing the chloro complexes of 1 mg each of platinum, palladium, rhodium, iridium, ruthenium, osmium, and gold in 4 M hydrochloric acid, was shaken for varying times with 10 ml of 5% (w/v) DDTU in DIBK. After the phases had separated, all the noble metals, except osmium, were determined in the aqueous phase by atomic-absorption spectrometry, uranium being used as the releasing agent [3, 4]. Adequate precision and accuracy of measurement were obtained by combining aqueous phases from several tests, evaporation to incipient dryness, and redissolution in a small volume (5 ml or less) of 4% (v/v) hydrochloric acid for measurement. After liquid—liquid extraction with toluene, osmium was determined with thiourea [7].

The kinetics of the extraction of platinum, palladium, gold, iridium, and osmium are very rapid, a quantitative extraction being achieved almost immediately on shaking (Fig. 1). For rhodium and ruthenium, a constant extraction is approached after 2 h of shaking, and equilibrium conditions are achieved only after 16 h, i.e. overnight.

The optimum concentration of DDTU in DIBK was then determined, 10-ml portions of solutions containing varying amounts of DDTU in DIBK being shaken for 10 min with 10 ml of a solution of platinum and rhodium in 4 M hydrochloric acid. The aqueous phase was analysed after phase separation. The dependence of the percentage extraction on reagent concentration is shown in Fig. 2. For maximum separation of the noble metals as a group, a reagent strength of 25% (w/v) DDTU in DIBK should be used.

If the noble metals are to be determined in the extract by atomic-absorption spectrometry, a lower concentration of reagent should be used so that the background contribution in the flame would be negligible. A solution of 5% (w/v) reagent gave satisfactory flame conditions and complete extraction of all the noble metals, except rhodium and ruthenium, after shaking for 2 h.

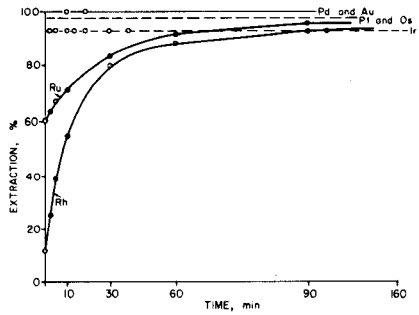

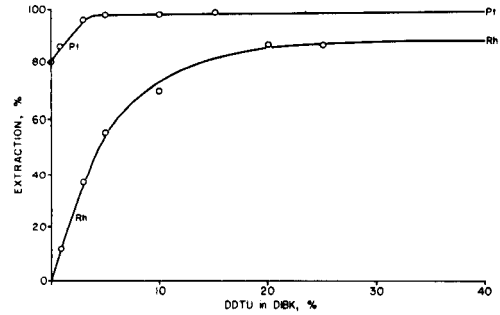

Fig. 1. Relation between time of shaking and extraction of the noble metals. Volume of aqueous phase, 10 ml. Acidity of aqueous phase, 4 M HCl. Volume of 5% DDTU in DIBK, 10 ml. Amount of each noble metal, 1 mg.

Fig. 2. Effect of increasing DDTU concentration on the extraction of platinum and rhodium. Volume of aqueous phase, 10 ml. Acidity of aqueous phase, 4 M HCl. Volume of organic phase, 10 ml. Shaking time, 10 min. Amount of platinum + rhodium, 5 mg each.

For all the noble metals except iridium, this concentration of reagent resulted in extractions of 96—100%; these extractions were obtained after overnight shaking for aqueous-to-organic ratios up to 3. For iridium, the recovery fell to 80% at a phase ratio of 3.

Equilibrium distribution coefficients

The distribution coefficients for the noble metals in varying molarities of hydrochloric acid were determined by shaking solutions containing 50 mg of each of the noble or base metals (except iridium and arsenic(III) where 5 mg was used) as their chloro complexes with 10 ml of solvent, i.e., 5% (w/v) DDTU in DIBK, for 16 h. The concentration of the metal in the aqueous phase was then determined by atomic absorption spectrometry [3, 4], by isotopic measurements (^{110m}Ag), or by spectrophotometry (osmium) [7]. The distribution coefficients (D) were calculated from

$$D = \frac{\text{Metal in organic phase (moles)} \times \text{volume of aqueous phase}}{\text{Metal in aqueous phase (moles)} \times \text{amount of DDTU (g)}}.$$

The distribution coefficients for the noble metals in 0.1 M, 0.5 M, 1.0 M, 2.0 M, 4.0 M, 6.0 M, 8.0 M, and 10.0 M hydrochloric acid are presented in Table 1. The equilibrium distribution coefficients for the chlorides of the noble metals and some other 23 elements with varying concentrations of hydrochloric acid show that the noble metals and silver are extracted from almost any concentration of hydrochloric acid. The equilibrium distribution coefficients range from 10^2 to 10^5, reaching a maximum in 1 M hydrochloric acid (Table 1). Under the given conditions, tin(II), iron(III), zinc(II), cadmium(II), selenium(IV), and bismuth(III) are extracted to various extents.

TABLE 1

Equilibrium distribution coefficients (D) of metal chlorides between varying molarities of hydrochloric acid and 5% DDTU in DIBK
(Amount of all metals except Ir and Ag = 50 mg. Amount of Ir and Ag = 5 mg. Aqueous-to-organic ratio = 1. Time of shaking = 16 h.)

Element	Molarity of hydrochloric acid							
	0.1	0.5	1.0	2.0	4.0	6.0	8.0	10.0
Pt(IV)	583	$>10^3$	$>10^3$	$>10^3$	954	674	352	298
Pd(II)	$>10^4$	$>10^5$	$>10^4$	$>10^4$	$>10^3$	257	126	80
Rh(III)	368	594	814	884	582	374	302	249
Ir(IV)	223	386	493	319	181	162	158	156
Ru(III)	103	151	218	226	187	142	107	38.3
Au(III)	$>10^4$	$>10^4$	$>10^5$	$>10^5$	$>10^5$	$>10^5$	$>10^4$	$>10^4$
Os(IV)	114	154	174	136	107	104	100	74
Sn(II)	NE[a]	2.5	9.4	24.1	68	157	157	157
Ni(II)	NE	0.8	0.8	1.9	2.5	4.8	7.3	7.5
Cu(II)	0.4	0.5	0.5	0.5	0.5	0.5	0.5	0.5
Co(II)	0.9	0.7	0.5	0.3	0.3	0.8	4.9	10.2
Fe(II)	0.8	0.8	1.7	2.9	4.2	5.1	53	$>10^4$
Fe(III)	1.2	2.1	7.2	20.6	140	863	10^4	$>10^4$
Cr(III)	NE	0.2	0.2	0.2	0.2	0.2	0.2	0.2
Ag(I)	960	$>10^3$	$>10^3$	$>10^3$	278	62	10.2	2.8
Al(III)	0.3	0.3	0.5	0.5	0.3	0.3	0.3	0.3
U(VI)	NE	NE	NE	NE	10.0	51	160	130
Sc(IV)	1.6	2.6	3.3	4.6	45.1	$>10^3$	$>10^3$	$>10^3$
Te(VI)	<0.1	0.1	0.3	1.1	3.5	17.0	127	706
Zn(II)	0.9	3.9	6.2	8.9	11.7	9.3	9.1	8.1
Cd(II)	2.8	18.6	28.7	30.8	27.1	24.0	20.1	15.4
Mg(II)	0.3	NE	NE	NE	NE	NE	NE	NE
Ba(II)	0.4	NE	NE	NE	NE	NE	NE	NE
Na(I)	NE	NE	NE	NE	NE	0.5	0.9	0.9
Ca(II)	0.8	NE	NE	NE	NE	NE	NE	NE
V(V)	1.7	1.8	1.8	2.2	1.8	0.8	0.8	0.8
Sb(III)	PPT	PPT	PPT	578	339	219	108	42
Pb(II)	PPT	PPT	PPT	PPT	54	8.8	5.0	3.9
Bi(III)	PPT	PPT	481	307	56	23.7	4.9	1.2
As(II)	NE	NE	NE	NE	2.4	27.4	87	100

[a]NE = not extracted. PPT = precipitate.

The other elements are not extracted, and their distribution coefficients range from 0 to 3. Extraction times of 30 min were also tested; the results confirmed the distribution coefficients and illustrated the need for a further step in the treatment.

The data used for calculation of the D values, which were obtained after shaking for 16 h, gave recoveries of 99, 100, 98, 92, 96, and 100% for platinum, palladium, rhodium, ruthenium, iridium, and gold, respectively. Similar recoveries for these elements were obtained from a solution of com-

bined noble metals (1 mg of each) after shaking for 2 h at an aqueous-to-organic ratio of 1 (99, 100, 93, 96, 96, and 100%, respectively) and 98% was obtained for osmium. The error associated with atomic-absorption measurement of the unextracted noble metals was 2—3%. These recoveries indicate that, with the possible exception of rhodium, overnight extraction would be satisfactory for the noble metals. Theoretically, much shorter periods could suffice, e.g., 30 min from 1 M hydrochloric acid. In this instance, with two extractions, the recovery of rhodium and ruthenium should not be less than 96%. However, it was found in practice that the rhodium and ruthenium remaining in the aqueous phase after the first extraction were further extracted at a reduced rate, probably because of lowering of the oxidation states of these elements during the first extraction. Therefore, three extractions are needed to yield recoveries of 91 and 95% for rhodium and ruthenium, respectively.

If the calibration is done by exactly the same procedure as that used for the samples, the somewhat low recoveries for rhodium and ruthenium and the possible loss of iridium are compensated for, irrespective of the equilibration time used.

Effect of back-washing

As the extraction of some of the base metals, notably iron(III) and tin(II) is high, back-washing was examined as a means of reducing the concentration in the organic phase to an acceptable level. After extraction of the platinum metals and gold from the base metals, the organic phase was washed by being shaken for 10 min with two 10-ml portions of 0.1 M or 1 M hydrochloric acid. The noble and base metals were determined in the aqueous phase after extraction, and in both back-washes, by atomic-absorption spectrometry. The tests with 0.1 M and 1 M hydrochloric acid (Table 2) show that only the 0.1 M solution is effective in this respect.

One wash was sufficient for complete removal of the tin(II) from the organic phase, whereas two washes reduced the iron(III), nickel(II), and copper(II) to 1% or less. Only bismuth(III) was resistant to the back-washing (8% remaining after two back-washes). Iron and possibly nickel and copper are the principal elements in platiniferous materials and process solutions that will be co-extracted.

The noble metals, with the possible exception of iridium(IV), are not affected by back-washing (Table 2). The error in the measurement of small concentrations of iridium is high (ca. 10%) because of its low sensitivity; this may account for the apparent loss. The back-washing procedure could therefore be used after the extraction to complete a group separation of the noble metals from the base metals.

Effect of butanol and pentanol as diluents

In an attempt to reduce the extraction of the base metals, more polar diluents, i.e., butanol and pentanol, were used, and the noble or base metals were determined in the aqueous phase and in the washing liquids by atomic-

TABLE 2

Extraction of noble and base metals and effect of back-washing with hydrochloric acid (Amount of metal present, 1 mg; Volume of aqueous phase, 10 ml; Volume of 5% (w/v) DDTU in DIBK, 10 ml; Time of shaking for extraction, 30 min; Time of shaking for back-washes, 10 min.)

Element	Amount in aqueous phase after extraction (%)	Extraction (%)	HCl (M)	Amount remaining in organic phase after	
				1 wash, %	2 washes, %
Fe(III)	18	82	0.1	5	1
Fe(III)	19	81	1.0	64	52
Cu(II)	99	1	0.1	0	0
Cu(II)	100	0	1.0	0	0
Ni(II)	97	3	0.1	1	0.8
Ni(II)	98	2	1.0	0	0
Cr(III)	100	0	0.1	0	0
Cr(III)	100	0	1.0	0	0
As(III)	100	0	0.1	0	0
As(III)	99	1	1.0	0	0
Se(IV)	96	4	0.1	2	1
Se(IV)	95	5	1.0	2	1
Te(VI)	100	0	0.1	0	0
Te(VI)	100	0	1.0	0	0
Sn(II)	41	59	0.1	0	0
Sn(II)	40	60	1.0	36	22
Al(III)	100	0	0.1	0	0
Al(III)	100	0	1.0	0	0
Bi(III)	4	96	0.1	55	8
Bi(III)	3	97	1.0	92	87
Fe(II)	37	63	0.1	31	29
Fe(II)	37	63	1.0	88	79
Pt(IV)	2	98	0.1	ND[a]	98
Pt(IV)	2	98	1.0	ND	98
Pd(II)	0	100	0.1	ND	100
Pd(II)	0	100	1.0	ND	100
Rh(III)	22	78	0.1	ND	77
Rh(III)	23	77	1.0	ND	76
Ir(IV)	7	93	0.1	ND	83
Ir(IV)	7	93	1.0	ND	83
Ru(III)	18	82	0.1	ND	81
Ru(III)	17	83	1.0	ND	82
Au(III)	0	100	0.1	ND	100
Au(III)	0	100	1.0	ND	100

[a]ND = Not determined.

absorption spectrometry [3, 4]. The results indicated that this procedure had absolutely no advantages, the extraction of the noble metals being reduced to unacceptable levels, and some elements, like arsenic(III), selenium(IV), and tellurium(IV), being co-extracted.

Effect of sulphate ions

The effect of sulphate ions derived from the original sulphide material was determined by shaking solutions containing 1 mg of each of the noble metals, or 1 mg of each of the base metals, in 10 ml of 1 M hydrochloric acid and varying amounts of sulphuric acid with 10 ml of 5% (w/v) DDTU in DIBK. The shaking time was 4 h — at which time equilibrium conditions are approached. The sulphuric acid in the aqueous phase was removed by precipitation as barium sulphate, and, after filtration, the noble and base metals were determined in the filtrate by atomic absorption, uranium being used as the releasing agent [5, 6] for the noble metals. After liquid—liquid extraction, osmium was determined by the use of thiourea [7]. The results are shown in Figs. 3—5.

The extraction of platinum, palladium, osmium, rhodium, and gold is not affected by the presence of sulphuric acid up to a concentration of 3 M. The extraction of iridium and ruthenium is marginally enhanced to a maximum when 1 M sulphuric acid is used (Fig. 3). In general, the extraction of the base metals increases slowly for solutions up to 3 M sulphuric acid. The exceptions are tin(II) and copper(II), for which the extraction increased by about 40%, and iron(III) for which the extraction increased by 20% to give an extraction of 100% at a sulphuric acid concentration of more than 2 M (Fig. 4). Nickel(II) was also extracted under these conditions, but should not present great difficulty, because it is easily eliminated by back-washing with 0.1 M hydrochloric acid. The extraction of arsenic and tellurium from sulphuric acid was enhanced at concentrations of 2 M or higher (Fig. 5). At lower acid concentrations, the extraction was low.

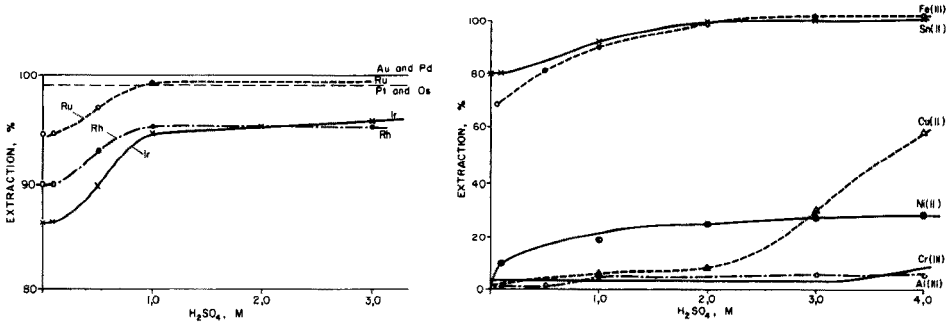

Fig. 3. Effect of sulphuric acid on the extraction of the noble metals. Volume of aqueous phase, 10 ml. Concentration of HCl in aqueous phase, 1 M HCl. Volume of organic phase, 10 ml of 5% DDTU in DIBK. Shaking time, 4 h. Amount of each noble metal, 1 mg.

Fig. 4. Effect of sulphuric acid on the extraction of iron, copper, nickel, and chromium. Volume of aqueous phase, 10 ml. Volume of 5% DDTU in DIBK, 10 ml. Concentration of HCl in aqueous phase, 1 M HCl. Shaking time for extraction, 30 min. Amount of each base metal, 1 mg.

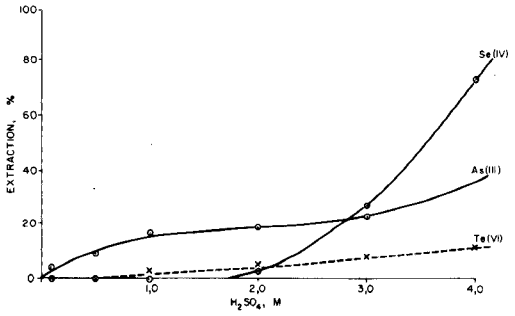

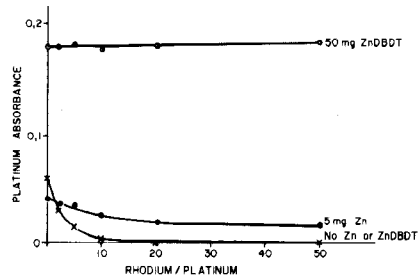

Fig. 5. Effect of sulphuric acid on the extraction of selenium, tellurium, and arsenic. Amount of each base metal, 1 mg. Other conditions as in Fig. 4.

Fig. 6. Effect of rhodium on platinum at high platinum-to-rhodium ratios. Amount of Pt, 100 μg. Methanol, 1 ml. DIBK, 8 ml. Zn—DBDT (5% w/v) in $CHCl_3$, 1 ml.

The amount of sulphate ions taken up in solutions of 1 M hydrochloric acid and 1 M sulphuric acid was determined after shaking with 10 ml of 5% (w/v) DDTU in DIBK for an arbitrary period of 20 min. The sulphate in the aqueous phase was determined gravimetrically after precipitation as barium sulphate. Approximately 3 mg of sulphate was found in 10 ml of organic extract, and this concentration should not cause any interference in the determination of the noble metals.

Determination in the organic extract

Uranium is less effective as a releasing agent in organic media than in aqueous media. Eckelmans et al. [8] have shown that addition of dithizone removes the mutual interferences between platinum, palladium, and gold. Macquet and Theophanides [9] have shown that thermally stable compounds of platinum yield maximum sensitivity in the flame, while Hilderbrand and Pickett [10] consider that the metal dithiocarbamates are more thermally stable than dithizonates. Therefore, zinc dibenzyldithiocarbamate (Zn—DBDT) was tested as a releasing agent with MIBK as the diluent, as reported by Nicolas and Jones [11]. Subsequently, it was found that the substitution of DIBK for MIBK did not affect the sensitivity of the atomic-absorption measurement or the degree of extraction, and had the advantage that the extraction of iron from samples containing appreciable amounts of iron was reduced. This diluent was therefore used in the remaining tests and the following procedure was adopted.

The concentrations of hydrochloric acid and sulphuric acid of the sample solution (up to 25 ml) were adjusted to 1 M, and, after addition of 0.02 g of sodium chlorate, the solutions were heated for 20 min at 80°C to ensure that the noble metals were present as their chloro complexes. The solution was shaken overnight with 10 ml of 5% (w/v) DDTU in DIBK. The aqueous phase was then removed, and the organic layer washed by shaking with 10 ml of

TABLE 3

Instrumental conditions for the determination of noble metals
(Light path, 3.5 mm above burner top. Flame, normal air—acetylene, with acetylene flow reduced to allow for presence of diluent.)

Element	Wavelength (nm)	Slit width (μm)	Lamp current (mA)	Scale expansion
Pt	265.9	25	10	2×
Pd	244.8	50	8	None
Rh	343.5	25	6	None
Ru	349.9	25	10	2×
Ir	264.0	25	12	3×
Au	242.8	50	4	None

TABLE 4

The recovery of noble metals after extraction with DDTU—DIBK
(Organic extract, 8 ml. Zn—DBDT (3%) solution, 2 ml. Time of shaking, 4 h. Phase ratio (aqueous-to-organic), 1.)

Metal	Pt	Pd	Rh	Ru	Ir	Au
Amount (μg)	300	100	50	100	100	100
Recovery (%)	100	100	96	98	97	97

0.1 M hydrochloric acid. The wash was repeated and the phases were separated. To 8 ml of the organic extract, 2 ml of releasing agent, i.e., 3% Zn—DBDT (w/v) in chloroform, was added; the solution was warmed on the edge of a steam-bath to ensure a clear solution and then cooled. Standards were extracted by the same procedure.

The conditions of measurement (Table 3) were similar to those used for the analysis of aqueous media.

The elimination of the interference of rhodium on platinum, one of the most severe of the mutual interferences encountered in the analysis of mixtures of noble metals, is shown in Fig. 6. A similar pattern is observed for binary mixtures of palladium, ruthenium, iridium, osmium, and gold. In all instances there was a significant enhancement, e.g. up to 300%, in the absorption reading for platinum. This enhancement was observed for the other noble metals when examined in admixture. The results obtained for noble metals in admixture after extraction into a DDTU—DIBK mixture are shown in Table 4; the recoveries range from 96 to 100%, i.e., within the accepted error for atomic-absorption measurements.

The solubility of the Zn—DBDT in a DDTU—MIBK or DIBK mixture was approximately 60 mg for 10 ml of solution. At this concentration of releasing agent, mutual interference effects were absent with a total noble-metal mass of 750 μg; only iridium showed a poor recovery (80%), and hence, possibly

TABLE 5

Analysis of leach liquors

	Found in sample A (ppm)		Found in sample B (ppm)	
	DDTU extraction[a] + Zn—DBDT	Ion exchange	DDTU extraction[a] + Zn-DBDT	Ion exchange
Pt	0.5 ± 0.1	0.3	<0.5	0.2
Pd	1.0 ± 0.1	0.8	<0.1	0.2
Ru	11.5 ± 0.3	12.0	11.3 ± 0.2	10.4
Ir	<2.0	ND[b]	<2.0	ND
Au	<0.1	ND	<0.1	ND

[a]Extraction for 16 h. The results quoted are the mean of triplicate determinations and the ± values indicate the range.
[b]ND = Not detected.

the presence of an interference effect when the mass of noble metals was doubled. In other media, such as DIBK—methanol mixtures, the releasing properties were effective for a total noble-metal mass of 15 000 μg.

The amount of sulphate extracted from a 1 M hydrochloric acid solution, to which sulphuric acid had been added to give a 1 M solution with respect to sulphuric acid, did not affect measurements made in the organic phase. However, for sulphate solutions of the platinum metals, the extraction of rhodium was very low (50%); rhodium is apparently resistant to conversion from a sulphate form to a chloro complex form before extraction. In these circumstances, the method of standard addition must be used with a consequent loss in precision and recovery when trace concentrations are measured.

Results for the analysis of two plant-processing solutions containing 80 g of $CuSO_4 \cdot 5H_2O$, 90 g of $NiSO_4 \cdot 6H_2O$, and 3 g of $Fe_2SO_4 \cdot 9H_2O$ per litre, as well as 25 ml of sulphuric acid per litre (about 0.5 M) and trace amounts of platinum metals, are given in Table 5, which also shows the values obtained by an ion-exchange procedure in which the free sulphuric acid originally present, and that formed as a result of the exchange process, was removed by evaporation [12]. The agreement is satisfactory in view of the complex nature of the solutions tested. No loss of noble metals was found after the removal of free sulphuric acid by evaporation.

This paper is published by permission of the Director General of the National Insititute for Metallurgy, Johannesburg, Republic of South Africa.

REFERENCES

1 W. Geilmann and R. Neeb, Z. Anal. Chem., 156 (1957) 420.
2 G. Koster and G. Schmuckler, Anal. Chim. Acta, 38 (1967) 179.

3 R. C. Mallett, D. C. G. Pearton and E. J. Ring, Johannesburg, Nat. Inst. Metall. Rep. no. 970. 5th June, 1970.
4 J. M. Scarborough, Anal. Chem., 41 (1969) 250.
5 Dutch patent No. 93, 872 (1st April, 1960). Chem. Abstr., vol. 55, 12754h.
6 R. C. Mallet, G. J. Wall, E. A. Jones and S. J. Royal, Johannesburg, Nat. Inst. Metall. Rep. no. 1864. 14th January, 1977.
7 K. Dixon, M. M. Kruger and A. J. Radford, Johannesburg, Nat. Inst. Metall. Rep. no. 1654. 27th March, 1975.
8 V. Eckelmans, E. Graauwmans and S. de Jaegere, Talanta, 21 (1974) 715.
9 J. P. Macquet and T. Theophanides, At. Absorpt. Newsl., 14 (1975) 23.
10 D. C. Hilderbrand and E. E. Pickett, Anal. Chem., 48 (1975) 424.
11 D. J. Nicolas and E. A. Jones, Johannesburg, Nat. Inst. Metall. Rep. no. 1826. 15th August, 1976.
12 K. Dixon, D. J. Nicolas, R. V. D. Robert and E. van Wyk, Johannesburg, Nat. Inst. Metall. Rep. no. 1739. 28th November, 1975.

Analytica Chimica Acta, 94 (1977) 269—274

THE RAPID DETERMINATION OF CADMIUM, LEAD, COPPER AND ZINC IN WHOLE BLOOD BY ATOMIC ABSORPTION SPECTROMETRY WITH ELECTROTHERMAL ATOMIZATION. IMPROVEMENTS IN PRECISION WITH A PEAK-SHAPE MONITORING DEVICE

PIERRE DEL CASTILHO* and ROBERT F. M. HERBER

Coronel Laboratory of Environmental and Occupational Hygiene, Faculty of Medicine, University of Amsterdam, Eerste Constantijn Huygensstraat 20, Amsterdam (The Netherlands)

(Received 28th April 1977)

SUMMARY

The Varian AA6 atomic absorption instrument with a CRA Model 63 in combination with a peak-shape monitoring system makes it possible to avoid losses of volatile elements during the ashing stage. Lead, cadmium, copper and zinc can be measured with sufficient precision even when only simple sample dilution is applied. Time is saved as laborious extraction procedures and frequent blank firings can be omitted. Zinc is measured above the oven so that 10—20 times lower dilutions with consequent gain in precision are possible.

About ten references can be found [1] which report attempts to increase the speed of analysis for lead in blood by atomic absorption spectrometry. However, methods with both speed and acceptable precision (standard deviation 4—6%) are rare. It is unnecessary to discuss here all the literature findings, but some difficulties encountered should be outlined. Posma et al. [2] indicated that only in fresh blood samples could sufficient precision be obtained. Garnys and Smythe [3] reported an improvement in precision but not on speed of analysis by applying the pipe-cleaner technique with prior acid decomposition. Rosen [4] applied a technically complicated method only feasible for the Varian CRA model 61, while Kubasik et al. [5] developed a method for this instrument which had acceptable precision only for higher concentrations.

For cadmium, four direct methods have been reported [2, 6—8]. Lundgren [6] reported that application of the method of Posma et al. [2] showed the disadvantage of residue formation after a few determinations.

The Massmann oven [9] has been used in three studies [5—7]; in the present study, the smaller oven of Matoušek and Brodie [10] is used.

The determination of copper is feasible provided that the ashing temperatures are not too high, as copper can be easily lost [11].

For zinc determinations, the flameless technique can offer a useful alternative to the commonly used flame techniques if sample size is limited.

Because of the great sensitivity obtained when the resonance line for zinc is used, blood should be diluted 1000—2000-fold to permit measurement. However, this dilution results in a great loss of precision and a high risk of contamination; in the present study, the absorption is measured above the oven after a 50—100-fold dilution.

Obviously, methods in which chemicals are used, e.g. digestion before measurement [3] or extraction and ion-exchange [12] procedures have their specific problems and are more vulnerable to contamination.

EXPERIMENTAL

Instrumentation

The carbon tube (pyrolytic graphite) atomizer Model CRA 63 was used with the AA-6 spectrophotometer equipped with a simultaneous background correction system (Model BC-6), all from Varian-Techtron. The monitoring device consisted of a lock-in amplifier (PAR Model 126) with preamplifier (Model 117) and a wave-form recorder (Biomation Model 805). A schematic diagram is shown in Fig. 1. Total, background-only or corrected absorbance signals can be monitored.

Graphite tube operating programme

Typical power supply settings are shown in Table 1. New ovens were heated for 60 s at the highest ashing temperature followed by a few atomization firings. For cadmium samples (5 μl) were introduced with an Oxford Ultra-Micropipet followed by 5 μl of concentrated nitric acid at the start of the drying stage.

Optical parameter settings were as recommended by the manufacturer. For lead, the monochromator bandwidth was 0.50 nm with a lead lamp current of 7 mA.

Nitrogen was used continuously as sheath gas at a flow rate of 4 l min^{-1}. For cadmium, the flow was stopped during drying and ashing to improve peak separation and to prevent cadmium losses [2]. The nitrogen flow was initiated automatically at the end of the ashing stage and stopped 10 s afterwards by instrumental modification.

For zinc the optical alignment was done in the usual way, after which the oven was lowered as far as possible with the vertical position knob. In this way, any variation of sensitivity caused by the position of the oven was minimized.

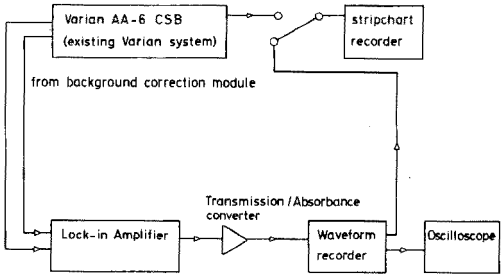

Fig. 1. Flow sheet of the apparatus.

TABLE 1

Power supply and read-out settings
(In all cases, drying was done at 3 V for 20 s.)

Element	Ash		Atomize		Peak mode absorbance setting
	Voltage	Time (s)	Voltage	Time (s)	
Cd	5.0—5.5	30	6.8[a]	4.2	corrected
Pb	5.0—5.5	50	7.5	3.8	corrected
Cu	5.0—5.5	20	8.5	3.5	total
Zn	4.5—5.0	20	7.5	3.8	total

[a]Every five determinations, a blank firing at 8.5 V for 3.5 s is included.

Sample preparation

Analytical-grade metal salts and nitric acid were used. Disposable polystyrene tubes with polyethylene caps and pipet tips were soaked in 10% (v/v) nitric acid for at least 24 h to avoid contamination. Blood dilutions and standard addition samples for the calibration lines were prepared in triplicate with the use of adjustable Finn pipets and shaken mechanically (Vortex). The dilutions contained 50 μl of blood each, and demineralized water was added to the following total volumes: for cadmium 250 μl, for lead and copper 1.0 ml, and for zinc 5.0 ml. A small amount (5 μl) of concentrated nitric acid was added to the dilutions for lead and copper at the time of sample preparation.

RESULTS

As can be seen from Table 1 the ashing voltage settings vary. Figure 2 shows the background absorbance signals for lead and cadmium measured with the monitoring device during the atomization stage; the arrows indicate

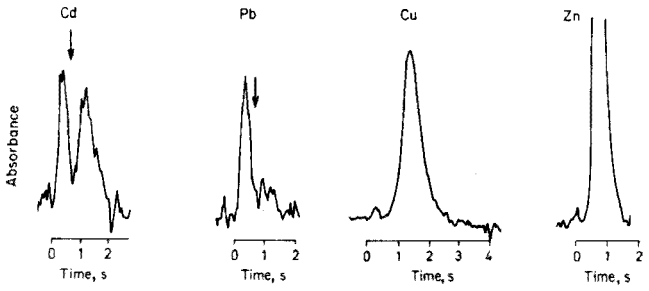

Fig. 2. Absorption during atomization. For cadmium and lead, non-atomic absorbance signals are shown; the arrows indicate the time of appearance of the analyte peak maxima. For copper and zinc total absorbance signals are given; a small non-atomic peak precedes the analyte peaks.

the time when the atomic signals appear. For copper and zinc total absorbance signals are given. In these cases, no loss of analyte occurs whereas the background is small or virtually absent at the analyte peak maxima. Thus the most important errors (except for contamination) according to a study of Baily and Kilroe-Smith [13], are avoided. Moreover, depression of the peaks by residue build-up [3] does not occur under the conditions selected, which involve the high dilution of samples, relatively high temperatures and prolonged atomization times. However, for fivefold diluted blood, a blank firing after every fifth measurement remains necessary to avoid residue build-up. Normally encountered levels, sensitivities, relative standard deviations and confidence intervals for triplicate measurements are shown in Table 2. It should be noted that the data given are realistic values: they were calculated from routine analysis series with 30 or more measurements of other samples interspersed.

The linearity of the calibration lines was tested by comparing the variation of the triplicate determinations with the variation from the best-fit line to the F-distribution. All calibration graphs were found to be straight lines.

DISCUSSION

The precision of the methods for lead and cadmium is satisfactory compared with those found in the literature for the low levels observed in populations (Table 2).

For lead measurements where 20-fold dilution is applied, it is possible to avoid the time-consuming pipecleaner technique described by Garnys and Smythe [3] where cleaning the oven with a pipecleaner followed by a blank firing after every lead measurement appeared necessary to maintain precision (relative standard deviation 3.4%) by preventing residue build-up. Absolute absorbance readings with the dilution method compared with the pipecleaner technique are only slightly smaller (0.060 versus 0.097). Application of a faster electronic response system (0.05 s versus 0.3 s for the time constant of the system) allows a higher atomization temperature setting with consequent increase of sensitivity while linear response is conserved for

TABLE 2

Precision and sensitivity for the metals in whole blood

Analyte	Concn. (ppm)	Sensitivity[a] (ppb)	R.s.d. (%)	95% confidence interval (± ppm)
Cd	0.003	0.1	7	0.001
Pb	0.150	0.5	4	0.02
Cu	1.1	4	6	0.2
Zn	7.0	1	5	0.9

[a]Sensitivity as the concentration in ppb of the dilution producing a 1% absorption signal.

these fast signals. Moreover, matrix peak depression during atomization is smaller for diluted samples. Slow response systems may conceal the amount of background present at the time of atomization of the analyte because of peak overlap, especially if a high rate of temperature increase is chosen to obtain better sensitivity. The measured background peaks (Fig. 2) yield information about the total conditions under which the atoms are formed. Changes in the shape and size of the background peaks indicate a change of physico-chemical conditions, e.g. temperature, surface structure or distribution of the sample in the oven. When a fast-response monitor is used, such effects which can lead to erroneous results are readily detected, and the original conditions can be restored before measurements are continued.

So far, four methods for the direct determination of cadmium in blood have been reported. An attempt to reproduce the method of Posma et al. [2] failed. Several authors [6—8] have reported direct methods for other types of ovens and apparatus; the precision is comparable with the present method. A drawback of Lundgren's method [6] is the somewhat lower sensitivity; for the other methods [7, 8], blank firings are necessary after each determination.

Direct methods yield appreciable saving of time compared with solvent extraction and ion-exchange procedures [12] for lead and cadmium in blood. The detection limits and precision of the direct methods are good enough to be applied at the low levels observed in the normal population, in contrast to the punched disk method of Cernik [14] which is of use in the field of industrial medicine.

The precision obtained for the copper and zinc measurements will meet the requirements for most purposes in clinical chemistry; the advantage of the micro method is that measurements are possible in the blood of young children or small animals where withdrawal of not more than 0.5 ml may be possible. According to Fuller [11] copper can be lost when the ashing temperature is too high. In our experience, the ashing voltage settings should be adjusted so that a small non-atomic peak precedes the atomic peak (Fig. 2), checking that no losses occur.

The method proposed for zinc has some resemblance to the older West and Williams filament atomizer method [15], when the problem of analyte soaking into the graphite had not been solved, and there was some loss of precision. If zinc is to be measured in the usual way, through the oven instead of above the oven, much higher dilutions (2000-fold) are necessary to permit measurement. As a result, the precision decreases dramatically (relative standard deviation, 25%) probably because of the higher risk of contamination and the instability of the dilutions.

Especially for the lead and cadmium determinations, the ashing voltage settings are critical; even temperature settings which are tenths of a volt too high can lead to losses of 20% or more. When ashing temperature settings are not high enough, so that much material must be evaporated during the atomization stage, erroneous results can be obtained because of

incorrect background correction as discussed by Baily and Kilroe-Smith [13]. Moreover, smoke may affect the concentration of free atoms in the oven as shown in the case of silver in copper and zinc matrices by Baudin et al. [16]. This possible effect has not so far been investigated for the blood matrices.

We thank H. J. Pieters and J. L. M. de Boer for technical assistance. The study was supported by a grant from the Netherlands Praeventie Fund.

REFERENCES

1 Annual Reports on Analytical Atomic Spectroscopy, Vols. 2—5, Soc. Anal. Chem. London, 1972—1975.
2 F. D. Posma, J. Balke, R. F. M. Herber and E. J. Stuik, Anal. Chem., 47 (1975) 834.
3 V. P. Garnys and L. E. Smythe, Talanta, 22 (1975) 881.
4 J. F. Rosen, J. Lab. Clin. Med., 80 (1972) 567.
5 N. P. Kubasik, M. T. Volosin and M. H. Murray, Clin. Chem., 18 (1972) 410.
6 G. Lundgren, Talanta, 23 (1976) 309.
7 R. T. Ross and J. G. Gonzales, Anal. Chim. Acta, 70 (1974) 443.
8 F. C. Wright and J. C. Riner, At. Absorpt. Newsl., 14 (1975) 103.
9 H. Massmann, Spectrochim. Acta, Part B, 23 (1968) 215.
10 J. P. Matoušek and K. G. Brodie, Anal. Chem., 45 (1973) 1606.
11 C. W. Fuller, Anal. Chim. Acta, 62 (1972) 442.
12 M. D. Vens and R. Lauwerys, Arch. Mal. Prof., 33 (1972) 7.
13 P. Baily and T. A. Kilroe-Smith, Anal. Chim. Acta, 77 (1975) 29.
14 A. A. Cernik, Brit. J. Ind. Med., 32 (1975) 155.
15 T. S. West and X. K. Williams, Anal. Chim. Acta, 45 (1969) 27.
16 G. Baudin, M. Chaput and L. Feve, Spectrochim. Acta, Part B, 26 (1971) 425.

Analytica Chimica Acta, 94 (1977) 275—281

A SIMPLE DECOMPOSITION AND CHELATING RESIN SEPARATION FOR THE DETERMINATION OF HEAVY METALS IN SILICATES BY ATOMIC ABSORPTION SPECTROMETRY

TETSUO UCHIDA, MASAYUKI NAGASE, ISAO KOJIMA, and CHUZO IIDA

Laboratory of Analytical Chemistry, Department of Engineering Sciences, Nagoya Institute of Technology, Showa-ku, Nagoya 466 (Japan)

(Received 1st June 1977)

SUMMARY

A simple method for the determination of copper, nickel, zinc, and cadmium in silicate rock samples is reported. Silicates are decomposed with hydrofluoric acid and aqua regia in a sealed Teflon vessel. After centrifugation and addition of malonic acid, the supernatant liquid is passed through a small column of Chelex 100. The metals are eluted with 2 M nitric acid, and determined by atomic absorption spectrometry. The method is rapid, simple, and free from contamination. The results obtained for 14 standard reference rock samples (USGS, GSJ, and CSRM) agree with literature data; the recovery, reproducibility, and accuracy of the proposed method are satisfactory.

For the determination of major [1, 2] and minor [2, 3] elements in silicates by atomic absorption spectrometry, the decomposition of silicates with a mixture of hydrofluoric acid and aqua regia in a sealed Teflon vessel has been reported. For accurate and precise determinations, minor and trace elements should preferably be separated from the sample solution to minimize interferences from the major elements. Recently, chelating resins have been applied for the separation and preconcentration of trace elements from large amounts of natural and sea waters [4—6] and from solutions containing high salt contents [7, 8]. In comparison with solvent extraction, this technique is convenient and free from contamination. The determination of copper in silicates by ordinary atomic absorption spectrometry after decomposition in a sealed Teflon vessel and separation on a chelating resin has already been described [9].

The present paper deals with separation on a chelating resin and the atomic absorption spectrometry of copper, nickel, zinc, and cadmium after decomposition of silicates in a sealed Teflon vessel. The method has been applied successfully to the determination of these metals in standard silicate samples.

EXPERIMENTAL

Apparatus and equipment

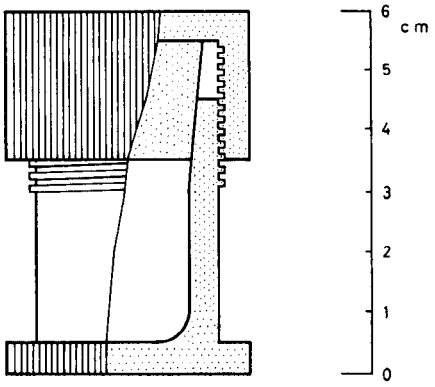

Fig. 1. Sealed Teflon vessel.

A Hitachi atomic absorption spectrophotometer, Model 518, with an acetylene—air flame was used for copper, nickel, and zinc, and an atomic absorption spectrophotometer having a long absorption tube [10] with a hydrogen—air flame was used for cadmium. The decomposition of sample was carried out in a sealed Teflon vessel of about 8-ml volume (Fig. 1). The chelating resin was used in a polypropylene column (BioRad, Cat. No. 7311110).

Chelating resin

Chelex 100 (BioRad, 100-200 mesh, sodium form) was used. Before use, the resin was repeatedly treated with 4 M hydrochloric acid and 4 M ammonia solution. The resin in the ammonium form was packed into the column (7 mm × 30 mm, 0.4 g dry weight) and finally conditioned with 0.1 M malonic acid solution of pH 6. The exchange capacity of the resin was 1.73 mM Cu g^{-1} (dry weight), determined by complexiметric titration of copper.

Reagents

Nitric, hydrochloric, and malonic acids and aqueous ammonia were obtained from Wako Pure Chemicals Co., and hydrofluoric acid from Toshiba. All reagents used were of super-pure grade except for malonic and hydrofluoric acids which were of reagent grade. Standard solutions (1000 ppm) were prepared by dissolving copper, zinc, and cadmium metals (99.999%, Mitsuwa Chemicals Co.,) and nickel oxide (Johnson Matthey, Specpure) in hydrochloric or nitric acids. Working solutions were obtained by diluting the standard solutions with 0.1 M hydrochloric acid.

Procedure

Into the Teflon vessel, place 0.5 g of powdered sample, 1 ml of aqua regia and 5 ml of 48% hydrofluoric acid. After sealing and standing for 36 h at 25°C, add 2 ml of 2.5 M malonic acid solution, and transfer the contents to a Teflon beaker with distilled water. Without removal of any residue, adjust the pH of the solution to 6 with concentrated ammonia liquor and dilute to ca. 50 ml with distilled water. After centrifugation, wash the residue with 5 ml of 0.05 M malonic acid solution of pH 6 containing about 1.3 M fluoride. Pass the supernatant liquid and the washings through the column at a flow rate of 3 ml min^{-1}, wash the column with 5 ml of distilled water, and elute the trace elements with three 10-ml portions of 2 M nitric acid. Evaporate the combined eluents to dryness, dissolve in 10 ml of 0.1 M hydrochloric acid, and determine the concentration of metals in the solution by atomic absorption spectrometry with calibration curves.

RESULTS AND DISCUSSION

Decomposition of silicates

The powdered silicates were completely decomposed with small amounts of aqua regia and hydrofluoric acid in the vessel at 25°C after 16 h; the decomposition time of about 36 h is recommended for security. This operation is very simple and free from airborne contamination.

Effect of pH and masking agents on adsorption of metals

Of the metals in silicates, copper, nickel, zinc, cadmium, cobalt, and lead are of particular interest. Preliminary experiments showed that these metals are completely adsorbed on the resin from Michaelis buffer or simple solutions in the pH range 3—9 for copper and nickel and 4—9 for lead, zinc, cadmium, and cobalt (Fig. 2). The order, Cu > Ni ~ Pb > Zn ~ Co ~ Cd, is consistent

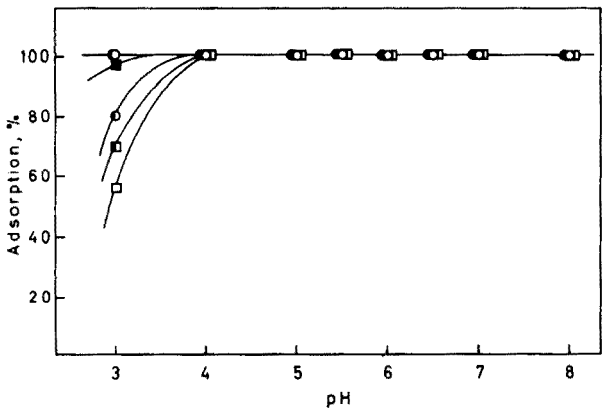

Fig. 2. Adsorption curves of metals from Michaelis buffer or simple solutions. Total volume, 50 ml. ○ Cu; ◐ Zn; ● Ni; □ Cd; ◧ Co; ■ Pb.

with that of the conditional stability constants, $K_{MY'}$, of the metals with *N*-(phenylmethyl)iminodiacetic acid, which is the functional group of the resin. These metals adsorbed on the resin are completely eluted with two 10-ml portions of 2 M nitric acid.

Of the major elements in silicates, iron and aluminum interfere with the adsorption of trace elements for two reasons: the large conditional stability constant of the iron(III) complex with *N*-(phenylmethyl)iminodiacetic acid, and the ease of hydrolysis of iron and aluminum at a rather low pH range, which causes coprecipitation of the trace elements with these hydroxides. Masking is therefore necessary. Of the masking agents studied, i.e. glycine, triethanolamine, malonic, tartaric, and citric acids, malonic acid is the best. Previously [9], citric acid was used as the masking agent and/or auxiliary complexing agent for iron and aluminum during the adsorption of copper at pH 4. Copper was completely adsorbed at pH 3—9, nickel, zinc, and cobalt at pH 7—9, cadmium at pH 7—8, and lead at pH 8—9 from 0.1 M citrate solution containing 100 mg of Fe and 1.8 g of NH_4F in 50 ml (Fig. 3). However, in practice, most of these metals were only partly adsorbed even at pH 7—8 from the digested solution of silicates. From 0.1 M malonate solution containing 100 mg of Fe and 1.8 g of NH_4F in 50 ml, these metals were completely adsorbed on the resin at pH values above 5.5 (Fig. 4). In both cases, lead was adsorbed only at higher pH values in the presence of fluoride ion. By taking the side-reaction coefficients for the metal complexes with malonate into account, the order, Cu > Ni > Zn > Co, is consistent with that of the conditional stability constants for the *N*-(phenylmethyl)iminodiacetic acid complexes (Table 1). At pH 7, hydrolysis of iron and aluminum does occur. Thus the optimum pH range for adsorption of metals is 5.5—6.5 (Fig. 4).

In the supernatant solution obtained after the decomposition of silicates, the cobalt ion seems to be present in the divalent and trivalent states. Only

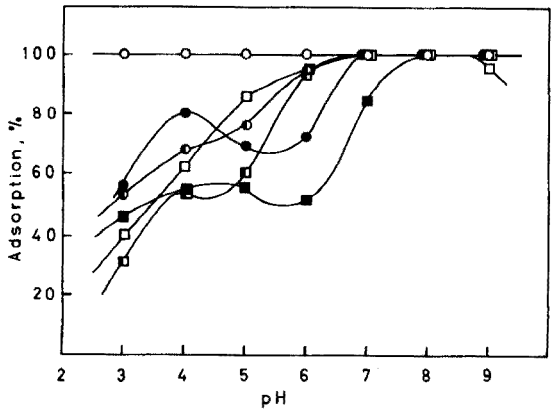

Fig. 3. Adsorption curves of metals from 0.1 M citrate solution. Total volume, 50 ml. Fe(III), 100 mg. NH_4F, 1.8 g. Symbols, see Fig. 2.

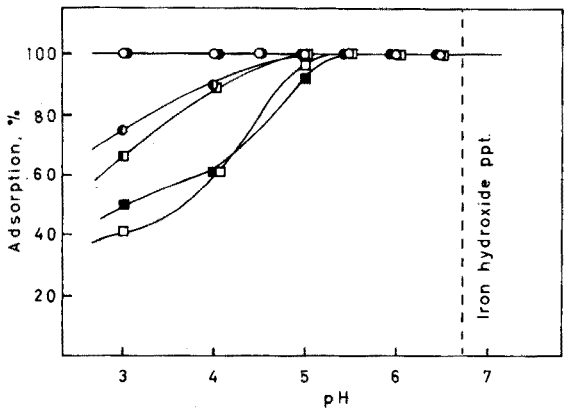

Fig. 4. Adsorption curves of metals from 0.1 M malonate solution. Conditions and symbols as for Fig. 2. Above pH 7, hydrated iron oxide precipitates.

TABLE 1

Conditional stability constants (log $K_{M'Y'}$[a]) for the copper, nickel, zinc, and cobalt complexes with *N*-(phenylmethyl)iminodiacetic acid in the presence of 0.1 M malonic acid

pH	Cu	Ni	Zn	Co
3	2.51	1.48	0.70	−0.13
4	2.95	2.38	1.72	1.11
5	2.75	2.30	1.69	1.44
6	3.25	2.82	2.22	2.07
7	4.26	3.82	3.23	3.08
8	5.13	4.69	4.10	3.95
9	5.69	5.25	4.66	4.52

[a] $K_{M'Y'} = [MY]/[M'][Y'] = K_{MY}\alpha^{-1}_{(M)}\alpha^{-1}_{Y(H)}$. The stability constants used are taken from ref. 11.

about 75% of the cobalt, presumably divalent, was adsorbed on the resin at pH 6 from malonate solution; cobalt(III) is not adsorbed. Cobalt can be completely adsorbed if the supernatant liquid is evaporated to dryness and dissolved in hydrochloric acid. Lead in silicates is included completely in the residue obtained during the decomposition, for lead fluoride is coprecipitated with calcium and aluminum fluorides. From these reasons and for simplicity, only copper, nickel, zinc, and cadmium were determined in this study.

Recovery, reproducibility, and accuracy for four metals

Table 2 shows the reproducibility and accuracy obtained for the four metals in the standard rock JB-1. The recoveries obtained by addition of standard solutions to this sample are shown in Table 3.

TABLE 2

Reproducibility and accuracy (n = 20) for the standard rock JB-1 (500-mg samples)

Element	Mean ± s (ppm)	Reported value (ppm)	Recovery (%)
Cu	52.9 ± 2.1	55.7	95
Cd	0.13 ± 0.02	0.11	114
Ni	131 ± 5	135	97
Zn	80.6 ± 3.6	84	96

TABLE 3

Recovery of copper, cadmium, nickel, and zinc (n = 5) added to samples (500 mg) of standard rock JB-1

Element	Present (μg)	Added (μg)	Found (μg)	Recovery (%)
Cu	26.4	25.0	51.6	100
Cd	0.065	0.050	0.11	97
Ni	65.5	60.0	127	101
Zn	40.3	40.0	79.3	99

TABLE 4

Results for trace metals in standard silicate rocks
(All results are given in ppm)

Silicate		Cu		Cd		Ni		Zn	
		Found	Reported	Found	Reported	Found	Reported	Found	Reported
GSJ	JG-1	2.5	3.9	0.04	0.046	8.4	8.2	39.6	40
	JB-1	52.9	55.7	0.13	0.114	131	135	80.6	84
	JA-1[a]	41.0	—	0.09	—	0.6	—	83.6	—
	JB-2[a]	261	—	0.15	—	12.0	—	104	—
USGS	G-2	9.1	11.7	0.02	0.039	1.8	5.1	80.1	85
	GSP-1	31.9	33.3	0.05	0.06	8.0	12.5	97.6	98
	AGV-1	57.4	59.7	0.07	0.09	15.9	18.5	83.6	84
	W-1	111	110	0.17	0.15	74.8	76	82.3	86
	BCR-1	15.8	18.4	0.14	0.12	9.9	15.8	119	120
	DTS-1	6.9	7.0	0.03	0.12	2260	2269	28.4	45
	PCC-1	9.8	11.3	0.04	0.1	2340	2339	30.2	36
CSRM	SY-2	2.9	6.6	0.23	—	6.7	11	228	247
	SY-3	17.3	18	0.24	—	7.2	11	225	245
	MRG-1	134	135	0.19	—	190	191	174	187

[a]New sample.

Results for copper, nickel, zinc, and cadmium in standard silicate samples of USGS, GSJ, and CSRM are summarized in Table 4. These values are in reasonably good agreement with the data reported by Flanagan [12], Ando et al. [13], and Abbey et al. [14].

The proposed method of decomposition of silicates at room temperature is simple, free from airborne contamination, and excellent for separating trace elements from major elements without using large amounts of reagents.

REFERENCES

1 B. Bernas, Anal. Chem., 40 (1968) 1682.
2 R. T. T. Rantala and D. H. Loring, At. Abs. Newsl., 12 (1973) 97.
3 D. E. Buckley and R. E. Cranstone, Chem. Geol., 7 (1971) 275.
4 D. G. Biechler, Anal. Chem., 37 (1965) 1054.
5 J. P. Riley and D. Taylor, Anal. Chim. Acta, 40 (1968) 479.
6 M. I. Abdullah and L. G. Royle, Anal. Chim. Acta, 58 (1972) 283.
7 H. Imoto, Bunseki Kagaku, 10 (1961) 1354.
8 K. Kawabuchi, M. Kanke, T. Muraoka, and M. Yamauchi, Bunseki Kagaku, 25 (1976) 213.
9 T. Uchida, M. Nagase, and C. Iida, Anal. Lett., 8 (1975) 825.
10 T. Uchida and C. Iida, Appl. Spectrosc., 29 (1975) 57.
11 L. G. Sillen and A. E. Martell, Stability Constants of Metal-Ion Complexes, The Chemical Society, London, 1964, Supplement No. 1, 1971.
12 F. J. Flanagan, Geochim. Cosmochim. Acta, 37 (1973) 1189.
13 A. Ando, H. Kurasawa, T. Ohmori, and E. Takeda, Geochem. J., 8 (1974) 175.
14 S. Abbey, A. H. Gillieson, and G. Perrault, A Report on the Collaborative Analysis of Three Canadian Rock Samples for Use as Certified Reference Materials, 1975.

Analytica Chimica Acta, 94 (1977) 283—287

THE SIMULTANEOUS DETERMINATION OF GOLD, SILVER AND CADMIUM AT PPB LEVELS IN SILICATE ROCKS BY ATOMIC ABSORPTION SPECTROMETRY WITH ELECTROTHERMAL ATOMIZATION

F. BEA BARREDO and C. POLO POLO

Geochemical Laboratory, Department of Petrology, University of Salamanca, Salamanca (Spain)

L. POLO DIEZ*

Department of Analytical Chemistry, University of Salamanca, Salamanca (Spain)

(Received 16th May 1977)

SUMMARY

A method for the determination of Au, Ag and Cd at ppb-levels in silicate rocks by flameless atomic absorption spectrometry after separation with an anion-exchange resin is described. The final test solutions are simple and calibration graphs can be prepared with pure salt solutions. The detection limits allow the determination of as little as 0.2, 0.05 and 0.03 ppb for Au, Ag and Cd, respectively, in 1-g rock samples.

The determination of gold in unmineralized silicate rocks is a difficult analytical problem because of the low gold concentrations. The estimated crustal average of gold is about 2.5 ppb [1]. Conventional flame atomic absorption spectrometry (a.a.s.) requires a preconcentration step, as well as large amounts of sample, which can be a serious inconvenience. Flameless atomic absorption spectrometry with a graphite furnace improves sensitivity, but chemical separations are necessary to avoid matrix effects and atypical matrix absorptions in the graphite tube. A recent method for the determination of gold in silicate rocks is based on selective extraction of gold as its bromide complex into methyl isobutyl ketone (MIBK), and injection into a graphite tube [2]. However MIBK injection involves some inconveniences, such as loss of sensitivity [3] and rigorous control of the time between injection and starting the atomizer program [4]. In addition, split peaks appear when gold is atomized from MIBK, so that reproducibility is poor [5]. Accordingly, efforts were made to eliminate interferences in the determination of gold by using other methods such as ion-exchange resins. When a method specially designed to determine gold was tested, it was found that silver and cadmium accompanied gold in the separation process. The crustal averages of silver and cadmium are about 80 and 200 ppb, respectively [6, 7] and, as in the case of gold, determination of these elements by flameless

a.a.s. can be interesting. Actually, cadmium has been determined by this technique after extraction of the iodocadmate complex into a secondary amine (Amberlite LA-2) [8]. The present paper reports a scheme for the simultaneous determination of gold, silver and cadmium and its application to the analysis of rocks.

EXPERIMENTAL

Reagents and equipment

Stock solutions (10 000 ppm) of gold, silver and cadmium were prepared by dissolving 1 g of the metal in 100 ml of aqua regia (for gold), in 25 ml of concentrated nitric acid followed by dilution to 100 ml with distilled water (for silver), or in 5 ml of concentrated hydrochloric acid followed by dilution to 100 ml with distilled water (for cadmium).

All reagents used were of analytical grade.

The ion-exchange resin Dowex 1-X8 (50-100 mesh) was used; the column of resin was 1 cm in diameter and 25 cm high.

A Pye-Unicam SP1900 atomic absorption spectrophotometer, equipped with a Pye-Unicam deuterium lamp, was used with a Pye-Unicam SP901 graphite electrothermal atomizer and a Pye-Unicam AR25 recorder.

Procedures

Sample dissolution. Solutions were prepared by a slight modification of the Abbey method [9]. Accurately weigh 2 g of the finely powdered rock (70 μm particle size). Then add 5 ml of concentrated nitric acid, 5 ml of concentrated hydrochloric acid, 5 ml of 70% perchloric acid and 15 ml of 40% hydrofluoric acid. Heat on a hotplate at about 120°C until dense vapors from decomposition of $HClO_4$ appear. Add 5 ml of distilled water and evaporate to dryness. To the residue, add 5 ml of concentrated hydrochloric acid and evaporate to dryness again. Add 30 ml of 0.5 M HCl and swirl, heating gently if necessary, to dissolve the residue completely.

Ion-exchange separation of Au, Ag and Cd. First saturate the anion exchanger (Cl^--form) with 0.5 M HCl. Pass the sample solution through the column at a rate of 1 ml min^{-1}, and wash the column with 60 ml of 0.5 M HCl.

Pass 2 M ammonia solution through the column at a rate of 1 ml min^{-1} and collect the first 50 ml of eluate in a flask. Evaporate this solution to dryness on a hotplate; moisten the residue with concentrated nitric acid and heat at 175°C on a hotplate for 1 h. Dissolve the residue in 5 ml of HNO_3—HCl reagent (5 ml of aqua regia diluted to 100 ml with distilled water). This solution is ready for injection.

Instrumental determination. Construct calibration graphs by injecting 50 μl of pure solutions with concentrations in the ranges: 1—10 ppb for Au, 5—150 ppb for Ag and 20—500 ppb for Cd. Instrumental conditions are as follows: dry the injected aliquot at 110°C for 60 s; ash the residues at 1000°C (Au), 750°C (Ag) and 550°C (Cd) for 40 s. For the atomization step, heat

at 2250°C for 9 s for gold, at 2050°C for 6 s for silver and at 2150°C for 6 s for cadmium. Clean the tube and establish the tube blank at 2500°C for 9.9 s in all cases. Argon is used as purge gas at a constant flow of 1 l min^{-1}.

RESULTS AND DISCUSSION

Fire-assay methods were not considered for dissolution of the samples because they are unsuitable for dissolving gold coordinated in silicate lattices. The slightly modified Abbey method was preferred because it produces complete decomposition of most of the common mineral-containing rocks. Concentrated hydrochloric acid was added to the acid mixture to assist dissolution of gold metal present as colloidal microdrops in silicate rocks [1].

Anion-exchange separation of gold from major elements

After the attack, the solid residue was dissolved in 0.5 M HCl. Strong fixation of some elements as their chloride complexes (Au(III), Ag(I), Cd(II), Pb(II), Ir(IV), Zn(II) partially, etc.) was expected when this solution was passed through the anion exchanger (chloride form), whereas none of the major elements in common silicate rocks should be retained [10]. This point was confirmed experimentally with different rock samples [5].

The chloroaurate complex has been eluted from strongly basic resins with thiourea [11]. This method was unsatisfactory for the present purpose, because complete elution of gold required a large volume of eluent, and the presence of thiourea in the solutions affected the instrumental determinations. High concentrations of the eluents are normally required, hence it is desirable that these reagents should be easily eliminated. Direct injection of concentrated eluates on the graphite tube produced atypical absorption for which the background correction was ineffective.

Ammonia was shown to be a very efficient eluent not only for gold but also for Ag and Cd from this resin. These elements form ammine complexes [12] and can be eluted; in the case of gold, displacement of the $AuCl_4^-$ complex is also possible. Figure 1 shows that the chloride complexes of Au, Ag and Cd were eluted in a small volume of eluate. Amounts below 2.5 mg of each element were quantitatively recovered from the resin in an eluate volume below 35 ml. This solution is not suitable for injection into the graphite tube because abnormally high signals are caused by the NH_4Cl smokes produced in the atomization step. Fortunately, NH_4Cl can be easily eliminated from the solutions by heating. The presence of NH_4NO_3 was preferred because of its lower volatilization temperature; accordingly, the residue obtained after evaporation of the eluate to dryness was moistened with concentrated nitric acid and evaporated to dryness again.

Instrumental determination

The test solutions contained only a small amount of solid matter (below 0.03%), which greatly simplified instrumental determinations because

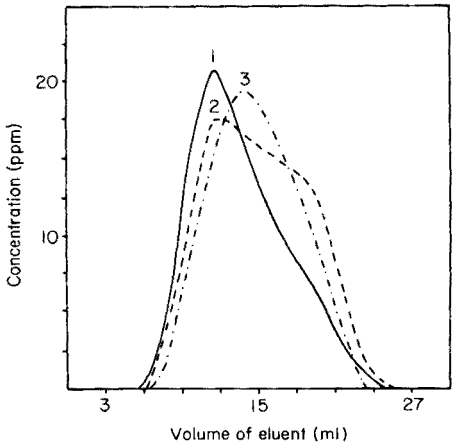

Fig. 1. Elution of Au, Cd and Ag from Dowex 1-X8 resin with 2 M NH_3 solution. (1) Au; (2) Ag; (3) Cd.

atypical absorptions did not occur. Silver and cadmium from the sample accompanied gold quantitatively in this solution. Of the other common components of silicate rocks, only a small percentage of zinc was also present. In this simple matrix interelement interferences were not observed and it was therefore possible to use calibration graphs prepared with pure chemical reagents. Instrumental parameters could also be determined on the electrothermal atomizer by using pure solutions, so that careful elimination of matrix by selective volatilization was avoided.

Detection limits, reproducibility and accuracy

Under the specified conditions, the detection limits, for a 1-g sample, were 0.2, 0.05 and 0.03 ppb for Au, Ag and Cd, respectively.

Reproducibility was determined by injecting 10 aliquots of each solution containing 10 ppb Au, 100 ppb Ag or 250 ppb Cd. Standard deviations were 0.8, 4 and 6.7 ppb for Au, Ag and Cd, respectively, the relative standard deviations being 8% for Au, 4% for Ag and 2.7% for Cd.

Accuracy was checked by determination of Au, Ag and Cd in the two standard rocks available (Table 1).

TABLE 1

Analysis of standard rocks
(Each result is the average of 8 analyses. Results are given in ppb.)

Rock	Au		Ag		Cd	
	Found	Rec.	Found	Rec.	Found	Rec.
GS-P1	1.9	1.6	98	100	72	60
PCC-1	1.6	1.6	4	5	105	100

REFERENCES

1 A. R. De Grazia and L. Haskin, Geochim. Cosmochim. Acta, 28 (1964) 559.
2 G. P. Sighinolfi and A. M. Santos, Mikrochim. Acta (Wien), (1976) 33.
3 G. P. Sighinolfi, At. Absorpt. Newsl., 12 (1973) 136.
4 M. J. Dudas, At. Absorpt. Newsl., 13 (1974) 67, 109.
5 C. Polo Polo, Thesis, Univ. Salamanca (Spain), 1977.
6 H. Hamaguchi and P. Kuroda, Geochim. Cosmochim. Acta 17 (1959) 44.
7 P. G. Jeffery, Chemical Methods of Rock Analysis, 2nd edn., Pergamon Press, Oxford, 1975.
8 G. P. Sighinolfi and A. M. Santos, Mikrochim. Acta (Wien), (1976) 477.
9 S. Abbey, Geol. Surv. Can., Paper 71-50 (1972).
10 K. A. Kraus and F. Nelson, Symposium on Ion Exchange and Chromatography in Analytical Chemistry, ASTM No. 195, Philadephia (1958).
11 R. K. Preobrazhensky and L. L. Moskivin, Radiokhimiya, 3 (1961) 309.
12 L. G. Sillen and A. E. Martell, Stability Constants of Metal-ion Complexes, The Chemical Society, London, 1964.
13 S. J. Flanagan, Geochim. Cosmochim. Acta, 37 (1973) 1189.

Analytica Chimica Acta, 94 (1977) 289—296

REPETITIVE DETERMINATIONS OF IRON(III) IN CLOSED FLOW-THROUGH SYSTEMS BY SERIES REACTIONS

V. V. S. ESWARA DUTT[§], DANIEL SCHEELER, and HORACIO A. MOTTOLA*

Department of Chemistry, Oklahoma State University, Stillwater, Oklahoma 74074 (U.S.A.)

(Received 5th May 1977)

SUMMARY

The determination of iron(III) with thiocyanate by means of sample injection into a chamber in a closed loop system of circulating reagent is described. Restitution of the absorbance to baseline by ligand exchange and by a redox process in the presence of iodide is discussed, together with some kinetic aspects of the decolorization reaction responsible for the return to the baseline. The iron content of the samples is deduced from the height of the generated transient signal, which is directly proportional to the iron(III) content. As many as 350 determinations/h can be processed when ligand exchange is used and 120/h when iodide is used for baseline restitution. Sample injection techniques of this type are particularly useful in industrial processes and quality control, and environmental monitoring, since they result in a decrease in operating cost and time.

Present trends in continuous-flow analyses focus on techniques based on sample injection into unsegmented streaming reagents [1, 2]. This is largely the result of attempts to meet the challenges of automation whereby, at low cost, a large number of samples can be processed with acceptable precision and accuracy, making statistical treatment of data meaningful. These attempts are particularly relevant to industrial process and quality control, to environmental monitoring, and to all situations in which large numbers of samples of similar nature have to be processed for the determination of a single species. In these situations, the use of pre-calculated concentrations of reagents for each sample increases the operating cost and time. The use of closed flow-through systems, such as that described by Bergmeyer and Hagen [3], which affords recirculation of the same reaction mixture for repetitive determinations greatly minimizes this problem. A chemical species commonly determined in industrial samples (e.g., non-ferrous metals and alloys, industrial waters, etc.) is iron, and this determination is used here to illustrate the principles of the method.

Many reagents are available for the determination of iron [4—8]; many of them are superior to thiocyanate but this reagent is still widely used because it provides a simple and rapid method, which can be employed in

§ Present address: Department of Health Science and Human Ecology, California State College at San Bernardino, California 92407, U.S.A.

strongly acidic medium, has few limitations, and requires inexpensive reagents. In view of the continuing popularity of thiocyanate as a chromogenic reagent for the direct determination of iron(III), and for that of total iron after adequate oxidation, conditions have been developed for its adaptation to determinations (repetitive) by sample injection in closed-loop flow systems. This type of determination produces transient signals generated and measured in a single reaction chamber by competitive reactions or by a chemical reaction and the competitive imposed flow. It offers several advantages over more conventional determinations with continuous-flow chemical analyzers. The experimental setup is very simple; it consists of a reaction chamber into which the sample is injected and a recirculation loop with a reservoir where the reagent is regenerated. The advantages of the system, which have been described recently [1, 2, 9] are: elimination of air segmentation, shorter manifolds, simpler apparatus, and more determinations per unit time. The ancillary advantages of main reagent (or background solution) recirculation and regeneration are easily achieved in procedures based on sample injection into flow systems [10]. In colorimetric determinations, successive sample injection with reagent recirculation can sometimes ignore the accumulation of colored product by taking advantage of dilution artefacts [11]; in other cases interplay of chemical reactions may regenerate the main reagent and eliminate baseline shift due to colored product accumulation [12]. In the work reported here, repetitive determinations of iron(III) with thiocyanate by sample injection and reagent recirculation, exploit the adjustment of the rates of two competitive chemical reactions to attain baseline restitution [9].

EXPERIMENTAL

Apparatus

The flow-through cell, reagent recirculation loop, and modular photometric unit used have already been described in detail [9—13]. The system used was essentially the same as that shown in ref. 9.

Reagents and solutions

All reagents used were of analytical-reagent grade. An iron(III) stock solution was prepared from iron(III) ammonium sulfate and 0.20 M hydrochloric acid. Working samples of iron(III) were prepared daily by diluting aliquots of this 0.100 M solution with 0.20 M hydrochloric acid.

Procedure

Typical aqueous reservoir solutions contained 0.20 M HCl, 0.27 M thiocyanate (as its sodium salt) and 0.10 M iodide (as its sodium salt) in a single mixture. This reservoir solution was circulated at a flow rate of 40.0 ml min^{-1}. Successive sample aliquots of 0.25 ml were then introduced into the detection zone by means of the injection system described earlier [11] and the peak height (absorbance) of the transient signal (monitored

at 480 nm) was recorded. The iron(III) concentration in the sample was deduced by reference to a calibration curve prepared from standards.

The flask containing the reservoir solution and the tubing transporting the solution were painted black to minimize photochemical effects.

RESULTS AND DISCUSSION

The determination of iron(III) with thiocyanate is based on the following reaction

$$Fe(H_2O)_6^{3+} + n\ SCN^- \rightleftharpoons [Fe(SCN)_n(H_2O)_{6-n}]^{3-n} + n\ H_2O \quad (1)$$

in which $n = 1.....6$, depending on the thiocyanate concentration. All the possible complexes are red and exhibit a bathochromic shift as the thiocyanate concentration increases [14]. Restitution of signal levels to baseline, under the optimum conditions reported for the formation of the iron(III)—thiocyanate complex(es) [4], was explored by using two approaches: (a) ligand substitution, i.e., use of an auxiliary ligand that displaces thiocyanate from the iron(III) complex; and (b) modification of one of the complex components by redox action so that the complex dissociates and/or decomposes.

Use of ligand substitution

Several ligands forming stable complexes with iron(III) were tested. Fluoride, oxalate, citrate, and nitrilotriacetate did not completely displace the iron from the thiocyanate complex. In the presence of these ligands a 50—80% loss of the "equilibrium" signal was observed as a result of preferential complexation of iron(III) with the auxiliary ligand. Phosphoric acid in high concentrations does displace the thiocyanate and can be used to generate transient signals, but a 20—30% decrease of the "equilibrium" signal was observed. The high-viscosity of this acid when concentrated also hampers homogeneous mixing in the detection zone. Ethylenediamine-*N,N,N',N'*-tetraacetic acid, EDTA, displaces the thiocyanate, but its low solubility in acidic medium diminishes its usefulness as an auxiliary ligand for transient signal generation. EDTA can be used, however, in the form of a complex with a metal ion that forms a less stable complex than iron(III) does in the reaction medium. Of several such EDTA—metal complexes tested, only that of nickel(II) was found suitable for thus supplying thiocyanate and generation of a transient signal. Typical signal profiles in the presence of nickel—EDTA and in its absence are illustrated in Fig. 1. As can be seen in curve B of Fig. 1, complete restitution to baseline could not be achieved. Figure 2 illustrates the effect of thiocyanate on signal height and duration. Changes in acid concentration, thiocyanate concentration, metal ion concentration, and EDTA concentration did not cause a total return to baseline. A clear and direct explanation for this behavior is lacking, but since the same behavior is observed when the thiocyanate concentration is increased

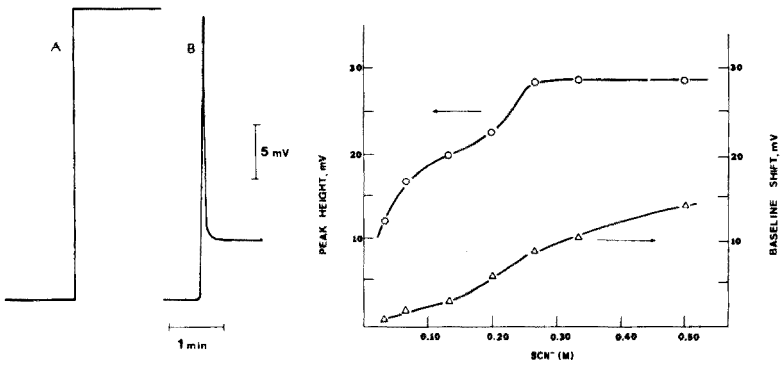

Fig. 1. Typical signal profiles in the presence and in the absence of the nickel(II)—EDTA complex. A: 0.20 M HCl, 0.27 M SCN^-. B: 0.20 M HCl, 0.27 M SCN^-, 0.03 M EDTA, 0.15 M Ni(II); 0.25 ml of 6.00×10^{-4} M iron(III) injected.

Fig. 2. Effect of thiocyanate concentration on signal height (○) and baseline shift (△). 0.20 M HCl, 0.030 M EDTA, 0.15 M Ni(II); 0.25 ml of 8.00×10^{-4} M iron(III) injected.

in the absence of the nickel—EDTA complex, the hysteresis may be ascribed to the presence of complexes with different stoichiometry, as discussed by Sandell [4]. Repetitive determinations of iron(III), in the range 0—1.0×10^3 M, could be carried out by use of a reservoir solution containing nickel—EDTA. A slight gradual increase in the baseline shift could not be avoided, however, with a single-beam instrument. The sampling rate under these conditions is highly satisfactory: 350 samples/h.

Modification by redox action

The large excess of thiocyanate necessarily present prevents the use of an oxidizing agent [e.g. Ce(IV)] for the "modification" of thiocyanate in the complex. Reducing agents such as hydroxylamine or hydrazine are not capable of reducing the iron(III) in the complex. The catalytic effect of iodide ions on the oxidation of thiocyanate by iron(III) reported by Iwasaki et al. [15] was tested as a way of inducing dissociation of the iron(III)—thiocyanate complex. For this purpose, of course, the concentration of iodide must be several orders of magnitude higher than that used in catalytic procedures for iodide determination. The effect of iodide concentration on the signal height (typical signals are shown in Fig. 3) and signal duration is illustrated in Fig. 4. From an analytical standpoint, a signal with the shortest duration and minimal signal loss is desirable; thus a concentration of 0.10 M iodide was chosen for further studies. In contrast to nickel—EDTA, iodide permits return to the original baseline.

Effect of hydrochloric acid and thiocyanate

Variation of HCl concentration between 0.05 and 1.0 M has negligible effect on both signal duration and signal height. A concentration of 0.2 M HCl

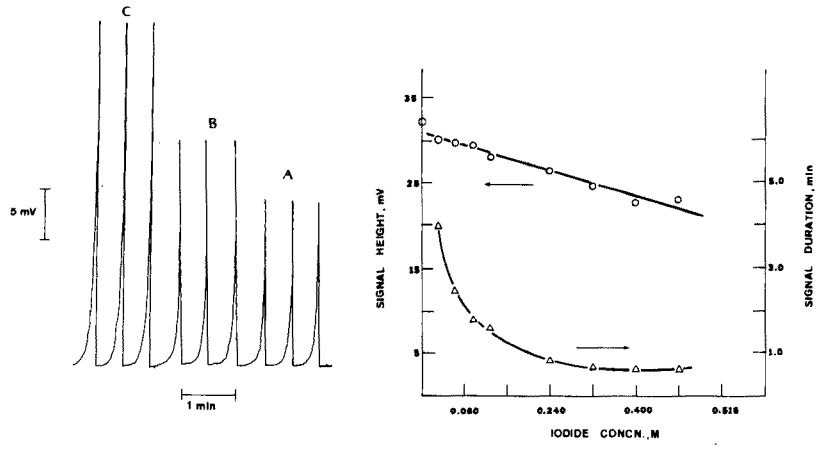

Fig. 3. Typical signal profiles for the determination of iron(III). 0.20 M HCl, 0.10 M I^-, 0.27 M SCN^-; flow rate 40 ml min^{-1}. A: 4.00×10^{-4} M Fe(III); B: 6.00×10^{-4} M Fe(III); C: 1.00×10^{-3} M Fe(III).

Fig. 4. Effect of iodide concentration on signal height (○) and signal duration (△). (Experimental conditions as in curve B, Fig. 3).

is considered convenient for iron(III) determination. The signal height sharply increases as the thiocyanate concentration is increased from 0.025 to 0.25 M. Further increase of thiocyanate from 0.25 to 0.50 M has a negligible effect on signal height. Signal duration is practically unaffected in the entire concentration range tested (0.025—0.50 M thiocyanate). Return to the baseline, however, is impaired as the thiocyanate concentration increases. A concentration of 0.27 M thiocyanate appears optimum for the iron(III) determination.

Effect of flow-rate

The reservoir solution must be kept in continuous circulation through the flow-cell and in a closed loop to allow fresh reagent solution to enter the reaction zone constantly. This helps to maintain constant distribution of products (removed from the detection zone) in the reservoir vessel. The effect of flow rate on the signal height and on its duration is illustrated in Fig. 5. A flow rate of 40 ml min^{-1} was chosen as it provides minimal signal loss and short signal duration.

Working curve, sampling rate, and reservoir capacity

Some typical signal profiles obtained with different concentrations of iron(III) are shown in Fig. 3. The working curve is linear over the range 10^{-4}–10^{-3} M iron(III). Above this concentration negative deviation occurs, probably because of a limiting local concentration of thiocyanate in the reaction (detection) zone. The relative standard deviation for 30 replicates

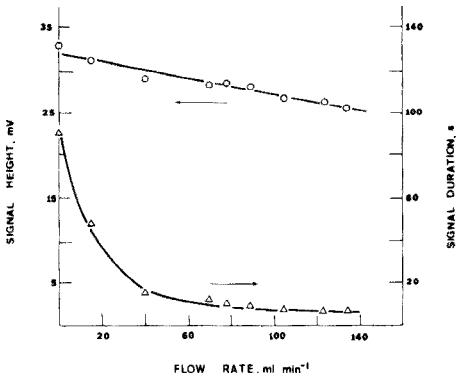

Fig. 5. Effect of flow rate on signal height (○) and signal duration (△). (Experimental conditions as in curve B, Fig. 3).

(0.25-ml aliquots of 7.90×10^{-4} M iron(III)) was found to be 2.2%. The calibration graph does not pass through the origin because of the blank absorbance contribution which results from a difference in the refractive indices of sample medium and reagent medium.

The selection of total reservoir volume is dictated by the number of samples to be processed and their approximate iron content. With a reservoir volume of 200 ml and a solution as described under Procedure, about 150 samples containing 7.9×10^{-4} M iron(III) (in 0.25-ml aliquots) could be processed with less than 5% signal loss in the 150th injection. A time interval of 30 s between successive injections is needed; this allows sample analysis at the rate of 120 samples per hour. A net signal loss of 16% results from the combined effects of iodide and flow rate, as compared to the signal obtained in absence of iodide and at zero flow rate.

Effect of acetone and dioxane

Lowering of the dielectric constant of the medium increases the color intensity of the iron(III)—thiocyanate complex(es) [4]. This results from a repression of the dissociation of the complex(es) as well as from a change of solvation species. A 60% signal increase was observed when the reaction medium contained 50% acetone. The time for return to baseline, however, was doubled and the increased sensitivity was traded for a smaller rate for analyses. The effect of dioxane was similar.

Some kinetic aspects relevant to the return to baseline

As stated above, the predominant species making up the iron(III)—thiocyanate complex depends on the overall thiocyanate concentration [4]. Rather wide variations can be seen in the reported values for the stepwise formation constants of the several complexes. On the basis of rounded values, the species $[Fe(SCN)]^{2+}$ predominates below $[SCN^-] = 0.032$ M at zero ionic strength and below 0.056 M at ionic strengths between 1 and 2.

Thence up to $[SCN^-] = 1.0$ M, the predominant species is $[Fe(SCN)_2]^+$ with its maximum value (roughly 75% of the species in solution) appearing at about $[SCN^-] = 0.10$. Above $[SCN^-] = 0.10$ M, the species $[Fe(SCN)_3]$ and $[Fe(SCN)_4]^-$ start to predominate and only negatively charged complexes seem to exist in solutions in which $[SCN^-] > 0.20$ M. The thiocyanate concentration in this work (0.27 M) should insure the predominance of negatively charged complexes, probably $[Fe(SCN)_4]^-$.

Kinetic information for the formation of $[Fe(SCN)]^{2+}$ is available [16, 17]. Yatsimirskii et al. [18] have reported studies of the kinetics of the iodide-catalyzed reaction in the presence of excess of iron, nitrite and substoichiometric concentrations of iodide. The catalytic effect of iodide in such a case is attributed to its participation in lowering the activation energy for the rate-controlling step of the following overall redox reaction: $2\ Fe(H_2O)_6^{3+} + 2\ SCN^- = 2\ Fe(H_2O)_6^{2+} + (SCN)_2$. Kinetic information for reactions in the presence of excess of thiocyanate, however, does not appear to be available. A study of the rate of formation of the colored specie(s) was not possible under the experimental conditions reported here. For all practical purposes, the reaction is completed in less than 20 ms, the approximate mixing time in the forced-flow mixing device. Figure 6 shows that, for the decolorization reaction in substantial excess of thiocyanate, the rate is second order with respect to the colored complex concentration, within the first minute after mixing. The reaction follows an apparently first-order dependence on iodide concentration. Extrapolation of the linear segments in Fig. 6 to zero reaction time should give the reciprocal of the initial absorbance; but as Fig. 6 shows, this is not the case, so that perhaps a

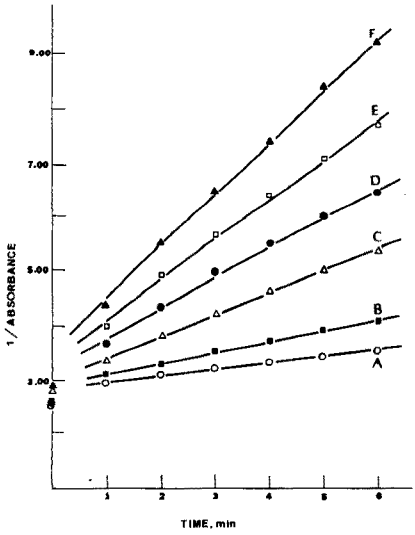

Fig. 6. Second-order plots for the decolorization of the iron(III)—thiocyanate complex(es). 0.20 M HCl, 0.27 M SCN^-, 8.33×10^{-5} M Fe(III), zero flow rate. Iodide concentration: A, 0.0025 M; B, 0.0050 M; C, 0.0100 M; D, 0.0150 M; E, 0.0200 M; F, 0.0250 M.

different mechanism takes over during the first minute after mixing. The dissociation rate in the absence of iodide is negligible during the first 10 min of reaction.

This work was supported by a National Science Foundation Grant (CHE 76-03739).

REFERENCES

1 J. Růžička and E. H. Hansen, Anal. Chim. Acta, 78 (1975) 145.
2 K. K. Stewart, G. R. Beecher, and P. E. Hare, Anal. Biochem., 70 (1976) 167.
3 H. V. Bergmeyer and A. Hagen, Fresenius' Z. Anal. Chem., 261 (1972) 333.
4 E. B. Sandell, Colorimetric Determination of Traces of Metals, 3rd edn., Interscience, 1959, Chapter XXII, New York, N.Y.
5 H. Diehl and G. F. Smith, The Iron Reagents: Bathophenanthroline, Bathophenanthroline-disulfonic acid, 2,4,6-Tripyridyl-S-triazine, Phenyl 2-pyridyl ketoxime, G. F. Smith Chemical Co., Columbus, Ohio, 2nd edn., 1965.
6 L. L. Stookey, Anal. Chem., 42 (1970) 779.
7 A. A. Schilt, C. D. Chriswell, and T. A. Fang, Talanta, 21 (1974) 831.
8 E. Kiss, Anal. Chim. Acta, 72 (1974) 127.
9 V. V. S. Eswara Dutt and H. A. Mottola, Anal. Chem., 49 (1977) 776.
10 V. V. S. Eswara Dutt and H. A. Mottola, Anal. Chem., 47 (1975) 357.
11 V. V. S. Eswara Dutt, A. Eskander-Hanna, and H. A. Mottola, Anal. Chem., 48 (1976) 1207.
12 V. V. S. Eswara Dutt and H. A. Mottola, Anal. Chem., 49 (1977) 319.
13 E. W. Chlapowski and H. A. Mottola, Anal. Chim. Acta, 76 (1975) 319.
14 T. C. J. Ovenston and C. A. Parker, Anal. Chim. Acta, 3 (1949) 277.
15 J. Iwasaki, S. Utsumi, and T. Ozawa, Bull. Chem. Soc. Jpn., 26 (1953) 108.
16 J. F. Below, Jr., R. E. Connick, and C. P. Coppel, J. Am. Chem. Soc., 80 (1958) 2961.
17 D. Seewald and N. Sutin, Inorg. Chem., 2 (1963) 643.
18 K. B. Yatsimirskii, L. I. Budarin, N. A. Blagoveshchenskaya, R. V. Smirnova, A. P. Fedorova, and V. K. Yatsimirskii, Zh. Anal. Khim., 18 (1963) 103.

Analytica Chimica Acta, 94 (1977) 297—305

SIMULTANEOUS DETERMINATION OF ARSENIC, GERMANIUM, AND ANTIMONY BY GAS CHROMATOGRAPHY AFTER HYDRIDE GENERATION

R. K. SKOGERBOE and A. P. BEJMUK

Department of Chemistry, Colorado State University, Fort Collins, Colorado 80523 (U.S.A.)

(Received 31st May 1977)

SUMMARY

A method is described for the simultaneous gas chromatographic determination of arsenic, germanium and antimony. The approach is based on conversion of the elements to their hydrides, collection of these via a semi-selective trapping procedure, desorption from the trap, and delivery to a gas chromatograph for separation and determination. Detection limits, based on the analysis of 100-ml natural water samples, are 1, 0.3, and 10 $\mu g\ l^{-1}$ for As, Ge, and Sb, respectively. Recovery studies indicate that the relatively simple method yields precise and accurate results.

The determination of As, Se, Sb and other similar elements by generation of hydrides and subsequent measurement by atomic absorption spectrometry has become a widely used approach [1—6]. While such methods have proved capable of solving numerous analytical problems involving these elements, the use of atomic absorption as the measurement tool essentially limits analyses to the determination of one element at a time. The possibility of determining simultaneously more than one element per sample offers obvious economic as well as analytical advantages. This factor, coupled with reports that the hydrides of As, Ge, Si, P and S can be effectively separated by gas chromatography [7, 8], suggested that the hydride generation approach might be combined with gas chromatography for simultaneous determination. This report summarizes the results of an evaluation of this possibility.

It has been shown that As, Ge, and Sb can be removed from aqueous samples via hydride generation and reliably determined by gas chromatography with a thermal conductivity detector. Attempts to determine selenium have not been successful.

EXPERIMENTAL

Apparatus

The hydride generation, trapping and chromatograph interface system is shown schematically in Fig. 1. The 200-ml generation vessel is equipped with a dosing stopcock to permit the addition of sodium borohydride pellets

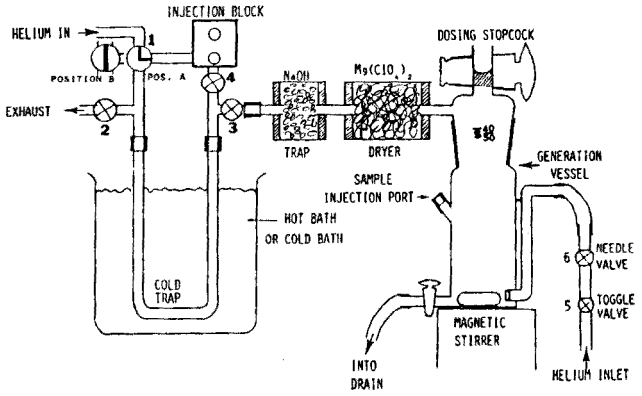

Fig. 1. Schematic diagram of hydride generation and trapping system.

without opening to the atmosphere, a gas dispersion inlet, a silicone rubber septum through which samples may be introduced, and a drain for sample removal. Gases leaving this vessel pass through drying traps to remove water, nitrous oxide, carbon dioxide, and sulfur dioxide. They subsequently enter a cryosorption trap packed with ca. 15 cm of 60-80 mesh silica gel and immersed in a dry ice—acetone bath. This trap is connected to the g.c. inlet via a gas manifold system. The gas chromatograph (Hewlett-Packard, Model 5750) was equipped with flame ionization and thermal conductivity detectors and was coupled to a 1-mV recorder (Hewlett-Packard, Model 7127A). The column was packed with 80-100 mesh silica gel (2.5 mm i.d. × 2.1 m) and maintained at 45°C with a helium flow of 20 ml min^{-1}. The injection port, detector, and auxiliary heaters were turned off and the detector bridge current was held at 300 mA.

Reagents

All reagents used were A.R. or spectroscopic grade. Sodium borohydride pellets (8 mm) were used for hydride generation when added to solutions preserved with H_2SO_4 at pH 2.0—2.1. Stock solutions (100 μg ml^{-1}) of the elements were prepared from oxides; subsequent dilutions of these were used to prepare standards of appropriate concentrations while maintaining the pH. Water samples were filtered through 0.45-μm filters and preserved with H_2SO_4 at pH 2.0.

Procedure

For analysis, the trap was immersed in the cold bath, valves 1 and 4 (Fig. 1) were set to maintain a constant helium flow of 20 ml min^{-1} to the column, valves 2 and 3 were opened so that the flow from the generation vessel passed through the trap to the exhaust, and valves 5 and 6 were set to pass a helium flow of 290 ml min^{-1} through the generation vessel. An appropriate sample volume, e.g. 100 ml, was introduced and two sodium borohydride

pellets were added through the dosing stopcock. Generation was allowed to continue for 5 min, after which valve 5 was closed, followed by valves 2 and 3 to isolate the trap. Valve 4 was opened and valve 1 was switched to divert the 20 ml min^{-1} helium flow through the trap and thence the column. The cold bath was replaced with a hot oil bath (140°C) to desorb the trapped hydrides. While the chromatogram was recorded, the generation vessel was drained, rinsed, and recharged for the next analysis.

RESULTS AND DISCUSSION

The use of a chemical reactor to form volatile entities for separation, as an integral part of the gas chromatographic system, may be regarded as one form of analytical reaction chromatography [9]. The optimal use of such a system requires that certain criteria be satisfied. An ideal reaction g.c. method would involve a chemical reaction which converts, instantaneously and completely, the species to be analyzed to compounds which can be efficiently separated on a chromatographic column. If the volatiles to be separated are to be delivered directly from the reactor to the chromatograph, the delivery must be rapid enough that neither the resolution nor the detection sensitivity are seriously affected. This is the first criterion.

The chemical reaction(s) used should also be such that they do not simultaneously produce other entities that can affect the separation or cause interferences of any type. Clearly, the selection of a reaction system that is applicable to all analytes of interest but not to any other entities present in the samples is not a trivial task.

Other criteria may be considered secondary. A suitable column material must be available. The volatiles should be stable at least over the time period required for analysis or they should undergo reproducible decomposition(s) to stable, separable species. The eluted compounds should be detectable by one or more g.c. detectors. Finally, the analytical reactions and the chromatographic procedures should be applicable to a wide variety of sample types.

Hydride generation

As indicated above, the conversion of the semi-metals to hydrides has often been used for separation and preconcentration purposes. A wide range of reaction media has been used. The recent uses of hydride generation to deliver elements such as arsenic and selenium to an atomic absorption measurement system appear to have led to improved conversion reactions. Since many investigators have indicated that the conversions and deliveries can be completed in less than 1 s, some recently recommended reaction approaches were examined.

Early hydride generation studies relied on a method described by Pollock and West [1]. Addition of $TiCl_3$ and magnesium to an acidic solution was the basis of $H^{\cdot}$ generation for hydride formation while the excess of hydrogen

produced purged the hydrides from the reaction medium. The present work demonstrates that complete conversions can be obtained, but that several minutes are required. In an attempt to reduce this time limitation, the procedure of collecting the evolved gases in a balloon followed by rapid expansion into the analytical measurement system [1, 8] was evaluated. Three general problems were encountered. First, the copious amounts of hydrogen effectively dilute the hydrides, and would be likely to affect the column separation. Secondly, moisture was also collected in the balloon and caused some decomposition of hydrides as reported by Devyatykh et al. [7]. Finally, it was noted that losses of arsine occurred even in the absence of moisture. This was observed with two different types of latex (balloon) material, and was probably caused by diffusion through the latex. This approach was therefore abandoned.

Subsequent efforts concentrated on the use of sodium borohydride as the reactant [1, 3—6]. This reagent could be added as a solid to the sample solution to form hydrides rapidly and efficiently. The reaction was 5—8 times faster than that with $TiCl_3$—Mg. The vessel shown in Fig. 1 was designed for carrying out the reaction. The device permits sample injection through the rubber septum while the $NaBH_4$ pellets are added through the dosing stopcock. Carrier gas (e.g. helium) may be introduced through a porous frit as a means of increasing and controlling the hydride removal rate. Initial experiments with this system coupled directly to a gas chromatograph indicated three problems. The gases evolved were essentially saturated with water. This was deleterious to the chromatographic column and the separation, and caused some hydride decomposition. A tube packed with magnesium perchlorate was consequently inserted to dry the gases; hydrides passed through the perchlorate quantitatively. The hydrogen evolved, however, was again found deleterious to both the separation and the detection processes. In addition, the generation reaction could not be completed in the short time required for optimal separation without using conditions that caused extreme rates of hydrogen generation. It was therefore necessary to devise a procedure for selectively trapping the hydrides. Because the trap functioned as an integral part of the generation system and its function was influenced by generating conditions, the two processes will be discussed jointly.

Hydride generation and trapping

The incorporation of a trap permitted the use of less rigorous (slower) reaction conditions where the hydrogen generation rate was lower. Under these conditions, the hydride residence times in contact with water were longer, so that decomposition might occur. Consequently, a carrier gas was used to remove the hydrides rapidly from the generation vessel.

Initial attempts to trap arsine relied on the use of a cold trap immersed in liquid nitrogen. Although the freezing point of arsine (—113.5°C) is above the temperature of liquid nitrogen (—195.8°C), trapping was highly inefficient.

Packing the trap with glass beads (2—3 mm diameter) to increase the cold surface was also unsuccessful. It was concluded that even low flow velocities through the trap were too rapid to permit adequate cooling and condensation.

A cryosorption trapping system with silica gel (60-80 mesh) was investigated, because this material was shown to be an effective column packing for hydride separation. Initial experiments with this cryosorption system at liquid nitrogen temperatures indicated low levels of collection efficiency but later studies with a dry ice—acetone coolant indicated quantitative removal. This suggests that the adsorption sites on the silica gel are "inactivated" at the lower temperatures. The experiments also indicated that hydrogen was inefficiently trapped at the dry ice—acetone temperature while quantitative results were obtained for As, Ge, and Sb. The trap design used is shown in Fig. 1. The valves are arranged to permit the operational sequence summarized in the Procedure. The following paragraphs reflect the interdependencies of the various segments of the reaction g.c. system.

Since hydride formation depends on reactions involving the hydrogen radical, the effects of pH on the generation-trapping processes were investigated. The results summarized for As and Ge in Fig. 2 indicate that low pH values are required for optimization. The occurrence of an optimum pH may be explained at least semi-quantitatively. The cryosorption trap functions essentially as a small chromatographic column; hydrides are sorbed on it and pass through it at rates dependent on gas flow conditions as well as their individual properties. Thus, at high pH values, the generation period is longer and the combined flow rate of carrier gas and the hydrogen produced is lower so that the rate of removal of the hydride from the generation vessel is slow. Under these conditions, the hydrides are probably distributed over a larger length of the trap because of their slower delivery rate, and the chromatographic effect occurs even at these low temperatures. During the desorption-removal process, the hydrides are delivered to the g.c. column at rates determined by their distributions in the trap. This affects the width and height of their chromatographic peaks. Although the peak areas were nearly constant over the 1.9—2.4 pH range, the lower resolution at higher pH values dictated the choice of peak height as the best indicator of optimum conditions. At the lower pH values, the helium plus hydrogen flow rate and the hydride generation rate were very rapid. The drop in peak height is apparently due to the fact that fractions of the hydrides are "chromatographed" through the trap causing peak broadening under these conditions. Thus, subsequent measurements were based on adjustment of the pH to the optimal range of 2.0—2.1.

Further verification of the trap efficiency—chromatographic effect can be obtained from Fig. 3. The pH was held constant at 2.0 and the helium purge rate was 290 ml min^{-1} for an examination of the effect of "trapping" time. Again the rise in peak height with trapping time was observed and it was noted that peak widths were greater for shorter times. Since generation and removal to the trap were accomplished in less than 1 min, this verifies the

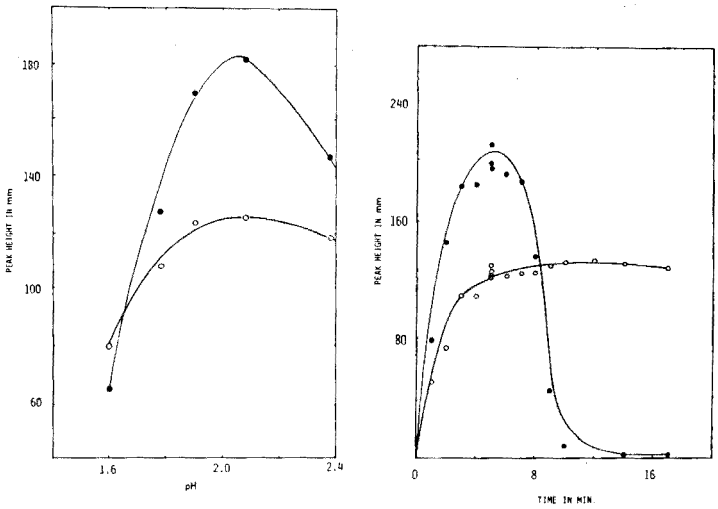

Fig. 2. Dependence of the generation—trapping efficiency on pH. He flow rate, 290 ml min^{-1}; • GeH_4, ○ AsH_3.

Fig. 3. Dependence of hydride recovery on generation (trapping) time. He flow rate, 290 ml min^{-1}; • GeH_4, ○ AsH_3.

"spreading" effect postulated above. Longer collection times resulted in loss of germanium hydride from the trap, since it is eluted from the silica gel trap/column earlier than arsine. A subsequent series of measurements used a lower helium purge rate (40 ml min^{-1}) and indicated that losses of As or Ge could be avoided at lower carrier gas flows even though relatively long generation-trapping times were used. Subsequent measurements used a 5-min time period at the 290 ml min^{-1} helium flow rate (see Fig. 3).

Desorption

Although it was shown that the cryosorbed hydrides could be eluted from the trap at the collection temperature, the slow removal rate adversely affected the column separation. Thus, desorption at higher temperatures was investigated. A hot oil bath was used. Figure 4 shows that desorption was complete above 140°C. Although higher temperatures were investigated, evidence for thermal decomposition was not noted for arsine or germanium hydride.

Column separation

Both alumina and silica gel columns were investigated. The hydrides were not eluted from alumina columns, but good separations were achieved with silica gel. Temperature and flow rate experiments indicated the optimum helium flow to be 20 ml min^{-1}, while a temperature of 10°C was best. However, increasing the column and/or the detector temperature resulted in nearly linear increases in the response of the thermal conductivity detector

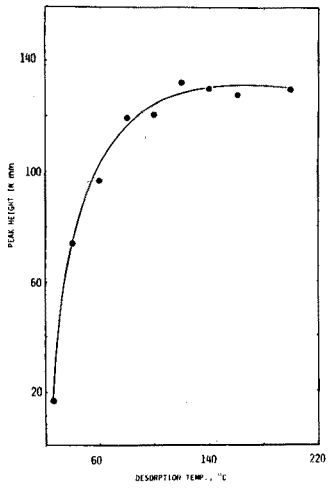

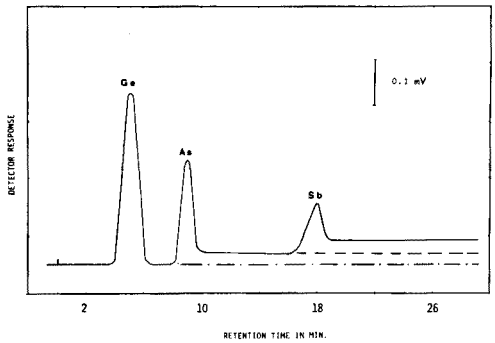

Fig. 4. Dependence of arsine desorption on trap temperature.

Fig. 5. Gas chromatogram of As, Ge, and Sb hydrides illustrating baseline shifts caused by thermal decomposition. Detector block temperature, 60°C; column temperature, 45°C.

for both arsenic and germanium. A chromatogram obtained at column and detector temperatures of 45 and 60°C, respectively, is shown in Fig. 5. This illustrates the separation capability and is indicative of the temperature-dependent problem that influenced the choice of the operational temperatures.

At detector temperatures above 50°C, considerable imbalance in the detector output occurred after elution of arsine and stibine. This baseline shift (Fig. 5) was in approximate proportion to the amount of hydride eluted and, once the shifts occurred, the baseline remained at that level for over 8 h. Examination of the detector filaments indicated the presence of a gray-white deposit, probably because of thermal decomposition of the hydrides with deposition on the filaments changing their effective thermal outputs. Thus, although higher detector temperatures produced an increase in the response, the detector was operated without heating to avoid this problem and a column temperature of 45°C was selected as a compromise between optimal separation and detector response.

Detectors

Thermal conductivity and flame ionization (f.i.d.) detectors were investigated. Arsine could not be detected with the f.i.d. even when 10 mg was introduced, probably because of the essentially instantaneous formation of stable oxides in the flame. Argon, nitrogen, and helium were investigated as carrier gases in conjunction with the thermal conductivity detector. The responses obtained with argon and nitrogen were nearly equivalent but more than five times lower than those obtained with helium. Thus, although

the thermal conductivities of the hydrides could not be found in the literature, their values differ most significantly from that of helium, making it the best choice as the carrier gas. Moreover, the response increase with temperature mentioned above probably reflects a divergence in the rates at which the hydride and helium thermal conductivities change with temperature.

Separation interferences

Studies in which nitric acid was used as the sample preservative indicated a large peak which obscured the arsine peak. This was due to the generation of N_2O during hydride formation. Subsequent analyses relied on the use of sulfuric acid as the preservative as recommended by EPA [2]. Although such usage eliminates excessive quantities of nitrogen which can cause the interference, many types of samples contain significant amounts of reducible nitrogen species. Under such circumstances, it was shown that the interference can be removed by placing an Ascarite or NaOH trap between the generator and the cryotrap. While such a trap does not remove the arsine or germanium hydride, it does cause decomposition of stibine. Stibine can be determined in the absence of the trap without the chromatographic interference.

Selenium

Studies involving selenium indicated that, although the hydride could be generated, it underwent rapid conversion to the oxide and/or the metal. Although a wide variety of experimental approaches and conditions were explored, none was found that prevented this problem. Efforts to determine selenium by this approach were consequently abandoned.

Analytical applicability

Analytical curves were determined for As, Ge, and Sb hydrides with 100-ml aliquots of standards. The results indicated that the curves were linear over 3—4 decades and were generally reproducible to ±5—10% (relative standard deviation) or better. Detection limits, defined as the concentration required to produce a signal twice the standard deviation of the baseline, were determined to be 1, 0.3, and 10 $\mu g\ l^{-1}$ for As, Ge, and Sb, respectively, based on 100-ml samples. Recovery studies were run on several natural water samples. These indicated that the recoveries obtained were consistently complete within experimental error over two decades of spike levels ranging from 3 to 300 $\mu g\ l^{-1}$.

In view of these results, the method described above can be used for the determination of As, Ge, and Sb on a simultaneous basis. The sensitivity, precision and accuracy are adequate for many analytical purposes. The method can clearly serve as an alternative, or a complement, to other means of analysis.

This research was funded (in part) by the U.S. Environmental Protection Agency, Duluth, Minnesota, Research Grant No. R-803950. The authors thank R. L. Munns for helpful advice.

REFERENCES

1 E. N. Pollock and S. J. West, At. Absorpt. Newsl., 12 (1973) 6.
2 Methods for Chemical Analysis of Water and Wastes, U.S. Environmental Protection Agency, Washington, D.C., 1974, p. 9.
3 F. J. Schmidt and J. L. Royer, Anal. Lett., 6 (1973) 17.
4 J. A. Fiorino, J. W. Jones and S. G. Capar, Anal. Chem., 48 (1976) 120.
5 K. C. Thompson and D. R. Thomerson, Analyst, 99 (1974) 595.
6 F. J. Fernandez, At. Absorpt. Newsl., 12 (1973) 93.
7 G. G. Devyatykh, A. D. Zorin, I. F. Frolov and I. V. Runovskaya, Works of Analytical Chemistry Commission of Academy of Science of U.S.S.R., XVI, 159 (1968) (in Russian).
8 K. W. Edwards and R. W. Klusman, Toxic Heavy Metals in Groundwater of a Portion of the Front Range Mineral Belt, Partial Completion Report, No. 67, Colorado School of Mines, Golden, Colorado, 1975.
9 V. G. Berezkin, Analytical Reaction Gas Chromatography, Plenum Press, New York, 1968.

Analytica Chimica Acta, 94 (1977) 307—315

EXTRACTION CHROMATOGRAPHY OF COPPER BY LIX-64N AND LIX-65N SUPPORTED ON THE MACROPOROUS RESIN, XAD-7

M. HEMMES and J. R. PARRISH*

Department of Chemistry, Rhodes University, Grahamstown (South Africa)

(Received 27th June 1977)

SUMMARY

The macroporous resin XAD-7 gives a fast rate of uptake of copper when used as a support for LIX-64N; it is superior to cellulose powder and other macroporous resins. The rate of uptake is satisfactory up to loadings of 60% (w/w), and the use of purified LIX-65N or the addition of LIX-63 gives no improvement in rate. The use of toluene as a diluent reduces the rate of extraction. Elution curves for copper show negligible tailing, and rapid separations of copper from other metals by selective absorption are demonstrated. Copper can be concentrated from very dilute solution at a flow rate of 50 ml min and a 99% recovery is obtained. The method has been applied to the rapid determination of copper in brass and bronze.

The separation of copper by extraction chromatography on cellulose powder treated with the commercial reagent, LIX-64, was studied by Cerrai and Ghersini [1]. They separated copper from five other metals, but the elution curve for copper showed considerable tailing, even at a flow rate of 1 ml min^{-1}. Fritz et al. [2] used Amberlite XAD-2 as a support for two aliphatic α-hydroxyoximes, which they had synthesized and used in preference to LIX-64, which they found to be impure. Copper was successfully separated from eighteen other metal ions at fast flow rates, but some tailing of copper was shown at a flow rate of 20 ml min^{-1}. It is not clear whether the improved results were caused by the use of a macroporous resin support or by the use of specially prepared hydroxyoximes.

The composition of the LIX extractants has been reviewed by Ashbrook [3], who purified them and separated the active isomers [4]. Methods for the synthesis of long-chain derivatives of salicylaldoxime, including 2-hydroxy-5-dodecylbenzophenoneoxime, the pure aromatic component of LIX-64, have been published [5]. Therefore the use of the commercially available LIX extractants for analytical separations of copper can be recommended. Warshawsky [6] pointed out the advantages of porous resins of high surface area as supports, and showed that XAD-7 had the highest "adsorption capacity" for LIX-64N of the XAD resins he investigated. A recent study [7] has shown that XAD-7 is the best support for the metal-chelating extractant, "Kelex 100". The effects of the properties of the support, the loading, and

the purification and dilution of the stationary liquid phase, have now been investigated for the LIX extractants.

EXPERIMENTAL

Extractants

LIX-64N (General Mills Inc.) was used as supplied, and also in purified form. The pure *anti* isomer of 2-hydroxy-5-nonylbenzophenoneoxime was obtained from LIX-64N by column chromatography on silica gel, but the method was slow, and the yield poor. Better results were obtained by precipitation of the copper chelate from alcoholic solution, a method previously used to separate the isomers of 2-hydroxy-5-t-octylbenzophenoneoxime [5]. An ethanolic solution of copper(II) acetate was heated under reflux with an excess of LIX-64N for 3 h. After standing overnight the precipitate was collected, washed with cold ethanol, and recrystallized from ethanol. The copper complex was decomposed by shaking a solution in carbon tetrachloride with 2 M hydrochloric acid. After washing and drying, the organic solvent was removed under reduced pressure, leaving the *anti* isomer as a yellow viscous liquid. This material produced a single spot on thin-layer chromatography; its mass spectrum showed a molecular ion at *m/e* 339, and its i.r., u.v., and n.m.r. spectra were in agreement with those published [8] for the pure *anti* isomer of LIX-65N. However, an additional peak was recorded in the u.v. spectrum at λ_{max} 211 nm, log ϵ_{max} 4.53. This wavelength is outside the range (225—350 nm) of the spectrum previously reported [8]. This pure *anti* isomer of 2-hydroxy-5-nonylbenzophenoneoxime will be referred to as "pure LIX-65N" whether obtained from LIX-64N or LIX-65N. LIX-65N was also used as supplied. This material reportedly [3] contained 39% of the *anti* isomer.

Supports

The Amberlite adsorbents, XAD-2, XAD-4, XAD-7, XAD-8 and XAD-11 (Rohm and Haas Co., Philadelphia, Pa.) were washed with ethanol to displace air from the pores and to remove residual monomers and solvents. They were then washed with water until the washings were free of chloride ions. The washed resins were dried at 110°C overnight before impregnation with a liquid ion-exchanger.

Since delays were experienced in obtaining fresh supplies of Amberlite XAD-7, a resin with very similar properties was made as follows. Azo-di-isobutyronitrile (0.1 g) was dissolved in ethyleneglycol dimethacrylate (25 ml) and amyl acetate (50 ml), and the mixture was suspended in a solution of gelatin (2.5 g) and sodium chloride (25 g) in water (250 ml). The flask (500 ml), fitted with a stirrer and reflux condenser, was heated to 60°C in a waterbath. The stirring rate was adjusted to give droplets of suitable size, and after 30 min the temperature was raised to 80—85°C and held there for 6 h. The resin beads were washed on a sieve with water, and then transferred to a sintered glass funnel. They were washed with acetone

and then alcohol, and were air-dried before the final sieving to 0.25—0.85-mm diameter. The water regain of this resin was 2.2, and when loaded with up to 60% (w/w) of a liquid ion-exchanger, its reaction rate and capacity were very close to those of similarly loaded XAD-7 resin.

Coating the supports

A known mass of the dry adsorbent in a round-bottomed flask was covered with a solution of the required amount of LIX extractant in heptane. The heptane was removed at room temperature on a rotary evaporator, and the temperature was then raised to 100°C. The coated resin was wetted before use by covering it with 1 M sodium hydroxide solution, and removing air from the pores by water-pump suction. It was then washed on a sintered glass filter with 1 M hydrochloric acid, water, acetate buffer (pH 5), and water, and was stored wet.

Measurements

Water regains of the coated resins were measured by blotting the wet resin between sheets of filter paper, weighing the blotted resin, and weighing the resin after drying at 110°C overnight.

Capacities were measured by equilibrating the wet resin (1.00 g) with 0.2 M copper sulphate solution (50 ml) and acetate buffer (15 ml). The pH of the buffer was adjusted, by mixing 1 M sodium acetate with 1 M hydrochloric acid, to give a final pH of 5.0 when added to the copper sulphate solution. After 24 h on a mechanical shaker at 20°C, the resin was filtered off and washed thoroughly with water. Absorbed copper was eluted with 2 M hydrochloric acid (50 ml), and was titrated with EDTA after adjustment to pH 5 with 4 M sodium hydroxide and with acetate buffer. Xylenol orange indicator was used in the presence of 1,10-phenanthroline.

As a practical measure of the exchange rates, the percentage attainment of equilibrium in 2 min by resins of particle diameter 0.25—0.85 mm (the $P_{2\,min}$ value) was determined. The capacity for copper was measured again, allowing only 2 min for contact with the copper sulphate solution, while the flask was shaken vigorously by hand. The capacity was expressed as a percentage of the equilibrium capacity.

Separations

The apparatus and procedure used for column separations have been described in detail elsewhere [9]. The separated metals were determined by titration with EDTA, or by atomic absorption spectrometry (a.a.s.) for the smaller amounts. The elution curves shown in Figs. 1 and 2 were obtained by the use of a commercial chromatographic column with a low dead volume (type LC-9MA; Laboratory Data Control, Florida). Fractions (2 ml) were collected and analysed by a.a.s. For the concentration of 10 μmol of copper from 1 l of solution, a column (9 × 30 mm) was used at a flow rate of 50 ml min^{-1}. The copper was recovered by elution with 2 M HCl (25 ml) at 10 ml min^{-1}.

Analysis of alloys

The alloy (0.2 g) was covered with a solution of tartaric acid (0.6 g) in water (3 ml). Concentrated nitric acid (3 ml) was then added. When dissolution was complete, the solution was diluted to 1 l, and a 25-ml aliquot was used for the separation of copper. Copper was eluted in the reverse direction with 25 ml of 2 M HCl, followed by 25 ml of water. After adjustment of the pH to 5, the copper was determined by titration with 0.01 M EDTA.

RESULTS AND DISCUSSION

Properties of the supports

The porosity, specific pore volume, specific surface area, and average pore diameter of each of the Amberlite adsorbents used in this work have been determined by the manufacturer [10]. These supports cover a wide range of physical properties, and range in polarity from the non-polar XAD-2 and XAD-4 (styrene—divinylbenzene copolymers), through XAD-7 and XAD-8 (acrylic ester polymers), to the polar XAD-11 (substituted acrylamide polymer). The more polar supports expand when the air in the pores is displaced by alcohol or water, and therefore the water regain is a more realistic property to measure than the pore volume of the dry support. Water regains of the uncoated supports have also been measured and are included in Table 1.

Rates of reaction

Since slow rates of diffusion of ions into and out of the solid phase can cause tailing, poor efficiency, and difficult elution in extraction chromatography,

TABLE 1

Comparison of macroporous resins loaded with LIX-64N

Water regain[a]	Resin	Loading (%)	$P_{2\,min}$ (%)	Water regain[b]	Capacity[c] (meq g^{-1})
0.70	XAD-2	10	44	0.44	0.16
0.70	XAD-2	60	20	0.51	0.68
1.10	XAD-4	10	44	0.27	0.01
1.10	XAD-4	60	34	0.63	0.68
2.16	XAD-7	10	82	1.96	0.31
2.16	XAD-7	50	73	1.42	0.58
2.16	XAD-7	60	72	1.43	0.62
1.36	XAD-8	10	53	0.72	0.16
1.36	XAD-8	60	53	0.79	0.62
1.44	XAD-11	10	57	0.84	0.19
1.44	XAD-11	60	42	0.70	0.61

[a]Water regain of bare support. [b]Water regain of coated support. [c]The capacity refers to the dry, loaded resin, and the $P_{2\,min}$ value is the percentage of the equilibrium capacity attained in 2 min.

the percentage attainment of equilibrium in 2 min ($P_{2\,min}$) was measured for each resin. Experience has shown that, under the conditions chosen for this measurement, a resin should have a $P_{2\,min}$ value of at least 50% for satisfactory performance when used in columns for rapid separations. The values in Table 1 show that XAD-7 is the best support. The rapid uptake of copper correlates with the high water regains of the bare and coated resin. A similar result has been found [7] for resins coated with the extractant "Kelex 100".

Loading

In general, the rate of uptake of copper decreases as the loading is increased from 10 to 60%, but the rate for XAD-7 with 60% loading is still very good. The very low capacity shown by XAD-4 with 10% loading is probably the result of inadequate wetting of the resin. This explanation is suggested by the low water regain found for the coated resin, and the effect is understandable in view of the hydrophobic nature, small pore diameter (5 nm), and high specific surface area (784 $m^2\ g^{-1}$) of the support. A loading of 10% of the more polar LIX-64N is probably insufficient to form even a monolayer on the internal surface of this resin, and alcohol cannot be used to displace air from the coated resin, because it would also remove the LIX-64N.

There is no significant difference between the capacities of the different resins at 60% loading, presumably because better wetting is achieved.

Effect of the addition of LIX-63 and of purification of LIX-65N

The structures and composition of the LIX extractants have been reported [3]. LIX-63 is an aliphatic α-hydroxyoxime, LIX-65N is 2-hydroxy-5-nonylbenzophenoneoxime with 40% (v/v) of an inert diluent, and LIX-64N is a mixture of LIX-65N with about 1% (v/v) of LIX-63. In solvent extraction LIX-63 accelerates the rate of extraction of copper by LIX-65N. When the extractants were supported on XAD-7, the results shown in Table 2 were obtained. The presence of LIX-63 made no significant difference to the rate. Thus the catalytic effect of LIX-63 is peculiar to solvent extraction, and does not apply to extraction chromatography.

Table 2 compares the properties of a resin loaded with the pure *anti*-isomer of LIX-65N with those of a resin loaded with the commercial LIX-65N (containing 39% of the active isomer [3]). At 60% loading, the extraction rate was slightly lower and the capacity slightly higher when the purified material was used. For analytical use, the commercial LIX-65N can be recommended.

Effect of other diluents

Since the addition of nonylphenol to Kelex 100 increased the rate of extraction of copper by a resin coated with the mixture [7], the addition of nonylphenol to LIX-64N was tried. It was without effect (Table 2). Many workers in the field of extraction chromatography [11] have used

TABLE 2

XAD-7 resin loaded with different combinations of LIX extractants and diluents

Stationary liquid phase	$P_{2\,min}$ (%)	Capacity (meq g^{-1})
55% LIX-65N + 5% LIX-63	73	0.75
60% LIX-64N	72	0.62
60% LIX-65N	73	0.78
55% pure LIX-65N + 5% LIX-63	69	1.20
60% pure LIX-65N	66	0.90
25% LIX-64N	86	0.35
25% LIX-64N + 25% nonylphenol	84	0.37
36% LIX-65N + toluene[a]	53	0.48
42% LIX-65N + toluene[a]	34	0.51

[a]Different methods of coating were used; see text.

diluents similar in nature and amount to those used in solvent extraction. To avoid evaporation of volatile diluents, a different method of coating is necessary. Thus Fritz et al. [2] used a 20% (w/w) solution of an oxime in toluene, passing this through a column of XAD-2 resin, and after equilibration, flushing out the excess of toluene solution with water. We applied the method to XAD-7, using a 20% (w/w) solution of LIX-65N in toluene. No evaporation of the toluene was allowed, but the toluene solution was left in contact with the resin for 1 d, before flushing it out with water. After removal of the toluene from an aliquot of this resin, the percentage of LIX-65N absorbed was 36%. The resin (with toluene diluent) had a slower rate of exchange (Table 2) than resins without the toluene diluent. Another method of coating the support [12] was tried. Dry XAD-7 resin was soaked in a 20% (w/w) solution of LIX-65N in toluene for 1 d, air being removed from the resin by initial evacuation, and then the resin was filtered off and the toluene was allowed to evaporate until the resin particles became free-flowing. The resin was then covered with water and air was removed. The resin coated in this way had a loading of 42% of LIX-65N (on a dry basis). The amount of toluene present was not determined. This resin had a rate of exchange even slower than that of the previous resin (Table 2).

Thus added diluents did not increase the exchange rate, and if any diluent was necessary, sufficient was present in the commercial LIX-65N.

Elution curves

The elution of 0.6 mg of copper from an XAD-7 resin loaded with 50% LIX-65N is shown in Fig. 1. The copper was absorbed at pH 5, and eluted with 2 M hydrochloric acid at a flow rate of 1 ml min^{-1}. The plate height was 2.0 mm, and tailing was negligible. This curve should be compared with those in Figs. 3 and 4 of reference 1, which showed considerable tailing and represented plate heights of 9.7 mm and 5.2 mm, respectively. The separations reported below were done rapidly by selective absorption, copper being held

while other metals passed through the column. However, separations by selective elution are possible with this resin. Figure 2 shows the selective elution of nickel and copper after both metals were absorbed on the resin at pH 5. All the nickel was eluted by acid of pH 2, before any copper appeared in the effluent.

Rapid separations

Solutions (0.01 M) of nickel, cobalt, or magnesium were mixed with 0.01 M copper solution and the pH was adjusted by the addition of sodium acetate—HCl buffers. The mixed solution was pumped at 10 ml min^{-1} through an 11 × 130 mm column of XAD-7 (75—150 μm particles) coated with 25% of LIX-64N. The metal not absorbed was washed through with 25 ml of buffer followed by 25 ml of water. The copper was then eluted in the reverse direction with 2 M HCl. Figures for individual separations are given in Table 3.

The separation of copper from iron(III) was not quantitative without an additional complexing agent to mask the iron. This finding is in agreement with previous work on hydroxy-oximes. Thus Cerrai and Ghersini [1] used fluoride ion in the eluent for the iron(III), and Fritz et al. [2] added tartaric acid to the iron solution "to minimize tailing". For the separations reported in Table 3, up to 0.5 g of potassium sodium tartrate was added per 0.1 mmol of iron. This prevented any retention of iron by the resin, but it also reduced the effective capacity of the resin for copper. It was therefore necessary to avoid overloading the column with copper. The resin used for

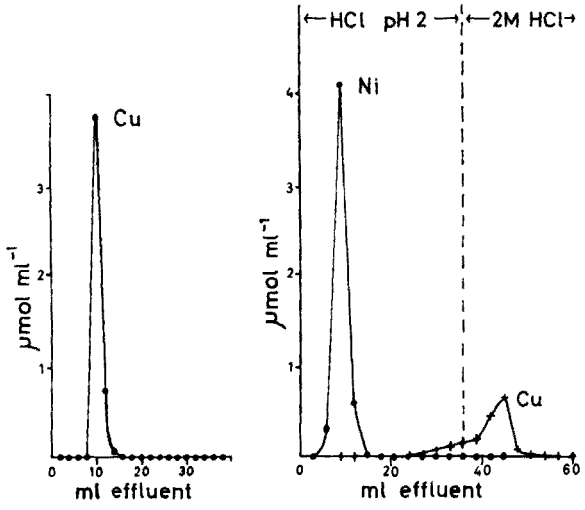

Fig. 1. Elution of copper (0.6 mg) from XAD-7 resin loaded with 50% (w/w) of LIX-65N. Eluent 2 M HCl. Column dimensions: 9 mm × 130 mm. Flow rate: 1 ml min^{-1}. Particle size of resin: 75—150 μm.

Fig. 2. Selective elution of nickel (0.01 mmol) and copper (0.005 mmol) with HCl of pH 2 and 2 M HCl. Other conditions as in Fig. 1.

TABLE 3

Rapid separations of metals from copper
(Flow rate, 10 ml min^{-1}. Elution of copper with 2 M HCl. Tartrate was added to solutions containing Fe(III).)

pH	Taken (mmol)	Found (mmol)	Recovery (%)	pH	Taken (mmol)	Found (mmol)	Recovery (%)
2.8	Ni 0.0991	0.0994	100.3	5.5	Fe(III) 0.1000	0.1009	100.9
	Cu 0.0990	0.0989	99.8		Cu 0.1000	0.0994	99.4
2.8	Ni 0.2463	0.2473	100.4	5.5	Fe(III) 0.1000	0.0998	99.8
	Cu 0.0990	0.0984	99.3		Cu 0.0100	0.0099	99.0
3.5	Co 0.2659	0.2676	100.6	5.5	Fe(III) 0.0250	0.02505	100.2
	Cu 0.0990	0.0989	99.9		Cu 0.0100	0.0099	99.0
3.5	Mg 0.2325	0.2325	100.0	5.5	Fe(III) 0.0100	0.0099	99.0
	Cu 0.0990	0.0999	100.9		Cu 0.0100	0.0099	99.0
3.5	Mg 0.0970	0.0973	100.3				
	Cu 0.0990	0.0988	99.8				

the separation of copper from iron was coated with 50% of LIX-65N. The same resin in a 9 × 30 mm column was used to concentrate copper from very dilute solution. Water (1 l) containing 0.623 mg of copper was adjusted to pH 5 and was pumped through the column at 50 ml min^{-1}. The recovery of copper was 99%.

The rapid determination of copper in analysed samples of bronze and brass was carried out by passing a solution of the alloy at pH 3.5 through a column of resin to remove the copper. A pH of 3.5 was necessary to avoid the absorption of zinc. The copper was then eluted and titrated with EDTA. Results are given in Table 4. Since tartaric acid was added to prevent the precipitation of tin, it was necessary to ensure that the column used had sufficient capacity to retain all the copper.

TABLE 4

Determination of copper in bronze and brass

Sample	Cu reported (%)	Cu found (%)
Bronze "C", No. 207 (British Chemical Standards)	86.84	86.65 86.72
Brass No. 5f (Bureau of Analysed Samples Ltd.)	70.8	71.1 70.5

Financial assistance from the South African Council for Scientific and Industrial Research, and from the National Institute for Metallurgy is acknowledged. This paper is published by permission of the Director-General of the National Institute for Metallurgy.

REFERENCES

1 E. Cerrai and G. Ghersini, Analyst, 94 (1969) 599.
2 J. S. Fritz, D. R. Beuerman and J. J. Richard, Talanta, 18 (1971) 1095.
3 A. W. Ashbrook, Coord. Chem. Rev., 16 (1975) 285.
4 A. W. Ashbrook, J. Chromatogr., 105 (1975) 141.
5 J. R. Parrish, J. S. Afr. Chem. Inst., 23 (1970) 129.
6 A. Warshawsky, Trans. Inst. Mining Metall., 83 (1974) C101.
7 J. R. Parrish, Anal. Chem., 49 (1977) 1189.
8 A. W. Ashbrook, Hydrometallurgy, 1 (1975) 5.
9 J. R. Parrish, Lab. Pract., 24 (1975) 399.
10 Amberlite XAD Macroreticular Adsorbents, Rohm and Haas Co., Philadelphia, Pa.
11 T. Braun and G. Ghersini (Eds.), Extraction Chromatography, Elsevier, Amsterdam, 1975.
12 Ref. 11, p. 51.

Analytica Chimica Acta, 94 (1977) 317—322

CHELATING ION-EXCHANGERS CONTAINING N-SUBSTITUTED HYDROXYLAMINE FUNCTIONAL GROUPS
Part V. Iron, Copper, and Uranium Separations on Duolite CS-346 Resin

F. VERNON* and T. W. KYFFIN

The Ramage Laboratories, Department of Chemistry and Applied Chemistry, University of Salford, Salford M5 4WT, Lancs. (U.K.)

(Received 7th July 1977)

SUMMARY

The separation of iron(III), copper(II) and uranyl(II) ions from a series of salt solutions by chelating ion exchange on Duolite CS-346 resin by pH control is described. Recoveries of these ions from cobalt and nickel salt solutions were quantitative. Iron may also be separated from copper by selective sorption with pH control, and uranium from iron and copper by selective desorption with sodium carbonate solution as eluent.

One of the few commercial chelating ion exchange resins available is Duolite CS-346 for which the chelating ability is attributed to amidoxime groups. Very little evaluation has been performed on this exchanger. The available data [1] give a brief description and suggestions that the resin chelates "very strongly" with nine elements including copper, iron and uranium; "strongly" with three elements, and "moderately" with a further six elements including cobalt and nickel. Stable complex formation with iron(III) is indicated at pH 1.5, with copper(II) at pH 3.0, and with uranyl(II) at pH 2.0. This exchanger should therefore be capable of separating iron, copper, and uranium from cobalt and nickel at the pH values recommended. In this respect it should behave in a manner similar to the hydroxamic acid exchanger described in Part III of this series [2]. The possibility of separating iron from copper by selective sorption of iron(III) is also indicated. The separation of uranyl ions from copper or iron by selective sorption is examined, together with selective elution of uranium by sodium carbonate solution. Removal of the three ions from solutions of other salts, and their separations from each other, are also investigated.

EXPERIMENTAL

Duolite CS-346, a microbead chelating ion exchanger containing the amidoxime functional group (Diamond Shamrock Chemical Co., U.S.A.) was washed with water, then with 1 M hydrochloric acid to convert it to the hydrogen form, and finally with deionized water until the effluent was

chloride-free. The resin was stored in an air-tight container in the fully swollen state.

Metal capacities

Sodium capacity. This was determined by equilibration of the resin with 0.25 M sodium hydrogencarbonate and measurement of the sodium uptake as previously described [2].

Multivalent metal capacities. To obtain more fundamental capacity data than have been reported previously for metal ion solutions containing acetate buffers, the following procedure, though tedious, was adopted for total capacity determination of a metal ion from a backing electrolyte which consisted only of sodium sulphate. The fully swollen Duolite CS-346 resin (0.50 ± 0.01 g) was equilibrated for 24 h with 1 M sodium sulphate solution whose pH had been adjusted to the required value by the addition of sodium hydroxide or sulphuric acid solutions. The pH of the equilibrating solution was adjusted regularly over the period until it remained constant at the selected value. This solution was decanted from the resin, which was then equilibrated for 48 h with 1 M sodium sulphate solution which was 20 mM with respect to the ion under test, and whose pH had been adjusted as described previously. During the equilibration, the pH was brought back regularly to the initial value by the addition of sodium hydroxide, the equilibration continuing for 24 h after the pH became constant. After filtration and washing of the resin with 1 M sodium sulphate solution of the same pH as the final equilibrating solution, the metal was eluted from the resin by equilibration for 48 h with 2 M sulphuric acid. For iron(III), 4 M sulphuric acid was used. The copper, iron, cobalt, and nickel contents of the eluates were determined with a Corning-EEL 240 mark II atomic absorption spectrophotometer. Uranium was determined colorimetrically by 8-hydroxyquinoline in the presence of EDTA [3]; acid elution or sodium carbonate elution techniques were employed.

Water regain and equilibration rate

These resin properties were determined as described previously [2, 4].

Cobalt sulphate, nickel sulphate and copper sulphate (Hopkin and Williams, Ltd.) were used.

Column separations

A glass column (length 50 cm, i.d. 1 cm) was filled to a height of ca. 30 cm with 15 g of fully swollen Duolite CS-346. The column was washed with 50 bed volumes of deionized water, and then conditioned with 10 bed volumes of backing electrolyte adjusted to the required pH. The sample solution was passed on to the column at a flow rate of 1 to 2 ml min^{-1}. The column was then washed with 5 bed volumes of water, adjusted for pH. The retained metal ions were eluted with 10 bed volumes of 2 M sulphuric acid (or 4 M sulphuric acid for iron), and the metal contents were

determined as described under metal capacities. Iron was separated from copper at pH 1.5; iron and copper were separated from other metals at pH 3.0. For the determination of the iron and copper contents of cobalt sulphate and nickel sulphate, 100 g of the salt was dissolved in 500 ml of deionized water and the pH adjusted to 3.0 by the addition of sulphuric acid solution. The solution was passed through the column at 2—3 ml min^{-1}, the column was washed with 10 bed volumes of water, and the iron and copper were eluted with acid as described. For the iron content of copper sulphate, 10 g of the salt was dissolved in 500 ml of deionized water and the pH was adjusted to 1.5 with sulphuric acid before the solution was passed through the column.

For tests on the selective sorption of uranyl ions over iron and copper at pH 3, resin was equilibrated with solutions containing various amounts of EDTA (disodium salt), which were 5 mM in each metal ion species. After the washing procedures described, the ions were eluted with 4 M sulphuric acid, and the concentration of each was determined.

RESULTS AND DISCUSSION

The properties of Duolite CS-346 are given in Table 1, the vanadium capacity of 1.7 mmol g^{-1} representing the functional group content of the resin. In comparison with a hydroxamic acid resin described earlier [2] the metal capacities are low and the time to 50% occupation of resin sites is quite high. This slow equilibration rate (ca. 100 min) is due to the low water regain of 1.2 g g^{-1}; with the hydroxamic acid resin, a water regain of 1.7 g g^{-1} results in a $t_{½}$ value for copper of 22 min. These apparently poor properties of the Duolite resin arise because the polymer is in better physical form than either hydroxamic acid or amidoxime bead polymers produced by the authors. This is because Duolite CS-346 contains a second monomeric vinyl species; it is a copolymer whereby suitable physical characteristics have been incorporated at the expense of high capacity and fast equilibration.

TABLE 1

Properties of Duolite CS-346 amidoxime ion-exchange resin

Water regain	1.2 g g^{-1}
Sodium-hydrogen exchange	1.66 mmol g^{-1}
Capacities:-	
Vanadium (V), (pH 3.2)	1.7 mmol g^{-1}
Iron(III), (pH 1.5)	0.4 mmol g^{-1}
Copper(II), (pH 3.0)	0.5 mmol g^{-1}
Uranyl(II), (pH 2.0)	0.2 mmol g^{-1}
Equilibration rate ($t_{½}$)	
for copper (pH 4)	98 min
for iron (pH 2.8)	120 min

Figure 1 shows the capacity vs. pH contours for iron, copper, and uranyl ions together with cobalt and nickel capacities; it is apparent that the former three ionic species should be capable of removal from cobalt and nickel solutions. The curves indicate the possibility of a quantitative separation of iron from copper but not of iron from uranium nor of uranium from copper by selective sorption at a chosen pH. Elution of 1 mg and 10 mg of uranium, which had been quantitatively removed from solution by the column, showed that 50 ml of 2 M sodium carbonate removed 81% of uranium from the resin; with 250 ml of 2 M sodium carbonate, quantitative removal of uranium was achieved and a complete separation of uranium, copper and iron was obtained, the copper and iron remaining on the column.

Table 2 shows that the recoveries of iron, copper, and uranium from solutions containing cobalt and nickel at pH 3 are quantitative. With a 25-fold excess of cobalt and nickel present, neither of these elements could

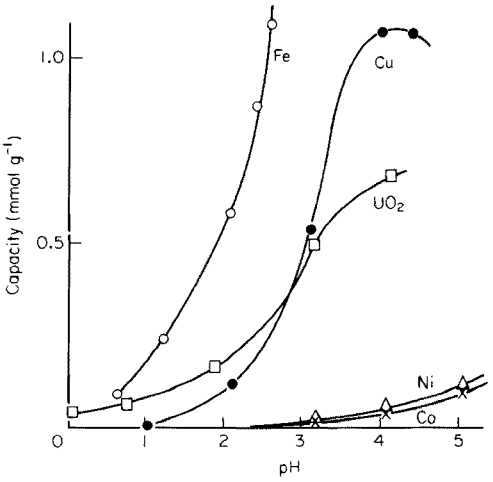

Fig. 1. Capacity vs. pH contours for iron, copper, uranyl, nickel, and cobalt on Duolite CS-346 resin.

TABLE 2

Recoveries of iron(III), copper(II) and uranyl(II) ions at pH 3.0 from solutions containing 25 mg each of cobalt and nickel ions in sodium sulphate backing electrolyte

Ion measured	Initial weight of ion present (mg)	Weight of ion eluted (mg)	Recovery (%)
Fe(III)	1.00	0.99	99
Fe(III)	5.00	5.06	101
Cu(II)	1.00	0.99	99
Cu(II)	5.00	4.96	99
UO_2(II)	1.00	0.99	99
UO_2(II)	5.00	4.98	100

be detected in the acid eluate containing the iron, copper, or uranium. Recoveries of 1 mg and 5 mg of iron from solutions containing 25 mg of copper at pH 1.5 were also studied: 99% of the iron was recovered in each case, and copper was not detected in the iron-containing acid eluate from the column.

As the recoveries were quantitative, the removal and determination of iron and copper from the various laboratory grades of cobalt and nickel salts was obvious, as was the determination of iron in copper salts. Table 3 gives the results obtained with a column of Duolite CS-346 to remove the two metals followed by their determination by atomic absorption spectrometry after elution; the grades of salts tested lie well within specification limits. Attempts to obtain comparative results by spraying the salt solutions directly into the flame of the atomic absorption spectrometer were not successful as the high salt concentration caused repeated blocking of the nebulizer unit. The determination of iron and copper in many systems is therefore possible; alkali and alkaline earth salts will not be retained on the exchanger and, from the metals whose retention is given as "moderate" or "weak", zinc, cadmium, chromium, tin, manganese, bismuth, and lead salts should be quantitatively stripped of iron and copper by this method.

Although the separation of iron, copper, and uranium can be quantitative, the procedure is tedious, involving their sorption at pH 3 followed by selective elution of uranium with 2 M sodium carbonate. As it is not possible to desorb copper ions selectively from a column loaded with copper and iron by control of eluent pH, it is necessary to elute both species with acid, increase the eluate pH to 1.5, and then selectively sorb iron. The copper in the effluent may then be sorbed at pH 3 as described.

As an alternative approach, the selective sorption of uranium from a solution containing a competing ligand for iron and copper was examined. As EDTA is well known as a masking agent for iron and copper in the determination of uranium [3], sorption characteristics of the ions in the

TABLE 3

The iron and copper contents of some cobalt and nickel salts, and iron content of copper sulphate

Salt	Iron content (ppm)		Copper content (ppm)	
	Found	Specification (max)	Found	Specification (max)
Cobalt sulphate (G.P.R.)	6.5	100	19.7	50
Cobalt sulphate (AnalaR)	2.9	20	2.3	10
Nickel sulphate (G.P.R.)	17.2	400[a]	14.4	400[a]
Nickel sulphate (AnalaR)	4.1	20	0.8	10
Copper sulphate (G.P.R.)	156.0	500	—	—
Copper sulphate (AnalaR)	30.0	100	—	—

[a]Specified as "heavy metals 0.04%"

TABLE 4

Selective sorption of uranyl ions as a function of EDTA content of a solution, 5 mM in iron(III), copper(II), and uranyl(II) ions

EDTA (mM)	Metal ion capacities at pH 3.0 (mmol g^{-1})		
	Fe(III)	Cu(II)	UO_2(II)
0	0.38	0.03	0.01
20	0.01	0.01	0.06
50	0.01	0.005	0.03

presence of this ligand were studied by batch equilibration. Table 4 shows the effect of EDTA on sorption characteristics. In its absence, the resin selectively retains iron(III) ions from the mixture. In the presence of a slight excess of EDTA, iron(III) and copper(II) chelation is suppressed with consequent increase in uranyl capacity. When the concentration of EDTA is further increased, the uranyl capacity is adversely affected.

Of the other species which the manufacturers claim to be strongly retained, Duolite CS-346 resin could be important in the recovery of gold and the platinum group metals if selective sorption is possible and efficient eluents are found.

The authors thank the Diamond Shamrock Company for the gift of the chelating ion exchanger.

REFERENCES

1 Diamond Shamrock Chemical Co. Duolite CS-346 Technical Sheet (1972).
2 F. Vernon and H. Eccles, Anal. Chim. Acta, 82 (1976) 369.
3 A. I. Vogel, A Text-book of Quantitative Inorganic Analysis, 3rd edn., Longmans, London, 1962.
4 F. Vernon and H. Eccles, Anal. Chim. Acta, 72 (1974) 331.

Analytica Chimica Acta, 94 (1977) 323—336

ÉTUDE DE L'EFFET DE QUELQUES FACTEURS SUR LES CARACTÉRISTIQUES DE FIXATION DU POTASSIUM ET DU RUBIDIUM SUR L'ACIDE ANTIMONIQUE, EN MILIEU NITRIQUE

I. N. BOURRELLY

Laboratoire Pierre Sue, C.N.R.S.,
C.E.N./SACLAY, B.P. 2, 91190 Gif sur Yvette (France)

(Reçu le 29 mars 1977)

RÉSUMÉ

L'influence de la concentration des ions des métaux alcalins, de la quantité d'acide antimonique mise en oeuvre et de la concentration en acide nitrique sur la fixation du potassium et du rubidium sur l'acide antimonique a été étudiée. Dans le domaine expérimental étudié, différents phénomènes gouvernent les mécanismes de fixation du potassium et du rubidium. La différence des caractéristiques de fixation apparaît de la comparaison des courbes de variation des coefficients de partage et des capacités de rétention de ces deux éléments en fonction des variables étudiées. L'étude des spectres infrarouge de l'acide antimonique et de ses dérivés deutérés a permis de mettre en évidence l'existence de plusieurs types de groupements OH qui se distinguent par la force des liaisons hydrogène. Le rubidium se fixe probablement sur les sites réactifs les plus accessibles, par des liaisons assez faibles, tandis que le potassium pourrait former des liaisons plus fortes avec des groupements Sb—O.

SUMMARY

Study of the effect of various factors on the retention characteristics of potassium and rubidium by antimonic acid in nitric acid.

The effects of the concentration of alkali metal ions, the amount of antimonic acid and the concentration of nitric acid on the retention of potassium and rubidium by antimonic acid have been studied. Different phenomena govern the retention mechanism of potassium and rubidium, under the experimental conditions of this study. The difference between the retention characteristics of the two elements appears from the different shapes of the curves showing their distribution coefficients and their uptake as functions of the various factors studied. Infrared spectroscopy of the antimonic acid and its deuterated compounds showed the presence of several types of OH groups which can be distinguished by the strength of their hydrogen bonds. Rubidium is probably retained on the most accessible exchange sites, forming weak bonds, while potassium could form stronger bonds with the Sb—O groups.

La sélectivité parfois très grande des échangeurs minéraux présente un intérêt particulier en analyse par activation où il est souvent indispensable d'isoler les isotopes radioactifs. Nous avons étudié les possibilités d'application de quelques composés minéraux pour la séparation de différents éléments en milieu acide [1—4]. Nos travaux sur la fixation des ions des

métaux alcalins sur l'acide antimonique ont fait apparaître une inversion dans l'ordre d'affinité pour le potassium et le rubidium en milieu acide fort par rapport à celui observé en milieu acide faible et en milieu ammoniacal, à savoir $Na^+ > K^+ > Rb^+ > Cs^+$ [5, 6]. D'autres ordres d'affinité ont été signalés par différents auteurs [7—9]. Il semblerait que la sélectivité de l'acide antimonique dépend d'une part de ses propriétés physico-chimiques et d'autre part du milieu de fixation des différents ions.

Nous avons considéré la réaction d'échange $x\ M^+ + HSbO_3 \rightleftharpoons x\ H^+ + M_xH_{1-x}SbO_3$, et nous avons étudié les effets des concentrations en ions métalliques M^+ et en ions H^+ dans la solution ainsi que l'effet de la quantité d'acide antimonique $HSbO_3$ solide mise en oeuvre, sur les rendements de fixation des ions K^+ et Rb^+, en milieu nitrique. La méthode de l'analyse de variance a été utilisée pour évaluer les effets des facteurs étudiés et pour mettre en évidence des interactions éventuelles entre ces facteurs.

MÉTHODE DE L'ANALYSE DE VARIANCE

Cette technique permet d'étudier plusieurs paramètres dans une même expérience. L'effet de chaque variable sur le résultat mesuré est évalué en même temps que la variation due à plusieurs autres facteurs différents [10—13]. Il est, en outre, possible de mettre en évidence des interactions éventuelles entre les paramètres pris en considération. Le gain de temps réalisé est, dans bien des cas, considérable, car cette méthode permet de réduire le nombre d'expériences à effectuer.

Description du plan d'expériences

Nous avons étudié les facteurs qui font l'objet de l'étude (facteurs contrôlés) dans un plan à modalités fixes, c'est à dire que des valeurs données à l'avance sont imposées aux facteurs maîtrisés. Les conclusions de l'analyse de variance ne s'appliquent qu'à ces modalités. Les valeurs retenues pour chaque facteur contrôlé constituent les modalités de ce facteur.

Faire l'analyse de variance, c'est caractériser les influences des facteurs contrôlés et isoler l'influence de tous les autres facteurs (non contrôlés), en décomposant la variance globale de la population des résultats expérimentaux en plusieurs parties. Pour obtenir ce résultat, il faut exprimer l'action des facteurs contrôlés sur le résultat mesuré par une hypothèse énoncée sous forme d'un modèle mathématique.

Additivité en interactions. Si l'on considère deux facteurs A et B, leur action sur le résultat mesuré x peut se faire selon deux modèles mathématiques différents:

$$x = x_0 + a + b + \epsilon$$

où x_0 = valeur moyenne; a = effet de A; b = effet de B; ϵ = erreur aléatoire.

a ne dépend que de la valeur du facteur A, b que de la valeur du facteur B. En d'autres termes, les effets de A et de B sont additifs. Dans le modèle $x = x_0 + a + b + (ab) + \epsilon$; les effets ne sont plus additifs; si le facteur A donne l'effet a quand il agit seul et le facteur B l'effet b quand il agit seul, l'action simultanée de A et B se traduit par un effet différent de $(a + b)$. D'où l'introduction du terme correctif $+ ab$ (terme d'interaction). Ce modèle ne concerne pas les facteurs non contrôlés dont l'action est toujours traduite par l'erreur aléatoire.

Plan factoriel à trois facteurs contrôlés. Les facteurs contrôlés A, B et C interviennent respectivement avec p, q et r modalités qui peuvent être fixes ou aléatoires.

On appelle facteur à modalités aléatoires, un facteur contrôlé pour lequel l'analyse de variance est faite sur les résultats de mesures effectuées pour un nombre p de modalités choisies au hasard parmi un nombre P, fini ou non, en général beaucoup plus grand, de modalités possibles ($p \ll P$). Pour un facteur à modalités fixes, le nombre de modalités possibles est restreint et les mesures sont effectuées pour toutes ces modalités ($p = P$). On dispose d'un résultat x_{ijk} pour chaque combinaison $A_iB_jC_k$ de l'ensemble de ces modalités. Le nombre total de résultats est $N = pqr$.

Un plan d'expériences avec répétitions permet d'étudier séparément les effets de chacun des trois facteurs contrôlés et permet, de plus, dans certains cas d'étudier une ou plusieurs interactions de premier ordre; le plan factoriel permet de distinguer l'effet des facteurs non contrôlés de l'interaction de deuxième ordre, si elle existe. On dispose de n résultats x_{ijk} pour chaque combinaison $A_iB_jC_k$ de l'ensemble de ces modalités. Le nombre total de résultats est $N = npqr$.

Facteurs et modalités étudiés

Dans un plan factoriel à trois facteurs contrôlés, à modalités fixes, avec répétition ($n = 2$), l'influence des paramètres suivants sur les rendements de fixation du potassium et du rubidium a été étudiée: facteur A = concentration des ions K^+ ou Rb^+; facteur B = quantité d'acide antimonique mise en oeuvre; facteur C = concentration en acide nitrique.
Les valeurs correspondants aux différentes modalités sont

$p = P = 3$ modalités fixes : $A_{i=1} = 2 \cdot 10^{-3}$ M ; $A_2 = 10^{-2}$ M; $A_3 = 2 \cdot 10^{-2}$ M

$q = Q = 2$ modalités fixes: $B_{j=1} = 0{,}5$ g; $B_2 = 2$ g

$r = R = 2$ modalités fixes: $C_{k=1} = 1$ N; $C_2 = 5$N

Conditions expérimentales

Les expériences ont été réalisées par la méthode dite statique (batch), à la température ambiante, à l'aide de traceurs radioactifs.

Les radioisotopes du potassium et du rubidium sont obtenus respectivement par les réactions nucléaires $^{41}K(n, \gamma)^{42}K^*$ et $^{85}Rb(n, \gamma)^{86}Rb^*$ dans un flux de

neutrons de 10^{13}—10^{14} n cm^{-2} s^{-1}. Les irradiations des éléments stables sous forme des sels nitrates ont été effectuées dans les réacteurs EL3 et Osiris du Commissariat à l'Energie Atomique à Saclay.

L'acide antimonique étudié est de provenance industrielle, fabriqué par hydrolyse du pentachlorure d'antimoine, séché pendant 5 h à 270°C. Tous les réactifs utilisés ont la qualité pour analyses.

La suspension d'acide antimonique dans 50 ml de la solution nitrique contenant les nitrates des métaux alcalins étudiés, ainsi que les radioisotopes correspondants, est agitée pendant 30 min. Les phases solide et liquide sont ensuite séparées par centrifugation. Une partie aliquote de la liqueur surnageante est prélevée et la radioactivité restante dans la solution (A_t) après fixation des ions initialement en solution sur l'acide antimonique solide est comparée à la radioactivité initiale A_0. La mesure des radioactivités est réalisée par spectrométrie gamme à l'aide d'un scintillateur NaI (Tl) relié à un sélecteur multicanaux. La radioactivité étant proportionnelle à la masse totale de l'élément, le rendement de fixation R est calculé suivant la relation: $R = [(A_0 - A_t)/A_0] \times 100\%$.

Résultats des calculs d'analyse de variance

L'ensemble des résultats, exprimés en rendement de fixation $R(\%)$, est présenté sous la forme d'un tableau qui fait apparaître aussi les sommes des résultats x par modalités ainsi que la somme globale. Dans le Tableau 1 sont rassemblés les résultats obtenus pour le potassium et dans le Tableau 2 ceux obtenus pour le rubidium.

TABLEAU 1

Les résultats obtenus pour le potassium

Facteur B (quantité acide antimonique)		Facteur C (N_{HNO_3})	Facteur A (concentration K^+) $i=1$	$i=2$	$i=3$	Sommes $\Sigma\Sigma_{ia}$		$\Sigma\Sigma\Sigma_{ika}$
$j=1$		$k=1$	57 60	32 34	17 16	$k=1$	$k=2$	
		Σ_a	117	66	33	216		
		$k=2$	5 6	8 6	6 9			
		Σ_a	11	14	15		40	
		$j=1$ $\Sigma_k\Sigma_a$	128	80	48			256
$j=2$		$k=1$	90 90	80 78	36 33			
		Σ_a	180	158	69	407		
		$k=2$	46 48	16 16	12 11			
		Σ_a	94	32	23		149	
		$j=2$ $\Sigma_k\Sigma_a$	274	190	92			556
Sommes		$k=1$ $\Sigma_j\Sigma_a$	297	224	102	623		$\Sigma\Sigma\Sigma\Sigma_{ijka}$
		$k=2$ $\Sigma_j\Sigma_a$	105	46	38		189	
		$\Sigma_j\Sigma_k\Sigma_a$	402	270	140	$\Sigma\Sigma\Sigma_{ija}$		812

TABLEAU 2

Les résultats obtenus pour le rubidium

Facteur B (quantité acide antimonique)		Facteur C (N_{HNO_3})	Facteur A (concentration Rb^+) $i=1$	$i=2$	$i=3$	Sommes $\Sigma\Sigma_{i\,a}$ $k=1$	$k=2$	$\Sigma\Sigma\Sigma_{i\,k\,a}$
$j=1$		$k=1$	91 91	43 43	22 20			
		Σ_a	182	86	42	310		
		$k=2$	41 41	27 24	15 17			
		Σ_a	82	51	32		165	
		$j=1$ $\Sigma\Sigma_{k\,a}$	264	137	74			475
$j=2$		$k=1$	98 98	95 96	77 79			
		Σ_a	196	191	156	543		
		$k=2$	84 81	66 68	52 48			
		Σ_a	165	134	100		399	
		$j=2$ $\Sigma\Sigma_{k\,a}$	361	325	256			942
Sommes		$k=1$ $\Sigma\Sigma_{j\,a}$	378	277	198	853		$\Sigma\Sigma\Sigma\Sigma_{i\,j\,k\,a}$
		$k=2$ $\Sigma\Sigma_{j\,a}$	247	185	132		564	
		$\Sigma\Sigma\Sigma_{j\,k\,a}$	625	462	330	$\Sigma\Sigma\Sigma_{i\,j\,a}$		1417

Les sommes de carrés, Q, et les carrés moyens, q, sont calculés à l'aide des équations habituelles d'analyse de variance [10—12]. Les effets de chacun des facteurs étudiés et leurs interactions éventuelles sont évalués en comparant la valeur numérique du rapport des carrés moyens q/q_R (q_R = erreur résiduelle) à la valeur tirée de la table de Snedecor pour le degré de liberté correspondant. D'après ces calculs nous avons tiré les conclusions suivantes.

Cas du potassium. Tous les facteurs étudiés exercent un effet significatif sur le rendement de fixation des ions K^+ sur l'acide antimonique en milieu nitrique. L'influence des interactions de premier ordre et de deuxième ordre entre ces facteurs a également pu être mise en évidence.

Cas du rubidium. Tous les facteurs étudiés exercent un effet significatif sur le rendement de fixation des ions Rb^+ sur l'acide antimonique en milieu nitrique. L'influence d'une interaction de deuxième ordre, ainsi que l'interaction de la concentration d'ions Rb^+ avec la quantité d'acide antimonique mise en oeuvre et la concentration en acide nitrique ont été mises en évidence.

Comparaison de l'influence des différents facteurs

S'il n'est pas possible, à partir des résultats d'un plan à modalités fixes, de comparer les facteurs entre eux par un même tableau, on peut cependant comparer les effets d'un facteur sur le rendement de fixation du potassium d'une part et sur celui du rubidium d'autre part, les modalités étant les mêmes dans les deux cas.

Les plans d'expériences pour le potassium et le rubidium étant identiques, on peut donc simplement comparer les carrés moyens ($q - q_R$) calculés.

D'autre part, la variance résiduelle q_R est pratiquement la même pour les deux éléments étudiés.

Dans le Tableau 3 sont rassemblées les valeurs de $q - q_R$ obtenues pour le potassium et le rubidium. L'effet de la concentration des ions alcalins en solution est du même ordre de grandeur dans les deux cas. L'effet de la quantité d'acide antimonique mise en oeuvre paraît plus grand pour le rubidium. Dans les deux cas l'influence de ce facteur dépend de la variation de la concentration des ions K^+ et Rb^+ (interaction *AB*) et de celle de la concentration en acide nitrique (interaction *ABC*). L'effet de la concentration en acide nitrique paraît plus faible pour le rubidium et l'interaction de ce facteur avec la concentration des ions en solution (interaction *CA*) paraît plus importante dans le cas du potassium.

Ces résultats nous amènent à conclure que les phénomènes de fixation du potassium et du rubidium sur l'acide antimonique, dans les conditions expérimentales étudiées, se distinguent par des mécanismes différents. Afin de mettre plus clairement en évidence cette différence, nous avons exprimé les caractéristiques de fixation tels le coefficient de partage limite et la quantité d'ions fixés sur le solide, en fonction des variables étudiées.

ÉTUDE DE L'INFLUENCE DE LA QUANTITÉ DU SOLIDE MISE EN OEUVRE

En application de la loi d'action de masse, on peut écrire la relation suivante

$$K_H^M = [M^+_{solide}] \cdot [H^+_{solution}] / [M^+_{solution}] \cdot [H^+_{solide}] \qquad (1)$$

où K_H^M représente la constante apparente d'échange et où les grandeurs entre paranthèses expriment les concentrations des ions M^+ et H^+ sur le solide et dans la solution. Le rapport $[M^+_{solide}] / [M^+_{solution}]$ représente le coefficient de partage limite P°, d'où

$$P^\circ = K_H^M [H^+_{solide}] / [H^+_{solution}] \qquad (2)$$

Dans le cas du potassium et du rubidium, la quantité d'ions H^+ échangés est faible par rapport à la quantité totale de groupements fonctionnels dans l'acide antimonique. La concentration d'ions H^+ restant dans le solide après échange $[H^+_{solide}]$ peut dans ce cas être considérée proportionnelle à la quantité

TABLEAU 3

Valeurs de $q - q_R$ pour le potassium et le rubidium

Source de variation	$q - q_R$		Source de variation	$q - q_R$	
	K	Rb		K	Rb
Concentration K^+, Rb^+ (*A*)	2143	2728	Interaction *AB*	332	322
Quantité $HSbO_3$ (*B*)	3748	9085	Interaction *BC*	278	0
Concentration HNO_3 (*C*)	7846	3478	Interaction *CA*	614	132
			Interaction *ABC*	274	458

d'acide antimonique mise en oeuvre (Q) et l'éqn. (2) peut s'écrire: $P^\circ = K_H^M \, a \cdot Q/[H^+_{solution}]$, où $a = [H^+_{solide}]/Q$ représente un facteur de proportionnalité.

Sur la Fig. 1 sont représentées les courbes correspondantes à la variation de $\log P^\circ$ en fonction de $\log Q$ pour le potassium et le rubidium. On voit que les valeurs de P° sont plus élevées pour le rubidium, ce qui signifie que l'affinité apparente de l'acide antimonique étudié est plus grande pour cet élément. La pente de la courbe $\log P^\circ/\log Q$ correspondant au rubidium est supérieure à celle du potassium, ce qui peut signifier que les sites de fixation accessibles aux ions Rb^+ sont plus nombreux que ceux qui sont accessibles aux ions K^+. La taille des ions anhydres Rb^+ est plus élevée que celle des ions anhydres K^+; si les ions en solution se fixent sous forme d'ions anhydres, ces résultats nous amènent à penser que des phénomènes de chimisorption sont prépondérants dans le cas du rubidium.

Ces conclusions peuvent s'appliquer au domaine expérimental étudié qui se caractérise par la présence d'ions H^+ en excès par rapport à la concentration d'ions K^+ et Rb^+ en solution.

ÉTUDE DE L'INFLUENCE DE LA CONCENTRATION EN ACIDE NITRIQUE

Sur les Figs. 2—4 sont représentées les courbes de la variation du rendement de fixation des ions K^+ et Rb^+ en fonction de la concentration d'acide nitrique pour différentes concentrations d'ions K^+ et Rb^+ initialement en solution. On voit que l'effet de la concentration en acide nitrique dépend de celle d'ions K^+ et Rb^+ en solution (influence de l'interaction entre ces deux facteurs).

Lorsque la concentration d'ions alcalins en solution est faible ($2 \cdot 10^{-4}$ M), le rendement de fixation du potassium baisse plus rapidement que celui du rubidium. Ceci pourrait confirmer la prépondérance des phénomènes d'adsorption dans le cas du rubidium (voir Fig. 2). Pour toutes les concentrations d'ions alcalins étudiées ($2 \cdot 10^{-4}$ M, $2 \cdot 10^{-3}$ M, $2 \cdot 10^{-2}$ M), l'affinité apparente de l'acide antimonique est plus grande pour le rubidium.

L'effet de la présence d'ions H^+ en excès peut avoir de multiples conséquences, notamment le déplacement de l'équilibre de la réaction d'échange d'ions (3) ainsi que celui de la réaction de dissociation des groupements fonctionnels (4), dans le sens (b), de la droite vers la gauche

$$M^+ + HSbO_3 \underset{(b)}{\overset{(a)}{\rightleftharpoons}} MSbO_3 + H^+ \qquad (3)$$

$$\text{>SbOH} \underset{(b)}{\overset{(a)}{\rightleftharpoons}} \text{>SbO}^- + H^+ \qquad (4)$$

et la formation de ponts hydrogène entre les groupements fonctionnels (5)

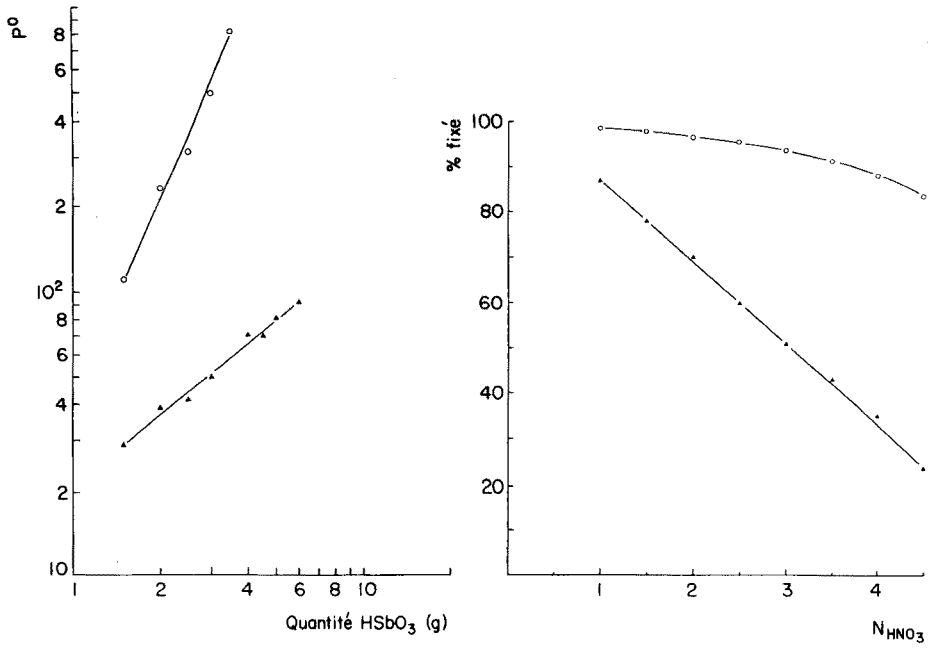

Fig. 1. Variation du coefficient de partage limite en fonction de la quantité d'acide antimonique mise en oeuvre. Milieu, HNO_3 1 M. Durée d'agitation: 1 h. (▲) K, (○) Rb.

Fig. 2. Variation du rendement de fixation sur 1 g d'acide antimonique en fonction de la concentration en acide nitrique. Concentration des ions K^+ et Rb^+ initialement en solution, $2 \cdot 10^{-4}$ M. (▲) K, (○) Rb.

$$\text{SbOH} + H^+ \rightleftharpoons \text{SbOH} \ldots H^+ \ldots \text{OHSb} \qquad (5)$$

Ces phénomènes peuvent se traduire par une baisse du rendement de fixation, qui semble être plus accusée pour le potassium et ceci d'autant plus que la concentration d'ions K^+ en solution est faible.

Nous avons posé l'hypothèse que les ions Rb^+ se fixent sur les sites réactifs les plus accessibles en formant des liaisons assez faibles, tandis que les ions K^+ se fixent par des liaisons plus fortes avec les groupements Sb—O.

Lorsque la réaction d'échange d'ions implique la dissociation préalable des groupements fonctionnels, un excès d'ions H^+ bloque la réaction (4) et la réactivité des groupements Sb—OH serait ainsi diminuée. De même, la réaction (5) peut être prépondérante en présence d'un excès d'ions H^+, réduisant le nombre de sites réactifs accessibles. L'influence de ces phénomènes serait moins importante pour la fixation des ions Rb^+, si des mécanismes d'adsorption sont prépondérants pour cet élément.

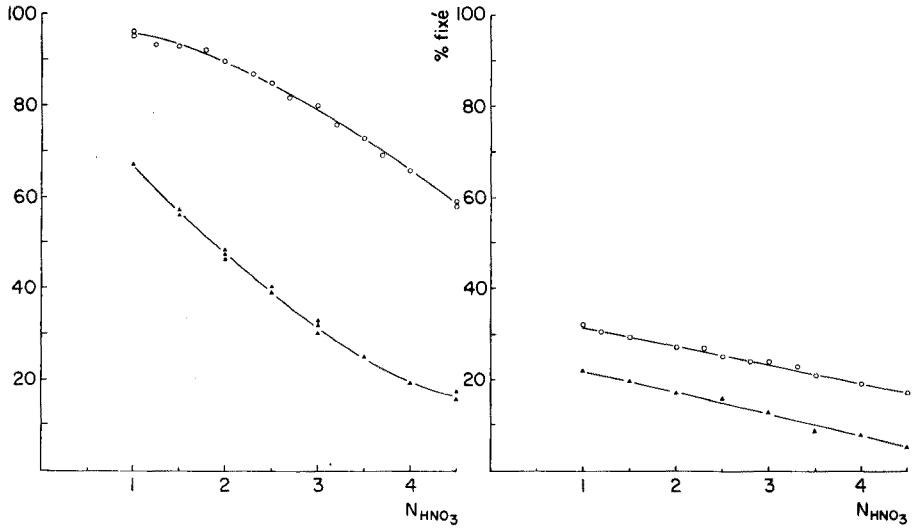

Fig. 3. Variation du rendement de fixation sur 1 g d'acide antimonique en fonction de la concentration en acide nitrique. Concentration des ions K^+ et Rb^+ initialement en solution, $2 \cdot 10^{-3}$ M. (▲) K, (○) Rb.

Fig. 4. Variation du rendement de fixation sur 1 g d'acide antimonique en fonction de la concentration en acide nitrique. Concentration des ions K^+ et Rb^+ initialement en solution, $2 \cdot 10^{-2}$ M. (▲) K, (○) Rb.

ÉTUDE DE L'INFLUENCE DE LA CONCENTRATION DES IONS ALCALINS EN SOLUTION

Sur la Fig. 5 sont représentées les courbes de variation de la quantité d'ions K^+ et Rb^+ fixés sur l'acide antimonique solide en fonction de la quantité d'ions initialement mise en solution. Lorsque la concentration d'ions en solution est faible, l'affinité apparente de l'acide antimonique pour le rubidium est plus grande et lorsque la concentration augmente, la capacité apparente pour le potassium atteint une valeur plus élevée que celle pour le rubidium.

L'acide antimonique que nous avons étudié n'est pas très bien cristallisé, il est fortement peptisé dans l'eau et dans des solutions de faible force ionique. Le phénomène inverse se produit lorsqu'on augmente la concentration des ions en solution. Cette gélification réversible ou thixotropie, est la cohésion de fines particules solides en enfermant de la solution [14]. Dans le milieu nitrique que nous avons étudié, cette cohésion pourrait être favorisée par la formation de ponts hydrogène entre les groupements OH de la surface.

Des phénomènes d'équilibre de Donnan peuvent avoir lieu entre les agglomérats ainsi formés et la solution; par conséquent, la solution extérieure peut pénétrer dans les agglomérats ou en être exclue, en fonction de facteurs tels que la capacité de fixation des ions en présence et la concentration de la solution.

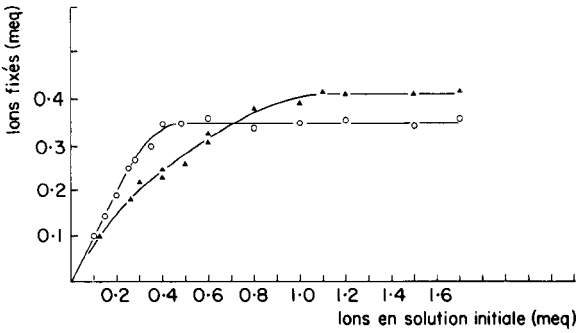

Fig. 5. Variation de la quantité du potassium et du rubidium fixés sur 1 g d'acide antimonique en fonction de la quantité des ions K^+ et Rb^+ initialement en solution nitrique 1 M. Durée d'agitation : 1 h. (▲) K, (○) Rb.

Lorsqu'on augmente la concentration d'ions alcalins en solution, un effet de tamis moléculaire peut favoriser la pénétration d'ions K^+ dans les agglomérats où les ions K^+ anhydres (1,33 Å) pourraient diffuser plus librement que les ions anhydres Rb^+ (1,49 Å) de plus grande taille, en l'absence de phénomènes de solvatation.

ÉTUDE DES GROUPEMENTS FONCTIONNELS DE L'ACIDE ANTIMONIQUE

L'hypothèse que les ions K^+ et Rb^+ se fixent sur des sites réactifs différents suppose l'existence de différents groupements fonctionnels dans l'acide antimonique.

Nous avons étudié l'acide antimonique par spectrophotométrie d'absorption infrarouge afin de connaître avec plus de précision les liaisons entre les atomes hydrogène et oxygène, qui peuvent correspondre aux groupements OH^-, OH^+ ou OH plus ou moins liés par des liaisons H, à des molécules d'eau également plus ou moins liées [15] ou à des ions hydronium

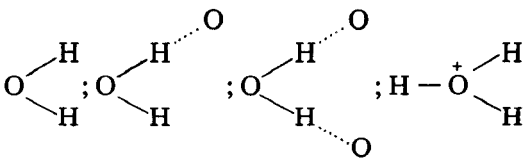

Nous avons utilisé la technique de la deutération pour attribuer les bandes de vibration dues aux liaisons hydrogène. La méthode de la dilution isotopique, qui consiste à faire un cristal mixte contenant quelques % d'un composé AH dans son dérivé deutéré AD, permet de distinguer les liaisons hydrogène de longueurs et de forces différentes [16].

Sur la Fig. 6 sont représentés les spectres d'absorption infrarouge entre 4000 et 2000 cm^{-1} de l'acide antimonique initial (a), du composé fortement deutéré (b) et du composé faiblement deutéré (c). Dans les dérivés deutérés

où les couplages intra et intermoléculaires des groupements OH sont supprimés, chaque bande fondamentale ν_{OH} correspond à un groupement OH distinct.

Sur la Fig. 7 sont représentés les spectres de l'échantillon partiellement deutéré (a) et du composé deutéré puis déshydraté sous vide pendant 2 h à 95°C (b).

De la Fig. 7b, on voit que l'intensité des bandes de vibrations des groupements OH et OD est diminuée dans le composé déshydraté. Une bande intense et bien définie à fréquence élevée (3580 cm^{-1}) signale la présence d'un nombre important de groupements OH avec des liaisons hydrogène faibles. Cette bande peut correspondre aux groupements OH libres de l'eau; toutefois sa présence dans l'acide antimonique déshydraté (Fig. 7b) indique qu'elle peut également correspondre aux groupements Sb—OH. Prost a récemment étudié les interactions entre différents types de molécules d'eau dans la sépiolite [17]. Cet auteur signale une intense bande de vibration à 3570 cm^{-1} correspondant aux groupements OH de l'eau.

D'après l'étude des dérivés deutérés, ces groupements OH forment d'une part des liaisons hydrogène faibles (ν_{OH} 3580 cm^{-1}; ν_{OD} 2630 cm^{-1}) et d'autre part des liaisons hydrogène fortes (ν_{OH} 3420 cm^{-1}; ν_{OD} 2500 cm^{-1}).

Dans l'acide antimonique PA, la présence de l'eau plus ou moins adsorbée est déduite d'après la bande de vibration ν_{OH} à 3300 cm^{-1} (ν_{OD} 2460 cm^{-1}).

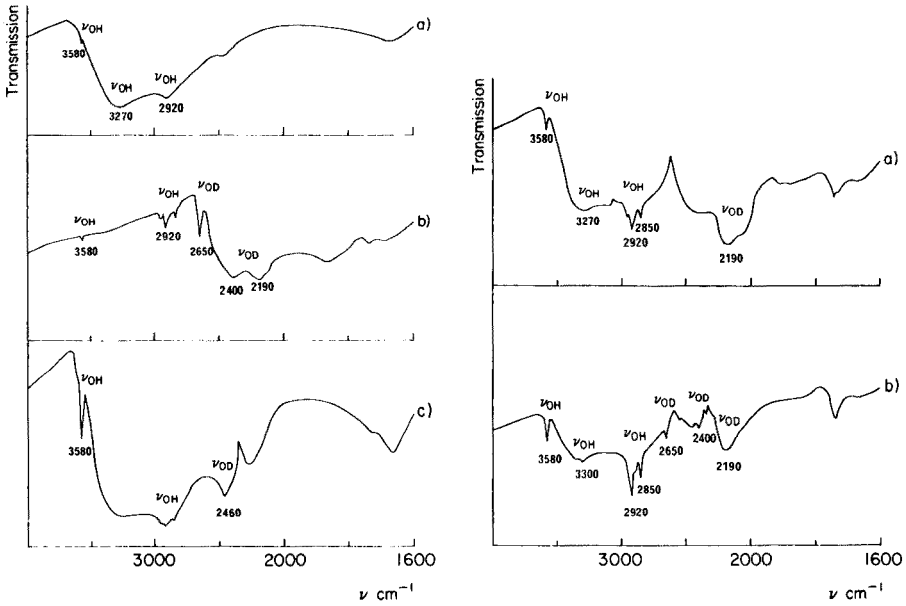

Fig. 6. Spectres infrarouge de l'acide antimonique initial (a), fortement deutéré (b) et faiblement deutéré (c).

Fig. 7. Spectres infrarouge de l'acide antimonique partiellement deutéré (a) et partiellement deutéré, puis déshydraté (b).

Les bandes de vibrations aux fréquences plus basses (ν_{OH} 3270 cm^{-1}; ν_{OD} 2400 cm^{-1}) indiquent la présence des liaisons hydrogène plus fortes des groupements OH de l'eau ou des groupements OH du type hydraté, Sb(OH).

Dans la région des fréquences inférieures à 3200 cm^{-1}, les vibrations ne sont habituellement pas dues à des molécules d'eau; d'autre part, des bandes de combinaison ou des harmoniques sont possibles, notamment $2\,\delta_{H_2O} \sim$ 3200 cm^{-1}.

Dans les échantillons partiellement deutérés, on peut distinguer un triplet (ν_{OH} vers 2920 cm^{-1}; ν_{OD} vers 2190 cm^{-1}) qui d'après la fréquence et le rapport isotopique (1,33) relativement moins élevés peut être attribué à des groupements Sb—OH moins libres et des liaisons hydrogène assez fortes.

Les différents types de groupements OH de l'acide antimonique

D'après leur fréquences d'absorption et leurs rapports isotopiques, trois types de groupements OH peuvent être distingués

Type 1: Groupements OH relativement "libres" correspondants aux groupements Sb—OH et aux groupements OH libres de l'eau

	ν_{OH}	ν_{OD}	rapport isotopique
Sb—OH	3580 cm^{-1}	2650 cm^{-1}	1,35
H_2O	3300 cm^{-1}	2460 cm^{-1}	1,35

Type II: Groupements OH de l'eau plus ou moins adsorbée ou des groupements Sb(OH) du type hydraté. Les bandes d'absorption correspondantes peuvent se superposer

ν_{OH}	ν_{OD}	rapport isotopique
3270 cm^{-1}	2400 cm^{-1}	1,36

Type III: Groupements Sb—OH moins libres et dont les liaisons hydrogène sont plus fortes

ν_{OH}	ν_{OD}	rapport isotopique
2920 cm^{-1}	2190 cm^{-1}	1,33

Etude de la réactivité des groupements OH

Nous avons étudié les spectres infrarouge de l'acide antimonique ayant fixé de l'argent; la capacité de fixation de cet élément étant la plus élevée, l'étude comparative avec l'acide antimonique initiale sera plus aisée. Sur la Fig. 8 sont représentés les spectres de l'acide antimonique initial partiellement deutéré (8a) et le composé deutéré après fixation de l'argent (8b). On peut noter une diminution importante des bandes de vibration correspondant aux groupements OH, ce qui confirme leur réactivité pour l'argent.

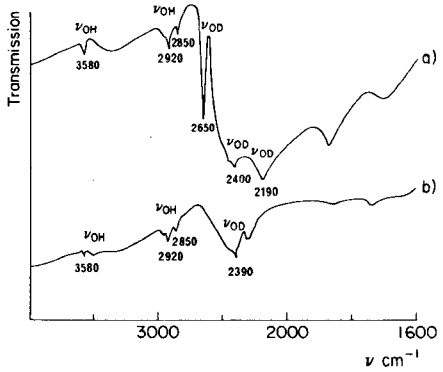

Fig. 8. Spectres infrarouge de l'acide antimonique partiellement deutéré (a) et deutéré après fixation de l'argent (b).

CONCLUSIONS

Une étude des caractéristiques de fixation du potassium et du rubidium en milieu nitrique par la méthode d'analyse de variance a permis de mettre en évidence que différents phénomènes peuvent gouverner les mécanismes de fixation de ces deux éléments.

L'examen des spectres infrarouge de l'acide antimonique et de ses dérivés deutérés montre que les groupements fonctionnels peuvent avoir des liaisons hydrogène assez faibles, du type hydraté ou assez fortes.

La réactivité des groupements fonctionnels dépend d'une part de la force des liaisons hydrogène et d'autre part de l'accessibilité des sites réactifs. Ces deux facteurs peuvent être influencés par la présence d'un excès d'ions H^+ et provoquer ainsi des modifications dans l'affinité apparente de l'acide antimonique pour les différents ions mis en présence.

Nous avons posé l'hypothèse que les ions Rb^+ se fixent sur les sites les plus accessibles et forment des liaisons assez faibles, tandis que les ions K^+ peuvent former des liaisons plus fortes avec les groupements Sb—O. Ceci expliquerait l'effet prépondérant de la présence d'ions H^+ en excès, qui se traduit par la diminution de la réactivité et de l'accessibilité des groupements Sb—OH, sur la fixation du potassium.

Il est important de noter que les propriétés physico-chimiques de l'acide antimonique sont fonction du milieu réactionnel, par conséquent ses propriétés de fixation se modifient au fur et à mesure que les réactions s'effectuent.

Lorsque des phénomènes de peptisation et de gélification peuvent se produire, ce qui est le cas de l'acide antimonique que nous avons étudié, la force ionique de la solution est un facteur déterminant pour la granulométrie des particules solides en suspension.

En effet, dans le milieu nitrique étudié, nous avons observé l'agglomération de fines particules solides qui sont peptisées dans des solutions de plus faible force ionique. En milieu acide fort, la cohésion est probablement favorisée par la formation de ponts hydrogène entre les groupements OH de la surface.

Des phénomènes d'équilibre de Donnan entre la solution renfermée dans les agglomérats et la solution extérieure pourraient se produire et influencer le rendement de fixation de certains ions.

La fixation du potassium semble particulièrement influencée par l'interaction entre les concentrations des ions K^+ et H^+ en solution. Ceci pourrait être dû à l'affinité de l'acide antimonique pour les ions H^+ d'une part et aux conséquences de ces phénomènes d'équilibre d'autre part. La capacité de fixation du potassium atteint une valeur plus élevée que celle du rubidium lorsqu'on augmente la concentration des ions alcalins en solution. On peut supposer que les ions K^+ anhydres ayant une plus petite taille que les ions Rb^+, pénètrent davantage dans les agglomérats (effet tamis moléculaire).

En présence d'un grand excès d'ions H^+, la sélectivité de l'acide antimonique est plus grande, car la formation de ponts hydrogène peut créer un encombrement stérique pour certains ions. L'élution des ions fixés par des acides forts peut également être rendue difficile par ces phénomènes.

BIBLIOGRAPHIE

1 I. N. Bourrelly, C. Cleyrergue, N. Deschamps, H. Jaffrezic, B. Vialatte et S. Alexandrov, Radiochem. Radioanal. Lett., 5 (1970) 43.
2 S. Alexandrov, J. N. Barrandon, I. N. Bourrelly, C. Cleyrergue, N. Deschamps, H. Jaffrezic et B. Vialatte, Radiochem. Radioanal. Lett., 5 (1970) 51.
3 B. Vialatte, J. N. Barrandon, S. Alexandrov, I. N. Bourrelly, C. Cleyrergue, N. Deschamps et H. Jaffrezic, Radiochem. Radioanal. Lett., 5 (1970) 59.
4 C. Cleyrergue, N. Deschamps, H. Jaffrezic, B. Vialatte, S. Alexandrov et I. N. Bourrelly, Radiochem. Radioanal. Lett., 6 (1971) 15.
5 I. N. Bourrelly et N. Deschamps, J. Radioanal. Chem., 8 (1971) 303.
6 I. N. Bourrelly, Thèse Univ. Pierre et Marie Curie, Paris 6, 1976.
7 L. H. Baetsle et D. Huys, J. Inorg. Nucl. Chem., 30 (1968) 639.
8 F. Girardi, R. Pietra et E. Sabbioni, Euratom Technical Report, EUR 42872 (1969).
9 M. Abe, Bull. Chem. Soc. Jpn., 42 (1969) 2683.
10 O. L. Davies, The Design and Analysis of Industrial Experiments, Hafner.
11 J. D. Hinchen, Practical Statistics for Chemical Research, Methuen and Co. Ltd.
12 P. Chapouille, Planification et analyse des expériences, Masson et Cie, Paris, 1973.
13 M. Neuilly, communications personnelles.
14 J. Lemere, Thèse Univ. Paris VI.
15 A. Novak, Structure and Bonding Vol. 18, Springer-Verlag, Berlin, Heidelberg et New York, 1974.
16 J. Guillermet, Spectroscopies infrarouge et Raman (B. F. Mentzen), Monographies du Centre d'Actualisation Scientifiques et Techniques de l'INSA, Masson et Cie, Paris, 1970.
17 R. Prost, Spectrochim. Acta, (1975) 1497.

Analytica Chimica Acta, 94 (1977) 337–342

THE DETERMINATION OF OXYGEN IN BRASS AND ZINC BY A VACUUM CARBON-REDUCTION TECHNIQUE§

A. COLOMBO* and R. VIVIAN

Chemistry Division, Joint Research Centre, Ispra Establishment, 21020 Ispra (Italy)

(Received 8th June 1977)

SUMMARY

A vacuum carbon-reduction technique for the determination of oxygen in brass and zinc has been studied. As a preliminary, zinc is removed from the samples, sealed in pre-degassed graphite capsules, in a silica furnace maintained at ca. 850°C under vacuum in a vacuum fusion instrument. The residual contents of the capsules are then analysed in sequence at 1450°C in the main furnace of the apparatus, to which they are transferred without breaking the vacuum. The procedure developed affords a detection limit of 0.5—1 ppm of oxygen for samples weighing ca. 1.5 g.

In 1969, the Eurisotop Office of the Commission of the European Communities, Brussels, organized a cooperative programme aimed at improving methods for the determination of bulk oxygen and nitrogen in non-ferrous metals. The participation of qualified laboratories in different countries of the European Economic Community area was extensive and involved the use of various analytical techniques, e.g. 14-MeV neutron, γ-photon and charged-particle activation analysis; vacuum and inert gas carbon-reduction techniques (sometimes referred to as "fusion" techniques); hydrogen reduction; spark-source mass spectrometry, and Kjeldahl digestion. Great attention was paid to the gas content of the sample surfaces; procedures to render them as low and reproducible as possible were provided [1, 2].

A natural consequence of such activities was their integration and continuation in a general programme set up by the Community Bureau of Reference† (BCR) aimed at the preparation of certified reference materials (RM's).

Within such a context, samples of non-ferrous metals (which will include brass and zinc) are under study and some oxygen-certified RM's are already available from BCR, together with their full certification reports. They include at the moment four types of copper (oxygen content 1—400 ppm), two types of zirconium (500 and 1200 ppm), titanium (600 ppm), molybdenum (15 ppm) and lead (1 ppm). A summary of the status of these activities, up to the end of 1975, has been published [3].

---

§Work performed in the framework of the "METRE" programme.

†Community Bureau of Reference, Directorate General XII, Commission of the European Communities, 86 Rue de la Loi, Brussels, Belgium.

This paper describes the method developed at the Joint Research Centre, Ispra, to determine oxygen in brass and zinc by a vacuum carbon-reduction technique.

EXPERIMENTAL

Equipment

Basically this technique consists of the extraction of oxygen as carbon monoxide from a molten sample in a graphite crucible by reaction with the carbon of the crucible, which is kept at a high temperature under a high vacuum.

The Feichtinger St Re 0583 commercial instrument was employed [4]: it makes use of a water-cooled, stainless-steel, carbon resistance-heated furnace and accumulates the analysed samples in an open graphite crucible. For the determination of carbon monoxide, it utilizes a gas chromatograph (helium carrier gas; molecular sieve column at 125°C; thermal conductivity detection) which is calibrated by the injection of known amounts of carbon monoxide delivered by a system of magnetic valves. The gaseous mixture (H_2, N_2, CO) extracted from the furnace is injected automatically into the gas chromatograph at predetermined time intervals (usually every 3 min; this period is sufficient for the complete elution of the components): this allows the operator to follow the degassing of the sample easily and to prolong it until the instrument blank value is reached. A horizontal glass side-arm, which is at the same high vacuum as the furnace, contains the samples to be analysed in sequence.

Preliminary experiments

These were aimed at determining oxygen in the brass (nominal composition of this brass is given in Table 1) to be used in the cooperative test.

The high volatility of zinc makes the direct analysis of brass by a vacuum carbon-reduction technique practically impossible; the preliminary removal of zinc from the analytical samples in a separate silica furnace at 750—800°C under high vacuum was therefore attempted.

Whilst zinc removal was practically complete in ca. 8 h, there was unquestionable evidence of sample oxidation, attributed to one or more of the following reasons: small, unavoidable air leaks in the vacuum system; silica permeability to air during the zinc removal treatment; exposure of the samples, which after zinc removal are likely to have surfaces in a rather reactive state, to air during the loading in the sample holder of the instrument.

TABLE 1

Nominal composition of brass used

Element	Al	Cu	Fe	Mn	Ni	Pb	Si	Sn	Zn (balance)
% weight	1.6	57.7	0.15	2.0	<0.1	0.6	0.6	<0.1	(37.3 by difference to 100)

To overcome these difficulties, it was decided to de-zinc the samples in the instrument itself, after sealing the samples in small pre-degassed lidded graphite capsules (o.d. 1 cm, height 1.8 cm), which would subsequently have been degassed with their residual content in the crucible of the instrument.

It was assumed that the capsules would provide a barrier against any possible sample oxidation and that there would also be the advantage of allowing the samples to be moved to the furnace of the instrument without breaking the vacuum. In addition, the capsules would enable the small residue left by unalloyed zinc samples to be transferred easily without loss.

The horizontal glass sample holder was then extended with a silica tube (i.d. 23 mm, length 300 mm) which could be heated by a cylindrical external furnace, in which the zinc removal treatment was carried out.

Final procedure

The following analytical procedure has been adopted for the analysis of brass and zinc as a result of some experiments to be discussed below. The samples are prepared, weighed, sealed into the pre-degassed capsules and loaded into the silica tube; the usual precautions, e.g. handling the samples and capsules with clean forceps, are observed. Since the largest graphite crucible which may be used for the analytical degassing has a limited volume capacity, the number of capsules is restricted to six, of which two are usually left empty and serve for blanks. The entire instrument is evacuated to a high vacuum and the capsules subjected to zinc removal at 850—870°C for 15—16 h (overnight) for brass samples or for 2 h for zinc samples. (The time period quoted extends from "heating on" to "heating off" and includes the time necessary to reach 850—870°C from room temperature; see below.) The graphite crucible can meanwhile be outgassed at 1650—1700°C. When the de-zincing treatment is finished and the instrument blank low enough, the capsules are pushed with an iron cylinder, advanced manually by a small external magnet, to the instrument furnace maintained at the constant operating temperature of 1450°C. They are then added successively and degassed for analysis until the instrument blank value at 1450°C is reached.

From the carbon monoxide evolved, the oxygen content of the samples is evaluated, allowance being made for the carbon monoxide coming from the capsules and from the instrument. The degassing time is usually of the order of 6—9 min; the instrument blank is measured before and after each analysis, the mean value being used in the calculations.

RESULTS AND DISCUSSION

Since graphite contains large amounts of gases, the capsules (weight ca. 2 g) need to be pre-degassed before use. This operation was carried out at ca. 1700°C under vacuum in the crucible of the instrument itself; after such treatment the capsules, stored in a clean beaker, did not appear to re-adsorb large quantities of gases even if exposed to the air for days: thus pre-degassing

immediately before analytical use is not mandatory. In addition, although the cover of each capsule was firmly screwed to the capsule body after the sample was added, they are not vacuum-tight: thus any air enclosed is removed when the silica tube is evacuated. Replicate analyses with empty capsules, by the procedure described, showed an average oxygen content of ca. 1.5 μg with a standard deviation of ca. 1 μg, which did not appear to bear a definite relationship either to the length of the zinc removal treatment or to the period of storage.

For the brass of nominal composition given in Table 1, 8 determinations gave results ranging from 0.8—3.3 ppm (mean, 1.7 ppm; s = 0.8); on the basis of preliminary results from 3 neutron and 1 He^3 activation laboratories thought to be free from important systematic errors [5], the probable oxygen content is 2.3 ± 0.5 ppm. The samples (1.15 g, length 0.7 cm, diam. 0.5 cm) were prepared by careful machining on a lathe and analysed according to the final procedure; from the geometric dimensions, their surface oxygen was estimated [1] to be 0.5 ppm, and this was deducted from the gross results.

Before performing these determinations, an independent test to estimate the efficiency of the zinc removal process, made on 4 samples of the same material of identical dimensions, showed that, on average, 35.3% of zinc was extracted from the samples after 16 h. This value compares favourably with the nominal zinc content of this brass (Table 1).

The de-zincing furnace reached ca. 750°C within 1 h, and reached its equilibrium temperature of 850—870°C after a further hour; the temperature fell from 850°C to less than 600°C in 10 min when heating was shut off. Zinc began to appear on the cooler parts of the silica tube ca. 30 min after heating was started (temperature then ca. 580—600°C): although a period of 16 h is more than sufficient to remove zinc from this brass sample and those of comparable dimensions, it was convenient to gain operator time by leaving the furnace unattended overnight. As expected, the samples did not gain oxygen during the treatment; nevertheless a partial sample reduction by the graphite of the capsule may have taken place at 850—870°C.

In general, brasses contain various proportions of alloying elements such as those indicated in Table 1 [6] and oxygen should be present as the oxide with greatest stability, i.e. as Al_2O_3; if Al, Si and Mn are not constituents, oxygen should be present as ZnO, which can be considered as the oxide of the lowest stability which could in practice be encountered in brasses. Although thermodynamics indicate the possible reduction of ZnO at 850—870°C, it should not proceed to any great extent, if at all, since brasses are not molten at the temperature of the zinc removal treatment [6]; thus it is unlikely that bulk oxygen will reach the sample surface brought into contact with graphite.

This assessment was verified, as far as possible, by submitting small amounts of ZnO to the treatment for 16 h and then to analysis at 1450°C. To avoid direct contact with the graphite and to simulate environmental conditions

ZnO was sealed into the capsules, together with either previously analysed or untreated pieces of brass weighing about 0.5 g, wrapped in thin (thickness 40—80 μm; weight 35—70 mg) copper foil. To check if the procedure could determine oxygen derived from very stable oxides, tests were also made by spiking the samples in the same manner with Al_2O_3. Before use, ZnO and Al_2O_3 were calcined in an air muffle at 800°C and 1100°C, respectively. Table 2 presents the results obtained; reduction of ZnO did not take place during the step at 850—870°C, and oxygen recovery from Al_2O_3 was practically complete. Although the oxygen extraction for ZnO at 1450°C took place in the usual 6—9 min, 9—30 min was necessary for Al_2O_3. Blanks of the copper foil and the brass pieces were deducted from the gross results, on the basis of analyses made under the same conditions.

As samples of known oxygen content were not available, the procedure for zinc was again assessed by means of zinc oxide-spiked samples. Environmental conditions were simulated by sealing into the capsules small amounts of oxide wrapped in zinc foil, together with 0.5 g of zinc in pieces. The experiments seemed to indicate a slow reduction of ZnO during the de-zincing treatment; this was attributed to the fact that the samples were in a liquid state (Zn m.p. 420°C) which favoured the kinetics of the reduction.

As a consequence, the shortest treatment time compatible with an acceptable degree of reduction and full zinc removal was selected on the basis of preliminary experiments; these showed that 550°C for 16 h was largely insufficient to remove zinc completely from the capsules, and that 650°C for 16 h, whilst sufficient, gave rise to a pronounced ZnO reduction.

TABLE 2

Oxygen recovery in spiked brass samples

Oxide added	mg	O added (μg)	O recovered (μg)	Recovery (%)
ZnO[a]	0.2014	39.6	43.8	110.6
	0.3570	70.2	71.1	101.3
	0.4655	91.5	99.1	108.3
ZnO[b]	0.1930	37.9	38.2	100.8
	0.4548	89.4	89.9	100.6
	0.1992	39.2	37.8	96.4
Al_2O_3[a]	0.1250	58.8	53.3	90.6
	0.2330	109.7	109.0	99.4
Al_2O_3[b]	0.2719	128.0	129.6	101.3
	0.2583	121.6	110.2	90.6

[a,b]Copper foil obtained by roll-pressing etched before use with a mixture of HNO_3 fum./H_2O (1/3) to remove surface contamination, rinsed with water and then with alcohol.
[a]0.5 g of previously analysed brass added to the capsule.
[b]0.5 g of untreated brass added to the capsule.

TABLE 3

Oxygen recovery in spiked zinc samples[a]

Oxide added	mg	O added (μg)	O recovered (μg)	Recovery (%)
ZnO[b]	0.8964	176.2	165.2	93.8
	0.3776	74.2	65.6	88.4
	0.9820	193.1	185.4	96.0
ZnO[c]	0.7334	144.2	117.6	81.6
	0.7108	139.7	127.8	91.5
	0.4859	95.5	90.5	94.8
ZnO[d]	0.5026	98.8	82.4	83.4
	0.4464	87.8	71.6	81.5

[a]Zinc foil obtained by roll-pressing and zinc pieces etched before use with a mixture of HNO_3 fum./H_2O (1/5) to remove surface contamination, rinsed with water and then with alcohol.
[b]De-zincing treatment at 850—870°C, 2 h.
[c]De-zincing treatment at 850—870°C, 4 h.
[d]De-zincing treatment at 650°C, 16 h.

Table 3 shows the results obtained for spiked zinc samples. Zinc removed from the samples remains on the walls of the silica tube and horizontal glass sample holder from which it is easily removed at the end of each working day by washing with dilute hydrochloric acid followed by rinses with water followed by alcohol.

The instrument blanks at 1450°C were of the order of 2—3 μg of oxygen in 3 min but showed an excellent stability, so that in the analysis of homogeneous samples the main cause of variability in the results should be given by the fluctuation of the oxygen content of the graphite capsules (see above). Capsules can accommodate up to 1.5-g samples: if the limit of detection of the procedure is defined as a sample oxygen content equal to the standard deviation of the oxygen content of the capsules, the limit is ca. 0.5—1 ppm.

REFERENCES

1 P. Boisot, M. Cuypers, G. Kraft, J. Pauwels, L. Quaglia and G. Weber, L'Influence du Traitement de Surface des Echantillons sur le Dosage de l'Oxygene dans les Metaux Non-ferreux, Eurisotop Office, ITE Report n° 76, 1972.
2 L. Quaglia, G. Weber, D. David, J. van Audenhove and J. Pauwels, Surface Treatment of Non-ferrous Metals for the Purpose of Gas Analysis, Eurisotop Office, ITE Report n° 90, 1976.
3 J. Pauwels, Community Programme on the Assay of Non-metals in Non-ferrous Metals, BCR Information, EUR Report 5517, 1976.
4 H. Feichtinger, H. Baechtold and W. Schuhknecht, Schweiz. Arch., 12 (1959) 426.
5 J. Pauwels, private communication.
6 C. J. Smithells, Metals Reference Book, Butterworths, London, 1962, p. 942—943.

Analytica Chimica Acta, 94 (1977) 343—350

LIQUID CHROMATOGRAPHIC SEPARATION OF ELECTROCHEMICAL OXIDATION PRODUCTS OF BIOLOGICALLY IMPORTANT PURINES

MICHAEL T. CLEARY and GLENN DRYHURST*

Department of Chemistry, University of Oklahoma, Norman, OK 73019 (U.S.A.)

(Received 19th July 1977)

SUMMARY

A liquid chromatographic method utilizing a dual column system (Sephadex G-10 gel permeation and Sephadex QAE A-25 anion exchange) has been developed for the quantitative separation of mixtures of compounds found as products of electrochemical oxidation of biologically important purines. Milligram quantities of such product mixtures may be separated and quantitative analysis is also possible in some cases.

Over the past several years, this laboratory has been concerned with the electrochemical oxidation of biologically important purine derivatives and the relationship between the electrochemical reaction mechanisms and products and the biological reactions of these molecules [1, 2]. A major difficulty has been the separation and identification of the large variety of reaction products formed. Previous studies have employed thin-layer chromatography, polarography, and spectrophotometric methods for both qualitative and quantitative analysis of reaction product mixtures. Many of these techniques, when applied to complex mixtures, are subject to a variety of uncertainties and errors; the complexity of the mixtures from the electrochemical oxidation of nucleoside and nucleotide derivatives of purines is such that these analytical techniques could not be utilized with confidence.

Accordingly, it became necessary to develop a technique for the separation of milligram quantities of relatively complex reaction mixtures such that sufficient pure product could be isolated for mass spectral, i.r., and other studies, and which could also be used to provide quantitative information on the yields of these reaction products.

The simplest and most straightforward purine electrooxidation is observed with uric acid [3]: at low pH, alloxan, urea, and CO_2 are the major products; at pH 2—7, allantoin, urea, and CO_2 are the major products. At some pH values parabanic acid is a minor product. It was decided to attempt to develop a suitable analytical technique which could separate all these organic materials simultaneously. In addition, oxaluric acid, which has also been observed in some purine electrooxidations [4] and D-ribose, a likely product from purine nucleoside electrooxidations, were also added to the

mixture. Thus, a mixture composed of D-ribose, urea, alloxan, parabanic acid, allantoin, and oxaluric acid was thought to contain the basic structural functionalities of products which might be expected from other purine electrooxidations. A technique which could separate and quantify this mixture satisfactorily on a milligram scale should provide a basic method for the separation of more complex reaction mixtures from purine nucleosides and nucleotides.

The technique reported here is based on a combination of gel permeation, ion exchange, and adsorption column chromatography.

EXPERIMENTAL

Chemicals

Alloxan monohydrate, oxaluric acid (Nutritional Biochemicals), D-ribose (Calbiochem), allantoin, parabanic acid (Eastman) and urea (Merck) were used. Buffer solutions were prepared from reagent-grade chemicals.

Sephadex G-10, Sephadex SP C-25 and Sephadex QAE A-25 resin (all 40—120-μm particle size) were obtained from Pharmacia.

Apparatus

Column chromatography utilized SR 25/45 (2.5 × 45 cm) and SR 25/100 (2.5 × 100 cm) columns (Pharmacia); a three-way valve (Pharmacia) was used to introduce samples. The eluant from the columns was collected with a Buchler Fractomat fraction collector; generally, each test tube collected 3-ml fractions. The u.v. absorbance of the fractions so collected was measured in 1-cm quartz cells at 199 nm, at which all compounds of interest exhibited significant absorption [5] in a Hitachi Model 124 spectrophotometer.

Column preparation

Prior to column preparation, Sephadex G-10 gel was allowed to swell in an excess of H_3PO_4—KH_2PO_4 buffer, pH 2.0, of ionic strength 0.1. Sephadex QAE A-25 anion-exchange gel and SP C-25 cation-exchange gel were allowed to swell in HOAc/KOAc buffer, pH 4.7, ionic strength 0.05. This initial swelling process was allowed to occur over 2 days at room temperature with continuous stirring; the excess of buffer solution was then removed and a fairly thick slurry of the appropriate gel was packed into a suitable column by recommended techniques [6, 7]. The packed columns were stabilized and equilibrated before use by passing at least two column volumes of the appropriate eluant, degassed by boiling and cooling, through the column at a flow rate similar to that employed for actual separations (e.g., 40 ml h^{-1}). For experiments with Sephadex SP C-25 gel, a SR 25/45 column was packed to a height of 35 cm. Sephadex QAE A-25 gel was packed (25 cm) in a SR 25/45 column. Sephadex G-10 gel was packed (91 cm) in a SR 25/100 column.

When Sephadex G-10 and Sephadex QAE A-25 columns were connected in series, the arrangement shown in Fig. 1 was used. The three-way valve V_2 (Fig. 1) was used to couple the two columns, equilibrated as described earlier, except that 0.025 M KH_2PO_4 (pH 4.3) was employed as the eluant for both columns; V_2 was also used to stop the flow of 0.025 M KH_2PO_4 eluant through the G-10 columns and allow introduction of 0.25 M KH_2PO_4 from a separate reservoir as the eluant for the second QAE A-25 column (Fig. 1). All liquid chromatography was carried out at room temperature.

Chromatographic procedure with coupled G-10 and QAE A-25 columns

Urea, D-ribose, allantoin, alloxan, parabanic acid and oxaluric acid were dissolved in 1 ml of 0.025 M KH_2PO_4 solution at appropriate concentration levels. This solution was drawn into a 2-ml syringe and applied to the top of the G-10 column through valve V_1 (Fig. 1). A flow rate of 40 ml h^{-1} was typically employed. Fractions (3 ml) of the eluant from the QAE A-25 column were collected. D-Ribose, urea, allantoin, alloxan and parabanic acid were separated with 0.025 M KH_2PO_4 as a the eluant; ca. 1050 ml of solvent was required to elute these five components (see below). Oxaluric acid is strongly retained on the QAE A-25 anion-exchange resin; to elute this compound (and, presumably, other anionic species) the eluant through

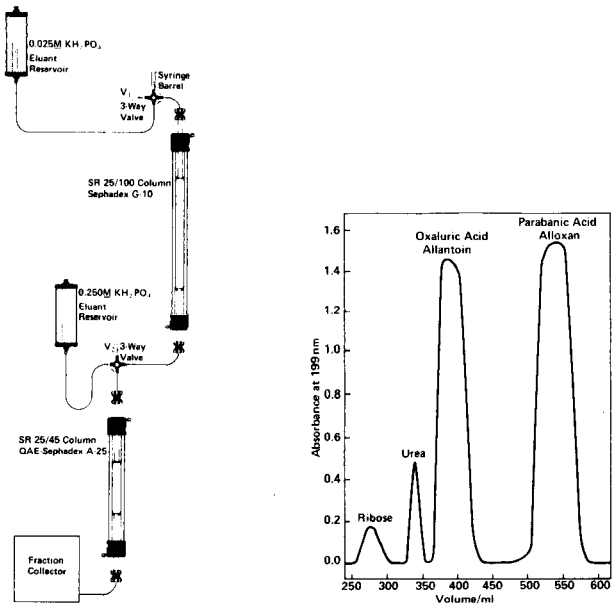

Fig. 1. Schematic arrangement for the dual column chromatographic system.

Fig. 2. Chromatogram of a mixture of urea (2 mg), D-ribose (20 mg), allantoin (1.3 mg), alloxan (1.3 mg), parabanic acid (1.3 mg), and oxaluric acid (1.3 mg) dissolved in 1 ml of KH_2PO_4/H_3PO_4, pH 2.0, ionic strength 0.5. Column: Sephadex G-10 91 × 2.5 cm. Eluant: phosphate buffer, pH 2.0, ionic strength 0.5. Flow rate, 40 ml h^{-1}.

the QAE A-25 column was changed to 0.25 M KH_2PO_4 by means of valve V_2 (Fig. 1).

Working curves were obtained for urea, allantoin, alloxan, parabanic acid, and oxaluric acid by running chromatograms on a series of solutions containing 0.25—1.5 mg ml^{-1} of each compound. The average detector response (i.e., of each fraction measured at 199 nm in a 1-cm cell) was determined as peak height (absorbance) or peak area, obtained by a conventional triangulation method.

When the eluant through the Sephadex QAE A-25 column is changed from 0.025 M KH_2PO_4 to 0.25 M KH_2PO_4 the column packing shrinks by about 2 cm. This occasionally results in a very substantial decrease in flow rate, which can only be increased by a reversed flow of 0.025 M KH_2PO_4 through the column at ca. 20 ml h^{-1} for 5 h.

RESULTS AND DISCUSSION

Solutions of alloxan are not stable, particularly at pH values above 4, when hydrolysis to alloxanic acid occurs [8, 9]. Parabanic acid also slowly hydrolyses to oxaluric acid at pH $\geqslant$ 6 and thence to oxalic acid and urea [10]. Accordingly, to minimize decomposition of alloxan, parabanic acid and oxaluric acid, eluant systems of pH 2—5 were employed. Within this pH range most of the compounds of interest are either neutral species or partially in their anionic form. Reported pK_a values are: allantoin, 8.96 [11], alloxan monohydrate, 7.20 [12]; oxaluric acid, 2.00 [10]; and parabanic acid, 6.10 [10].

Initial attempts to separate a mixture of alloxan, allantoin, parabanic acid, oxaluric acid, D-ribose, and urea utilized various types of ion-exchange resins as the column packing. With Sephadex SP C-25 resin, and eluants of various ionic strength at pH values of 2—4, only oxaluric acid could be separated from the other five components, which eluted as a single peak. With Sephadex QAE A-25 resin and an acetate buffer system similar to that recommended by Pit et al. [13], alloxan, parabanic acid, and oxaluric acid could be adequately separated. However, it was not possible to separate alloxan from allantoin or urea and D-ribose even though a variety of ionic strength buffer gradients, column lengths and flow rates were employed.

Accordingly, the use of Sephadex G-type gel permeation packings were examined. These are normally used to fractionate high-molecular-weight substances according to their molecular dimensions [14], but they adsorb molecules with π-electron systems reversibly provided that their molecular sizes are small enough to permit diffusion into the gel matrix [15]. The extent of adsorption which can take place depends on the amount of gel accessible to the solute; the greater the penetration, the greater the extent of adsorption [17]. In buffer systems of low pH, unionized organic acids tend to be adsorbed by π-electron interactions or by hydrogen bonding to the gel matrix [16]. Thus, by control of the pH of the eluting medium, it is

possible to effect separations of acidic organic compounds with different dissociation constants.

With eluant systems of pH 2—5 and ionic strengths ranging from 0.025 to 0.5, separations of the six-component mixture of interest were attempted with Sephadex G-10 gel. With only minor differences, all chromatograms had the appearance of that shown in Fig. 2. Thus, although D-ribose and urea could be separated from the other components, oxaluric acid and allantoin eluted together, as did parabanic acid and alloxan. As previous studies (see above) indicated that parabanic acid and alloxan and allantoin and oxaluric acid could be separated with Sephadex QAE A-25, a two-column separation involving Sephadex G-10 gel and Sephadex QAE A-25 resin was investigated (see Fig. 1). With phosphate buffer pH 4.3 as the eluting medium, at ionic strengths greater than 0.1, alloxan and parabanic acid could not be completely resolved. However, with 0.025 M potassium phosphate pH 4.3 as the eluant, D-ribose, urea, allantoin, alloxan, and parabanic acid gave well-resolved chromatographic peaks, although oxaluric acid was not eluted. Experiments revealed that oxaluric acid was strongly retained by the QAE A-25 resin and could only be eluted in a reasonable period by increasing the ionic strengths of the KH_2PO_4 eluant to 0.25 M. Accordingly, a complete separation of all six components could be accomplished with 0.025 M KH_2PO_4 as the initial eluant through both columns. When the first five components had been eluted, the eluant through the anion-exchange column was changed to 0.25 M KH_2PO_4, using the arrangement shown in Fig. 1; oxaluric acid was then eluted. A typical chromatogram showing the separation of the six-component mixture under these conditions is shown in Fig. 3.

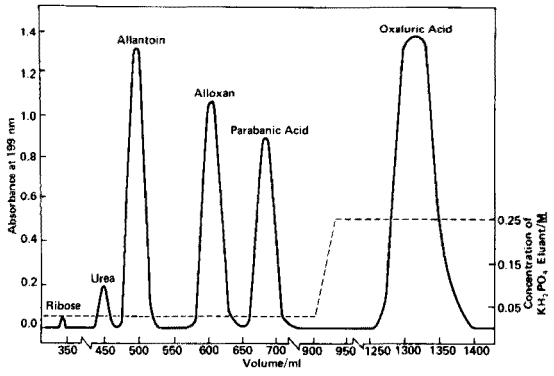

Fig. 3. Chromatogram of a mixture of urea (2 mg), D-ribose (13 mg), allantoin (1.3 mg), alloxan (1.3 mg), parabanic acid (1.3 mg), and oxaluric acid (1.3 mg) dissolved in 1 ml of 0.025 M KH_2PO_4, pH 4.3. The arrangement of chromatographic columns is shown in Fig. 1. Bed-heights; Sephadex G-10, 70 cm; Sephadex QAE A-25, 35 cm. Step elution method for the first five components (0.025 M KH_2PO_4); the last component was eluted with 0.25 M KH_2PO_4 from the QAE A-25 column. Flow rate, 40 ml h^{-1}.

Retention volume data for all six components under optimum chromatographic conditions are presented in Table 1; these retention volumes are not influenced by the presence of the other test species in solution, and the retention volume data may be used for qualitative identification of the eluting species.

The resolution (R_s) of adjacent chromatographic peaks was determined from

$$R_s = 2(V_2 - V_1)/(w_1 + w_2) \quad (1)$$

where V_1 and V_2 are the retention volumes of two adjacent peaks and w_1 and w_2 are their baseline peak widths, respectively [17]. The resolution values for adjacent peaks in the six-component mixture under conditions such as those described in Fig. 3, were all $\geqslant 1.5$. At R_s values of 1.5, or greater, the two peaks may be regarded as being completely separated with less than 1% cross contamination between the components under each peak [17]. However, injection of 1-ml samples containing more than 1.3 mg of parabanic acid and alloxan (see Fig. 3) caused the R_s value to decrease; when the amount of both parabanic acid and alloxan in the 1-ml sample injected was 1.49 mg, the R_s value decreased to 1.0. A smilar effect was noted for the urea and allantoin peaks when the injected amounts exceeded 2.0 mg and 1.3 mg, respectively.

Analytical curves

To evaluate the use of chromatograms, such as that shown in Fig. 3, for quantitative analysis of the individual components, a series of analytical curves were prepared. For D-ribose, the absorbance at 199 nm of even relatively concentrated solutions is so low that useful absorbance vs. concentration curves could not be obtained. Oxaluric acid also gave non-reproducible peak height or peak area vs. concentration results, presumably because the solvent change required to elute oxaluric acid from the QAE A-25 column caused distorted chromatographic peaks.

TABLE 1

Retention volumes for the chromatographic separation of typical purine electrooxidation products[a]

Compound	Retention[b] volume (ml)	Relative retention volume[c]
D-Ribose	344	0.69
Urea	448	0.90
Allantoin	498	1.00
Alloxan	602	1.21
Parabanic acid	682	1.37
Oxaluric acid	1314	2.64

[a]Under conditions outlined in Experimental and Fig. 3. [b]Flow rate 40 ml h^{-1}. [c]Relative to allantoin.

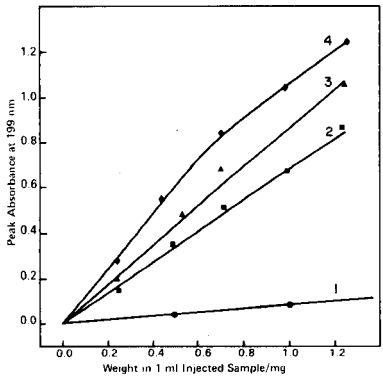

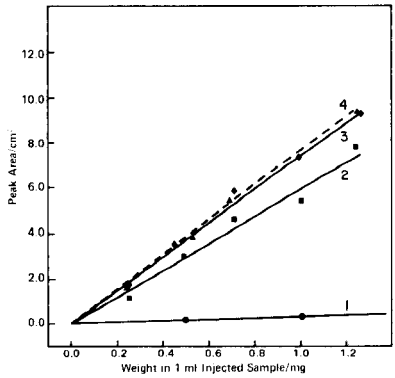

Fig. 4. Peak height vs. concentration curves for urea (1), parabanic acid (2), alloxan (3) and allantoin (4). Chromatographic conditions as described in Fig. 3.

Fig. 5. Peak area vs. concentration curves for urea (1), parabanic acid (2), alloxan (3), and allantoin (4,---). Chromatographic conditions as described in Fig. 3.

For urea, allantoin, parabanic acid and alloxan, analytical curves based on peak height measurements are shown in Fig. 4. With the exception of allantoin, the compounds give reasonably linear plots. Plots of peak area vs. concentration gave more reproducible and linear analytical curves (Fig. 5). The absorbance of urea at 199 nm is significantly less than those for alloxan, allantoin, and parabanic acid, and analyses for urea based on curves such as those shown in Figs. 4 and 5 would be, at best, only semi-quantitative.

When the amount of urea, alloxan, allantoin, and parabanic acid in the 1-ml injected sample exceeded 1.3 mg, appreciable peak broadening and distortion occurred and plots of peaks absorbance or peak area vs. concentration became non-linear.

Conclusions

The dual gel permeation-anion-exchange column liquid chromatographic method is useful for the separation of six common electrochemical oxidation products of purines; milligram quantities of these material are sufficient to allow their isolation and identification by conventional chemical and instrumental methods. In the case of urea, alloxan, allantoin, and parabanic acid, the height or area of the chromatographic peaks may be used for quantitative analysis.

The general methodology reported should be applicable to the separation and analysis of electrochemical (and biochemical) oxidation products of more complex purine and other *N*-heterocyclic systems.

The authors acknowledge the assistance of Victor Savage in some aspects of this work, which was supported by the National Institutes of Health through Grant No. GM-21034.

REFERENCES

1 G. Dryhurst, Topics in Current Chemistry, 34 (1972) 47.
2 G. Dryhurst, Electrochemistry of Biological Molecules, Academic Press, New York, 1977.
3 G. Dryhurst, J. Electrochem. Soc., 119 (1972) 1559.
4 G. Dryhurst and P. J. Elving, J. Electrochem. Soc., 115 (1968) 1014.
5 D. H. Rodgers, Am. Lab., 9 (1977) 133.
6 Gel Filtration in Theory and Practice, Pharmacia Fine Chemicals AB, Uppsala, Sweden, 1974.
7 D. Eaker and J. Porath, Sep. Sci., 2 (1967) 507.
8 G. M. Richardson and R. R. Cannon, Biochem. J., 23 (1929) 68.
9 D. Seligson and H. Seligson, J. Biol. Chem., 190 (1951) 647.
10 J. C. Andrews and L. T. Sell, Arch. Biochem. Biophys., 56 (1955) 405.
11 R. C. Weast (Ed.), CRC Handbook of Chemistry and Physics, 1972—1973.
12 W. A. Struck and P. J. Elving, J. Am. Chem. Soc., 86 (1964) 1229.
13 W. W. Pit, C. D. Scott, W. F. Johnson and G. Jones, Clin. Chem., 16 (1970) 657.
14 J. Porath and P. Flodin, Nature, 183 (1959) 1657.
15 B. Gelotte, J. Chromatogr., 3 (1960) 330.
16 A. J. W. Brook and S. Housley, J. Chromatogr., 42 (1969) 112.
17 B. L. Karger, L. R. Snyder and C. Horvath, An Introduction to Separation Science, J. Wiley, New York, 1973.

Analytica Chimica Acta, 94 (1977) 351—356

TURBULENT HYDRODYNAMIC VOLTAMMETRY
Part III. Analytical Investigations with a Turbulent Voltammetric Cell and Applications to Amino Acid Analysis

M. VARADI[§] and E. PUNGOR*

Institute for General and Analytical Chemistry, Technical University, Budapest (Hungary)

(Received 10th June 1977)

SUMMARY

The analytical applicability of a turbulent voltammetric cell in a flowing stream has been studied. A silicone rubber-based graphite electrode is used. Under optimal conditions, the distortion of the signal in the cell as well as the fluctuations of the signal cause a relative standard deviation of 1% in the results. An examination of the amino acids which occur in protein hydrolyzates is reported. Proline, histidine and arginine can be determined with standard deviations of about 4%; the standard deviations range from 10% to 16% for the other amino acids, except threonine, serine and tyrosine which cannot be determined.

Some of the important characteristics of a turbulent hydrodynamic voltammetric cell have been reported in earlier papers [1, 2]. In these studies, the effect of the electrode surface on the measured electric current and the way in which the Prandtl layer was established through the turbulent flow were examined. The results showed that the diameter of the electrode should be smaller than the cross-section of the jet flowing at a high rate, and that the turbulent mass transport produces oscillations in the current signal corresponding to the oscillations on the boundary layer surface. These oscillations obey the energy transfer rules.

The aim of the work described here was to examine, on the basis of the knowledge accumulated earlier about the physical characteristics of the turbulent cell, whether or not analytical applications of this cell would be possible. The first aspects investigated were the distortion of the voltammetric signal established at the measuring electrode and the standard deviation of the results obtained. Analytical applications were then demonstrated for a few examples.

EXPERIMENTAL

Materials and equipment

The chemicals used were of analytical grade (Reanal, Budapest).

[§] Permanent address: Labor MIM Laboratory Instruments and Equipment Works, Budapest, Hungary.

The equipment has already been described [1, 2]. In the measuring cell the jet was placed perpendicular to the surface of the silicone rubber-based graphite electrode, thus ensuring the establishment of the turbulent flow. The liquid was transferred by means of a micro-pump (Labor MIM Type LS-204) which ensured a nearly sinusoidal transport of the solution. The voltammetric signal was recorded with a Phillips oscilloscope (PM 3251). The analytical measurements were made with a Radelkis polarograph (Type OH-102) or a voltammetric unit (Labor MIM) with a Radelkis recorder (Type OH-814/1).

RESULTS AND DISCUSSION

Distortion of the voltammetric signal formed at the measuring electrode

The voltammetric signal in relation to the flow rate of the streaming solution before the jet was measured, and simultaneously the signal established at the electrode placed after the jet was recorded. The streaming liquid was 10^{-3} M $K_4Fe(CN)_6$ solution. The solution was passed continuously through the measuring equipment, an almost sinusoidal transport being ensured by the pump. The measuring electrodes were a platinum wire before the jet, and a silicone rubber-based graphite electrode after the jet. The results are shown in Fig. 1. On the basis of the record obtained with a memory oscilloscope, it was found that under the conditions applied (frequency of the feeding pump, 30/min; stroke length, 12 mm; jet diameter, 0.5 mm; distance between the electrodes placed before and behind the jet, ca. 20 cm), the signal starts on the electrode after the jet with a delay of 20 ms. The time was measured accurately with the help of a superimposed current signal of 50 Hz. The current signal which starts on the electrode after the jet after 20 ms, does not increase sinusoidally; the function is distorted so that the increase in the current intensity is steeper than behind the pump, i.e. in the space before the jet.

Because of the compressibility of the solution, the sinusoidal pump action does not provide a sinusoidal liquid flow at the electrode surface, and so the voltammetric signal obtained is not regular either.

At the maximum movement of the piston, i.e. at the end of the feed, the signal shows an exponential decay.

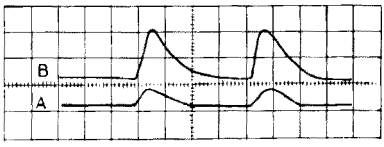

Fig. 1. (A) The current signal measured on the electrode placed before the jet. Amplification, 110; sensitivity, 10 mV/div; time axis, 0.5 s/div. (B) The current signal measured on the electrode placed after the jet. Amplification, 110; sensitivity, 100 mV/div; time axis, 0.5 s/div.

Standard deviation of the results

It has been shown [2] that the current fluctuation corresponding to the turbulence is superimposed on the distorted sinusoidal signal. If the other physical conditions which may cause distortion of the signal are unchanged, then the standard deviation must include the current fluctuations originating from turbulence. These current fluctuations have components of various frequencies and amplitudes. Hence, the analytical signals corresponding to the amounts of individual substance transferred can be compared only if the integral of the resultant current for the whole signal interval is considered.

To calculate the standard deviation, a 10^{-3} M $K_4Fe(CN)_6$ solution was passed through the cell, and the area under the curve of the individual current signals was determined graphically. The data obtained are summarized in Table 1. The standard deviation of the current signal established at the electrode placed opposite the jet, i.e. in the axis of the jet, was less than 1%; even when the electrode was placed on the periphery, the standard deviation was below 3%, i.e. the turbulent flow fluctuations did not cause errors greater than are generally encountered in analytical measurements. Only if the electrode is placed at a greater distance from the jet is the standard deviation significantly greater: because of reduction in the flow rate and back-mixing, the noise level increases significantly and the whole flow pattern becomes more complicated.

Analytical application

These measurements proved that the sensitivity of this turbulent voltammetric cell, the relationship between concentration and current signal, and the noise conditions, meet the requirements of modern chemical analysis.

Earlier work showed that the lower detection limit was 10^{-10} mol [3]; the turbulent measuring cell was applied to the liquid chromatography of purine bases, after preliminary tests with stationary and then flowing systems. In the present work, the measuring cell was applied to the determination of amino acids. Fleet and Little [4] suggested the application of

TABLE 1

Standard deviation of the signals measured with the electrode in different positions (Sample, 10^{-3} M $K_4Fe(CN)_6$; flow rate, 108 cm s^{-1}; potential, +0.80 V vs. Ag/AgCl.)

Position of electrode		n	R.s.d. (%)
x[a]	y[b]		
0	1.5	12	0.93
3.5	1.5	8	2.45
0	4.5	8	4.25

[a]Distance from the axis of the jet (mm).
[b]Distance from the tip of the jet measuring in the axis of the jet (mm).

a voltammetric cell with a glassy carbon indicator electrode to the chromatographic determination of amino acids.

The amino acids were first examined in a stationary system; under such conditions, amino acids could not be electrochemically oxidized at the silicone rubber-based graphite electrode by changing the electrode potential. However, with some amino acids, quite usable analytical curves could be obtained if the measurements were made in a flowing solution at constant voltage. Figure 2 shows the voltammetric curves obtained by injecting 1-ml aliquots of proline solutions of different concentrations into a supporting electrolyte containing 0.1 M KCl solution and borate buffer pH 8.99. A good linear relationship was found for the range 0.1—2.5 × 10^{-6} mol of proline; the signals were the average areas of the time—current curves obtained for three injections.

An examination of the amino acids occurring in protein hydrolyzates yielded the results summarized in Table 2. In each case, 1 ml of the injected sample volume contained 2.5 μmol of the amino acid. The experimental conditions were the same as described above for proline. Because of the different structures of the amino acids, their kinetic behaviour during oxidation also differs. As Table 2 shows, histidine, arginine and proline gave reproducible voltammetric peaks. With these three amino acids, there is a linear relationship between the concentration of the amino acid and

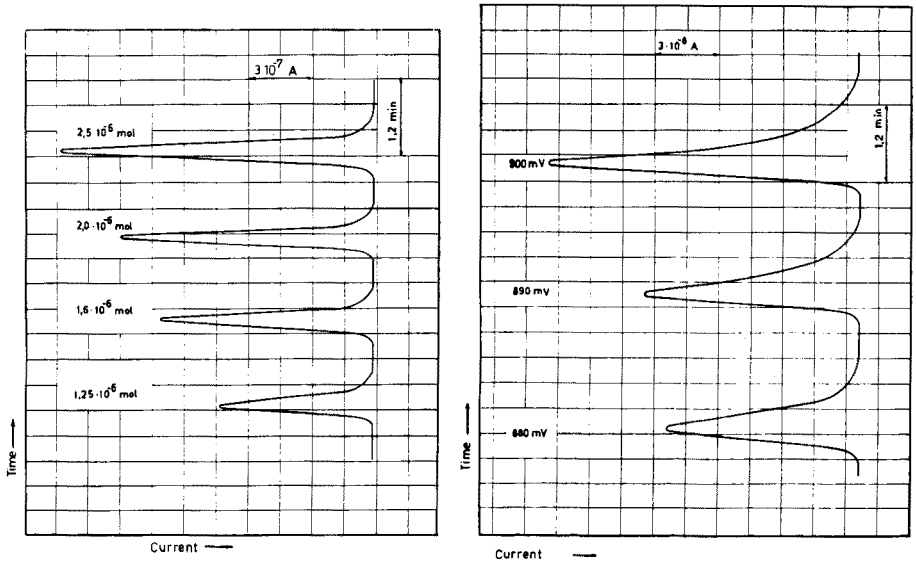

Fig. 2. The current signal obtained by the injection of proline. Supporting electrolyte, 0.1 M KCl and borate buffer pH 8.99. Volume of sample, 1 ml. Flow rate, 108 cm s^{-1}. Potential, 1.0 V (vs. Ag/AgCl).

Fig. 3. Injection of cystine at different applied voltages. Amount of sample, 2.5 × 10^{-6} mol. Volume of sample, 1 ml. Supporting electrolyte, 0.1 M KCl and borate buffer pH 8.99. Flow rate, 108 cm s^{-1}.

TABLE 2

Examination of the amino acids occurring in protein hydrolyzates at a silicon rubber-based graphite electrode with the injection technique
(Supporting electrolyte, 0.1 M KCl and borate buffer pH 8.99. Amount of sample, 2.5 μmol. Volume of sample, 1 ml. Flow rate, 108 cm s^{-1}.)

Amino acid	Area under the curve (Cb)	Standard deviation (%)	Applied potential (V)[a]
Lysine	2.8×10^{-5}	15.7	1.0
Histidine	4.2×10^{-5}	4.3	1.0
Arginine	10.8×10^{-5}	3.9	1.0
Aspartic acid	2.5×10^{-6}	8.9	0.9
Threonine	Signal with decreasing amplitude		0.9
Serine	Signal with decreasing amplitude		0.9
Glutamic acid	2.1×10^{-7}	15	0.9
Proline	2.6×10^{-5}	4	1.0
Glycine	2.2×10^{-7}	14.5	0.9
Alanine	1.8×10^{-7}	16	0.9
Valine	2.1×10^{-6}	10.8	0.9
Cystine	4.3×10^{-6}	11	0.9
Methionine	5.2×10^{-7}	15.6	0.9
Leucine	7.6×10^{-7}	10.5	0.9
Tyrosine	Signal with decreasing amplitude		1.0
Phenylalanine	3.4×10^{-7}	16	0.9

[a]Referred to Ag/AgCl electrode.

the signal measured. Accordingly, this method is suitable for the separate measurement of these compounds; if they are present as mixtures, they can be determined after chromatographic separation.

In the case of the other amino acids, the relative standard deviation was 10—15%, and there was a significant reduction in sensitivity. The half-wave potentials for oxidation of these amino acids lie very near the potential of oxygen evolution; accordingly, they can be measured only at potentials where the rate of electrochemical oxidation is low while the current caused by oxygen formation is significant. Figure 3 shows the formation of the current signal when identical amounts of cystine were injected while different voltages were applied to the measuring electrode.

At potentials of 880, 890 and 900 mV, increasing peaks were obtained; but above 900 mV the curves became totally irreproducible. The instrumental sensitivity used for these measurements was about 10 times that used for proline, histidine and arginine.

The signals of reduced amplitude obtained for threonine, serine and tyrosine indicate that the products or intermediates formed in the electrochemical oxidation contaminate the electrode surface. The method is therefore unsuitable for these compounds.

In addition to the compounds mentioned the measuring cell can be applied in analysis for any component that yields a reproducible signal at a silicone rubber-based graphite electrode, i.e. that can be reduced or oxidized within the available potential range. The silicone rubber-based graphite electrodes are suitable for the determination of various pharmaceutical derivatives, alkaloids, amines, chlorine, etc. A table listing these compounds, and the experimental conditions suitable for their measurement, has been reported [5].

The authors thank Mr. M. Gratzl for his valuable help in connection with the turbulence studies.

REFERENCES

1 M. Varadi and E. Pungor, Anal. Chim. Acta, 80 (1975) 31.
2 M. Varadi, M. Gratzl and E. Pungor, Anal. Chim. Acta, 83 (1976) 1.
3 M. Varadi, Zs. Feher and E. Pungor, J. Chromatogr., 90 (1974) 259.
4 B. Fleet and C. J. Little, J. Chromatogr. Sci., 12 (1974) 747.
5 E. Pungor, K. Toth, Zs. Feher, G. Nagy and M. Varadi, Anal. Lett., 8(12) (1975) ix.

Analytica Chimica Acta, 94 (1977) 357—365

A BIO-SELECTIVE MEMBRANE ELECTRODE PREPARED WITH LIVING BACTERIAL CELLS

G. A. RECHNITZ, R. K. KOBOS, S. J. RIECHEL and C. R. GEBAUER

Department of Chemistry, State University of New York, Buffalo, New York 14214 (U.S.A.)

(Received 25th April 1977)

SUMMARY

A novel potentiometric sensor has been devised by coupling intact microorganisms (*Streptococcus faecium*) with an ammonia gas-sensing membrane electrode. The resulting electrode provides a linear response to arginine over the concentration range 5.0×10^{-5}—1.0×10^{-3} M in phosphate buffer pH 7.4, with selectivity over other amino acids. The slope of the calibration graph is —40 to —45 mV/decade during the period 2—20 days after preparation. This membrane electrode with living bacterial cells may serve as a model for the development of other new sensing systems.

Membrane electrodes for many important substances have been developed by coupling an enzyme to an appropriate ion-selective or gas-sensing electrode; progress in this field has been reviewed [1—4]. Recent improvements in gas-sensing membrane electrodes have led to the development of better enzyme electrodes [5—7] which are free from ionic and protein interferences [8]. However, the development of such enzyme electrodes is still limited by the need to isolate, purify, and concentrate the required enzymes, especially since many enzymes which could be used in principle, are not commercially available at the present time.

A novel approach to the development of bio-selective sensors is described here: living microorganisms, such as bacteria, are employed in place of isolated enzymes at the surface of a gas-sensing membrane electrode. This approach offers several possible advantages over conventional enzyme electrodes, e.g. the enzyme extraction and purification steps are eliminated, loss of enzyme activity is often less than in the case of isolated enzymes, thus prolonging the life of the electrode, and the biological activity is optimized through the use of living systems [9]. Moreover, processes requiring a number of enzymes or enzyme cofactors are easy to achieve, since the required substances are already present in the living cell. It has been shown [10—13] that living cells can be immobilized for extended periods with little loss of biological activity.

In this study, a bacterial electrode with response and selectivity to L-arginine is reported. This sensor uses an ammonia gas-sensing electrode in conjunction with the microorganism *Streptococcus faecium*, American Type

Culture Collection No. 9790, formerly classified as *Streptococcus faecalis*, which has been studied extensively in connection with microbiological assays of amino acids [14—16]. This microorganism metabolizes L-arginine to produce ammonia by the sequence [17]:

$$\text{L-Arginine} \xrightarrow{\text{arginine deaminase}} \text{citrulline} + NH_3 \quad (1)$$

$$\text{Citrulline} + H_3PO_4 \xrightarrow{\text{ornithine transcarbamylase}} \text{ornithine} + \text{carbamoylphosphate} \quad (2)$$

$$\text{Carbamoylphosphate} + \text{ADP} \xrightarrow{\text{carbamate kinase}} \text{carbamic acid} + \text{ATP} \quad (3)$$

$$\text{Carbamic acid} \longrightarrow CO_2 + NH_3 \quad (4)$$

Ammonia is produced in large quantities only from L-arginine by this organism [18], a finding which suggests that this bacterial electrode should be selective for L-arginine; apparently citrulline does not penetrate the walls of the intact cells.

EXPERIMENTAL

Apparatus

An Orion Model 95-10 ammonia gas-sensing electrode was used in the construction of the bacterial electrode. Potentials were monitored with a Corning Model 12 Research pH meter in conjunction with a Heath- Schlumberger strip-chart recorder, Model SR-255B. Measurements were made in a thermostated cell at 28.0 ± 0.2°C. A Branson Sonifier cell disrupter was used to obtain broken cell preparations.

Reagents

Streptococcus faecium No. 9790 was obtained from the American Type Culture Collection, Rockville, Maryland. The growth medium included Difco tryptone and yeast extract (VWR Scientific, Buffalo, N.Y.) and glucose (Sigma Chemical Co., St. Louis, Mo). The amino acids L-arginine, L-glutamine, L-asparagine, L-histidine, L-lysine, and L-citrulline, as well as urea (Sigma Chemical Co.), were used without further purification. The stock solutions were prepared in 0.1 M phosphate buffer (pH 7.0 and 7.4), 0.2 M carbonate buffer (pH 10.0) and 0.1 M Tris—HCl buffer (pH 7.4). These stock solutions were prepared fresh as needed and their background ammonia levels were checked with the ammonia gas-sensing electrode. The potentials obtained in all cases indicated the presence of negligible amounts of ammonia.

Procedure

The bacteria were initially grown in a tomato juice—yeast extract—skim milk medium as recommended by the supplier. The medium was prepared as follows: the content of a can of tomatoes was filtered and was allowed to

stand overnight at 10°C. The next day the pH was adjusted to 7.0 with NaOH; 100 ml of this tomato juice was then combined with 100 g of skim milk and 5.0 g of yeast extract. Distilled water was added until the final volume was 1 l. This medium was autoclaved for 10 min. The inoculation was made aseptically with the freeze-dried bacteria (American Type Culture Collection) and growth was carried out at 30°C.

The bacteria grown in the tomato juice—yeast extract—skim milk medium were used to inoculate the tryptone—yeast extract—glucose medium which was used in all subsequent cultivations. This growth medium consisted of 1.0% tryptone, 0.5% yeast extract, 1.0% glucose, 0.25% K_2HPO_4 and 0.25% NaCl, in 0.2 M carbonate buffer [19] at pH 10.0. The glucose-free medium and the glucose solution were autoclaved separately for 5 min. After the solutions had cooled, the glucose solution was added to the medium and the culture was aseptically inoculated with the microorganisms. The growth was carried out at 30.0°C and was measured turbidimetrically at 640 nm with a Bausch and Lomb Spectronic 20 photometer. An uninoculated tube of the medium served as the reference blank. After ca. 11 h, growth began and was completed after ca. 18 h. Cultures could be carried in the medium for 3—4 weeks [14], but new cultures were grown from time to time.

Volumes (10—20 ml) of the culture were centrifuged and the collected cells were washed several times with buffer. The washed cells were collected by centrifugation and applied as a paste to the gas-permeable membrane of the ammonia electrode. The paste was allowed to air-dry and was then weighed. The quantities of bacteria employed were 1—20 mg in the various trials. Such amounts correspond to approximately 10^9 living cells as determined by a viable count [20] carried out in the following manner. A known volume of the culture was taken aseptically and diluted by serial steps over a large range with sterile buffer. Each solution was spread out evenly on the surface of a nutrient agar plate, which consisted of the growth medium plus 1.0% agar. After incubation at room temperature for several days, the colonies in the final plates, which contained 10—100 colonies, were counted visually.

The bacterial paste was held on the electrode membrane by means of a circular dialysis membrane, as previously described for the preparation of enzyme electrodes [5]. The resulting electrode was preconditioned by soaking in buffer for several hours and was stored in buffer when not in use.

For purposes of comparison, several electrodes were also prepared with a cell preparation consisting of an approximately equal number of broken cells. A portion (1 l) of the culture was centrifuged and the collected cells were washed several times with buffer. The cells were ruptured by ultrasonic treatment and the resulting broken cell preparation was concentrated by molecular filtration [21]. The broken cell solution (ca. 4 ml) was passed through a PSED Pellicon molecular filter (25 000 molecular wt. cut off) at 4°C under 50 psi for ca. 8 h. The concentrated broken cell preparation (ca. 0.5 ml) was stored at 4°C. Electrodes were prepared by placing 15 μl of the

concentrated broken cell preparation between a circular cellophane dialysis membrane and the gas-permeable membrane of the ammonia electrode. The broken cell electrode was preconditioned and stored in the same manner as the bacterial electrode.

RESULTS AND DISCUSSION

The design of the bacterial electrode is illustrated in Fig. 1. The dialysis membrane serves to hold the bacteria in place on the electrode, while allowing the passage of the low-molecular-weight amino acids into the bacterial layer. This membrane also allows for the escape of any bacterial waste products.

Typical calibration curves are shown in Fig. 2 for the response of the bacterial electrode to L-arginine in 0.1 M phosphate buffer pH 7.40 at 28°C. Freshly prepared electrodes exhibited a response slope of −52.5 mV/decade with a correlation coefficient of 0.998 in the linear range of 1.0×10^{-4}—6.5×10^{-3} M arginine. By the second day, the response slope dropped to −42.0 mV/decade with a correlation coefficient of 0.999 over the concentration range of 5.0×10^{-5}—1.0×10^{-3} M. After the initial drop in slope between the first and second day, the electrode response remained fairly constant for many days with slopes ranging between −40 and −45 mV/decade. The reproducibility of the electrode between the second and third day is shown in Table 1. A calibration curve for the bacterial electrode after a period of 20 days is also shown in Fig. 2. There is little change in the slope (slope = −41.8 mV/decade; correlation coefficient of 0.999), but the curve is shifted to more positive potentials and has a shorter linear range, levelling

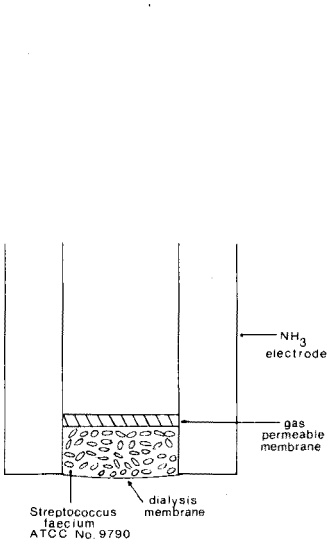

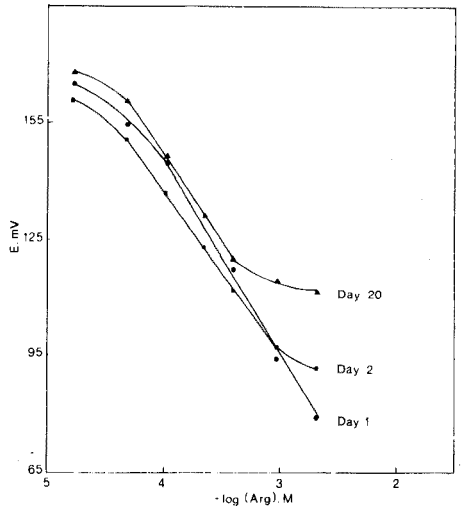

Fig. 1. Schematic diagram of the bacterial electrode.

Fig. 2. Calibration curves for L-arginine with the bacterial electrode.

TABLE 1

Reproducibility of the bacterial electrode in phosphate buffer pH 7.4 at 28°C

[L-Arginine] (M)	Potential (mV)	
	Day 2	Day 3
1.64×10^{-5}	162.0	159.1
4.46×10^{-5}	151.6	146.7
1.04×10^{-4}	137.9	134.4
3.91×10^{-4}	124.1	119.2
9.18×10^{-4}	112.9	109.2
2.01×10^{-3}	98.0	96.4
Response slopes, mV/decade	−42.0	−40.0

off at an arginine concentration of 4.0×10^{-4} M. This response behavior remained fairly constant for more than 40 days.

The decrease in response slope between the first and second day was observed for all of the bacterial electrodes tested, but the reason for this effect is not clear. Initially, it was thought that the effect might be due to the death of a large fraction of the bacteria held on the electrodes in contact with the buffer solution. To test this hypothesis, viable counts, taken as described above, were made on a small volume of the culture and on an equal volume of the culture which was washed with sterile buffer and allowed to remain overnight in the buffer solution. The number of viable cells counted in both cases was approximately equal, indicating that the bacteria do not expire rapidly in the buffer solution. Therefore, the change in response of the electrode between day 1 and day 2 cannot be attributed to a high mortality rate of the bacteria and requires future investigation.

The response time, i.e. the time required for the potential reading to come within 1 mV of the steady-state value, was approximately 20 min when the electrode was new and was not dependent on the arginine concentration in the linear range 5×10^{-5}—1.0×10^{-3} M. Enzyme electrodes typically have a response time of about 10 min. in this concentration range. The longer response time of the bacterial electrode could be due to the required additional diffusion step through the bacterial cell wall. As the bacterial electrode aged, the response time increased slightly.

The selection of optimum operating conditions involves a compromise between optimum conditions for the enzymatic reactions and those of the NH_3—NH_4^+ equilibrium involved in the gas electrode. Consequently, a study of the electrode response at different pH conditions and in different buffers was undertaken. The response of the electrode in pH 10.0 carbonate buffer, pH 7.0 and 7.4 phosphate buffer, and pH 7.4 Tris—HCl buffer is shown in Fig. 3. The electrode was first tested in the pH 10.0 carbonate buffer, since the bacteria used can grow at pH 10.0 [19] and this pH would be favorable for the gas electrode. However, the response slope at this pH was low,

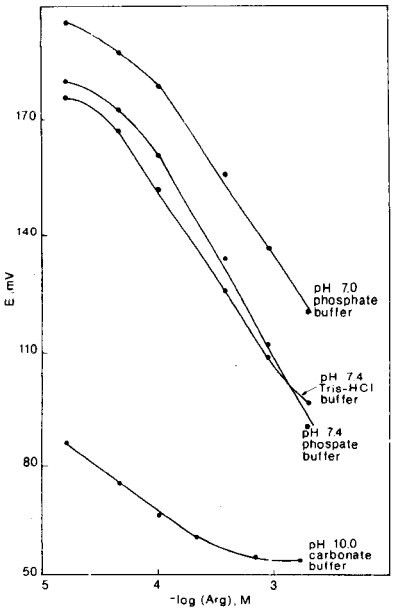

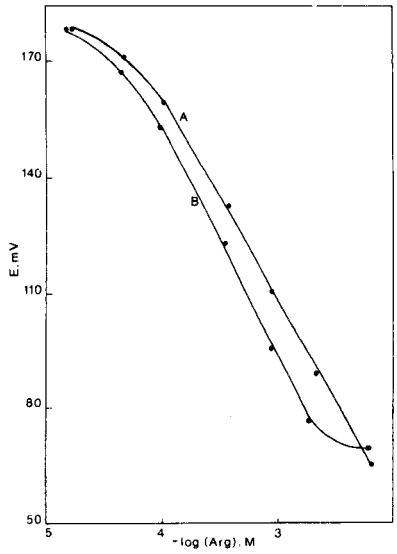

Fig. 3. Calibration curves for bacterial electrodes in various buffers.

Fig. 4. Calibration curves for bacterial electrodes with varying amounts of bacteria. A, 7 mg of bacteria. B, 1 mg of bacteria.

i.e. —21.8 mV/decade. A calibration curve of the ammonia gas electrode alone in carbonate buffer showed a Nernstian response, indicating that the low slope of the bacterial electrode in this buffer cannot be due to any CO_2 interference at the ammonia electrode. The calibration curves of the electrode in the pH 7.0 and 7.4 phosphate buffer and the pH 7.4 Tris—HCl buffer were similar. The response slope was greatest in the pH 7.4 phosphate buffer and, therefore, this buffer was used in subsequent studies.

The effect of using different amounts of bacteria on the electrode was also investigated. The response of two bacterial electrodes, one with 1 mg of bacterial cells and the other with 7 mg, is shown in Fig. 4. As can be seen, the slope in both cases is approximately equal; the slope of curve A is —53.2 mV/decade, and the slope of curve B is —55.7 mV/decade. However, the electrode with 7 mg of bacteria has a more extensive linear range. Increasing the amount of cells to 20 mg produced no further effect on the response of the electrode. In fact, with the larger amounts of bacteria, aggregates would form on the dialysis membrane, causing longer response times and requiring a longer time for the potential to return to its original value when the electrode was placed in a buffer solution after a calibration of the electrode. Therefore, amounts of bacteria in the 1—2 mg range were used for further study.

The selectivity of the bacterial electrode for L-arginine over other amino acids is shown in Fig. 5. The electrode showed little response to L-histidine, L-lysine, L-citrulline, and urea, but responded moderately to L-asparagine and L-glutamine. The order of selectivity of the electrode — arginine > glutamine ≃ asparagine > urea > histidine ≃ lysine — is similar to the order of NH_3 production reported for the bacteria in a non-electrochemical study [18]. Since the enzyme responsible for ammonia production from L-arginine, arginine deaminase E.C. No. 3.5.3.6, has been shown to be highly selective for L-arginine (22, 23), the cells must contain other enzymes that produce ammonia from L-asparagine and L-glutamine, making these substrates interferences. This illustrates a possible limitation of bacterial electrodes. Whereas the selectivity of an enzyme electrode is determined by the selectivity of the enzyme employed, bacteria may contain other enzymes or factors which produce the desired product from other substances, making them interferences. This problem may be overcome or diminished by proper initial selection of bacteria or by adjustment of the growth media to limit undesirable biochemical pathways.

In order to determine if the bacteria remain viable on the electrode for extensive time periods and to test the possibility of regenerating electrode activity by natural regrowth of the bacteria, a 20-day old electrode was placed back into the growth medium for 48 h at room temperature. After this period, the electrode response was tested; the calibration curves before and after regeneration are shown in Fig. 6. It should be noted from Fig. 2 that the decline in electrode response after 20 days was very small, with the calibration curve shifted to more positive potentials and the linear portion slightly shortened. After regeneration, the curve was shifted back to lower potentials and the linear portion was extended. A comparison of the second day curve (Fig. 2) and the regenerated curve (Fig. 6) indicates

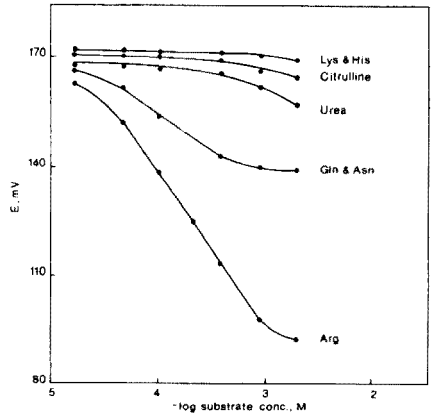

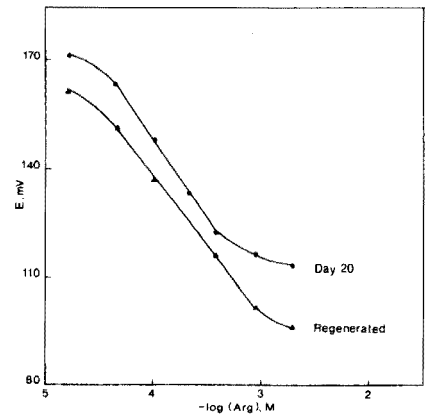

Fig. 5. Selectivity studies of bacterial electrodes.

Fig. 6. Regeneration study of the bacterial electrode.

that the response of the electrode after regeneration was fully restored. This result seems to indicate that the bacteria are still viable after 20 days on the electrode. However, owing to the intrinsic stability of the electrode, the response curves of the electrode on day 20 and of the regenerated electrode are not sufficiently different to make the observed regeneration effect one of practical importance. Other, less stable strains of bacteria might be regenerated in this manner with a resulting practical extension of electrode lifetimes. In principle, the use of bacteria in place of enzymes could greatly reduce the cost of bio-selective electrodes via direct generation or external culture growth.

Electrodes prepared from the ruptured bacterial cells gave calibration curves essentially similar to those of the living bacterial electrode with slopes ranging between −38 and −42 mV/decade for arginine. These slopes were comparable to those obtained with intact cell electrodes aged two days or longer. The response of the broken cell electrode remained fairly constant over a period of 40 days, indicating the unusual stability of the cell enzyme involved. The response time of the broken cell electrode was comparable to that of conventional enzyme electrodes, i.e. approximately 10 min in the linear range 5×10^{-5}—1.0×10^{-3} M arginine. This observation supports the belief that the longer response times of the intact cell bacterial electrodes are due to an additional diffusion step involving the cell wall. The response time of the broken cell electrode also increased as the electrode aged.

This study has demonstrated the feasibility of using living micro-organisms in conjunction with membrane electrodes to prepare workable bio-selective sensors. The present electrode, although of possible practical use for arginine measurements, is primarily intended to illustrate the novel concept involved and to serve as a model for the development of future sensors. If the basic concept can be applied to systems for which enzymes are not available, or are insufficiently stable, or require complex sequences of steps, then the coupling of living bacteria or other suitable cells to ion- or gas-sensing membrane electrodes could indeed provide new biochemical measurement capabilities beyond those of conventional electrodes. Divies [24] has reported attempts to employ a microbial electrode, based on an oxygen probe, for ethanol assays.

We acknowledge the valuable assistance of Michael Ryan, Department of Microbiology, in the preparation of the broken cell solutions.

REFERENCES

1 G. J. Moody and J. D. R. Thomas, Analyst, 100 (1975) 609.
2 P. J. Elving, Bioelectrochem. Bioenerg., 2 (1975) 251.
3 G. A. Rechnitz, Chem. Eng. News, 53 (1975) 29.
4 G. G. Guilbault, in H. H. Weetall (Ed.), Immobilized Enzymes, Antigens, Antibodies and Peptides, M. Dekker, New York, 1975, p. 293.
5 D. S. Papastathopoulos and G. A. Rechnitz, Anal. Chim. Acta, 79 (1975) 17.

6 D. S. Papastathopoulos and G. A. Rechnitz, Anal. Chem., 48 (1976) 862.
7 M. Meyerhoff and G. A. Rechnitz, Anal. Chim. Acta, 85 (1976) 277.
8 G. A. Rechnitz, Science, 190 (1975) 234.
9 S. Bascomb and C. A. Grantham, in R. G. Board and D. W. Lovelock (Eds.), Some Methods for Microbiological Assay, Academic Press, New York, 1975, p. 29.
10 K. Mosbach and R. Mosbach, Acta Chem. Scand., 20 (1966) 2807.
11 W. B. Vieth, S. S. Wang and R. Saini, Biotechnol. Bioeng., 15 (1973) 565.
12 S. J. Updike, D. R. Harris, and E. Shrago, Nature, 224 (1969) 1122.
13 J. F. Kennedy, S. A. Barker, and J. D. Humphreys, Nature, 261 (1976) 242.
14 F. Kavanagh, Analytical Microbiology, Vol. 1, Academic Press, New York, 1963.
15 J. L. Stokes, M. Gunness, I. M. Dwyer, and M. C. Caswell, J. Biol. Chem., 160 (1945) 35.
16 J. L. Stokes and M. Gunness, J. Biol. Chem., 157 (1945) 651.
17 J. R. Sokatch, Bacterial Physiology and Metabolism, Academic Press, New York, 1969, p. 170.
18 G. M. Hills, Biochem. J., 34 (1940) 1057.
19 W. R. Chesbro and J. B. Evans, J. Bacteriol., 78 (1959) 858.
20 G. G. Meynell and E. Meynell, Theory and Practice in Experimental Bacteriology, Cambridge Press, 1970, p. 23.
21 Molecular Filtration, Publication AR801, Millipore Corp., Bedford, Mass., 1974.
22 B. Petrack, L. Sullivan, and S. Ratner, Arch. Biochem. Biophys., 69 (1957) 186.
23 S. Ratner, in F. F. Nord (Ed.), Advances in Enzymology, Interscience, New York, 1954, p. 319.
24 C. Divies, Ann. Microbiol., 126A (1975) 175.

Analytica Chimica Acta, 94 (1977) 367—376

CONSTRUCTION, ANALYTICAL STUDY AND APPLICATION OF A NEW CHLORAMINE-T SELECTIVE ELECTRODE

M. A. KOUPPARIS and T. P. HADJIIOANNOU*

Laboratory of Analytical Chemistry, University of Athens, Athens (Greece)

(Received 16th May 1977)

SUMMARY

A chloramine-T (CAT) selective electrode with a liquid membrane of nickel bathophenanthroline—chloramine-T dissolved in 2-nitro-*p*-cymene is described. The liquid membrane electrode exhibits rapid and near Nernstian response to chloramine-T activity from 10^{-1} to 10^{-4} M. The response is unaffected by pH in the range 5—9. Major interferences are periodate and perchlorate. In analytical applications, direct potentiometric methods for the determination of chloramine-T, ascorbic acid, and arsenic(III), and a titrimetric method for ascorbic acid are described. Ascorbic acid and arsenic(III) in the ranges 0.4—40 and 0.5—2 mg, respectively, can be determined with relative errors of 1—2%. The method has been applied to the determination of ascorbic acid in pharmaceutical preparations.

Ion-selective electrodes based on a wide variety of sensors are now available for about 50 different ions; most of them have useful activity response ranges and selectivity [1]. However, while there has been considerable research on electrodes selective for charged inorganic species, electrodes selective for organic ions have received much less attention, and only scattered references have been made to the possibilities in this area [1—3].

Recently, the interference of an ion with an ion-selective electrode has been exploited for monitoring the interferent and for the construction of new electrodes [4—7]. In this paper, a new chloramine-T selective electrode is described; it is prepared by modifying an Orion nitrate-selective electrode by converting its liquid ion-exchanger, consisting of [(bathophenanthroline)$_3$Ni] nitrate in 2-nitro-p-cymene, to the chloramine-T (CAT) form. The CAT-selective membrane electrode has been used successfully in direct potentiometry for the determination of chloramine-T, ascorbic acid, and arsenic(III), and in the indirect potentiometric titration of ascorbic acid with chloramine-T.

EXPERIMENTAL

Preparation of the liquid ion-exchanger

The Orion 92-07-01 nitrate liquid ion-exchanger was converted to the chloramine-T form by diluting 2 ml of exchanger with 10 ml of dichloromethane,

shaking the resulting solution with 50 ml of a 0.1 M CAT solution and decanting the aqueous phase. After evaporation of the dichloromethane, the organic phase was treated with anhydrous sodium sulfate to remove any traces of water. The liquid ion-exchanger obtained consists of a solution of [(bathophenanthroline)$_3$Ni]—chloramine-T salt in the initial organic solvent, 2-nitro-*p*-cymene. The Orion 92-05-01 fluoroborate ion-exchanger consists of the same active substance as the Orion 92-07-01 nitrate electrode and therefore can also be used as the starting material for the preparation of the CAT ion-exchanger.

The body of an Orion series 92 electrode equipped with an Orion polycellulose acetate membrane (e.g. a 92-07-04 nitrate membrane) was used as the liquid membrane electrode. The electrode was assembled according to the manufacturer's directions. The internal reference solution consisted of 0.1 M CAT and 0.1 M NaCl in a saturated solution of AgCl. The reference electrode was an Orion 90-02 Ag—AgCl double-junction electrode; its outer chamber was filled weekly with a 10% (w/v) KNO_3 solution.

The measuring cell can be represented as:

Ag/AgCl	Internal solution 0.1 M CAT + 0.1 M NaCl	Membrane saturated with CAT-exchanger	Test solution	KNO_3 salt bridge	KCl	AgCl/Ag

The CAT electrode was conditioned by soaking in a stirred 0.1 M CAT solution for at least 12 h. When not in use, the electrode was stored in a 0.01 M CAT solution. Exposure to direct sunlight must be avoided to prevent decomposition of the CAT solution. The operative life of the electrode is about 30 days.

Apparatus

E.m.f. values were measured with an Orion Model 801 digital pH/mV meter, connected to an Orion Model 751 digital printer. This system allows the e.m.f. to be read to ± 0.1 mV. All solutions were stirred magnetically during measurements of potentials. For pH measurements, a Metrohm Model E-350B pH meter with a combination glass electrode was used. Cell potentials were recorded with a Heath-Schlumberger recording system, consisting of a pH/pIon electrometer (EU-200-30) acting as a follower for impedance matching, a potentiometric amplifier (EU-200-01), a d.c.-offset module (EU-200-02) and a strip-chart recorder (EU-205-11). For the semi-automatic titrations, the system was as previously described [8]. All measurements were carried out in a 50-ml double-wall glass cell, coated with a black nylon sheet for sunlight protection, at 25.0°C, except where stated. The distance between the electrodes and their position in the reaction cell were rigidly maintained during all measurements. The reaction cell was emptied by suction. A magnetic stirring bar agitated the solution to provide mixing and achieve steady, reproducible potentials.

Reagents

All solutions were prepared in double-distilled water from reagent-grade materials.

Chloramine-T (CAT) solutions. For a 0.1000 M stock solution, dissolve 28.17 g of chloramine-T trihydrate (Merck) in water, dilute to 1 l and store in an amber bottle. This solution is stable for at least one month. Standardize with standard arsenite solution [9]. Prepare the working solutions fresh daily by suitable dilution. The purity of chloramine-T may be increased to 99.5% by recrystallization from aqueous solution [9].

Ascorbic acid solutions. For the 0.1000 M stock solution, dissolve 17.61 g of ascorbic acid (Merck) in water, dilute to 1 l and store in an amber bottle in a refrigerator. Prepare working standard solutions fresh daily by dilution.

Phosphate and citrate buffers pH 7.0 (0.1 M). Mix 10 ml of 1 M NaH_2PO_4 or citric acid solution with 80 ml of water. Neutralize with 5 M NaOH to a pH of 7.0 and dilute to 100 ml.

p-*Toluenesulfonamide (1.00 × 10^{-3} M).* Dissolve 0.1712 g of *p*-toluenesulfonamide in 1 l of water.

Composite 0.05 M phosphate—25 ppm osmium(VIII) buffer pH 7.0. Mix 10 ml of 0.5 M NaH_2PO_4, 25 ml of 100-ppm osmium solution (133.6 mg of OsO_4 in 1 l of 0.05 M NaOH) and 50 ml of water, neutralize with 2 M NaOH to pH 7.0, and dilute to 100 ml.

Composite working standards of CAT—p-*toluenesulfonamide* (for the determination of arsenic). Prepare four working standards containing $n \times 10^{-4}$ M CAT, $(10 - n) \times 10^{-4}$ M *p*-toluenesulfonamide and 5 ml of the composite phosphate—osmium buffer per 25 ml of standard.

RESULTS AND DISCUSSION

Characteristics of the electrode

A typical calibration curve for the CAT electrode in stirred chloramine-T solutions is shown in Fig. 1. The solutions were buffered at pH 7.0 with 0.1 M phosphate buffer, so that the ionic strength and thus the activity coefficients remained constant. Figure 1 shows that the response is linear in the 10^{-4}—10^{-1} M range. At lower CAT concentrations, curvature is observed because the solubility of the liquid ion-exchanger itself contributes a small but significant amount of CAT to the test solution. During the operative life of the electrode, which is about 1 month, the slope of the calibration curve was 59—62 mV at 25°C; after 1 month, the slope decreased gradually. All slopes were calculated by regression analysis on the linear part of the calibration curves.

The limit of detection, i.e. the activity of that point on the calibration curve where ΔE between that curve and the extrapolated Nernstian line is 18 mV (as recommended by IUPAC), was found to be 1.8×10^{-5} M (Fig. 1). This limit remained practically constant during the operative life of the electrode.

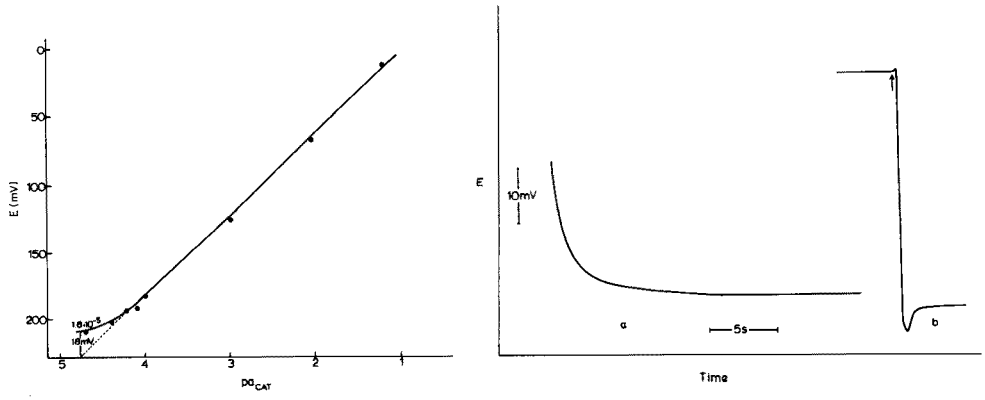

Fig. 1. Response of the chloramine-T selective electrode in chloramine-T solutions.

Fig. 2. (a) Time trace for the electrode immersed in 1.00×10^{-3} M chloramine-T solution (static method). (b) Time trace for the electrode following an increase of CAT concentration from 1.00×10^{-3} to 5.7×10^{-3} M (dynamic method).

During a period of 15 min there was a drift of 0.9, 0.5, and 0.4 mV, in the e.m.f. of the cell in 1×10^{-4}, 1×10^{-3} and 1×10^{-2} M CAT solutions, respectively. The e.m.f. of the cell was reproducible within ±2mV over a span of 1 month.

The static response times [10] were measured in terms of the period necessary for the recorder to show a stable potential to within ±1 mV on immersing the CAT and reference electrodes in an unstirred test solution at 25°C. The static response time was about 20 s for CAT solutions in the range 10^{-4}—10^{-1} M (Fig. 2a). Dynamic response times were tested for 10^{-4}—10^{-1} M CAT solutions; the sequence of measurements was from low concentrations to high concentrations and vice versa. The dynamic response times (Fig. 2b) for a 5.7-fold increase in CAT concentration or for a 20% decrease in CAT concentration (by injection of CAT solution or water) were quite short (less than 2 s, including the mixing and recorder time). It should therefore be possible to employ the CAT electrode in titrations with continuous addition of titrant and for the continuous monitoring of rapidly changing systems.

pH in the range 6—10 and temperature in the range 5—25°C had no practical effect on the response time. There was a gradual increase of response time with age for electrodes older than 1 month.

When potentials were measured over the range 10^{-4}—10^{-1} M, from low concentrations to high concentrations and back, no practical hysteresis phenomenon was noticed.

Effect of pH

In order to check the pH-dependence of the potential of the electrode, potential—pH curves at various CAT concentrations were constructed. The

pH of the initial solution was altered by addition of very small volumes (less than 0.1 ml per 30 ml of test solution) of NaOH or H_2SO_4. The plots (Fig. 3) show that the potential is practically independent of pH in the range 5—9 for 10^{-2} and 10^{-3} M CAT solutions, and in the range 5—8 for 10^{-4} M CAT solution.

At lower pH values there is an increase in potential because of the decrease in the CAT concentration caused by a shift in the equilibrium between the CAT-anion ($RNCl^-$) and the free acid (RNHCl): $RNCl^- + H^+ \rightleftharpoons RNHCl$; $K_a = (2.8 \pm 0.2) \times 10^{-5}$ at 25°C (where $R = CH_3C_6H_4SO_2$). The free acid disproportionates to give *p*-toluenesulfonamide and sparingly soluble dichloramine-T: $2RNHCl \rightleftharpoons RNH_2 + RNCl_2$; $K = 6.1 \times 10^{-2}$ [11]. Accordingly, a white precipitate appeared in CAT solutions below pH 4.8.

Potentiometric selectivity coefficients

The interference of various anions was studied by the separate solution and the mixed solution methods, graphically (Fig. 4) and from the formula

$$K^{pot}_{CAT,j} = \{[10^{(E_1 - E_2)F/2.303\,RT}]\,\alpha_{CAT} - \alpha'_{CAT}\}/\alpha_j^{1/z} \qquad (1)$$

where E_1 is the potential in a chloramine-T solution of activity α_{CAT}, E_2 is the potential in a solution containing chloramine-T and interfering anion j of activities α'_{CAT} and α_j, respectively, and z is the valency of the anion j [1]. The concentration of the tested anion was kept constant, while the CAT concentration was varied in the range 10^{-1}—10^{-5} M. All concentrations were converted to activities by means of the expression $\log f = -0.511\,\mu^{1/2}/(1 + \mu^{1/2})$, where f is the activity coefficient and μ is the ionic strength. In the case of weak acids the anion concentration was calculated from the measured pH, K_a, and the analytical concentration. Potentiometric selectivity coefficients are presented in Table 1.

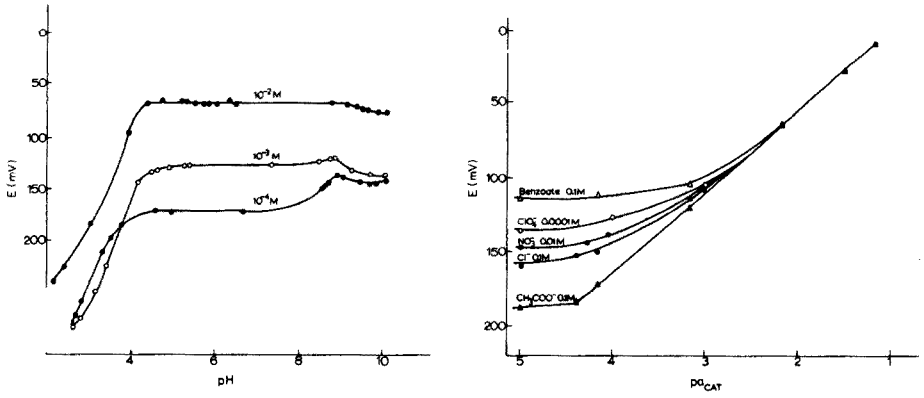

Fig. 3. Effect of pH on the potential of the electrode.

Fig. 4. Potential response of the electrode in mixed CAT—interferent solutions at 25°C.

TABLE 1

Potentiometric selectivity coefficients of chloramine-T selective electrode

Interferent, j	Separate solutions method[a]	Mixed solution method	
		Graphically[b]	Calculated[c]
IO_4^-	$7.2(1 \times 10^{-4})$	$1.8(1 \times 10^{-4})$	$9.5(1 \times 10^{-4}/1 \times 10^{-4})$
ClO_4^-	$6.1(1 \times 10^{-4})$, $5.5(5 \times 10^{-4})$	$6.2(1 \times 10^{-4})$	$7.9(1 \times 10^{-4}/1 \times 10^{-4})$
Benzoate	$1.6 \times 10^{-2}(1 \times 10^{-1})$	$6.2 \times 10^{-3}(1 \times 10^{-1})$	$1.3 \times 10^{-2}(1 \times 10^{-3}/1 \times 10^{-1})$
NO_3^-	$4.6 \times 10^{-2}(1 \times 10^{-2})$	$2.9 \times 10^{-3}(1 \times 10^{-2})$	$5.4 \times 10^{-2}(1 \times 10^{-4}/1 \times 10^{-2})$
Cl^-	$3.4 \times 10^{-3}(1 \times 10^{-1})$	$3.1 \times 10^{-3}(1 \times 10^{-1})$	$7.0 \times 10^{-3}(1 \times 10^{-3}/1 \times 10^{-1})$
Phthalate	$3.4 \times 10^{-3}(1 \times 10^{-1})$	$1.3 \times 10^{-3}(1 \times 10^{-1})$	
$H_2BO_3^-$	$6.8 \times 10^{-3}(1 \times 10^{-1})$	$6.6 \times 10^{-3}(1 \times 10^{-1})$	$5.0 \times 10^{-3}(1 \times 10^{-3}/1 \times 10^{-1})$
HCO_3^-	$1.0 \times 10^{-3}(1 \times 10^{-1})$	$9.7 \times 10^{-4}(1 \times 10^{-1})$	$1.3 \times 10^{-3}(1 \times 10^{-4}/1 \times 10^{-1})$
HPO_4^{2-}	$1.2 \times 10^{-3}(1 \times 10^{-2})$	$7.0 \times 10^{-4}(1 \times 10^{-2})$	$9.0 \times 10^{-4}(1 \times 10^{-4}/1 \times 10^{-1})$
CH_3COCOO^-	$1.0 \times 10^{-3}(1 \times 10^{-1})$	$7.0 \times 10^{-4}(1 \times 10^{-1})$	$1.3 \times 10^{-3}(1 \times 10^{-4}/1 \times 10^{-3})$
CH_3COO^-	$9.3 \times 10^{-4}(1 \times 10^{-1})$	$8.8 \times 10^{-4}(1 \times 10^{-1})$	$7.6 \times 10^{-4}(1 \times 10^{-4}/1 \times 10^{-1})$
Malonate	$8.7 \times 10^{-4}(8.9 \times 10^{-2})$	$6.0 \times 10^{-4}(1 \times 10^{-2})$	$8.1 \times 10^{-4}(1 \times 10^{-4}/8.9 \times 10^{-2})$
F^-	$8.4 \times 10^{-4}(1 \times 10^{-1})$	$4.4 \times 10^{-4}(1 \times 10^{-1})$	$6.4 \times 10^{-4}(1 \times 10^{-3}/1 \times 10^{-1})$
Tartrate	$5.1 \times 10^{-4}(1 \times 10^{-1})$	$3.1 \times 10^{-4}(1 \times 10^{-1})$	
CrO_4^{2-}	$5.9 \times 10^{-4}(1 \times 10^{-1})$	$2.5 \times 10^{-4}(1 \times 10^{-1})$	
Citrate	$5.2 \times 10^{-4}(8.4 \times 10^{-2})$	$5.0 \times 10^{-4}(8.4 \times 10^{-2})$	
MoO_4^{2-}	$4.4 \times 10^{-4}(1 \times 10^{-1})$	$2.6 \times 10^{-4}(1 \times 10^{-1})$	
SO_4^{2-}	$9.5 \times 10^{-5}(1 \times 10^{-2})$	$9.0 \times 10^{-5}(1 \times 10^{-1})$	

[a]The values in parentheses show the interferent and chloramine-T concentrations.
[b]The values in parentheses show the interferent concentration. The chloramine-T was 1×10^{-2}—1×10^{-5} M.
[c]The values in parentheses show the ratio [CAT]/[Interferent].

Analytical applications

The chloramine-T selective electrode can be used practically for the determination of chloramine-T either by direct potentiometry or by potentiometric titration. The electrode can also be used as indicator electrode in potentiometric titrations of reducing agents with chloramine-T and in kinetic methods [12]. As examples, the titrimetric determination of ascorbic acid and the determination of ascorbic acid and arsenic(III) by direct potentiometry with the CAT-electrode were examined. The method for the determination of ascorbic acid by direct potentiometry was applied to the analysis of pharmaceutical preparations.

Semi-automatic potentiometric titration of ascorbic acid. Pipet a 20.00-ml aliquot of the sample containing 20—200 μmol of ascorbic acid, 2.00 ml of phosphate buffer and 5.00 ml of 0.0500 M chloramine-T solution into the reaction cell, and titrate the excess of chloramine-T with 0.0500 M standard ascorbic acid solution. Carry out a blank titration in duplicate to determine the blank and subtract the blank from the volume of the standard ascorbic solution used.

Determination of ascorbic acid by direct potentiometry. Procedure A. (For the 20—200 μmol range). Pipet 5.00 ml of 5.00×10^{-2} M CAT solution (250 μmol), 20.00 ml of sample, and 2.00 ml of phosphate buffer pH 7.0 into the reaction cell. Start the magnetic stirrer and when the potential has stabilized to within ±0.1 mV (in about 1—2 min), read the digital ion meter. Include four

ascorbic acid standards in the range 1×10^{-3}—1×10^{-2} M, containing 2.00 ml of buffer per 20.00 ml of standard solution, with each series of unknown samples. The excess of CAT is found from a plot of E vs. log [CAT] in excess (Fig. 5). The amount of ascorbic acid in the sample is equivalent to the amount of CAT consumed, the stoichiometry of the reaction being 1:1.

Procedure B. (For the 2—20 μmol range) is similar except that 5.00 ml of 5.00×10^{-3} M CAT solution (25 μmol) and standard ascorbic solutions in the range 1×10^{-4}—1×10^{-3} M are used. In this case the abscissa in the calibration curve (Fig. 5) is log (25-μmol ascorbic).

Determination of ascorbic acid in injection solutions. Dilute an exactly measured volume of the injection solution so that 20.00 ml of the dilute solution contain 20—200 or 2—20 μmol of ascorbic acid and apply procedure A or B, respectively.

Determination of ascorbic acid in tablets. Weigh at least 20 tablets of the sample and pulverize in a mortar. Weigh an appropriate amount of the pulverized sample in water, transfer the solution to a 100-ml volumetric flask and dilute to the mark, so that 20.00 ml of the solution contain 20—200 or 2—20 μmol of ascorbic acid. If a residue remains, filter through a Whatman paper filter. Proceed as above using procedure A or B. Calculate the mean ascorbic acid content per tablet. If the tablets contain calcium, substitute 0.1 M citrate buffer pH 7.0 for the phosphate buffer to prevent calcium phosphate precipitation.

Determination of arsenic(III) by direct potentiometry. Pipet 10.00 ml of 2.50×10^{-3} M CAT solution (25 μmol), 5.00 ml of composite phosphate-osmium buffer pH 7.0, and 10.00 ml of arsenic sample containing 5—22.5 μmol of arsenic(III) into the reaction cell. Start the stirrer and when the potential has stabilized to within ± 0.1 mV (1—2 min), read the digital ion meter. Include four composite—CAT standards in duplicate with each series of unknown samples.

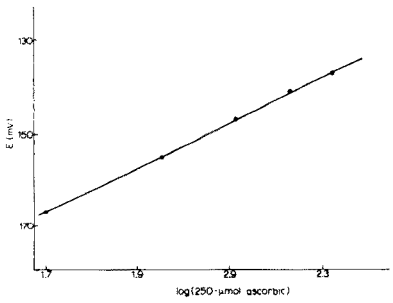

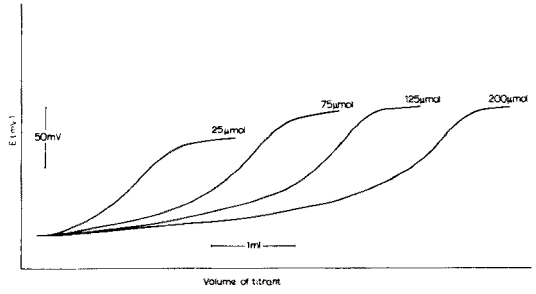

Fig. 5. Calibration curve for ascorbic acid determination.

Fig. 6. Recorded curves for the semi-automatic titration of chloramine-T with standard ascorbic acid solution.

Typical recorded curves for the semi-automatic potentiometric titration of chloramine-T with ascorbic acid are shown in Fig. 6. Analysis of aqueous ascorbic acid solutions of known concentrations gave the results shown in Table 2. The data indicate that ascorbic acid in the range 4—40 mg can be determined with relative errors and relative standard deviation (s_r) of about 1%.

Results for the determination of ascorbic acid by direct potentiometry are given in Table 3. The relative errors and the relative standard deviation for the determination of 0.7—35 mg of ascorbic acid were about 1—2%. The values for ascorbic acid in pharmaceutical preparations obtained by direct potentiometry are compared with those obtained by the dichlorophenol—indophenol titrimetric method [13] in Table 4. There is satisfactory agreement between the results obtained by the two methods.

Table 5 shows the results for the determination of arsenic(III) by direct potentiometry. Arsenic in the range 0.5—2 mg can be determined with relative errors and relative standard deviation of 1—2%.

Although the applications reported here deal with the determination of chloramine-T, ascorbic acid, and arsenic(III), the scope of the applications of the chloramine-T selective electrode should be more general. The rapid response of the chloramine-T selective electrode to changes in chloramine-T concentration makes it a valuable sensor for following the rate of chloramine-T reactions. Work in progress indicates that hydrazine and isonicotinic acid hydrazide can be determined by direct potentiometry and trace amounts of various ions can be determined on the basis of their catalytic effect on various chloramine-T redox reactions. This work and other analytical possibilities of the chloramine-T selective electrode will be published in the near future.

TABLE 2

Semi-automatic potentiometric titration of ascorbic acid in aqueous solutions

Ascorbic acid in 20-ml sample (mg)		Error (%)	s_r (%)
Taken	Found[a]		
3.52	3.45	−2.0	
14.1	14.3	+1.4	
17.6	17.6	—	1.1(n = 5)
24.7	24.6	−0.4	
35.2	35.0	−0.6	

[a] Average of two measurements.

TABLE 3

Results for aqueous ascorbic acid solutions by direct potentiometry

Ascorbic acid in 20-ml sample (mg)					
Taken	Found[a]	Error(%)	Taken	Found[a]	Error(%)
Procedure B			*Procedure A*		
0.705	0.713	+1.1	3.52	3.91	+11.1
1.06	1.07	+0.9	10.6	10.4	− 1.9
1.76	1.78	+1.1	17.6	17.5	− 0.6
2.82	2.82	—	24.7	24.7	—
3.52	3.48	−1.1	35.2	35.4	+ 0.6
		Av. 0.8			Av. 2.8

[a]Average of two measurements.

TABLE 4

Comparison of potentiometric and titrimetric methods for the determination of ascorbic acid in pharmaceutical preparations

Preparation	Potentiometric method	Dichlorophenol—indophenol titrimetric method
Redoxon ampoules, 500 mg/5ml (Roche)	98.5 mg/ml 101.3 mg/ml 102.1 mg/ml	99.2 mg/ml 100.4 mg/ml 102.7 mg/ml
Redoxon Quiksolv. tablets 500 mg (Roche)	492 mg/tablet 502 mg/tablet 506 mg/tablet	494 mg/tablet 503 mg/tablet 504 mg/tablet

TABLE 5

Determination of aqueous arsenic(III) solutions by direct potentiometry (Results are given as mg As/10 ml)

As(III) taken	0.562	0.936	1.31	1.50	1.69
As(III) found[a]	0.586	0.966	1.33	1.49	1.65
Error(%)	+4.3	+3.2	+1.5	−0.7	−2.4

[a]Single measurements.

The authors are grateful to H. Freiser and C. Efstathiou for valuable suggestions.

REFERENCES

1 N. Lakshminarayanaiah, Membrane Electrodes, Academic, New York, 1976.
2 E. Pungor, Anal. Chem., 39 (1967) 28A.
3 T. P. Hadjiioannou and E. P. Diamandis, Anal. Chim. Acta, 94 (1977) 443.

4 R. F. Hirsch and J. D. Rortock, Anal. Lett., 2 (1969) 295.
5 K. Hiiro, G. J. Moody and J. D. R. Thomas, Talanta, 22 (1975) 918.
6 C. E. Efstathiou and T. P. Hadjiioannou, Anal. Chem., 47 (1975) 864.
7 L. A. Lazarou and T. P. Hadjiioannou, unpublished work, University of Athens, 1977.
8 T. P. Hadjiioannou, M. A. Koupparis and C. E. Efstathiou, Anal. Chim. Acta, 88 (1977) 281.
9 V. J. Jennings, CRC Crit. Revs. Anal. Chem., 3 (1974) 413.
10 G. J. Moody and J. D. R. Thomas, Lab. Pract., 23 (1974) 475.
11 F. G. Soper, J. Chem. Soc. (London), (1924) 1899.
12 M. A. Koupparis and T. P. Hadjiioannou, Anal. Chim. Acta, in press.
13 The United States Pharmacopeia VIII (1965) p. 47.

Analytica Chimica Acta, 94 (1977) 377—384

A.C. POLAROGRAPHIC DETERMINATION OF POLYETHYLENE GLYCOLS — APPLICATION TO ANALYSIS OF PHOTOGRAPHIC PROCESSING SOLUTIONS

D. R. CANTERFORD

Research Laboratories, Kodak (Australasia) Pty. Ltd., P.O. Box 90, Coburg, 3058, Victoria (Australia)

(Received 15th July 1977)

SUMMARY

The tensammetric behaviour of several polyethylene glycol (PEG) molecules is described. At neutral pH, PEG gives both a positive and a negative peak. At high pH the positive peak is obscured by the anodic dissolution of mercury and at low pH the negative peak is obscured by the hydrogen evolution reaction. Tensammetry is shown to be applicable to the direct determination of PEG in photographic processing solutions. Despite the complex chemical composition of these solutions the only pre-treatment required was dilution of samples.

The non-ionic surfactant polyethylene glycol (PEG) has a wide variety of practical applications in industries ranging from pharmaceutical manufacture to metal fabrication [1]. Among the many applications in the photographic industry, PEG has been used as a development accelerator [2].

It has been established from electrocapillary [3] and differential capacity [4, 5] measurements that PEG molecules are strongly adsorbed on mercury. The fact that maxima on d.c. polarographic waves are suppressed by surface-active compounds is well known [6]. In many analytical applications of polarography a surfactant such as Triton X-100 (a polyethylene glycol ether) is added to solutions to suppress maxima. This ability of surfactants to suppress maxima has led to the development of indirect methods for the determination of surface-active compounds, including PEG. For example, Badinand and Boucherle [7] reported that suppression of the maximum on the nickel(II) reduction wave and displacement of the maximum on the copper(II) reduction wave were related to PEG concentration. More recently [8], it has been established that suppression of the oxygen maximum in 0.001 M KCl is related to PEG concentration. A disadvantage of these indirect methods is that they are non-specific, since all surface-active agents have qualitatively similar effects on maxima [6, 7]. This would greatly restrict the practical application of the methods.

Another consequence of the adsorption of PEG on mercury is that, in common with many other surface-active compounds, it gives tensammetric [9]

(adsorption/desorption) peaks under a.c. polarographic conditions. Although PEG of mean molecular weight 1000 (PEG 1000) has been used as a test compound in a fundamental study of the sensitivity of various forms of tensammetry [10, 11], this technique has apparently not been applied to the determination of PEG in any practical situation.

In this paper the tensammetric behaviour of several PEG molecules, ranging in molecular weight from 300 to 6000, is described. Application of the method to the direct determination of PEG 1540 and PEG 4000 in photographic processing solutions illustrates the usefulness of the technique.

EXPERIMENTAL

Apparatus

Polarograms were obtained with a Metrohm Polarecord E261 in conjunction with a Metrohm AC Modulator E393. An applied alternating voltage of 10 mV (r.m.s.) at 50 Hz was used. A conventional dropping mercury electrode (DME) was used as the working electrode. A silver—silver chloride (sat. KCl) reference electrode and a tungsten wire auxiliary electrode were used. The reference electrode was separated from the test solution by a salt bridge containing 1 M KNO_3. This solution was replaced daily.

Chemicals

PEGs from several sources were used without further purification. Nominal mean molecular weights were 300, 1540, 4000 and 6000. Chemicals used for preparing developer solutions were of normal photographic quality. Supporting electrolyte solutions were prepared from analytical-grade chemicals. The supporting electrolytes used were: 0.1 M NaOH; borate buffer (pH 10.4); borate—phosphate buffer (pH 8.0); acetate buffer (pH 3.8).

Procedures

A known volume of supporting electrolyte was transferred to the polarographic cell. Dissolved oxygen was removed by bubbling oxygen-free nitrogen through the solution for 10 min. The required PEG concentration was obtained by adding an appropriate aliquot of PEG stock solution by microsyringe. For analysis of photographic processing solutions, dissolved oxygen was removed from the supporting electrolyte (pH 10.4 buffer) by the addition of 0.1 M sodium sulfite.

RESULTS AND DISCUSSION

Tensammetric behaviour of PEG

Figure 1 shows the tensammetric behaviour of PEG 4000 in several supporting electrolytes. (For clarity, only the maximum current has been traced.) The background or base current recorded in the absence of PEG is indicated (dashed line). As with many other non-ionic surfactants [9],

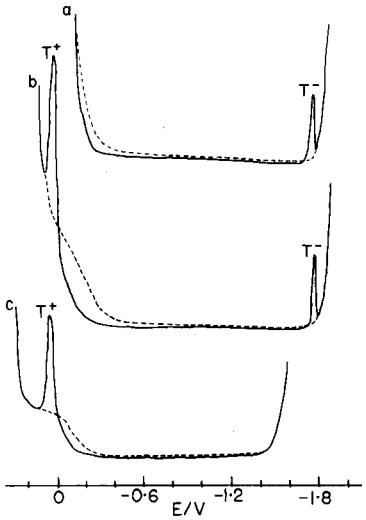

Fig. 1. Positive (T^+) and negative (T^-) tensammetric peaks for 5×10^{-6} M PEG 4000 in (a) 0.1 M NaOH, (b) pH 8.0 buffer, and (c) pH 3.8 buffer. (-----) Background current.

PEG gives both a positive and a negative peak, indicated by T^+ and T^-, respectively. These peaks are similar to the sharp peaks on the differential capacity curves reported by Dobren'kov and Guseva [4] and Yoshida et al. [5] (Jehring et al. [10, 11] discussed only the negative peak of PEG.).

In agreement with the observation of Dobren'kov and Guseva [4], adsorption of PEG molecules extends over a very wide potential range. Thus the positive and negative peaks occur close to the anodic and cathodic limits of the mercury electrode. Only at intermediate pH values are both peaks observed (Fig. 1, curve b). In supporting electrolytes of high pH the anodic dissolution of mercury is shifted to more negative potentials and thus obscures the positive peak (Fig. 1, curve a); at low pH, the negative peak is obscured by the hydrogen evolution reaction (Fig. 1, curve c). Yoshida et al. [5] reported that the negative peak on the differential capacity curve was not revealed in acidic solution for the same reason.

The tensammetric behaviour of the other PEG molecules studied was similar to that of PEG 4000. As expected [9], for a particular PEG the positive and negative peaks became sharper and further separated with increasing concentration. As for the differential capacity curves [4, 5], there was only a relatively small change in peak potential with change in concentration. For a given concentration the positive and negative peaks also became sharper and further separated with increasing molecular weight.

Figure 2 shows peak current vs. concentration data for the various PEG in pH 8.0 buffer. Data for both the positive and negative peaks are given. As expected [9] the curves have the form of an adsorption isotherm with a saturation limit. The concentration at which the peak current becomes independent of concentration decreases as the molecular weight increases.

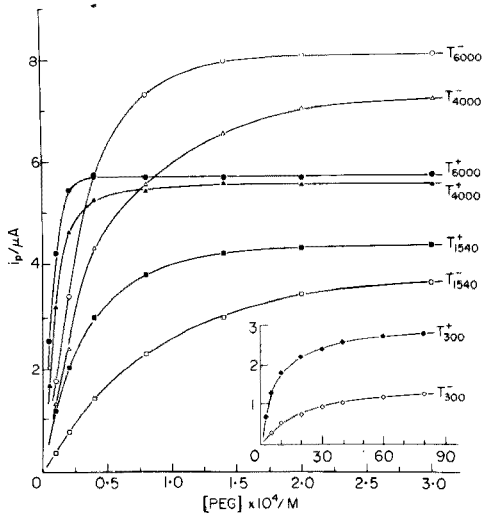

Fig. 2. Dependence of peak current (i_p) on PEG concentration in pH 8.0 buffer. Data refer to the positive and negative peaks respectively for (♦, ◇) PEG 300; (■, □) PEG 1540; (▲, △) PEG 4000; (●, ○) PEG 6000.

For analytical applications only the lower, approximately linear, portion of the peak current vs. concentration curve is useful. If either the positive or negative peak can be used for a particular determination, the positive peak is more sensitive.

As illustrated in Fig. 3, dissolved oxygen interferes with both positive and negative peaks of PEG and must be removed prior to analysis. For example, the first oxygen reduction peak occurs at approximately the same potential as the positive peak of PEG 1540 (Fig. 3A). Thus a higher peak is obtained in the presence of oxygen. Figure 3B shows the effect of PEG 1540 on the second reduction peak of oxygen in pH 10.4 buffer. With increasing PEG concentration, the oxygen peak shifts to more negative potentials and begins to overlap the PEG peak (Fig. 3B, curves a—d). (With d.c. polarography, the ability of surfactants to shift reduction waves to more negative potentials is well known [6].) Because of the empirical method by which the height of the tensammetric peak is measured, dissolved oxygen causes an apparent decrease in PEG peak height (compare curves d and e in Fig. 3B). For both the positive and negative peaks the extent of interference from oxygen depends on the molecular weight and concentration of PEG since, as previously discussed, the positions of the peaks depend on both these factors.

Application to analysis of photographic processing solutions

Photographic processing solutions, which consist of a complex mixture of organic and inorganic compounds, often present difficult analytical problems.

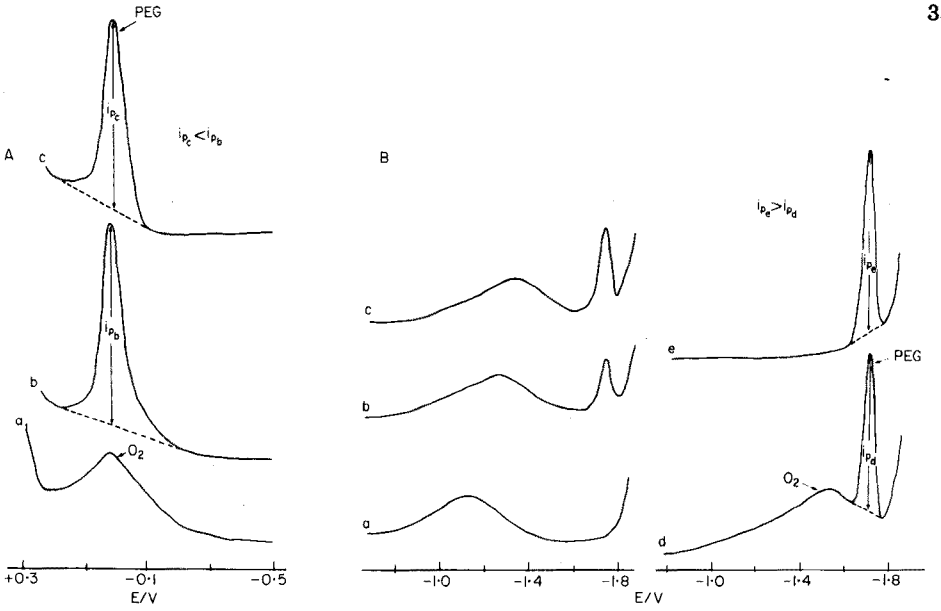

Fig 3. Interference by oxygen on the positive peak of PEG 1540 in pH 3.8 buffer (A) and on the negative peak of PEG 1540 in pH 10.4 buffer (B).
A, (a) oxygen; (b) oxygen + 2×10^{-5} M PEG 1540; (c) 2×10^{-5} M PEG 1540.
B, (a) oxygen; (b), (c) and (d) oxygen + 1×10^{-5}, 2×10^{-5}, and 4×10^{-5} M PEG 1540, respectively; (e) 4×10^{-5} M PEG 1540.

Many existing methods require complicated and time-consuming separation procedures before a constituent can be determined [12]. It has recently been shown that a.c. polarography can be used for the direct determination of color developing agents in a variety of photographic processing solutions [13]. The method has now been applied to the determination of PEG 1540 and PEG 4000 in the cyan, yellow, and magenta developers used for processing Kodachrome film (K-14 Process).

For the present application it is more convenient to use the negative peak. Halide and sulphite ions present in photographic developers shift the anodic dissolution of mercury to more negative potentials and are thus likely to interfere with the positive peak of PEG. Furthermore, it is convenient to maintain the developers being analysed at high pH (i.e., pH 10—12) to prevent precipitation of other constituents. At high pH only the negative peak is observed (Fig. 1, curve a).

Figure 4 shows a.c. polarograms recorded directly on samples of cyan and yellow developer, which contained approximately 7.8×10^{-4} M PEG 1540 and 1.3×10^{-4} M PEG 4000, respectively. In both cases, the PEG peak is very well-defined. The previously reported [15] reduction peaks for Kodak antifoggant AF-2 (5-nitrobenzimidazole) occur at much more negative potentials and do not interfere with the PEG peaks. Figure 5, curve a shows the a.c. polarogram recorded directly on a sample of magenta developer, which contained ca. 2.6×10^{-4} M PEG 4000. The PEG peak is much broader and

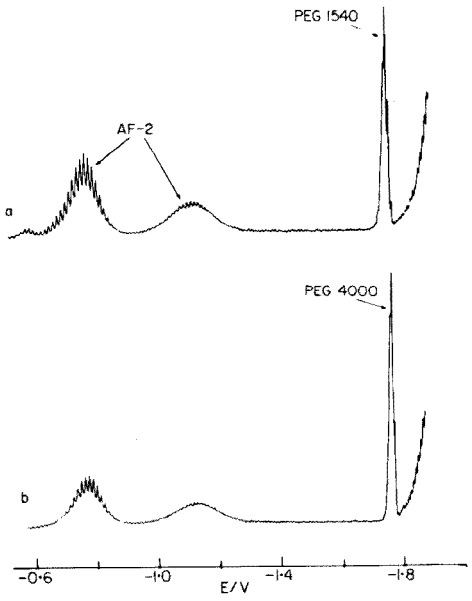

Fig. 4. (Left) A.c. polarograms of (a) cyan and (b) yellow developer.

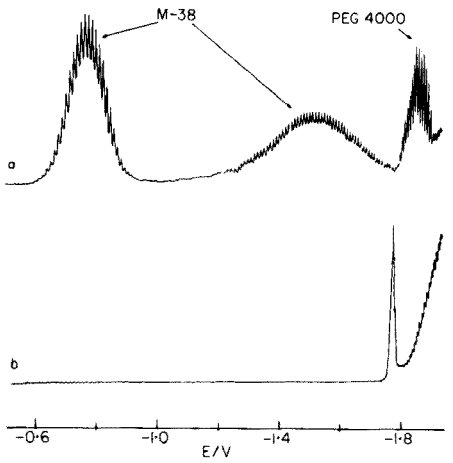

Fig. 5. (Right) A.c. polarograms of magenta developer in the (a) presence and (b) absence of M-38.

at a more negative potential than expected. The other two peaks are due to reduction of Kodak coupling agent M-38 (1-[2,4,6-trichlorophenyl]-3-*p*-nitroanilino-2-pyrazoline-5-one). Comparison with the polarogram recorded for the developer containing no M-38 (Fig. 5, curve b) shows that M-38 is responsible for distortion of the PEG peak.

In alkaline media, calibration curves for the negative peaks of PEG 1540 and PEG 4000 are similar in shape to the curves obtained in pH 8.0 buffer (Fig. 2). Ideally, the concentrations should be less than about 6.5×10^{-5} and 4×10^{-5} M, respectively, since only the lower portion of the curves are analytically useful. It is therefore necessary to dilute the developer samples prior to analysis. A potassium borate buffer of pH 10.4 was used for this purpose. For the magenta developer, dilution had the advantage that it eliminated interference from M-38. For example, after 20-fold dilution of the sample used to obtain the polarograms in Fig. 5, the PEG peak had the same shape and height in the presence and absence of M-38.

The processing solutions under consideration contain other surface-active species, apart from PEG, which give rise to tensammetric peaks under a.c. polarographic conditions. These include color developing agents of the *p*-phenylenediamine type [13, 14] and hexylene glycol. Although some of these species are present at greater molar concentrations than PEG, they do not interfere with the determination of PEG since they are less strongly adsorbed on the mercury electrode. Suppression of the peak of the color developer by PEG has been reported [13].

For freshly prepared developers, the only interference with the PEG peak is from M-38, which is readily overcome by diluting the magenta developer. When methods suitable for control purposes for continuous processing machines are being established, it must be recognised that the composition of a developer may vary as a result of species being leached from the film passing through it and also as a result of aerial oxidation. As shown recently [13], simple dilution experiments are a convenient method of establishing whether or not species introduced by these processes (usually of unknown identity) interfere with tensammetric peaks. Indirect interferences on the peaks of the color developers by species leached from various films has previously been established [13]. Figure 6 shows the effect of dilution on PEG peak current for fresh and used cyan and yellow developers. For used cyan developer the PEG peak is partially suppressed, perhaps by a surface-active species leached from the film. With 10-fold or greater dilution, the curves for fresh and used developer have the same shape, indicating that this indirect interference could be overcome simply by diluting the used developer. Similar interference for the used magenta developer was also overcome by dilution. Although no interference occurs for the used yellow developer (Fig. 6b) it is still necessary to dilute this developer prior to analysis to ensure that the PEG concentration falls on the appropriate portion of the peak current vs. concentration curve.

For analysis of used processing solutions, dilution factors of the order of 20-fold for the cyan and magenta developer and 10-fold for the yellow developer are appropriate. For convenience, analyses may be carried out by pipetting aliquots of the used developer and supporting electrolyte (pH 10.4 buffer/0.1 M Na_2SO_3) directly into the polarographic cell. The a.c. polarogram is recorded after mixing the solutions with a brief burst of nitrogen, and the PEG concentration in the dilute sample is estimated from the appropriate calibration curve. By incorporating sulphite in the supporting electrolyte the time-consuming degassing step is avoided.

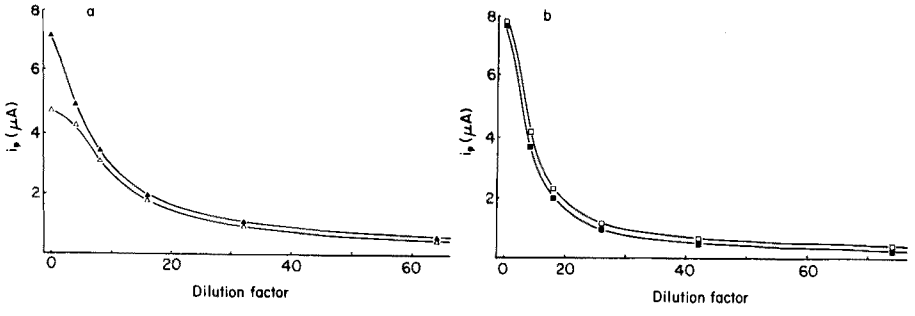

Fig. 6. Effect of dilution with pH 10.4 buffer on PEG peak current. (a) PEG 1540 in (▲) fresh and (△) used cyan developer. (b) PEG 4000 in (■) fresh and (□) used yellow developer.

Conclusions

Tensammetry provides a very rapid and simple method for the direct determination of PEG in photographic processing solutions. Despite the complex chemical composition of these solutions, the only pre-treatment required is dilution of samples with an alkaline supporting electrolyte. Since the processing solutions under consideration contain a number of surface-active agents, the non-specific indirect methods based on suppression of maxima [6, 7] could not be used for the determination of PEG.

For the present application the conventional a.c. technique and a DME with a normal drop time of 2—3 s provided more than adequate sensitivity. If necessary, sensitivity can be greatly improved by using techniques such as second harmonic a.c. polarography or a stationary mercury electrode [10, 11]. Because of the widespread industrial use of PEG (and other surfactants) many other practical applications of tensammetry should become apparent.

The author is grateful to Thelma Lobb for technical assistance, and to J. T. van Gemert for encouragement and helpful criticism of the manuscript.

REFERENCES

1 A. M. Schwartz, J. W. Perry and J. Berch, Surface Active Agents and Detergents, Vol. II, Interscience, New York, 1958.
2 T. H. James, in C. E. K. Mees and T. H. James (Eds.), The Theory of the Photographic Process, Macmillan, New York, 3rd edn., 1966.
3 P. J. Hillson, J. Phot. Sci., 11 (1963) 225.
4 G. A. Dobren'kov and L. T. Guseva, Elektrokhimiya, 7 (1971) 563.
5 T. Yoshida, T. Ohsaka and M. Suzuki, Bull. Chem. Soc. Jpn., 45 (1972) 3245.
6 L. Meites, Polarographic Techniques, Interscience, New York, 2nd edn., 1965.
7 A. Badinand and A. Boucherle, 9th Cong. Soc. Pharm. France, Clermont-Ferrand, 1957, p. 147.
8 K. Linhart, Tenside, 9 (1972) 241.
9 B. Breyer and H. H. Bauer, Alternating Current Polarography and Tensammetry, Interscience, New York/London, 1963.
10 H. Jehring, E. Horn, A. Reklat and W. Stolle, Collect. Czech. Chem. Commun., 33 (1968) 1038.
11 H. Jehring and W. Stolle, Collect. Czech. Chem. Commun., 33 (1968) 1670.
12 G. Russell, Chemical Analysis in Photography, Focal Press, London, 1965.
13 D. R. Canterford, Photogr. Sci. Eng., 21 (1977) 215.
14 D. R. Canterford, J. Electroanal. Chem., 73 (1976) 247.
15 D. R. Canterford, Photogr. Sci. Eng., 20 (1976) 230.

Analytica Chimica Acta, 94 (1977) 385—394

ÉTUDE DES RÉACTIONS D'OXYDO—RÉDUCTION DU NEPTUNIUM DANS LE MÉLANGE RbCl—CsCl (25—75% mol)

R. LYSY et G. DUYCKAERTS*

Laboratoire de Chimie analytique et Radiochimie, Université de Liège au Sart-Tilman, B-4000, Liège (Belgique)

(Reçu le 20 juin 1977)

RÉSUMÉ

Les potentiels normaux des couples $NpO_2(VI)$—$NpO_2(V)$ et Np(IV)—Np(III) et la constante d'équilibre de la réaction de dismutation—amphotérisation $2Np^{4+} + 2H_2O + 2\,Cl^- \rightleftarrows NpO_2^+ + Np^{3+} + 4\,HCl$ ont été déterminés dans un bain fondu de (Rb 0,25; Cs 0,75) Cl entre 660° et 750°C par spectrophotométrie d'absorption visible et proche infrarouge. Les résultats obtenus sont comparés à ceux trouvés antérieurement dans (Li 0,7; K 0,3)Cl, (Li, K)Cl eutectique, (Li 0,55; Cs 0,45)Cl.

SUMMARY

The oxidation—reduction reactions of neptunium in molten RbCl—CsCl.

Standard potentials of the systems $NpO_2(VI)$—$NpO_2(V)$ and Np(IV)—Np(III) and the equilibrium constant of the following disproportionation reaction $2Np^{4+} + 2H_2O + 2Cl^- \rightleftarrows NpO_2^+ + Np^{3+} + 4HCl$ have been determined in a (Rb 0,25; Cs 0,75)Cl melt in the temperature range 660—750°C by absorption spectrophotometry. The results are compared with those obtained previously in (Li 0,7; K 0,3)Cl, (Li, K)Cl eutectic and (Li 0,55; Cs 0,45)Cl.

La spectrophotométrie d'absorption visible et proche i.r. constitue une méthode de choix pour l'étude des réactions d'oxydo —réduction du neptunium dans les chlorures alcalins fondus, ainsi qu'en témoignent plusieurs travaux antérieurs [1—6]. Cette étude a été étendue au cas du solvant constitué du mélange RbCl—CsCl (25—75% mol).

CONDITIONS EXPERIMENTALES

Le neptunium est introduit dans le bain fondu sous forme de complexes Cs_2NpCl_6 et $Cs_3NpO_2Cl_4$. Le solvant est préparé en mélangeant, dans les proportions requises, les sels purs (CsCl et RbCl; Merck p.a.); ce mélange est ensuite séché par chauffage sous vide à 300°C.

Les dispositifs expérimentaux utilisés, ainsi que les manipulations ont été décrits précédemment [1, 2, 7, 8].

Les Figs. 1 et 2 montrent les spectres d'absorption du neptunium aux différents états d'oxydation. Les longueurs d'onde des maxima des différentes bandes d'absorption sont consignées au Tableau 1.

Ainsi que le montrent la Fig. 3 et le Tableau 2, la loi de Beer est vérifiée dans le domaine de concentration considéré, pour les différents états d'oxydation III, IV et V du neptunium dans RbCl—CsCl (25—75% mol). Dès lors, il nous est possible d'étudier, de manière quantitative, quelques réactions d'oxydo—réduction du neptunium dans ce bain.

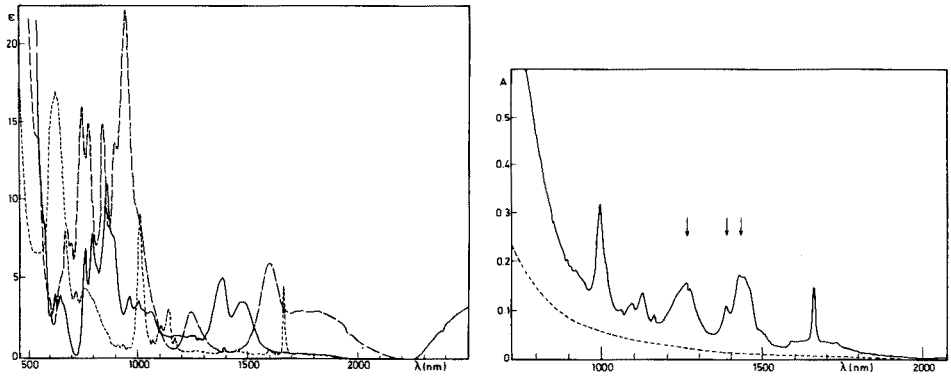

Fig. 1. Spectres d'absorption du neptunium aux différents états d'oxydation dans RbCl—CsCl (25—75% mol); Np(III) —— Np(V) —— NpO_2(V) ------- T = 660°C.

Fig. 2. Spectre d'absorption d'une solution de NpO_2(VI) + NpO_2(V) dans le mélange RbCl—CsCl (25—75% mol). Les bandes d'absorption caractéristiques de NpO_2(VI) sont représentées par des flèches. T = 660°C, P_{Cl_2} = 1 atm. ---------: fond continu.

TABLEAU 1

Position des maxima des bandes d'absorption (λ en nm) des différents états d'oxydation du neptunium dans le mélange RbCl—CsCl (25—75% mol) à 690°C

Np(III)	Np(IV)	NpO_2(V)	NpO_2(VI)
1460	1590	1658	1440
1380	1235	1162	1428
1053	936	1129	1261
1002	893	1097	
960	836	1085	
887	768	1058	
857	736	993	
791	686	746	
761	664	708	
659	529	625	
629		439	

TABLEAU 2

Variation des coefficients d'extinction molaire (ϵ en $l\,mol^{-1}\,cm^{-1}$) dans le mélange RbCl—CsCl (25—75% mol)

T (°C)	ϵ^3_{857}	ϵ^3_{1380}	ϵ^3_{1460}	ϵ^4_{936}	ϵ^5_{993}	ϵ^5_{1658}
660	11,1	4,90	3,35	22,2	9,13	4,58
690	11,2	4,92	3,44	22,5	9,09	4,47
720	11,3	4,82	3,48	22,8	9,05	4,37
750	11,4	4,82	3,53	22,9	8,99	4,26

RESULTATS

Détermination du potentiel normal du couple $NpO_2(VI)$—$NpO_2(V)$ dans le mélange RbCl—CsCl (25—75% mol)

Un barbotage de chlore dans une solution de $NpO_2(V)$ dans les chlorures alcalins fondus provoque l'apparition de $NpO_2(VI)$ selon la réaction

$$NpO_2^{2+} + Cl^- \rightleftarrows NpO_2^+ + \tfrac{1}{2}Cl_2 \qquad (1)$$

Le rapport des concentrations en $NpO_2(VI)$ (désignée par C_6) et $NpO_2(V)$ (C_5) ne dépend que de la pression partielle en chlore (P_{Cl_2}). La loi de Guldberg et Waage, appliquée à cet équilibre, s'écrit

$$K_1 = [NpO_2^+]\, P^{1/2}_{Cl_2}/[NpO_2^{2+}] \qquad (2)$$

A 993 nm, longueur d'onde du maximum d'absorption de la bande intense de $NpO_2(V)$, et aux hautes températures de travail (> 650°C), l'absorption due au Cl_2 gazeux n'est plus négligeable; cela rend malaisé une détermination précise de C_5 par mesure de l'absorbance à cette longueur d'onde. C'est pourquoi nous avons considéré l'absorption à 1658 et 1700 nm, laquelle est uniquement due à $NpO_2(V)$; on a alors

$$A_{1658} - A_{1700} = (\epsilon^5_{1658} - \epsilon^5_{1700})\, C_5 \cdot l$$

On calcule C_6 par différence entre la concentration totale et C_5.

Etant donné la température de fusion de mélange RbCl—CsCl (642°C), l'étude quantitative de l'équilibre [1] a été effectuée dans un domaine de température s'étendant de 660 à 750°C. Par barbotage de différents mélanges ($N_2 + Cl_2$) dans la solution fondue, on impose des potentiels redox à cette solution; lorsque l'équilibre est atteint, on enregistre le spectre de la solution qui fournit les valeurs de C_5 et C_6. La relation (2) peut encore s'écrire

$$\log C_5/C_6 = \log K_1 - 0.5 \log P_{Cl_2} \qquad (3)$$

Si on porte $\log C_5/C_6$ en fonction de $\log P_{Cl_2}$, on doit obtenir une droite de pente (—0,5) dont l'ordonnée à l'origine nous permet de calculer la valeur de la constante K_1. La Fig. 4 montre l'évolution de $\log C_5/C_6$ en fonction de $\log P_{Cl_2}$. Des mesures ont été effectuées aux températures de 660, 690, 720 et 750°C (Tableau 3). Les pentes obtenues (Tableau 4) correspondent aux

TABLEAU 3

Etude de l'équilibre NpO_2^{2+}—NpO_2^{+} dans le mélange RbCl—CsCl (25—75% mol)

T (°C)	No. exp.	Conc. tot. (10^2 mol l^{-1}) en Np	log ($P_{Cl_2} \cdot 10^3$ atm)	log C_5/C_6
660	I 1	2,71	2,64	0,17
	2		2,44	0,27
	3		2,32	0,35
	4		1,95	0,52
	5		1,58	0,70
	6		0,98	1,00
	7		2,99	0,039
	II 1	4,71	2,64	0,15
	2		2,53	0,21
	3		2,34	0,33
	4		2,15	0,42
	5		1,72	0,63
	6		1,45	0,77
	7		1,17	0,90
	8		2,99	0,025
690	I 1	2,68	1,37	0,90
	2		1,83	0,66
	3		2,58	0,29
	4		2,73	0,24
	5		2,99	0,10
	6		2,53	0,29
	7		2,24	0,46
	8		1,64	0,77
	II 1	4,65	1,18	0,98
	2		1,43	0,88
	3		2,16	0,49
	4		2,40	0,35
	5		2,67	0,23
720	I 1	2,65	1,63	0,89
	2		1,73	0,78
	3		2,01	0,64
	4		2,24	0,50
	5		2,67	0,32
	6		2,99	0,14
	II 1	4,58	2,49	0,39
	2		2,10	0,59
	3		1,58	0,86
	4		2,99	0,13
750	I 1	1,82	2,24	0,56
	2		2,39	0,49
	3		2,61	0,40
	4		2,84	0,29
	5		1,36	1,05
	II 1	4,54	1,58	0,92
	2		2,20	0,59
	3		2,99	0,19

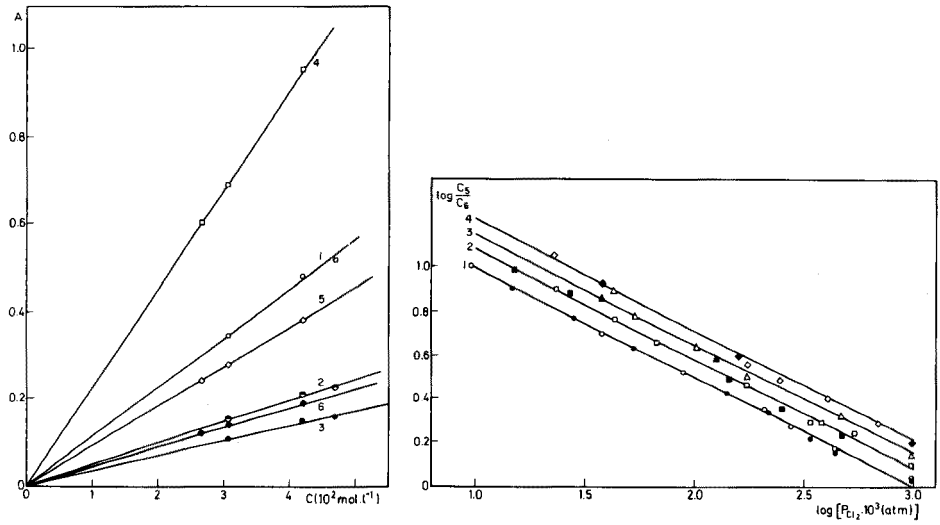

Fig. 3. Vérification de la loi de Beer dans le mélange RbCl—CsCl (25—75% mol) à 690°C. (1) Np(III) à 857 nm. (2) Np(III) à 1380 nm. (3) Np(III) à 1460 nm. (4) Np(IV) à 936 nm. (5) $NpO_2(V)$ à 993 nm. (6) $NpO_2(V)$ à 1658 nm.

Fig. 4. Evolution du degré d'avancement de la réaction d'oxydo—réduction $NpO_2(V)$—$NpO_2(VI)$ en fonction de log P_{Cl_2}. (1) 660°C, ○ Exp. I, ● Exp. II. (2) 690°C, □ Exp. I, ■ Exp II. (3) 720°C, △ Exp. I, ▲ Exp. II. (4) 750°C, ◇ Exp. I, ◆ Exp. II.

erreurs expérimentales près, à la valeur théorique, confirmant ainsi la stoechiométrie de la réaction (1). La Fig. 5 montre l'évolution de ln K_1 (Tableau 4) avec l'inverse de la température absolue. Dans le domaine de température considéré, on obtient une droite dont la pente et l'ordonnée à l'origine fournissent les valeurs moyennes des variations enthalpique et entropique de la réaction (1) (Tableau 4). On peut également calculer la valeur du potentiel normal du couple $NpO_2(VI)$—$NpO_2(V)$ par rapport au système

TABLEAU 4

Etude de la réaction $NpO_2^{2+} + Cl^- \rightleftarrows NpO_2^+ + \frac{1}{2}Cl_2$ dans le mélange RbCl—CsCl (25—75% mol)

$K_1 = [NpO_2^+]\, P_{Cl_2}^{1/2}/[NpO_2^{2+}]$

T (°C)	n[a]	pente	K_1 (atm$^{1/2}$)	ln K_1	E^0(V)
660	15	(—0,49 ± 0,01)	0,99 ± 0,07	—0,010	—0,001
690	13	(—0,50 ± 0,02)	1,20 ± 0,11	0,18	+0,015
720	10	(—0,52 ± 0,03)	1,40 ± 0,21	0,34	+0,029
750	8	(—0,52 ± 0,02)	1,58 ± 0,20	0,46	+0,041
			ΔH = (41,6 ± 6,5) kJ mol^{-1}		
			ΔS = (44,6 ± 6,6) j mol^{-1} K^{-1}		

[a]Nombre de mesures.

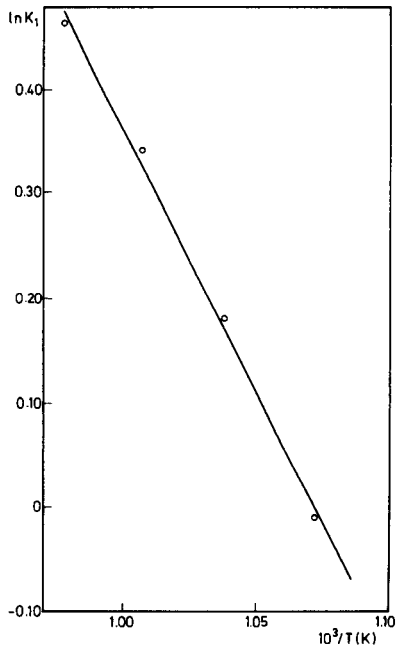

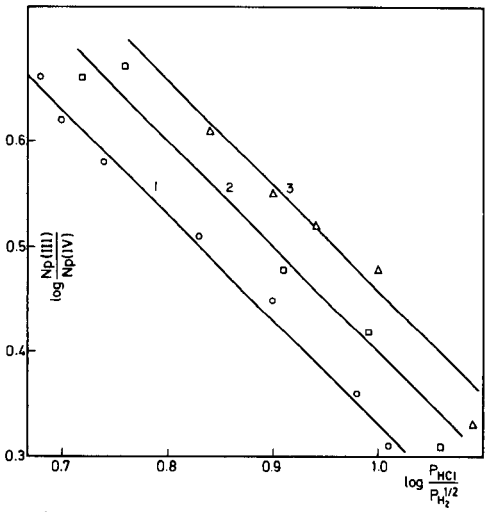

Fig. 5. Evolution du ln K_1 en fonction de l'inverse de la température absolue.

Fig. 6. Evolution du degré d'avancement de la réaction d'oxydo—réduction Np(IV)—Np(III) en fonction de log ($P_{HCl}/P_{H_2}^{1/2}$. (1) 660°C. (2) 700°C. (3) 750°C. Concentration totale en Np: (1) $4{,}35 \cdot 10^{-2}$ mol l^{-1}; (2) $4{,}28 \cdot 10^{-2}$ mol l^{-1}; (3) $4{,}20 \cdot 10^{-2}$ mol l^{-1}.

Cl_2—Cl^-; on a, en effet

$$E^\circ_{NpO_2(VI)/NpO_2(V)} = (2.3RT/F) \log K_1 \qquad (4)$$

Ces valeurs de E° sont reprises au Tableau 4. On peut remarquer qu'à 660° C, ce potentiel normal est très proche de $E^\circ_{Cl_2-Cl^-}$; ceci signifie que, si $P_{Cl_2} = 1$ atm, le rapport C_5/C_6 est voisin de l'unité ce qui fixe la concentration maximum en NpO_2(VI) accessible, dans nos conditions expérimentales.

Détermination du potentiel normal du couple Np(IV)—Np(III) dans RbCl—CsCl (25—75% mol)

En contrôlant la composition de la phase gazeuse (H_2 + HCl) au contact avec la solution fondue et en mesurant les concentrations en Np(IV) et Np(III) à l'équilibre, il devient possible de déterminer la valeur de la constante d'équilibre de la réaction

$$Np^{4+} + \tfrac{1}{2}H_2 + Cl^- \rightleftarrows Np^{3+} + HCl \qquad (5)$$

avec

$$K_2 = [Np^{3+}]\, P_{HCl}/[Np^{4+}]\, P_{H_2}^{1/2} \qquad (6)$$

L'expression (6) peut se mettre sous la forme logarithmique suivante

$$\log (C_3/C_4) = \log K_2 - \log (P_{HCl}/P_{H_2}^{1/2}) \quad (7)$$

Si on porte log (C_3/C_4) en fonction de log $(P_{HCl}/P_{H_2}^{1/2})$, on doit obtenir une droite de pente −1 dont l'ordonnée, à l'origine, permet de calculer K_2. La détermination des concentrations en Np(III) (C_3) et Np(IV) (C_4) est effectuée comme pour les solutions dans LiCl—CsCl [6].

Des expériences ont été réalisées entre 660 et 750°C; la Fig. 6 montre l'évolution du rapport des concentrations C_3 et C_4 en fonction du rapport des pressions partielles en HCl et H_2. Les pentes des différentes droites (Tableau 5) correspondent à la valeur théorique, aux erreurs expérimentales près, et semblent donc confirmer la validité de la stoechiométrie de la réaction (5). La Fig. 7 montre l'évolution de ln K_2 en fonction de l'inverse de la température absolue, dans le domaine de température considéré; on en déduit les valeurs moyennes des variations enthalpique et entropique de la réaction (5) (Tableau 5). Le potentiel normal du couple Np(IV) –Np(III) par rapport au système H^+—H_2 aux différentes températures considérées, est obtenu par la relation suivante:

$$E^0_{Np(IV)—Np(III)} = (2{,}3RT/F) \log K_2 \quad (8)$$

Les différentes valeurs de $E^0_{Np(IV)—Np(III)}$ sont reprises au Tableau 5.

Dismutation de Np(IV) dans RbCl—CsCl

L'action du mélange gazeux (HCl + H_2O + Cl_2) sur une solution de neptunium dans les chlorures fondus donne lieu à la réaction

$$NpO_2^+ + 4HCl \rightleftarrows Np^{4+} + 2H_2O + \tfrac{1}{2}Cl_2 + 3Cl^- \quad (9)$$

ainsi qu'en témoignent plusieurs publications antérieures [2, 3, 5]. Dans le solvant RbCl–CsCl, on obtient plus aisément NpO_2(VI) que dans les autres

TABLEAU 5

Etude de l'équilibre $Np^{4+} + \frac{1}{2}H_2 + Cl^- \rightleftarrows Np^{3+} + HCl$ dans le mélange RbCl—CsCl (25—75% mol)

$K_2 = [Np^{3+}]P_{HCl}/[Np^{4+}]P_{H_2}^{1/2}$

T (°C)	n[a]	Pente	K_2 (atm$^{\frac{1}{2}}$)	ln K_2	$E^0_{Np(IV)/(Np(III)}$[b]
660	7	−0,98 ± 0,10	20,9 ± 3,9	3,04	0,244
700	5	−1,06 ± 0,24	28,0 ± 11,9	3,33	0,281
750	5	−1,08 ± 0,30	33,6 ± 17,5	3,52	0,311
			ΔH = (42,0 ± 29,0) kJ mol^{-1}		
			ΔS = (70,5 ± 30,0) J mol K^{-1}		

[a] Nombre de mesures.

[b] Par rapport au système H^+/H_2.

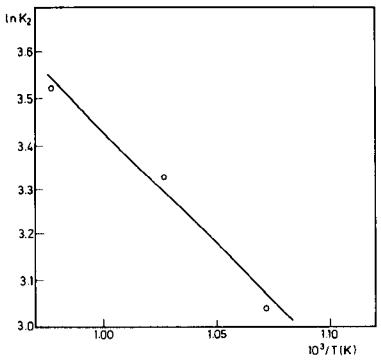

Fig. 7. Evolution du ln K_2 en fonction de l'inverse de la température absolue.

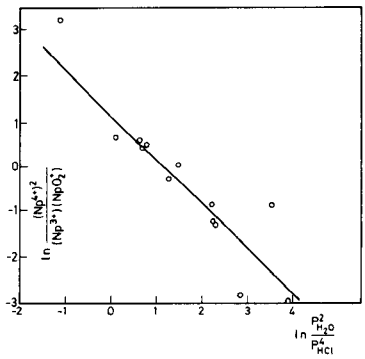

Fig. 8. Evolution du degré d'avancement de la réaction de dismutation de Np(IV) en fonction de ln $(P^2_{H_2O}/P^4_{HCl})$. T = 660°C. Concentration totale en Np: $4{,}75 \cdot 10^{-2}$ mol l^{-1}.

solvants étudiés, rendant difficile la préparation de solutions contenant uniquement Np(IV) et NpO_2(V). On y arrive cependant pour des valeurs importantes de P_{HCl}, mais, dans ce cas, l'espèce Np(IV) est prépondérante. Lorsque P_{H_2O} et P_{Cl_2} croissent vis-à-vis de P_{HCl}, on observe rapidement la réapparition de NpO_2(V) et NpO_2(VI) jusqu'à disparition totale de Np(IV); les trois espèces peuvent ainsi être obtenues dans un certain domaine de pressions partielles des trois gaz considérés.

Dans ces conditions, nous nous sommes demandés s'il était possible d'observer, par analogie avec la réaction de dismutation de UO_2(V) étudiée précédemment [8, 9], l'équilibre

$$2NpO_2^+ + 4HCl \rightleftarrows Np^{4+} + NpO_2^{2+} + 2H_2O + 4Cl^- \qquad (10)$$

A cet effet, nous avons fait réagir diverses solutions de neptunium avec des mélanges HCl—H_2O de compositions variables. Dans toutes les expériences effectuées, nous avons obtenu, contrairement à notre attente, des solutions contenant Np(III), Np(IV) et NpO_2(V), NpO_2(VI) ayant totalement disparu. De plus, la concentration en Np(IV) augmente avec le rapport P_{HCl}/P_{H_2O}, tandis que, simultanément, les concentrations en Np(III) et NpO_2(V) diminuent; ce phénomène est réversible et aisément reproductible.

Ces observations semblent montrer qu'en présence d'une phase gazeuse contenant HCl et H_2O nous pouvons observer la réaction de dismutation—amphotérisation de Np(IV) en NpO_2(V) et Np(III), soit

$$2Np^{4+} + 2H_2O + 2Cl^- \rightleftarrows NpO_2^+ + Np^{3+} + 4HCl \qquad (11)$$

En contrôlant le $p_{O^{2-}}$ de la solution au moyen de mélanges gazeux (HCl + H_2O) définis et en mesurant les concentrations en Np(III), Np(IV) et NpO_2(V) à l'équilibre, nous pouvons déterminer, pour l'équilibre (11) la valeur de la constante d'équilibre K_3 définie comme suit

$$K_3 = [Np^{4+}]^2 P^2_{H_2O} / [Np^{3+}]\ [NpO_2^+]\ P^4_{HCl} \quad (12)$$

Cette expression peut se mettre sous la forme logarithmique suivante

$$\ln (C_4^2/C_3\ C_5) = \ln K_3 - \ln (P^2_{H_2O}/P^4_{HCl}) \quad (13)$$

Si on porte ln $(C_4^2/C_3\ C_5)$ en fonction de ln $(P^2_{H_2O}/P^4_{HCl})$, on doit obtenir une droite de pente —1 dont l'ordonnée à l'origine permet de calculer K_3. Les concentrations sont déterminées en mesurant les absorptions à 1380 et 1423 nm pour le calcul de C_3 et 1658 et 1700 nm pour le calcul de C_4 et C_5. La Fig. 8 montre les résultats obtenus dans RbCl—CsCl à 660° C. La valeur de la pente (n = —1,06 ± 0,28) correspond à la valeur théorique, ce qui semble confirmer l'existence d'une dismutation de Np(IV) suivant la réaction (11). Le valeur de la constante d'équilibre K_3 est (3,8 ± 1,8) atm^{-2}.

DISCUSSION

Les équilibres (1) et (5) évoluent dans le sens de la formation des espèces NpO_2(V) et Np(III) lorsque la température augmente; cette évolution est analogue à celle observée dans les autres bains de chlorures fondus.

Si l'on considère, à une température déterminée, la série des solvants utilisés, en l'occurrence: LiCl—KCl (70—30% mol), eutectique LiCl—KCl, LiCl—CsCl (55—45% mol), RbCl—CsCl (25—75% mol), on constate qu'en passant de la gauche vers la droite les valeurs de K_1 et K_2 diminuent. L'anion des différents solvants étant commun, ceci signifie que les espèces NpO_2(VI) et Np(IV) vont être de plus en plus stables en passant de solvants riches en lithium à ceux riches en césium. Cette stabilité se traduit par une évolution des potentiels normaux. On mesure, par exemple, pour le système NpO_2(VI)—NpO_2(V) à 660°C:

	$E^0_{NpO_2(VI)-NpO_2(V)} - E^0_{Cl_2-Cl^-}$
LiCl—KCl (70—30% mol)	+0,38 V
LiCl—KCl (eutectique)	+0,36 V
LiCl—CsCl (55—45% mol)	+0,12 V
RbCl—CsCl (25—75% mol)	0,00 V

On constate que, dans les différents milieux considérés, le pouvoir oxydant de NpO_2(VI) diminue lorsqu'on passe d'un solvant dont les cations ont un rayon ionique faible, comme le mélange LiCl—KCl, à un solvant dont les cations sont plus volumineux, comme le mélange RbCl—CsCl. Il est à noter que l'on observe une stabilité comparable pour NpO_2(VI) dans RbCl—CsCl à 660°C et LiCl—CsCl à 387°C; on a alors, dans ces deux milieux: $E^0_{NpO_2(VI)-NpO_2(V)} - E^0_{Cl_2-Cl^-} = 0$ V.

En ce qui concerne le couple oxydo—réducteur Np(IV)—Np(III), nous avons à 660°C:

	$E^0_{Np(IV)-Np(III)} - E^0_{H(I)-H_2}$
LiCl—CsCl (55—45% mol)	+0,26 V
RbCl—CsCl (25—75% mol)	+0,24 V

Ainsi que nous l'avions signalé dans un précédent travail [6], la méthode spectrophotométrique n'est pas adaptée à l'étude du système Np(IV)–Np(III) dans l'eutectique LiCl–KCl et le mélange LiCl–KCl (70–30% mol). Si l'on considère les effets de solvant observés pour les couples NpO_2(VI)–NpO_2(V) et Pu(IV)–Pu(III) [10–12], il semble raisonnable d'admettre que la valeur de $[E^0_{Np(IV)-Np(III)} - E^0_{Cl_2-Cl^-}]$ décroît en remplaçant Li par Cs dans le solvant.

Les auteurs remercient l'Institut Interuniversitaire des Sciences Nucléaires pour les subsides accordés au laboratoire et qui ont permis la réalisation de ce travail.

BIBLIOGRAPHIE

1 R. Lysy, G. Landresse et G. Duyckaerts, Bull. Soc. Chim. Belg., 83 (1974) 227.
2 R. Lysy, G. Landresse et G. Duyckaerts, Anal. Chim. Acta, 72 (1974) 307.
3 R. Lysy et G. Duyckaerts, Inorg. Nucl. Chem. Lett., 12 (1976) 205.
4 R. Lysy et G. Duyckaerts, Inorg. Nucl. Chem. Lett., 11 (1975) 79.
5 R. Lysy et G. Duyckaerts, Inorg. Nucl. Chem. Lett., 11 (1975) 89.
6 R. Lysy et G. Duyckaerts, Rev. Chim. Minér., 14 (1977) 119.
7 G. Landresse, Anal. Chim. Acta, 56 (1971) 29.
8 R. Lysy, G. Landresse et G. Duyckaerts, Inorg. Nucl. Chem. Lett., 10 (1974) 685.
9 G. Landresse et G. Duyckaerts, Anal. Chim. Acta, 58 (1972) 369.
10 G. Landresse et G. Duyckaerts, Inorg. Nucl. Chem. Lett., 10 (1974) 675.
11 G. Landresse et G. Duyckaerts, Inorg. Nucl. Chem. Lett., 10 (1974) 1051.
12 G. Landresse et G. Duyckaerts, J. Radioanal. Chem., 35 (1977) 63.

Analytica Chimica Acta, 94 (1977) 395—403

MECHANISM AND REACTION RATE OF THE KARL FISCHER TITRATION REACTION
Part V. Analytical Implications

J. C. VERHOEF

Laboratory of Analytical Chemistry, Free University, de Boelelaan 1083, Amsterdam (The Netherlands)

E. BARENDRECHT

Laboratory of Electrochemistry, University of Technology, P.O. Box 513, Eindhoven (The Netherlands)

(Received 16th May 1977)

SUMMARY

The Karl Fischer titration procedure for the determination of water has been studied. In view of the results of previous investigations, a methanolic sodium acetate—sulfur dioxide solution is recommended as solvent and an iodine solution in methanol as titrant. The advantages of this procedure over a conventional Karl Fischer titration are: a much more rapidly reacting reagent, the possibility of a visual end-point detection, a titrant of constant titre over a long period of time, and the absence of the disagreeable odour of pyridine.

The two-step mechanism proposed by Smith et al. [1] for the Karl Fischer titration reaction is, in spite of some severe criticism [2, 3], still generally accepted

$$I_2 + SO_2 + 3\,Py + H_2O = 2\,PyHI + PySO_3 \quad (1)$$

$$PySO_3 + CH_3OH = PyHSO_4CH_3 \quad (2)$$

where Py = C_5H_5N. It has been shown [4, 5] that pyridine plays no role in the mechanism, provided that the pH of the solution is kept constant. The oxidizable species in the reagent is neither sulfur dioxide, nor a pyridine—sulfur dioxide complex, but the monomethyl sulfite ion

$$SO_2 + 2CH_3OH \rightleftharpoons CH_3SO_3^- + CH_3OH_2^+ \quad (3)$$

It is therefore necessary to buffer the solution to be titrated to convert as much sulfur dioxide into methyl sulfite as possible. Another advantage of good buffering is that little of the yellow complex of sulfur dioxide and iodide [6] ($K_c \approx 1\ 1\ mol^{-1}$) is formed

$$SO_2 + I^- \rightleftharpoons SO_2I^- \quad (4)$$

Thus, a visual end-point detection is possible, for this complex is the cause of the yellow color of spent reagent; the equipment for a biamperometric or a bipotentiometric end-point detection is not then required. The titration reaction is first order in methyl sulfite, in water, and in iodine, with a third-order rate constant, $k_{3,I_2} = 8 \times 10^6$ l^2 mol^{-2} s^{-1} (average of the values published [4—6] previously. Because of the great stability of the triiodide ion in methanol [7]

$$K_s = c_{I_3^-}/c_{I^-} \cdot c_{I_2} = 2 \times 10^4 \text{ l mol}^{-1}, \quad (5)$$

generally most of the iodine will be converted into triiodide. The reaction is also first order in triiodide, but the rate constant for this species is much smaller than that for iodine: $k_{3,I_3^-} = 5 \times 10^2$ l^2 mol^{-2} s^{-1}. The effective rate constant for the reaction of both iodine and triiodide can be expressed as

$$k_3 = (k_{3,I_2} + k_{3,I_3^-} K_s c_{I^-})/(1 + K_s c_{I^-}) \quad (6)$$

Thus the greater the iodide concentration, the greater the conversion of iodine into triiodide and the lower the effective rate constant k_3.

THEORETICAL CONSIDERATIONS

It is customary with the Karl Fischer method for methanol to be used as solvent. Before the sample is added, the solvent is pre-titrated to a sensitive, but arbitrary end-point (e.g., in biamperometric end-point detection to a current greater than 10 μA, lasting for at least 20 s when one drop of reagent is added). After addition of the sample, the solution is titrated to the same end-point.

This procedure introduces a systematic error: the volume at the end of the pre-titration differs from that at the end of the sample titration [8]. This error can be kept within acceptable limits by proper choice of the initial volume, concentration of the reagent and volume of the sample added. More important, however, is the difference in reaction rate. Usually, the reagent contains an approximately three-fold excess of sulfur dioxide over iodine, so that on addition of each drop of reagent the sulfur dioxide concentration in the titration vessel increases. At the end of the pre-titration, the sulfur dioxide concentration (assuming that the original solvent is reasonably dry) will be small; generally, this will not be so at the end of the sample titration. Since the detection of the end-point depends on the lifetime of a drop of reagent, and therefore on the reaction rate, this difference could cause serious errors. However, the iodide concentration will also increase during the titration so that, according to eqn. (6), the effective rate constant will decrease. These effects compensate each other to a large extent, so that in practice the systematic error is small. Nevertheless one of the drawbacks of the Karl Fischer reagent is the slow reaction rate and, therefore, the tedious titration and the dragging end-point. The remedy is to increase the reaction rate by increasing the sulfur dioxide concentration, or better, by

increasing the pH of the solution. Normally, pyridine is added as buffer with each drop of reagent (usually, the reagent contains a seven-fold excess of pyridine over iodine). Pyridine and sulfur dioxide have approximately the same acidity constant [4] in methanol

$$K_{a,Py} = c_{Py}\ c_{H^+}/c_{PyH^+} = 10^{-5.6} \quad (7)$$

$$K_{a,SO_2} = c_{RSO_3^-}\ c_{H^+}/c_{SO_2} = 10^{-6.0} \quad (8)$$

(these values depend somewhat on the ionic strength of the solution), so that a reasonable estimation of the methyl sulfite concentration is

$$c_{RSO_3^-} \approx 0.5\ f_{SO_2} \quad (9)$$

where f_{SO_2} is the formal (analytical) concentration of sulfur dioxide. Unless very large amounts of water are titrated, the sulfur dioxide concentration will remain relatively low. It is therefore proposed that a methanolic solution of sulfur dioxide (ca. 0.5 M) and sodium acetate (ca. 1 M) is used as solvent and a solution of iodine in methanol as titrant. Because the dissociation constant of acetic acid in methanol is very small [9]

$$K_{a,HAc} = c_{Ac^-}\ c_{H^+}/c_{HAc} = 10^{-9.7}, \quad (10)$$

the sodium acetate will convert virtually all of the sulfur dioxide into methyl sulfite

$$SO_2 + Ac^- + CH_3OH \rightleftharpoons HAc + CH_3SO_3^-. \quad (11)$$

and the solution in effect contains a solution (0.5 M + 0.5 M) of acetate—acetic acid buffer.

The advantages of this procedure are: (1) the good buffer action and the large methyl sulfite concentration give a high reaction rate; (2) the absence of sulfur dioxide prevents the formation of the yellow SO_2I^- complex and makes a visual end-point possible; (3) the absence of pyridine makes the reagent more agreeable to use; (4) the iodine titre remains constant.

The only disadvantages are: (1) two separate solutions are necessary; (2) the maximum amount of water that can be titrated depends on the amount of buffer present, i.e. on the buffering capacity of the solution. The appearance of a yellow colour before the end-point is a good indication that the buffer capacity is not adequate. If, on further addition of iodine, the intensity of the colour does not increase, formation of the SO_2I^- complex is indicated.

Some titration curves, whereby the lifetime of a drop of reagent is calculated as a function of the total amount of reagent added, have been constructed. By the lifetime of a drop is understood the time needed for the iodine therein to be consumed and a certain detection limit to be reached (expressed in terms of concentration in the titration vessel, see below). For the sake of simplicity, some approximations are made: (1) the mixing time of the drop with the sample solution is neglected; (2) the overall third-order rate constant does not change during the drop life; (3) the methyl sulfite concentration of the solution is constant during the drop life.

The first approximation is required as it would be very difficult — if not impossible — to calculate the flow patterns of the mixing of the drop, the concentration profiles in the solution and the influence of these factors on the drop life. In practice, the mixing time is ca. 1 s. The second approximation implies that variation of the iodide concentration during a drop life is small. For the first few drops this condition is not fulfilled but, from an analytical point of view, these first few drops are not important. Figure 1 shows the dependence of the overall third-order rate constant, k_3, on the iodide concentration (eqn. 6). When the iodide concentration is very small, the reaction rate constant decreases very rapidly with increasing iodide concentration; for the relatively large iodide concentration usually found at the end of a titration, the decrease in rate constant is much smaller and the second approximation is justified.

The third approximation makes it possible to calculate the drop life with pseudo-second order kinetics. If the initial sulfur dioxide concentration (at the beginning of the customary titration) is zero, some error is incurred; again, this is not pertinent analytically. The calculation is as follows: for the n th drop of reagent added, the initial concentrations of water and methyl sulfite, $c^{n,0}_{H_2O}$ and $c^{n,0}_{RSO_3^-}$, are calculated. Then, the initial concentrations of iodine, triiodide and iodide are calculated. From eqn. 6, the third-order rate constant for the n th drop, k^n_3, is found, and multiplication by $c^{n,0}_{RSO_3^-}$ gives the second-order rate constant, k^n_2: this is considered to remain constant during the lifetime of the n th drop τ_n.

Second-order kinetics give:

$$\tau_n = \frac{1}{k^n_2 (c^{n,0}_{Ox} - c^{n,0}_{H_2O})} \ln \frac{c^{n,0}_{H_2O} \cdot c^{n,\tau}_{Ox}}{c^{n,0}_{Ox} (c^{n,0}_{H_2O} - c^{n,0}_{Ox} + c^{n,\tau}_{Ox})} \qquad (12)$$

where $c^{n,0}_{Ox} = c^{n,0}_{I_2} + c^{n,0}_{I_3^-}$ and $c^{n,\tau}_{Ox}$ is the detection limit of iodine and triiodide at the end of the life of the n th drop.

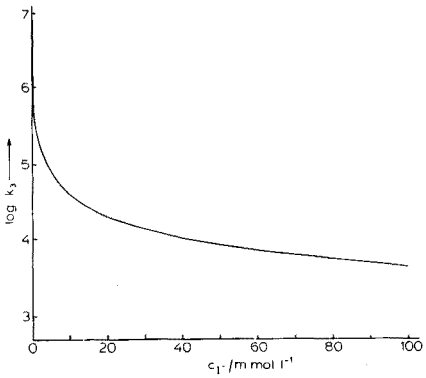

Fig. 1. Dependence of the effective third-order rate constant on the iodide concentration.

In Fig. 2, some titration curves are shown for a pre-titration with a sample titration. The following values for the various quantities have been used in the calculation. The initial volume and the volume of a drop of reagent are taken as 10 ml and 0.01 ml, respectively. Before addition of the sample, the water concentration in the titration vessel is 1 mM, and the sample increases the water concentration in the vessel by a further 10 mM. The pre-titration, therefore, demands 10 drops of reagent (0.1 ml) and the sample consumes 100 drops of reagent (1 ml). The detection limit is estimated as 0.03 mM ($I_2 + I_3^-$). Figure 2(a) shows the titration curve for the customary reagent ($pH \simeq pK_a$; threefold excess of sulfur dioxide over iodine in the reagent). Figure 2(b) shows the titration curve for the same reagent, but with increased pH. Figure 2(c) shows the titration curve for the modified procedure in which the initial solution contains 0.5 M methyl sulfite and sulfur dioxide is not added during the titration. For the sake of clarity, the titration curves are drawn as solid lines rather than as discrete points for each drop. The amount of reagent used for the sample titration equals the distance between corresponding points in the pre-titration curve and the sample titration curve. If the end-point corresponds to a drop life of 20 s, this distance corresponds in Fig. 2(a) to 0.95 ml of reagent (i.e. a systematic error of −5%). At 30 s, the systematic error is −2.5%, at the expense of a more tedious titration. For the modified reagent, however, this error is negligible at 2 s or more.

Figure 3 shows the values of the second-order rate constant for the different cases in Fig. 2. Except for the first few drops, the decrease in the rate constant as a result of the increasing concentration of iodide is compensated largely by the increase in sulfur dioxide concentration (Fig. 3a and b). For the modified procedure (Fig. 3c), there is no such compensation and the variation of the second-order rate constant is much larger. However, this rate constant is, even at the end of the titration, so high that all drops are very rapidly consumed and the variation in the second-order rate constant has no effect.

Because of the approximations mentioned above, the results of the calculations are indicative rather than absolute. They show, however, the shortcomings of the customary reagent and the improvements obtained by increasing the pH and the methyl sulfite concentration. For the measurement of rate constants, the calculations are, of course, not suitable. The better-defined conditions and more accurate measuring techniques of previous parts of this series are much more suitable for this purpose.

EXPERIMENTAL

Reagents and procedure

The methanol used to prepare the titration solutions (Baker, A.R.) was dried by distillation after refluxing with magnesium. Sodium iodide (Baker A.R.) and sodium acetate (Merck, A.R., anhydrous) were dried at 150°C for

at least 24 h. Iodine (Baker, A.R.) and sulfur dioxide (Baker—Matheson, anhydrous gas) were used without further purification. Both single and double Karl Fischer reagents (Merck and Baker) were used. The titre of the reagents was determined with water, injected into the titration vessel through a rubber septum with a 10-μl Hamilton microsyringe.

Apparatus

The customary Karl Fischer reagent and methanolic iodine solution were inserted into the titration vessel from a 5-ml electronic burette (Metrohm Dosimat E 535/E 552-5B) with a resolution of 0.001 ml. The original Teflon tip was replaced by a very fine glass capillary that just reached the solution surface. The methanol and the methanolic solution of sulfur dioxide and sodium acetate were added from a 20-ml burette (Metrohm Dosimat E 415/E 552-20B) with a resolution of 0.01 ml. The burettes were fitted with Teflon cocks. The supply vessels of the burettes could be opened to the atmosphere via a drying tube, filled with silica gel or phosphorus pentoxide; a cock between the supply vessels and the drying tubes was opened occasionally for a few seconds to equalize the pressure in the supply vessels, thus preventing the drying material from interacting with the methanol vapours.

Bipotentiometric and biamperometric end-points were detected with a pair of platinum wire electrodes (ca. 5 mm long, 5 mm apart) and a laboratory-made potentiostat/galvanostat. Some titrations were performed with a Metrohm autotitrator E 526-1 to which some minor modifications were made. The coulometric experiments were performed as described [4] with a cell of reduced size (main compartment, 9-ml capacity).

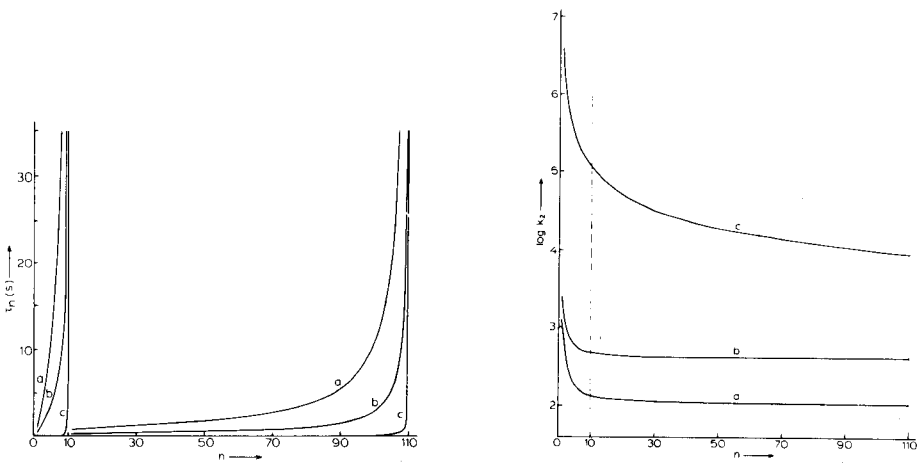

Fig. 2. Calculated titration curves. (a) Customary Karl Fischer reagent, (b) effect on (a) of increased pH, (c) modified procedure (see text).

Fig. 3. Second-order rate constants for the titration of Fig. 2.

RESULTS AND DISCUSSION

For a customary Karl Fischer reagent, electroanalytical end-point detection is normally used. Figure 4 shows bipotentiometric detection curves (E vs. total c_{I_2}, i.e. inclusive triiodide) for various electrode currents. Bipotentiometric detection is well-suited for triggering purposes because of the steep drop in potential difference. A potential-controlled timing device was started when the potential difference fell below 100 mV and was stopped when the difference exceeded 150 mV, thus indicating the lifetime of a drop of reagent. The hysteresis of 50 mV made the timing device insensitive to small fluctuations in the potential difference.

Figure 5 shows biamperometric detection curves (i vs. total c_{I_2}) for various potential differences between the indicator electrodes. The indication is approximately proportional to the total concentration of iodine (inclusive triiodide) and much more dependent on factors such as the rotation speed of the stirring magnet and concentration gradients in the titration vessel. The fluctuations in the indication are much larger, so that an automatic timing device cannot easily be used. Bipotentiometric end-point detection was therefore used. The electrode current was usually set at 2 μA, corresponding to a detection limit of about 3×10^{-5} M. The bipotentiometric detection mode is acceptable in modern analytical practice; many pH meters have a Karl Fischer polarization current source.

For the modified procedure, a methanolic solution of sulfur dioxide (0.5 M) and sodium acetate (1 M) was used as solvent; the titration was made with either a customary Karl Fischer reagent or with a solution of iodine in methanol (0.1 M). Both titration reagents are equally satisfactory but the iodine solution is preferred; the titre of the customary Karl Fischer reagent decreases from ca. 0.3 M to 0.1 M over a period of a few months, but the effective titre of a methanolic iodine solution decreases by only 3% over a period of five months, probably through penetration of water into the supply vessel). The effective titre of the iodine solution is the difference between the analytical iodine concentration and the water concentration in that solution; in practice it differed by ca. 5% from the amount of iodine dissolved in the methanol.

Both bipotentiometric and visual end-points are possible; the latter is somewhat more sensitive (about 1×10^{-5} M).

The use of sodium acetate instead of pyridine has been reported previously [10]. A Karl Fischer reagent with the pyridine replaced by sodium acetate is not very stable and it was recommended that the reagent be stabilized by adding iodide. This, however, lowers the reaction rate; the stabilization and the lowering of the reaction rate can be attributed to the same effect. It has been suggested [4] that an iodine—methyl sulfite complex might be an intermediate in the Karl Fischer reaction

$$CH_3SO_3^- + I_2 \rightleftharpoons CH_3SO_3I_2^- \qquad (13)$$

The actual Karl Fischer reaction then involves the hydrolysis of this complex

$$CH_3SO_3I_2^- + H_2O \rightarrow CH_3SO_4^- + 2\,I^- + 2\,H^+ \quad (14)$$

The complex is also thought to react with methanol, but the rate of solvolysis is much smaller

$$CH_3SO_3\,I_2^- + CH_3OH \rightarrow (CH_3)_2SO_4 + 2\,I^- + H^+ \quad (15)$$

Dimethyl sulfate is very toxic; a Karl Fischer reagent should therefore be handled with care. The introduction of a large amount of iodide will convert most of the iodine into triiodide. In this respect, the use of separate solutions for sulfur dioxide and iodine contributes to safety in the laboratory; the use of separate solutions has been suggested previously [11, 12]. In Fig. 6, the experimental titration curves are shown for (a) a customary Karl Fischer titration and (b) the modified titration. There is a fair similarity between these curves and the theoretical predictions. For ca. 1 y, a customary and a modified reagent have been compared in use. The water content of many non-aqueous solvents used in the laboratory has been measured, e.g. the methanolic solutions used previously [4—6] and non-aqueous solutions for electrochemical experiments, e.g. dimethyl sulfoxide, dimethylformamide, propylene carbonate, etc. The variations in the determinations by the two methods are of the same order of magnitude as the variation within one method (1—2%). The modified procedure is much faster. It is sufficient to check the titre of the iodine solution weekly.

The applicability of the modified reagent to coulometric determinations has been tested. The cell was filled with the sulfur dioxide — sodium acetate solution and iodide (0.1 M). The solution was coulometrically pre-titrated (if the glassware is not very dry, it is faster to pre-titrate the solution with

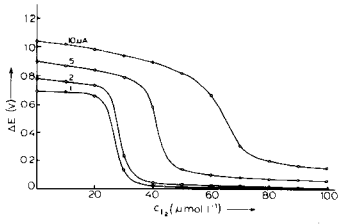

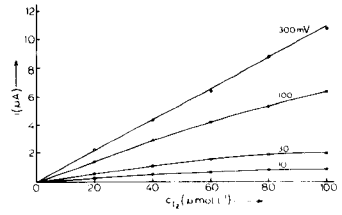

Fig. 4. Bipotentiometric detection curves for different electrode currents; c_{I^-} = 0.1 M in methanol.

Fig. 5. Biamperometric detection curves for different potential differences c_{I^-} = 0.1 M in methanol.

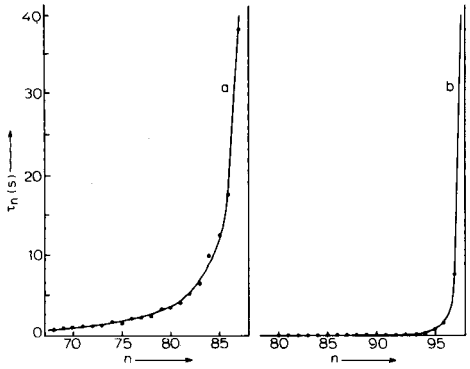

Fig. 6. Experimental titration curves. (a) Titration of 4 μl of water with 0.25 M Karl Fischer reagent; (b) titration of 2 μl of water with 0.11 M iodine solution in methanol; c_{NaAc} = 1 M, c_{SO_2} = 0.5 M, drop volume = 0.01 ml.

an iodine solution) and small amounts of water were injected with a Hamilton 1-μl microsyringe through a rubber septum. For the coulometric determinations, the current source for the generation of iodine, set at 25 mA, was controlled by the Metrohm autotitrator. The switching potential was set at 100 mV. The autotitrator was slightly modified; e.g. a polarization current source (2 μA) for the platinum wire detector electrodes was added. The overall current efficiency was excellent (99.1 ± 0.1% inclusive of the tolerances in the electronic equipment and the microsyringe) when the method was tested over the range 1—12 μg of water.

REFERENCES

1 D. M. Smith, W. M. D. Bryant and J. Mitchell, Jr., J. Am. Chem. Soc., 61 (1939) 2407.
2 E. Bonauguri and G. Seniga, Z. Anal. Chem., 144 (1954) 161.
3 E. Eberius, Wasserbestimmung mit Karl Fischer Lösung, Verlag Chemie, Weinheim, 2e Aufl., 1958.
4 J. C. Verhoef and E. Barendrecht, J. Electroanal. Chem., 71 (1976) 305.
5 J. C. Verhoef, W. P. Cofino and E. Barendrecht, to be published.
6 J. C. Verhoef and E. Barendrecht, J. Electroanal. Chem., 75 (1977) 705.
7 J. C. Verhoef and E. Barendrecht, Electrochim. Acta, in press.
8 A. Cedergren, Talanta, 21 (1974) 367.
9 B. Trémillon, La chimie en solvants non-aqueux, Presses Universitaires de France, Paris, 1971.
10 F. B. Sherman, M. P. Zabokritskii and V. A. Klimova, J. Anal. Chem. U.S.S.R., 28 (1974) 1450.
11 A. Johansson, Svensk Papperstidn., 50, 11B (1947) 124; Acta Chem. Scand., 3 (1949) 1058.
12 W. Seaman, W. H. McComas and G. A. Allen, Anal. Chem., 21 (1949) 510.

Analytica Chimica Acta, 94 (1977) 405—413

KINETIC DETERMINATION OF TRACES OF MANGANESE(II) BY ITS CATALYTIC EFFECT ON THE AUTOXIDATION OF 1,4-DIHYDROXY-PHTHALIMIDE DITHIOSEMICARBAZONE

D. PEREZ-BENDITO* and M. VALCARCEL

Department of Analytical Chemistry, University of Córdoba (Spain)

M. TERNERO and F. PINO

Department of Analytical Chemistry, University of Sevilla (Spain)

(Received 10th May 1977)

SUMMARY

A kinetic method is described for the determination of trace amounts of manganese(II) based on its catalytic effect on the aerial oxidation of 1,4-dihydroxyphthalimide dithiosemicarbazone. The reaction is followed spectrophotometrically by measuring the rate of change in absorbance at 594 nm. The calibration graph (rate constant vs. manganese concentration) is linear in the range 10—90 ng Mn ml^{-1}. The preparation and properties of the reagent are described and the kinetic parameters of the reaction are reported. There are few interferences.

The catalytic effect of osmium on the oxidation of phthalimide dithiosemicarbazone with cerium(IV) has been described [1]. The new reagent, 1,4-dihydroxyphthalimide dithiosemicarbazone (OH-PDT) is easily oxidized because of the presence of hydroxy groups, and a chemical oxidizing agent is not necessary. Traces of manganese(II) catalyze the aerial oxidation of reagent in alkaline medium, and a red-violet colour is developed. Other ions such as Os(VIII), Rh(III), Pt(IV) and Pd(II) do not exhibit this catalytic effect under the recommended conditions. There are several catalytic methods for the determination of microgram amounts of manganese, based on various reactions [2—7], but all these methods require an oxidizing agent.

The present paper describes the properties of the reagent and a kinetic catalytic reaction which can be utilized in several methods for the determination of traces of manganese. The method described here allows the determination of as little as 10 ng Mn ml^{-1}. A later paper will report the application of the reaction to the determination of manganese, nickel and other metal ions by complexiметric titration with catalytic end-point detection.

EXPERIMENTAL

Synthesis of 1,4-dihydroxyphthalimide dithiosemicarbazone

The reagent was synthesized from 1,4-dihydroxyphthalimidedioxime and thiosemicarbazide.

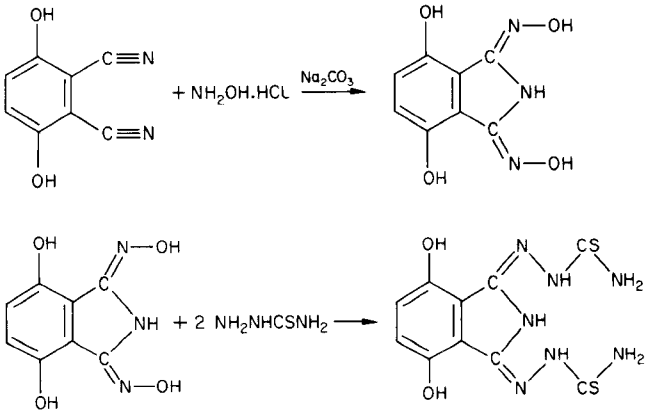

To prepare the dioxime, dissolve 2,3-dicyanohydroquinone (5 g) in 50 ml of ethanol and add 10 g of Na_2CO_3 in 50 ml of water. Add the mixture to 14 g of hydroxylammonium chloride in 100 ml of water, reflux for 2 h, and then cool to 0°C. Filter off the yellow product and wash with (1 + 1) ethanol—water. (Yield, 70%.)

Dissolve the 1,4-dihydroxyphthalimidedioxime (1 g) in 50 ml of hot ethanol and add to 5 g of thiosemicarbazide in 50 ml of water; add 2 ml of 11 M hydrochloric acid, and reflux for 5—6 h. Filter off the yellow product and wash with (1 + 1) ethanol—water. (Yield 50%. M.p., 297°C. Found: 37.2% C, 3.5% H, 29.8% N, 19.8% S; calculated for $C_{10}N_7H_{11}O_2S_2$: 36.9% C, 3.4% H, 30.1% N, 19.7% S.)

Reagents

1,4-Dihydroxyphthalimide dithiosemicarbazone solution. Prepare 0.05% and 0.1% (w/v) solutions in dimethylformamide (DMF).

Standard manganese(II) solution. Prepare from manganese sulphate (ignited at 500°C) dissolved in hot dilute sulphuric acid and standardize by titration with EDTA. Dilute the stock (1.0000 g l^{-1}) solution as required immediately before use.

All solvents and reagents were of analytical-reagent grade.

Apparatus

Pye-Unicam SP600, SP800 and SP8000 spectrophotometers with 1.0-cm glass cells and equipped with a thermostat for kinetic measurements, a Metrohm E1009 photometric titrator with a 4.0-cm glass cell, and a Phillips PW9408 digital pH meter with a combined glass—calomel electrode were used.

Procedure for determination

The reaction conditions were chosen so that the rate of the uncatalyzed reaction was very small compared with that of the catalyzed reaction.

To a solution containing up to 0.9 μg of Mn(II) in a 10-ml volumetric flask, add 5 ml of 0.429 M ammonia solution and 1.5 ml of 0.05% reagent solution in DMF, and dilute to 10 ml with distilled water. Transfer a portion of the reaction mixture to a thermostated 1.0-cm cell at 33 ± 0.1°C, and follow the reaction by recording the absorbance at 594 nm at various reaction times against a similar solution containing no Mn(II). Begin the measurements 8 min after preparation of the samples. Calculate the reaction rate from the slope of the absorbance—time curve.

RESULTS

Analytical properties of the reagent

OH-PDT is insoluble in water, very slightly soluble in ethanol, methanol, acetone or nitrobenzene, and moderately soluble in sodium hydroxide solution or dimethylformamide (25.5 g l^{-1}) at room temperature. Infrared spectra (KBr disc) showed bands assigned (cm^{-1}) to the stretching vibrations of —NH and NH_2 (3410 and 3010), C=N (1610 and 1530) and C=S (1100).

The variation of the u.v.—visible spectra of OH-PDT with pH is shown in Fig. 1. A simultaneous potentiometric—photometric method [8] was used to measure the pK values of the reagent at 420 and 430 nm in DMF—H_2O (1 + 12) with hydroxylamine present to prevent oxidation of the reagent in alkaline medium. The values found are 7.5 (assigned to the NH and OH groups together) and 11.5 (thiosemicarbazone group).

The yellow-orange reagent solution in alkaline media (pH 10) becomes red-violet very slowly, and the absorption spectrum then shows a maximum at about 600 nm with a shoulder at about 550 nm. This evolution is not observed when an inert atmosphere is used.

Reducing agents in moderate concentration, e.g. hydroxylamine and hydrazine, do not alter the absorption spectrum of OH-PDT.

In the presence of cerium(IV), potassium persulphate or sodium periodate in acidic media, the absorption band at 370 nm is displaced towards 430 nm (at pH 5) and 470 nm (at pH 1.2), and the solution becomes green. In alkaline medium (pH 10), persulphate and periodate produce an absorption band at 550 nm, and the yellow-orange reagent solution changes to brown; the solution is red-violet above pH 10 but quickly becomes brown, and the absorption spectrum shows a weak band at 600 nm in addition to the 550-nm band.

Reactions with cations

The reactions of 36 ions with OH-PDT were tested at various pH values. The samples were prepared in 25-ml volumetric flasks with 1—6 ppm of metal ion, 2 ml of 0.1% OH-PDT solution in DMF and 5 ml of buffer

solution; final dilution was with distilled water. The spectra from 400 to 600 nm were measured against a reagent blank. The most important results are shown in Fig. 2.

Catalytic action of manganese(II)

The aerial oxidation of the reagent in alkaline medium is very slow. In the presence of traces of Mn(II), the oxidation rate is increased and new absorption bands at 550 and 594 nm appear rapidly (red-violet colour; Fig. 3). Manganese(II) catalyzes the oxidation, and the absorptivity is proportional to the manganese concentration. This reaction does not proceed in an inert atmosphere, and when other oxidants, e.g. persulphate, Ce(IV), periodate, etc., are used, the reagent is oxidized immediately, so that Mn(II) does not have a catalytic effect.

The oxidation of the reagent depends on the relative concentrations of reagent and Mn(II), the pH, the ammonia concentration and the temperature. At pH 10 (ammonia—ammonium chloride buffer) there is no reaction, but the reaction proceeds above about pH 11; a dilute ammonia solution was therefore used. The reaction rate increases with temperature. When the mixture is heated at 80°C for 5 min, the red-violet colour formed fades rapidly unless $Na_4P_2O_7$ is added after the heating. However, at 33°C (as recommended), $Na_4P_2O_7$ prevents the reaction.

Effects of reaction variables

The influence of temperature on the reaction rate ($dA/dt = \tan\alpha$) was studied in the range 30—40°C. The absorbance—time curves at different temperatures (Fig. 4) show that the absorbance increases linearly during the first 15 min, and becomes constant after 40 min. The slopes of these curves during the first 15 min increase linearly by a factor of about 15 as the temperature is raised from 30 to 38°C. These results indicate that the

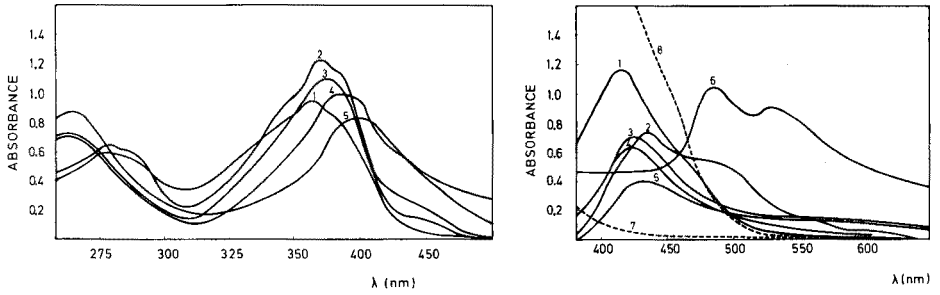

Fig. 1. Absorption spectra of OH-PDT (4×10^{-5} M) in DMF—water (1 + 12) solution at different pH values. Curves 1—5 correspond to pH 1.8, 3—5.8, 7, 9 and 11, respectively.

Fig. 2. Absorption spectra of the reaction products of OH-PDT with metal ions at different pH values. (1) Co(II), 3 ppm, pH 5. (2) Co(II), 6 ppm, pH 10. (3) Fe(II), 1 ppm, pH 5. (4) Fe(III), 1 ppm, pH 5. (5) Ni(II), 1 ppm, pH 5. (6) Mn(II), 1 ppm, pH10. (7) Reagent blank, pH 5. (8) Reagent blank at pH 10.

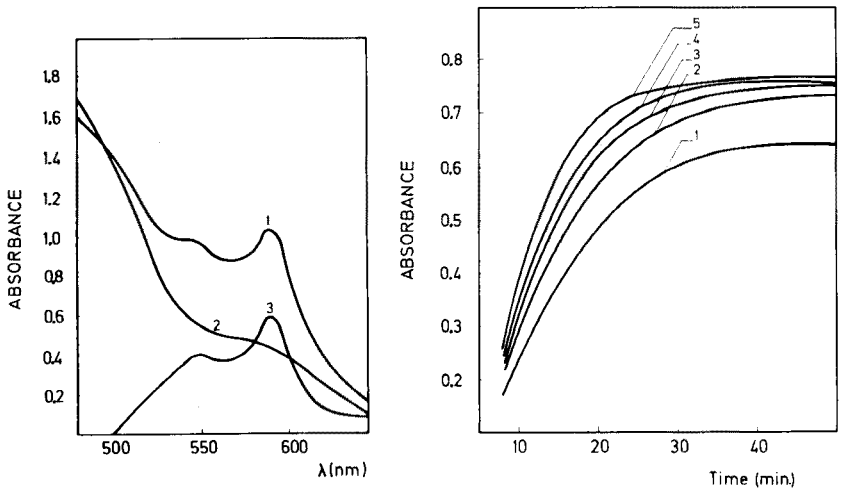

Fig. 3. Effect of manganese(II) on the absorption spectra of the autoxidation product of OH-PDT. Curve 1: in the presence of manganese; curve 2: without manganese; both against a distilled water reference. Curve 3: differential spectra. Conditions: 40 ng Mn ml^{-1}, 0.214 M ammonia and 2.3×10^{-4} M OH-PDT. The curves were recorded after 30 min.

Fig. 4. Effect of temperature on the catalyzed autoxidation of OH-PDT. Curves 1—5 correspond to 30.0, 32.5, 35.0, 37.5 and 40°C, respectively. Conditions: 50 ng Mn ml^{-1}, 0.214 M ammonia and 2.3×10^{-4} M OH-PDT.

activation energy for the catalyzed reaction is large. A temperature of 33°C was selected.

The effect of the reagent concentration on the reaction rate was studied in the range 7.6×10^{-5} —3.8×10^{-4} M. The rate of the catalytic reaction depends linearly on the reagent concentration up to $1.5—1.7 \times 10^{-4}$ M, but the slope of the relationship then changes (Fig. 5). A 2.3×10^{-4} M concentration of reagent (1.5 ml of 0.05% solution) was selected. A logarithmic plot showed that the reaction rate is proportional to the square root of the reagent concentration below 1.7×10^{-4} M and inversely proportional to the reagent concentration at higher values.

The reaction rate depends linearly (Fig. 6, curve 1) on the ammonia concentration in the range 0.085—0.300 M (2—7 ml of 0.429 M ammonia solution). The pH dependence of the system was studied for mixtures of ammonium chloride and ammonia containing a total 0.257 M ammonia concentration. The slopes of the absorbance—time curves against the H^+ and NH_4^+ concentrations, respectively, are shown in Fig. 6 (cf. Table 1). The reaction rate decreases exponentially as the H^+ and NH_4^+ concentrations increase.

The manganese-catalyzed autoxidation of OH-PDT is first order with respect to ammonia concentration. From plots of the data in Table 1, the reaction rate is inversely proportional to the hydrogen ion concentration

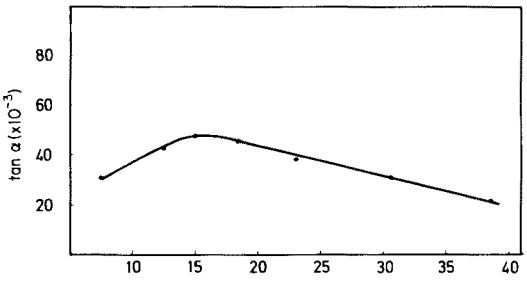

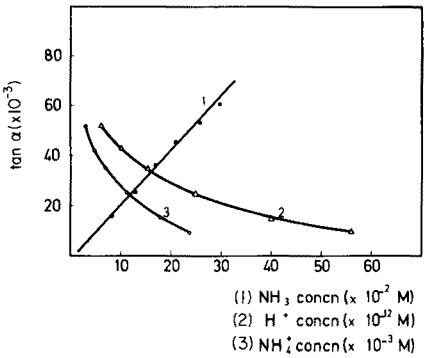

Fig. 5. Effect of OH-PDT concentration on the catalyzed autoxidation of OH-PDT. Conditions: 50 ng Mn ml^{-1} and 0.214 M ammonia.

Fig. 6. Effect of ammonia concentration (curve 1), proton concentration (curve 2) and ammonium ion concentration (curve 3). Conditions for curve 1: 50 ng Mn ml^{-1}, 1.5×10^{-4} M OH-PDT; and for curves 2 and 3: 50 ng Mn ml^{-1}, 0.257 M ammonia and 1.5×10^{-4} M OH-PDT.

TABLE 1

Dependence of reaction rate on hydrogen and ammonium ion concentration

Initial composition (mol l^{-1})		Actual concentrations (mol l^{-1})		Curve slope $\tan\alpha \cdot 10^{-3}$	Values of	
$(NH_3) \cdot 10^{-1}$	$(HCl) \cdot 10^{-2}$	$(H^+) \cdot 10^{-12}$	$(NH_4^+) \cdot 10^{-3}$		$\frac{\tan\alpha}{(H^+)^{-1}(NH_3)} 10^{-12}$	$\frac{\tan\alpha}{(H^+)^{-\frac{1}{2}}(NH_3)} 10^{-7}$
2.57	7.5	56.2	24.33	10.0	2.42	3.23
2.57	5.0	39.8	17.72	15.0	2.49	3.95
2.57	2.0	25.1	11.47	25.0	2.56	5.11
2.57	1.0	15.8	7.36	36.2	2.29	5.47
2.57	0.5	10.0	4.68	42.5	1.68	5.33
2.57	0.0	6.3	2.98	52.0	1.29	5.14

below pH 10.6, and inversely proportional to the square root of the hydrogen ion concentration above pH 10.6.

Rate equation and calibration graphs

The absorbance—time curves for solutions containing different amounts of Mn(II) were recorded against a similar solution containing no Mn(II) (Fig. 7); the curves indicate a first-order reaction with respect to manganese.

On the basis of the kinetic investigation, the following kinetic equation is suggested for the manganese(II)-catalyzed autoxidation of the reagent in ammoniacal medium at pH 11.2:

$$d[\text{OH-PDT}]_{ox}/dt = K\,[\text{OH-PDT}]^{-1}\,[Mn^{2+}]\,[NH_3]\,[H^+]^{-\frac{1}{2}}$$

where $[\text{OH-PDT}]_{ox}$ is the concentration of the oxidized reagent and K is the conditional rate constant. The indicated equation is not absolute, for

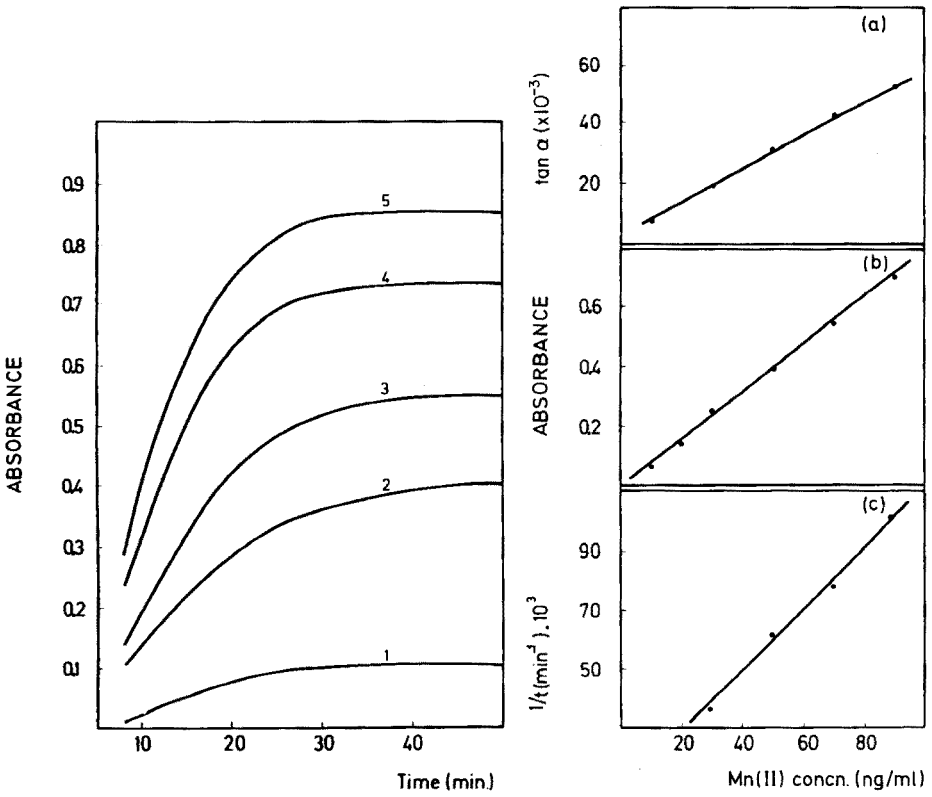

Fig. 7. Effect of manganese concentration. Curves 1—5 correspond to 10, 30, 50, 70 and 90 ng Mn ml^{-1}, respectively. Conditions: 0.214 M ammonia and 2.3 × 10^{-4} M OH—PDT.

Fig. 8. Calibration graphs for manganese(II). (a) Tangent method. (b) Fixed time method (t = 16 min). (c) Fixed absorbance method (A = 0.400). Conditions: 0.214 M ammonia and 2.3 × 10^{-4} M OH—PDT.

another conditional rate constant, K', relative to the uncatalyzed reaction, must be included.

The tangent method was applied to the data in Fig. 7, and the rate of the catalyzed reaction was plotted as a function of Mn(II) concentration. The calibration graph (Fig. 8a) is linear in the concentration range 10—90 ng Mn ml^{-1}. The relative standard deviation for 50 ng Mn ml^{-1} was 1.8% (n = 11).

The fixed time and fixed absorbance (variable time) methods were also applied. For the fixed time method, a time of 16 min was selected; the calibration graph is shown in Fig. 8(b). The relative standard deviation for 50 ng Mn ml^{-1} was 2.4% (n = 11). For the fixed absorbance method, the inverse of the time necessary to obtain an absorbance of 0.400 is plotted against the manganese concentration (Fig. 8c); with this method, the permissible concentration range is narrower than with the other methods.

The relative standard deviation for 50 ng Mn ml^{-1} was 2.0% (n = 11). In general, the tangent method is recommended.

The catalyzed reaction can also be used to determine manganese(II) simply by measuring the absorbance of the samples at 594 nm after 45 min against a reagent blank solution. After this time, the reaction is virtually complete (Fig. 7) and the results are reproducible. The absorbances are measured at room temperature (20—21°C) and the relationship between the manganese concentration and the absorbance is linear in the range 20—90 ng Mn(II) ml^{-1}. The relative standard deviation (P = 0.05) is 1.1%, which is very satisfactory for this type of reaction.

Study of interferences

In order to assess possible analytical applications of the kinetic reaction, the influence of foreign ions on the reaction rate in the presence of manganese(II) was examined. The tangent method was applied. The results are summarized in Table 2. Alkali metals and alkaline earth metals do not interfere. Zn(II), Cd(II), Hg(II), etc., interfere above twentyfold amounts probably because ammine complexes are formed and so alter the ammonia concentration. The interference of Co(II) indicates that there is a catalytic effect when the cobalt concentration is very small.

TABLE 2

Influence of foreign ions on the kinetic determination of 50.0 ng Mn ml^{-1} by the tangent method

Foreign ion	[ion]/[Mn(II)]	$\tan\alpha \cdot 10^{-3}$	Mn found (ng ml^{-1})	Foreign ion	[ion]/[Mn(II)]	$\tan\alpha \cdot 10^{-3}$	Mn found (ng ml^{-1})
—	—	30.6		Zn(II)	20	27.5	46.0
Pyrophosphate	200	27.5	46.0	Cd(II)	20	30.0	49.5
	100	30.0	49.5	Hg(II)	20	30.0	49.5
Sulphate	100	29.5	49.0	Co(II)	10	27.5	46.0
Chloride	100	30.0	49.5		0.5	35.0	59.0
Nitrate	100	30.0	49.5	Pd(II)	10	27.5	46.0
Phosphate	100	28.7	48.0		1	30.0	49.5
Tartrate	100	30.0	49.5	Pt(IV)	10	32.5	54.0
V(V)	100	28.7	48.0	Ag(I)	10	20.0	31.5
Cr(VI)	100	32.5	54.0	Cu(II)	5	27.5	46.0
Mo(VI)	100	31.2	50.5	Pb(II)	1	27.5	46.0
W(VI)	100	27.5	46.0	Sn(II)	1	27.5	46.0
La(III)	100	32.5	54.0	Ti(IV)	1	25.0	41.0
UO_2(II)	100	27.5	46.0	Fe(III)	1	30.0	49.5
Al(III)	100	30.0	49.5	Fe(II)	1	30.0	49.5
Au(III)	100	31.2	50.5	Rh(III)	1	30.0	49.5
Ni(II)	60	30.0	49.5	Ru(IV)	1	22.5	36.0
Mg(II)	20	27.5	46.0	Os(VIII)	1	27.5	46.0

DISCUSSION

Above pH 10, the spectrum of the reagent oxidation product shows two absorption bands at 550 and 600 nm (brown and red-violet, respectively). With chemical oxidizing agents, a red-violet colour is formed rapidly, but it is very unstable and only the 550-nm band appears. Aerial oxidation of the reagent causes the slow formation of the 600-nm band, with an absorptivity greater than that of the 550-nm band. Manganese(II) catalyzes the formation of the oxidation product. The 550-nm band can therefore be attributed to a higher oxidation state than the 600-nm band.

The mechanism of this catalytic reaction has not been elucidated completely, but the rate equation derived is adequate for discussion of the use of the reaction in the catalytic determination of manganese. The catalytic reaction probably involves the oxidation of manganese(II) to Mn(III), and possibly Mn(IV), by atmospheric oxygen in alkaline medium. The Mn(II) serves as a mediator in the electron transfer, and the reaction steps are probably:

$$Mn(II) + \tfrac{1}{2}O_2 \rightleftharpoons Mn(III)$$

$$OH\text{—}PDT_{red} + Mn(III) \rightleftharpoons OH\text{—}PDT_{ox} + Mn(II)$$

The cycle can be stopped by the addition of complexing agents for Mn(III) e.g. pyrophosphate, which prevent the formation of the red-violet colour, probably because the Mn(III)/Mn(II) redox potential is decreased.

The oxidation of 1,4-dihydroxyphthalimide dithiosemicarbazone probably involves the hydroxy groups forming a quinone, rather than the imido group. This is supported by the fact that osmium(VIII), which catalyzes the oxidation of phthalimide dithiosemicarbazone by cerium(IV) [1], does not exhibit catalytic activity in this system.

REFERENCES

1 M. Guzman, D. Pérez-Bendito and F. Pino, Anal. Chim. Acta, 83 (1976) 259.
2 A. Fernandez, C. Sobel and S. Jakobs, Anal. Chem., 35 (1963) 1721.
3 H. A. Mottola and C. R. Harrison, Talanta, 18 (1971) 683.
4 T. Janjic, G. A. Milovanovic and H. B. Celap, Anal. Chem., 42 (1970) 27.
5 I. F. Dolmanova, V. P. Poddubienko and V. M. Peskova, Zh. Anal. Khim., 25 (1970) 2146.
6 I. F. Dolmanova, N. T. Yatsimirskaya, V. P. Poddubienko and V. M. Peskova, Zh. Anal. Khim., 26 (1970) 1540.
7 S. Abe, K. Takahashi and T. Matsuo, Anal. Chim. Acta, 80 (1975) 135.
8 J. A. Muñoz Leyva and F. Pino, Inf. Quim. Anal., 27 (1973) 67.

Analytica Chimica Acta, 94 (1977) 415—420

KINETIC STUDY OF THE IODATE—IODIDE AND CHLORATE—IODIDE REACTIONS IN ACIDIC SOLUTIONS, AND A METHOD FOR THE MICRODETERMINATION OF BROMIDE

D. P. NIKOLELIS, M. I. KARAYANNIS and T. P. HADJIIOANNOU*

Laboratory of Analytical Chemistry, University of Athens, Athens (Greece)

(Received 10th May 1977)

SUMMARY

The iodate—iodide and chlorate—iodide reactions were studied spectrophotometrically in acidic solutions by stopped-flow techniques. Intermediate products(I^+) were followed; reaction rate constants and activation energies of the reactions were determined. A method of determining bromide was developed on the basis of its accelerating effect on the iodate—iodide reaction; microamounts of bromide in the range 16—320 μg (10^{-4}—2×10^{-3} M) were determined with relative errors and relative standard deviation of about 2%.

The iodate—iodide and chlorate—iodide reactions are well known [1—6]. In acidic solution they proceed according to the equations

$$5I^- + IO_3^- + 6H^+ \rightarrow 3I_2 + 3H_2O \quad (1)$$

$$6I^- + ClO_3^- + 6H^+ \rightarrow Cl^- + 3I_2 + 3H_2O \quad (2)$$

When the iodide is in excess, a more probable scheme for process (1) appears [4, 6] to be

$$IO_3^- + 8I^- + 6H^+ \rightarrow 3I_3^- + 3H_2O \quad (3)$$

These reactions were studied earlier [1—4] titrimetrically under conditions of variable ionic strength. In the present paper, the kinetics of these reactions are studied by stopped-flow techniques at constant ionic strength; intermediate products are followed spectrophotometrically, and reaction rate constants and activation energies are determined. In addition, a spectrophotometric kinetic method is described for the determination of bromide, based on its accelerating effect on the iodate—iodide reaction. Microamounts of bromide in the range 16—320 μg (1.0×10^{-4}—2.0×10^{-3} M) were determined with relative errors and relative standard deviation of about 2%.

EXPERIMENTAL

Apparatus

A commercial spectrophotometer (Durrum Gibson Stopped-Flow spectrophotometer, Model D-131) was used for the kinetic study, as previously

described [7]. The signal from the photomultiplier was fed to a photometric log amplifier (Durrum D-131); the course of the absorbance of the reacting system, followed on the screen of the storage oscilloscope, was photographed with a polaroid camera. A modified Heath-701 single-beam spectrophotometer connected with a "double-switching" network was used for the kinetic determination of bromide [8, 9]. The "double-switching" network was adjusted to measure the time required for the recorder pen to cross preselected positions on the chart, corresponding to about 0.5 and 0.3 absorbance units.

Reagents

All solutions were prepared in twice-distilled deionized water from reagent-grade substances.

Buffer (pH 2.30). This was based on the sulfuric acid—sodium sulfate system and was prepared from 0.1 M stock solutions, the appropriate amount of sodium perchlorate being added to achieve ionic strength 1.94 (1.65 M $NaClO_4$). For the kinetic study of the iodate—iodide reaction, prepare buffers from 0.1 M stock solutions of sulfuric acid and sodium sulfate and the appropriate amount of sodium perchlorate, with the ionic strength kept constant at 1.00.

Sodium iodate solutions, 0.100 M. Dissolve 19.8 g of $NaIO_3$ in 1l of sulfate buffer, pH 2.30. For the kinetic study use the sulfate buffers with ionic strength 1.00.

Potassium chlorate solutions 0.200 M. Dissolve 24.5 g of $KClO_3$ in 1 l of various mixtures of sulfuric acid and sodium sulfate, with the ionic strength kept constant at 1.00.

Sodium iodide solution, 0.100 M. Dissolve 15.0 g of KI in water and dilute to 1l. Prepare more dilute solutions as required. For the kinetic study of the iodate—iodide reaction use the sulfate buffers with ionic strength 1.00.

Potassium bromide stock solution, 0.01000 M. Dissolve 1.1901 g of KBr in water and dilute to 1l. Prepare working standards of 1.00×10^{-4}, 3.00×10^{-4}, 6.00×10^{-4} and 1.00×10^{-3} M from the stock solution by dilution.

Procedure for kinetic studies

All runs were performed at 25 ± 0.1°C, unless otherwise stated, with the reagents thermostated before mixing. The formation of iodine and monovalent iodine was followed at 460 and 340 nm, respectively. Follow the procedure previously described [7, 8].

Procedure for bromide

For the kinetic determination of bromide in aqueous solutions, on the basis of its accelerating effect on the iodate—iodide reaction, proceed as follows. Into the thermostated reaction cell (25°C) of the Heath-701 single beam spectrophotometer (with the monochromator set at 340 nm) pipet 2.00 ml of 0.100 M sodium iodate solution in sulfate buffer of pH 2.30 and 2.00 ml of sample or standard bromide solution. Start the reaction by

injecting 1.00 ml of aqueous 0.0015 M sodium iodide solution into the cell. Close the compartment and after 10 s press the start button on the U.D.I. The analysis is completed automatically and the result, in hundredths of a second, is recorded on the U.D.I. Press the Reset button and empty the cell with suction. Repeat the procedure for each analysis.

RESULTS AND DISCUSSION

The initial rate of formation of iodine when iodate is in excess over iodide can be expressed as

$$d[I_2]/dt = k\,[I^-]^x\,[IO_3^-]^y\,[H^+]^z \qquad (4)$$

where x, y and z are the orders with respect to I^-, IO_3^- and H^+ respectively.

In order to study the effect of the reactant concentrations on the reaction rate, the initial rate method was used [10]. Thus, for constant concentrations of iodate and hydrogen ion, eqn. (4), in relation to Beer's law, becomes

$$dA/dt = K_{obs}\,\epsilon_{I_2}\,b[I^-]^x \qquad (5)$$

where

$$K_{obs} = k[IO_3^-]^y\,[H^+]^z \qquad (6)$$

Equation (5) can be written as

$$\log (dA/dt)_i = \log (K_{obs}\,\epsilon_{I_2}\,b) + x \log [I^-]_i \qquad (7)$$

where the subscript i indicates initial rate and concentrations. The initial values of dA/dt can be determined from the slopes of the linear parts of curves such as that shown in Fig. 1. Plotting $\log (dA/dt)_i$ vs. $\log[I^-]_i$ gave a straight line (Fig. 2) from which x was calculated to be 1.98. The same technique gave $y = 1.00$ and $z = 2.01$.

From the x-intercept in Fig. 2, equal to $\log (K_{obs}\,\epsilon_{I_2}\,b)$ in relation to eqn. (6), the rate constant k was calculated to be $(6.5 \pm 0.20) \times 10^8\ M^{-4}\ s^{-1}$, at 25°C and ionic strength of 1.00.

The formation of hypoiodous acid, HIO, as an intermediate in reaction (1), has been suggested [5, 6]. By stopped-flow techniques, the intermediate monovalent iodine can be followed spectrophotometrically at 340 nm, as shown in Fig. 3. With iodate in large excess over iodide, the formation of monovalent iodine obeys the rate law

$$\frac{d[I^+]}{dt} = k'[IO_3^-]\,[I^-]^2\,[H^+]^2 \qquad (8)$$

To calculate the value of the rate constant k', the molar absorptivity of I^+ is necessary. From oscilloscope traces, e.g. that shown in Fig. 3, the molar absorptivity of I^+, ϵ_{I^+}, was calculated as follows. The decaying flank of the curve of Fig. 3, extrapolated to zero time, corresponds to the concentration

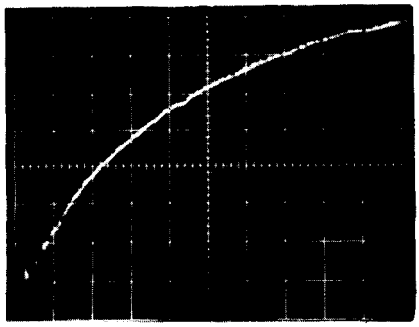

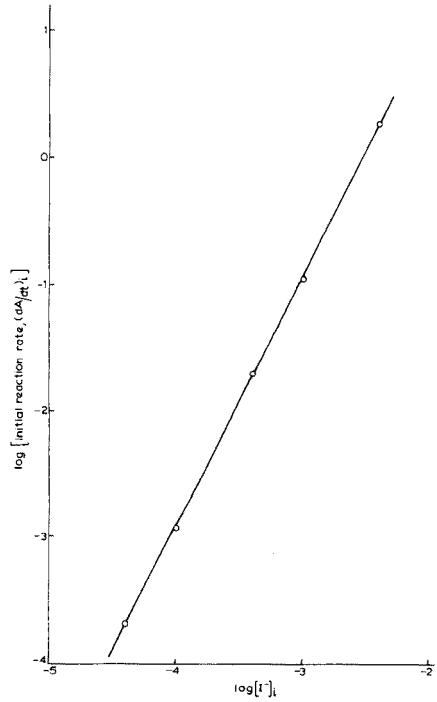

Fig. 1. Typical oscilloscope picture (absorbance vs. time at 460 nm) of the iodate—iodide reaction, when iodate is in excess over iodide. [IO_3^-], 0.05 M; [I^-], 2.5 × 10^{-4} M; pH, 2.0. Ordinate scale 0.02 a.u./div; abscissa scale 100 ms/div. Base line 0.02 a.u.

Fig. 2. Effect of [I^-] on the initial reaction rate, $(dA/dt)_i$.

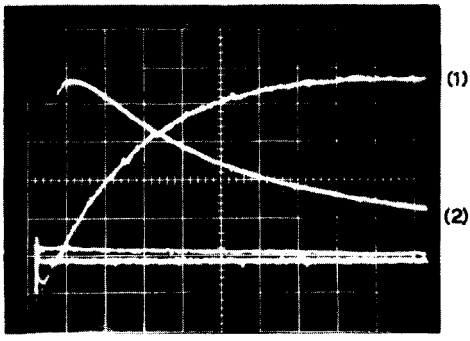

Fig. 3. Oscilloscope picture (absorbance vs. time at 340 nm) showing the formation and consumption of monovalent iodine. [IO_3^-], 0.05 M; [I^-], 2.5 × 10^{-4} M; pH, 2.0. Ordinate scale (1) 0.02 a.u./div; (2) 0.02 a.u./div. Abscissa scale (1) 50 ms/div; (2) 500 ms/div. Base line 0.03 a.u.

of I^+, if no destruction of I^+ occurs. According to the proposed mechanism [5], the concentration of I^+ must be 50% greater than the initial concentration of I^-. From Beer's law, $\epsilon_{I^+} = 180$ l mol^{-1} cm^{-1}, for $[I^-]_i = 5.0 \times 10^{-5}$, in good agreement with the value of 189 l mol^{-1} cm^{-1} found by measuring the absorbance of a solution of ICl_2^- of known concentration at 340 nm. Taking $\epsilon_{I^+} = 180$ l mol^{-1} cm^{-1}, $k' = (6.3 \pm 0.19) \times 10^9$ M^{-4} s^{-1} at 25°C and ionic strength 1.00.

The rate of reaction (1) decreased with increased ionic strength of the solution, indicating that the reacting species in the rate-determining step are oppositely charged.

With the stopped-flow technique, reaction (2) was found to obey the rate law

$$-d[ClO_3^-]/dt = k^* [ClO_3^-] [I^-]^{1.5} [H^+]^2 \quad (9)$$

The calculated value of the rate constant k^* was 35 ± 1.0 M$^{-3.5}$ s^{-1}, at 30°C and ionic strength 1.00.

The rate of reaction (2) increased with increased ionic strength of the solution, indicating that the reacting species in the rate-determining step have the same charge.

The rate of reaction (1) did not change effectively with increasing temperature. From Arrhenius plots of $\log(dA/dt)_i$ vs. T^{-1} the activation energy for reaction (2) was calculated to be 9.7 kcal mol^{-1}.

Determination of bromide

Aqueous bromide solutions of known concentrations gave the results shown in Table 1 when the recommended procedure was used. The data indicate that bromide in the range 16—320 μg (1.0×10^{-4}—2.0×10^{-3} M) can be determined with relative errors of about 2%. The relative standard deviation for a 6.0×10^{-4} M KBr sample was 2.4% ($n = 6$). The slope of the calibration curve increases at higher concentrations and therefore the bromide

TABLE 1

Results for aqueous bromide solutions

Reciprocal time ($s^{-1} \times 10^3$)	Bromide in 2-ml sample (μg)		Relative error (%)
	Taken	Found[a]	
11.9	16.0	16.0	0.0
13.6	32.0	32.0	0.0
16.3	63.9	60.7	−5.0
18.2	79.9	79.9	0.0
19.4	95.9	92.7	−3.3
21.3	112	112	0.0
25.9	160	160	0.0
42.5	320	331	+3.4

[a] Average of two values.

TABLE 2

Effect of various ions on bromide determination at a concentration of 5×10^{-4} M

Ion[a]	Source	Ratio of added ion concn. to bromide concn.	Ion[b]	Source	Ratio of added ion concn. to bromide concn.
S^{2-}	$Na_2S \cdot 9H_2O$	1.2	SCN^-	KSCN	0.6
Al^{3+}	$Al(NO_3)_3 \cdot 9H_2O$	6.2	Ag^+	$AgNO_3$	0.6
Mn^{2+}	$Mn(NO_3)_2 \cdot 6H_2O$	6.2	Fe^{3+}	$Fe(NO_3)_3 \cdot 9H_2O$	1.0
Cl^-	NaCl	100	Pb^{2+}	$Pb(NO_3)_2$	1.2
			Hg^{2+}	$Hg(NO_3)_2 \cdot \frac{1}{2}H_2O$	2.5
			Ba^{2+}	$Ba(NO_3)_2$	3.8
			Ca^{2+}	$Ca(NO_3)_2 \cdot 4H_2O$	12

[a]These ions in the stated ratio caused a positive relative error of less than 5%.
[b]These ions in the stated ratio caused a negative relative error of less than 5%.

concentration of the samples should be adjusted to lie within the range 10^{-4}—2×10^{-3} M by appropriate dilution.

The following ions did not affect the reaction rate at concentrations several thousand times that of the bromide: potassium, sodium, zinc, magnesium, nitrate, sulfate, and perchlorate. Table 2 summarizes the effect of interfering ions; thiocyanate and silver exert the strongest interference effects.

REFERENCES

1 W. C. Bray, J. Phys. Chem., 7 (1903) 92.
2 S. Dushman, J. Phys. Chem., 8 (1904) 453.
3 E. Abel and F. Stadler, Z. Phys. Chem., 122 (1926) 49.
4 E. Abel and K. Hilferding, Z. Phys. Chem., 136 (1928) 186.
5 K. J. Morgan, M. G. Peard and C. F. Cullis, J. Chem. Soc., (1951) 1865.
6 Yu. V. Efremov, Zh. Neorg. Khim., 13 (1968) 58.
7 M. I. Karayannis, S. M. Tzouwara-Karayanni and T. P. Hadjiioannou, Anal. Chim. Acta, 70 (1974) 351.
8 D. P. Nikolelis and T. P. Hadjiioannou, Mikrochim. Acta (Wien), (1977) 125.
9 C. E. Efstathiou and T. P. Hadjiioannou, Anal. Chim. Acta, 89 (1977) 55.
10 G. M. Fleck, Chemical Reaction Mechanisms, Holt, Rinehart and Winston, New York, 1971, p. 47.

Analytica Chimica Acta, 94 (1977) 421—427

THE EFFECT OF AMMONIUM THIOCYANATE AND SODIUM CHLORIDE ON LOSS AND RECOVERY OF MERCURY FROM WATER DURING STORAGE

I. SANEMASA*, T. DEGUCHI, K. URATA, J. TOMOOKA§, and H. NAGAI

Department of Chemistry, Faculty of Science, Kumamoto University, Kurokami-machi, Kumamoto 860 (Japan)

(Received 4th May 1977)

SUMMARY

The effect of inorganic complexing agents such as thiocyanate and chloride on the stability of distilled water and natural waters spiked with 1 μg Hg l^{-1} in polyethylene containers is reported. Distilled water solutions can be stored for several months without significant losses of mercury if they contain HNO_3(0.05—0.1 M) + NH_4SCN(0.001—0.01 M) or HNO_3(0.1 M) + NaCl(higher than 0.01 M). For river and pond waters, addition of HNO_3(0.1 M) + NH_4SCN(0.01 M) not only has a pronounced effect on preventing mercury losses, but also gives quantitative recoveries from spiked sample solutions from which mercury has been "lost". Thiocyanate ion favors desorption of mercury from solid phases; chloride is less effective in this respect.

In trace analysis for mercury in solutions, the problems of storage for periods of time before analysis are of prime importance. Losses of mercury from waters during storage, which have been recognized by many investigators [1—4], can occur by sorption to container walls, association with particulate matter and vaporization. The simplest preservative technique is acidification with mineral acids [5, 6]; some of the data reported in the literature have been tabulated by Feldman [7]. The use of acids and oxidants, e.g. H_2SO_4 with $KMnO_4$ [8] or HNO_3 with $K_2Cr_2O_7$ [7], has been recommended. These methods appear to be effective especially in determining the sum of both inorganic and organic mercury. The use of complex-forming agents such as iodide, cyanide [9] and cystine [2], has also been reported. These preservation techniques, however, have not been widely accepted, largely because of lack of supporting data for their efficacy for natural water samples.

The effects of ligands which form stable mercury(II) complexes on preventing losses of mercury are of interest. The present paper describes the preservation of mercury solutions stored in polyethylene containers in the

---

§Present address: Prefectural Institute of Public Health and Environmental Pollution, 4-33 Minami-sendanbata, Kumamoto 860 (Japan).

presence of ammonium thiocyanate or sodium chloride. These media are effective in preventing mercury losses, and also appear to be effective in preconcentrating trace amounts of mercury by using SCN- or Cl-form anion-exchange resins.

EXPERIMENTAL

Reagents

Redistilled water was used for reagent preparation. All chemicals used were of analytical grade except the mineral acids, (HNO_3, HCl, H_2SO_4, and $HClO_4$) which were superspecial grade (Wako Pure Chemical Industries Ltd., Osaka, Japan). A 1 M ammonium thiocyanate stock solution was prepared by dissolving the required amount of NH_4SCN in water and adjusting to pH 7 with ammonia water. This stock solution was standardized titrimetrically against silver nitrate with iron(III) alum as indicator. A 1 M sodium chloride stock solution was prepared from dried NaCl.

Sample preparation

The samples used were redistilled water, river, and pond waters. River water samples (R-I, -II, -III, -IV, and -V) were collected from five different rivers in the Kumamoto Prefectures. A pond water sample was collected near the laboratory. All these samples were brought to the laboratory in 20-l polyethylene containers and were stored until use. Samples were prepared as follows: suitable volumes were transferred to 1-l polyethylene bottles and adequate volumes of the preservative stock solutions were added to yield final volumes of 1 l. Then, the solutions were spiked with 1 ml of 1-ppm mercury standard to give 1-ppb concentrations. In the recovery studies of mercury lost during storage, the order of addition of preservative and mercury spike was reversed.

Pre-cleaning of sample containers, preparation of mercury standard solutions, apparatus, and measurements have been described previously [10].

RESULTS

Mercury blanks from reagents

Table 1 shows the results of determining mercury blanks in ammonium thiocyanate, sodium chloride, and mineral acids at the concentrations indicated. The concentrations of mercury present in NH_4SCN, NaCl, and

TABLE 1

Mercury contents (in ppb) of the reagents

0.1 M NH_4SCN	2 M NaCl	1 M HNO_3	1 M HCl	1 M H_2SO_4	1 M $HClO_4$
<0.02	<0.02	<0.02	1.48	0.55	0.72

TABLE 2

Change in mercury contents of acids during storage

Reagent	Hg (ppb)/Standing time[a]						
1 M HCl	1.48/1 h	1.52/2	1.52/5	1.60/9	1.56/16	1.60/28	1.60/60
1 M H_2SO_4	0.55/1 h	0.60/2	0.64/5	0.60/9	0.56/16	0.46/28	0.22/60
1 M $HClO_4$	0.72/1 h	0.41/2	0.36/4	0.33/6	0.05/11	0.05/20	

[a]Times are expressed in days except for the first 1 h.

HNO_3 were all below the detection limit (0.02 ppb), while HCl, H_2SO_4, and $HClO_4$ contained considerable amounts of mercury. These acids, when stored in polyethylene containers for 2 months (Table 2), showed no significant losses of mercury, except for $HClO_4$. HNO_3 appears to be the most suitable acid owing to its relatively high oxidation potential as well as its low mercury blank; in certain situations $HClO_4$ can also be used.

Distilled water sample

The behavior of mercury in distilled water is of prime importance in connection with stable storage of dilute mercury standard solutions. The stability of spiked distilled water acidified with HNO_3 is shown in Fig. 1. Substantial losses were observed, and the initial rapid decreases in concentration were not prevented even in 1 M HNO_3, which is consistent with Feldman's results [7]. Rosain and Wai [3] reported that solutions acidified to pH 0.5 with HNO_3 can reduce mercury losses significantly. However,

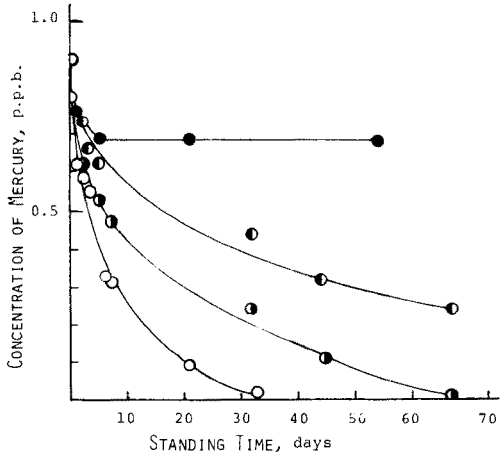

Fig. 1. Change in mercury concentration during storage of the spiked distilled water acidified with HNO_3. ● 1 M, ◐ 0.1 M, ◑ 0.01 M, ○ None (acidity is ca. 10^{-4} M HNO_3, derived from the mercury standard solution).

Coyne and Collins [1] emphasized that this was effective only if the acid was present in the container before the water sample was introduced. In the present study, the pre-acidification method with HNO_3 was not adopted, because interferences may occur, as pointed out by Fitzgerald et al. [5], by formation of volatile organic matter leached by the concentrated nitric acid.

The effect of ammonium thiocyanate on mercury losses in the absence of nitiric acid was first investigated; NH_4SCN alone was ineffective in stabilizing the mercury although the initial rapid decreases were less. Combinations of HNO_3 and NH_4SCN were then examined (Table 3). Characteristic decreases in mercury concentrations were observed at HNO_3 concentrations higher than 0.2 M, probably because of the decomposition of thiocyanate. The optimum conditions for storing the spiked distilled water were HNO_3(0.05—0.1 M) + NH_4SCN(0.001—0.01 M), which were effective for at least 2 months without significant loss of mercury. With addition of HNO_3(0.1 M) + NH_4SCN(0.01 M), the spiked solutions were reasonably stable for 10 months. The stability of mercury in the HNO_3—NH_4SCN medium is probably due to the formation of stable mercury(II) thiocyanate complexes, mainly $Hg(SCN)_2$ and $Hg(SCN)_3^-$.

From the standpoint of complex formation, the effect of sodium chloride on mercury preservation was studied. Table 4 shows that NaCl, at concentrations above 0.01 M, with the addition of 0.1 M HNO_3, is effective in preventing mercury losses. This supports the assumption that the stability of mercury in acidified sea water is due to chloro-mercury complexes [10].

TABLE 3

The effect of HNO_3—NH_4SCN on the stability of mercury in distilled water during storage

Reagent (M)	Hg (ppb)/Standing time[a]					
[NH_4SCN] (with 0.1 M HNO_3)						
0.0001	1.04/1 h	1.06/1	1.08/3	1.07/7	1.06/12	0.92/28
	0.80/42	0.72/65	0.64/78			
0.001	1.05/1 h	1.05/28	1.00/42	1.04/65	0.92/78	0.72/118
0.01	1.00/1 h	1.02/3	1.01/8	1.02/13	1.04/19	1.04/28
	1.04/35	1.06/76	1.05/153	1.06/300		
0.02	1.04/1 h	0.98/78	0.72/118			
[HNO_3] (with 0.01 M NH_4SCN)						
None[b]	1.02/3 h	1.00/1	1.02/2	0.66/6	0.57/8	<0.02/38
0.01	0.98/1 h	0.93/2	0.96/4	0.92/7	0.88/11	0.03/18
0.05	1.02/1 h	1.02/1	1.01/3	1.00/6	1.00/9	1.04/13
	1.04/19	1.07/26	1.07/42	1.06/143		
0.2	1.02/1 h	1.01/1	1.01/3	<0.02/4		

[a] Times are given in days except for the first 1 h or 3 h.
[b] Acidity was ca. 10^{-4} M HNO_3, derived from the mercury standard solution.

TABLE 4

The effect of HNO_3—NaCl on the stability of mercury in distilled water during storage

Reagent (M)	Hg (ppb)/Standing time[a]					
[NaCl] (with 0.1 M HNO_3)						
0	0.90/2 h	0.76/1	0.60/2	0.53/5	0.47/7	0.24/32
	0.12/45	<0.02/67				
0.001	1.06/33 min	1.03/1	0.96/4	0.86/11	0.84/19	0.60/23
0.01	1.02/16 h	1.02/12	1.00/26	1.01/44	0.90/96	
0.1	1.01/43 min	1.04/15 h	1.04/6	1.06/16	1.07/26	1.08/44
	1.07/96	1.08/138	1.10/250			
0.5	1.02/2 h	1.04/1	1.05/4	1.03/6	1.04/8	1.04/12
	1.04/19	1.04/24	1.08/36	1.08/36	1.12/140	
[HNO_3] (with 0.1 M NaCl)						
None[b]	1.08/30 min	1.08/1	1.00/3	0.96/6	0.93/8	0.78/13
	0.20/21	0.04/33	<0.02/53			
0.001	1.00/20 min	1.01/1	0.94/3	0.93/5	0.86/8	0.83/16
	0.68/31					
0.01	1.00/10 min	1.00/1	1.00/3	0.98/5	1.00/8	0.98/16
	0.84/32					

[a] Times are given in days except for the initial times of minutes or hours.
[b] Acidity was ca. 10^{-4} M HNO_3, as previously.

River and pond water samples

Losses of spiked mercury from river and pond waters with time were investigated. Typical results are given in Table 5. Without preservatives, losses of mercury were essentially complete within 3—5 days. The initial rapid decreases were not prevented by acidifying the solutions to 0.1 M with HNO_3. After the spiked sample solutions had been allowed to stand for 3—5 days, HNO_3 and NH_4SCN stock solutions were added to yield final concentrations of 0.1 and 0.01 M, respectively. The results obtained by this treatment are also shown in Table 5. Within at least 1 day after HNO_3—NH_4SCN treatment, quantitative recoveries were obtained. These data indicate that mercury can be leached by treatment with acidified thiocyanate from the container walls and particulate matter on which mercury would be adsorbed. The concentrations of the spiked mercury during storage were followed for 2 months. For the R-I, R-II, and R-III samples, mercury losses were not observed, while for the R-IV, R-V, and pond water samples there were decreases in mercury concentration after 10—20 days. However, there did not seem to be any differences in the appearances of the sample solutions. The preservation effect of the HNO_3—NH_4SCN treatment probably depends on the properties of the natural waters, e.g. the content of dissolved ions and organics, and the amount and nature of particulate matter. These natural water samples were re-examined at a later time, and it appeared that the HNO_3—NH_4SCN treatment was especially effective in the winter season. At room temperatures

TABLE 5

Loss, recovery and preservation of mercury spiked in natural waters

Sample	Hg (ppb)/Standing time[a]					
Loss of mercury[b]						
R-I	0.76/2 min	0.20/1 h	0.05/14 h	0.03/2	<0.02/4	
R-I[c]	0.80/5 min	0.42/30 min	0.52/10 h	0.46/1	0.36/2	0.33/4
Recovery and preservation after HNO_3(0.1 M)—NH_4SCN(0.01 M) treatment						
R-I	0.24/1 min	0.68/20 min	0.97/2 h	1.04/6 h	1.10/10	1.02/30
	1.08/60					
R-II	0.16/10 min	0.32/1 h	0.48/3 h	0.60/5 h	1.03/15 h	1.00/3
	1.02/30	1.08/60				
R-III	1.04/1	0.98/10	1.00/20	1.02/30	1.08/60	
R-IV	0.96/12 h	1.02/3	0.96/10	0.88/20	0.80/30	0.36/60
R-V	1.02/1	0.90/3	0.98/10	0.90/20	0.70/30	0.23/60
Pond water	0.98/1	0.96/10	0.84/20	0.43/30	<0.02/60	

[a] See footnote 'a', Table 4.
[b] Data are given for only the R-I sample since the other samples behaved similarly.
[c] Acidified to 0.1 M with HNO_3.

below ca. 15°C, mercury losses for R-IV, R-V, and pond water samples were not observed during storage for 2 months. The treatment was ineffective in preventing mercury losses when the sample solutions were allowed to stand for several weeks prior to the mercury addition and the subsequent HNO_3—NH_4SCN treatment. This indicated that microbial activity might interfere with the effectiveness of the treatment. For natural waters, HNO_3 and NH_4SCN should be added to sample solutions as soon as possible after collection, otherwise the greenish algae which appear will affect the treatment.

The conditions, HNO_3(0.1 M)—NaCl(0.1—0.5 M), which were favorable for preserving spiked distilled water, were applied to the river and pond waters. However, the sample solutions did not always give quantitative recoveries even at the higher NaCl concentrations. On some occasions, quantitative recoveries were obtained, but only 10—20 days after HNO_3—NaCl treatments. The irreproducible results indicate that chloride is less effective than thiocyanate in desorbing mercury from solid phases.

DISCUSSION

Numerous investigators have demonstrated that mercury losses are due to volatilization of elemental mercury and to adsorption on container walls and/or particulate matter. However, the present work and the previous study [10] suggest that the "loss" of mercury does not mean its disappearance, but is rather due to faults in analytical technique. This has already been pointed out by Carr and Wilkniss [4] in their radioactive isotope study. Recent

studies [11] on liberation of mercury from anion-exchange resin (Cl-form) by direct reduction with tin(II) in a reduction-aeration bottle combined with atomic absorption measurement, showed that a long aeration time was necessary for quantitative recoveries of mercury adsorbed on the resin, especially at low temperatures, e.g., it required more than 30 min at 10°C. Inorganic complexing reagents, such as thiocyanate or chloride, which form stable complexes with mercury even in acidic medium, probably remove mercury strongly adsorbed on solid phases into the aqueous phase or convert the mercury to readily reducible forms. Less rigorous experiments were conducted in which spiked distilled waters were stored in polyethylene bottles until their mercury concentrations dropped below the detection limit and the contents were discarded; then the containers were filled with HNO_3 (0.1 M)—NH_4SCN (0.01 M) solution without washing. The results obtained made it clear that the acidified thiocyanate solutions can leach mercury from container walls and can therefore be used as "cleaning solutions" for polyethylene containers.

REFERENCES

1 R. V. Coyne and J. A. Collins, Anal. Chem., 44 (1972) 1093.
2 Y. Dokiya, S. Yamazaki and K. Fuwa, Environ. Lett., 7 (1974) 67.
3 R. M. Rosain and C. M. Wai, Anal. Chim. Acta, 65 (1973) 279.
4 R. A. Carr and P. E. Wilkniss, Environ. Sci. Technol., 7 (1973) 62.
5 W. F. Fitzgerald, W. B. Lyons and C. D. Hunt, Anal. Chem., 46 (1974) 1882.
6 M. H. Bothner and D. E. Robertson, Anal. Chem., 47 (1975) 592.
7 C. Feldman, Anal. Chem., 46 (1974) 99.
8 S. H. Omang, Anal. Chim. Acta, 53 (1971) 415.
9 S. Shimomura, Y. Nishihara and Y. Tanase, Jpn. Anal., 18 (1969) 1072.
10 I. Sanemasa, T. Deguchi, K. Urata, J. Tomooka and H. Nagai, Anal. Chim. Acta, 87 (1976) 479.
11 I. Sanemasa, E. Takagi, T. Deguchi and H. Nagai, Chem. Lett., submitted.

Analytica Chimica Acta, 94 (1977) 429—434

SULFONEPHTHALEIN DYES
Part VII. Chromogenic Reactions of Semi-Glycinethymol Blue§

K. VYTŘAS* and F. J. LANGMYHR

Department of Chemistry, University of Oslo, Oslo-Blindern (Norway)

(Received 2nd May 1977)

SUMMARY

The chromogenic reactions of semi-glycinethymol blue have been studied spectrophotometrically and by complementary tristimulus colorimetry. The separation of the dye from a commercial product of glycinethymol blue is described. The five dissociation constants were determined; the means of the pK_a (H_iI) values for i = 5, 4, 3, etc. are —1.5, 0.3, 1.5, 7.5, and 12.7, respectively. Colour reactions with some metal ions are reported; the reaction with copper(II) is suggested for the determination of the composition of commercial samples of glycinethymol blue.

Semi-glycinethymol blue (SGTB) is a mono-substituted by-product in the synthesis of glycinethymol blue from thymol blue, formaldehyde, and glycine by Mannich condensation [2]. Similarly, the mono-substituted derivatives can accompany the di-substituted compounds in commercial reagents such as xylenol orange, methylthymol blue, methylxylenol blue, glycinecresol red, etc. [3, 4]. It is evident that this contamination does not matter when these dyes are used as indicators in titrimetric analysis or as spectrophotometric reagents, but for detailed studies of dissociation or complexation equilibria it is imperative that only pure preparations be employed.

Nevertheless, the mono-substituted products are an interesting group of compounds. They form simpler complexes with metals [5, 6] than the di-substituted ligands, and have been used advantageously for the verification of the theory of photometric titration curves [7, 8] and for interpreting the kinetic behaviour of complex formation [9]. Semi-xylenol orange has also been applied as a sensitive reagent for a spectrophotometric determination of zirconium(IV) [10] and in a complexiметric titration of submicromolar amounts of thorium(IV) with photometric end-point detection [8]. The present paper deals with the separation of SGTB and elucidates its basic optical and equilibrium properties.

---

§ For Part VI, see ref. [1].

*On leave from the Department of Analytical Chemistry, College of Chemical Technology, 53210-Pardubice, Czechoslovakia.

EXPERIMENTAL

SGTB was separated from a commercial preparation (Lachema) of glycinethymol blue as follows. About 3 g of the above preparation was gradually mixed with saturated sodium acetate solution (12 ml), ethanol was added to a total volume of 250 ml, and the mixture was left for two days. The sticky matter formed on the bottom of the beaker was separated by decantation, and the ethanolic solution was mixed with the same volume of diethyl ether. The sticky sediment was formed again and separated (both the sediments contained mostly glycinethymol blue contaminated by SGTB, which was confirmed chromatographically). Then, most of the sodium acetate was precipitated by a further portion of ether, and the filtrate was evaporated to dryness. The chromatographic check applied [1] showed only one spot with an R_F value of 0.81 corresponding to SGTB.

As the absorptivity of the product isolated by evaporation was unsatisfactory (it contained some sodium acetate), further purification was needed. A strong acid cation-exchanger (Ionenaustauscher I, Merck) was applied as described earlier [1] to convert the dye completely to its acid form; the acetic acid formed from the acetate was removed by evaporation of the eluates. Elemental analysis of the sample gave the following results (theoretical percentages for $C_{30}H_{35}O_7NS \cdot 3H_2O$ are given in parentheses): C, 58.2% (59.3%); H, 6.79% (6.80%); N, 2.76% (2.30%); S, 5.30% (5.28%); O (by difference), 27.0% (26.3%).

The stock solution of SGTB (ca. 0.1%), with a small admixture of nitric acid, was stable for over a month.

The instrumentation, reagents, and method of measurement have been described [1].

RESULTS AND DISCUSSION

Protolytic equilibria

SGTB exhibits colour changes with varying pH. In strongly acidic solutions, the fully protonated cation H_5I^{2+} gives off a proton from the $-SO_3H$ group between H_0 −3 and −1.5 (H_2SO_4). The dissociation is accompanied by a decrease of the main absorption band at 546 nm, and the spectra

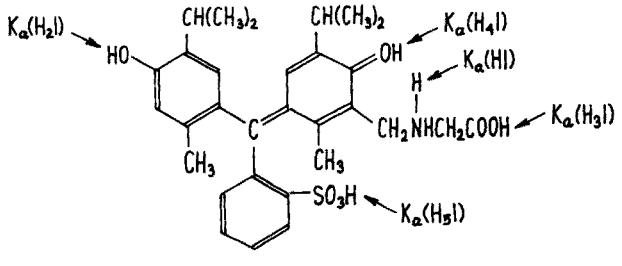

(SGTB)

exhibit an isosbestic point at 490 nm, although the secondary absorption band at 407 nm is almost unaffected by acidity. A colour change from reddish-purple to orange accompanies the dissociation of the proton bonded on the quinoidal oxygen ($H_4I^+ \rightarrow H_3I$) over the H_0 range −0.89 to +0.69 (formic acid); an isosbestic point occurs at 487 nm. Finally, the last equilibrium occurring in acidic solutions (H_0 1.08 to pH 2.7) can be ascribed to the dissociation of the hydrogen from the carboxyl group, with ill-defined isosbestic points at 443 and ca. 386 nm.

Between pH 5 and 9, the proton of the hydroxyl group dissociates, and there is a marked colour change from yellow to purplish-blue. This transition is characterized by a new absorption band at 598 nm, and by an isosbestic point at 488 nm. The dissociation of the last proton connected to the nitrogen atom and linked by a hydrogen bond to the adjacent oxygen atom occurs in strongly alkaline solutions. A pure blue colour is developed (λ_{max} = 605 nm), and isosbestic points appear at 534 and ca. 415 nm.

The overall colour transition curve of SGTB is illustrated in the $Q_x Q_y$ complementary tristimulus triangle in Fig. 1. In general, the curve is similar to that of glycinethymol blue [1]. However, unlike the latter, the colour change from yellow to blue corresponding to the dissociation of the proton from a phenolic group goes through purplish-grey hues (see the line connecting the complementary colour points of the species H_2I and HI in Fig. 1). The dependence of the tristimulus values X_c, Y_c, Z_c (generally R_c) of SGTB on pH (or acidity functions) is given in Fig. 2.

The dissociation constants evaluated from the tristimulus components R_c or from the modified tristimulus values (see [11]) are listed in Table 1 together with the results of a statistical treatment [12]. As expected, the

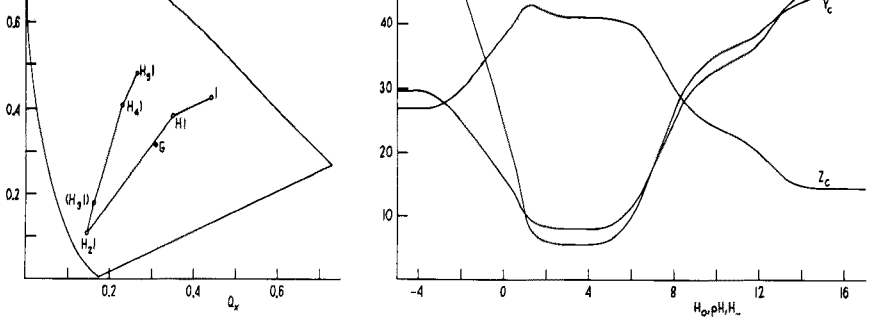

Fig. 1. Colour transitions of SGTB in the $Q_x Q_y$ complementary tristimulus diagram with marked colour points of the individual species. G, grey point corresponding to the CIE standard source C.

Fig. 2. R_c—pH curves for protolytic equilibria of SGTB.

TABLE 1

Evaluation of dissociation constants of SGTB

Equilibrium	$pK_a(H_iI)$[a]		
	n	$\bar{x}$	s
$H_5I^{2+} \rightleftharpoons H_4I^+ + H^+$	5	−1.53	0.09
$H_4I^+ \rightleftharpoons H_3I + H^+$	7	0.30	0.03
$H_3I \rightleftharpoons H_2I^- + H^+$	4	1.5	0.2
$H_2I^- \rightleftharpoons HI^{2-} + H^+$	11	7.48	0.02
$HI^{2-} \rightleftharpoons I^{3-} + H^+$	7	12.68	0.06

[a] n, number of points considered, $\bar{x}$, average value, s, standard deviation.

values for the same kinds of transition are higher than those of glycinethymol blue [1] and lower than those of thymol blue [13]. Two related dyes — semi-methylthymol blue [14] and semi-xylenol orange [15] — show similar effects.

Reactions with metal ions

Glycinethymol blue forms intensely blue complexes with a number of metals [2]. When the chromogenic reactions of SGTB with metal ions were tested over the pH range 2—7, very poor or no colour changes were observed except for the reactions with iron(III) and copper(II). Iron(III) reacts with SGTB in the presence of acetate buffer to form a complex with a wide u.v. absorption band, which overlaps well into the visible range. The resulting absorbance depends on the concentrations of both the iron(III) salt and the dye.

In the presence of acetate buffer (pH 5.5), copper(II) forms a complex which exhibits a wide, asymmetrical absorption band with a maximum at 503 nm; the colour is purplish-pink. The absorption spectrum of the copper(II)—SGTB complex is shown in Fig. 3 (curve 1). For comparison, the spectrum of the copper(II)—glycinethymol blue complex (λ_{max} at 601 and 397 nm) was also recorded (curve 2); this was obtained with the purified [1] reagent. The absorption spectra of the copper(II) complexes with commercial preparations of glycinethymol blue were recorded under the same conditions: it is evident from Fig. 3 that the use of the unpurified reagents in studies of metal complex equilibria would give greatly distorted results. It may be concluded that SGTB will not be useful for analytical applications as, e.g., semi-xylenol orange or semi-methylthymol blue.

Analysis of commercial preparations of glycinethymol blue

The broadening of the absorption bands of the copper(II) complexes of glycinethymol blue by the presence of SGTB could be advantageously used to determine the ratio of the two dyes in commercial preparations. The ratio of the colour components can be found by using a simple graphical

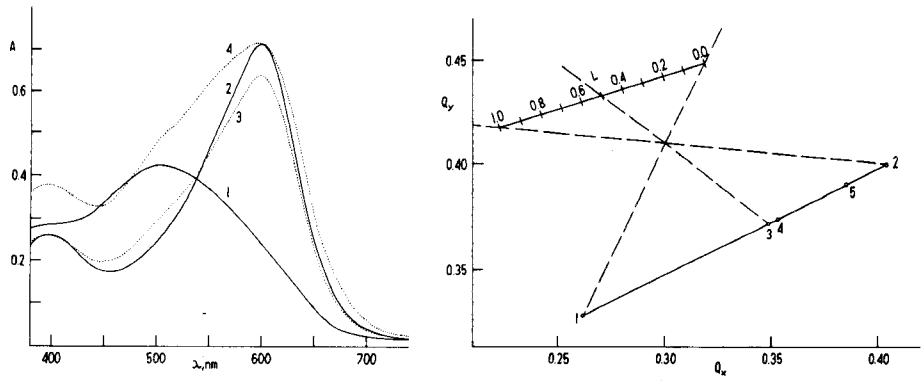

Fig. 3. Absorption spectra of the copper(II) complexes of (1) semi-glycinethymol blue, $3.9 \cdot 10^{-5}$ M; (2) glycinethymol blue, $3.4 \cdot 10^{-5}$ M; (3) the Lachema preparation of glycinethymol blue, 0.0282 mg ml^{-1}; (4) the Fluka preparation, 0.0374 mg ml^{-1}. pH 5.51, 10-mm cells, [Cu] $\approx 10^{-3}$ M, 20°C.

Fig. 4. Graphical determination of the proportion between glycinethymol blue and semi-glycinethymol blue in commercial samples of glycinethymol blue. Complementary colour points of the copper(II) complexes of (1) semi-glycinethymol blue, (2) glycinethymol blue, (3) a 50:50 mixture of 1 and 2, (4) the Fluka preparation, (5) the Lachema preparation. L is a linear scale calibrated by values of the glycinethymol blue relative concentration [GTB]/([GTB] + [SGTB]) in the binary dye system.

method suggested by Flaschka [16]. The method is based on a graphical linear calibration of the non-linear plot connecting the complementary colour points of the copper(II) complexes of both glycinethymol blue and SGTB (Fig. 4). The solutions of the complexes formed from commercial specimens are then analysed like binary systems, and their composition can be estimated from the linear calibration scale.

Of course, the normal procedure can also be used; thus the absorbance values are measured at two wavelengths (480 and 600 nm) and simultaneous equations are solved:

$$A_{480} = 9.25\,[\mathrm{GTB}]l + 15.89\,[\mathrm{SGTB}]l$$
$$A_{600} = 32.95\,[\mathrm{GTB}]l + 9.53\,[\mathrm{SGTB}]l$$

where l is the cell path-length. As the absorptivity values are given in ml mg^{-1} cm^{-1}, the resulting concentrations of glycinethymol blue [GTB] and semi-glycinethymol blue [SGTB] will be obtained in mg ml^{-1}. The total copper(II) concentration should not exceed 10^{-3} M because of the absorption of $Cu(OH_2)_4^{2+}$ ions. The results for two commercial preparations obtained by the two methods are shown in Table 2; the data are in quite good agreement with the first estimate [1] made by a comparison of chromatographic spots.

TABLE 2

Composition of commercial specimens of glycinethymol blue

Sample	Ratio [GTB]/([GTB] + [SGTB])		Composition		
	Graphically	Numerically	%GTB	%SGTB	%Imp.[a]
Fluka	0.54	0.524	46	42	12
Lachema	0.81	0.802	64	16	20

[a]Colourless impurities.

REFERENCES

1 K. Vytřas and F. J. Langmyhr, Anal. Chim. Acta, 92 (1977) 155.
2 J. Körbl, E. Kraus and R. Přibil, Chem. Listy, 51 (1957) 1809; Collect. Czech. Chem. Commun., 23 (1958) 1219.
3 J. Körbl and E. Přibil, Chem. Ind., (1957) 233.
4 J. Körbl, V. Svoboda, D. Terzijská and R. Přibil, Chem. Ind., (1957) 1624.
5 T. Yoshino, S. Murakami, M. Kagawa and T. Araragi, Talanta, 21 (1974) 79.
6 T. Yoshino, H. Okazaki, S. Murakami and M. Kagawa, Talanta, 21 (1974) 673.
7 V. Řiha, M. Meloun, M. Franz and J. Čermák, Sb. Věd. Pr., Vys. Šk. Chemickotechnol., Pardubice, 33 (1975) 39.
8 C. J. C. Pijpers, L. G. Decnop-Weever, G. den Boef and W. E. van der Linden, Mikrochimica Acta, (1976) 667.
9 Y. Kawai, T. Takahashi, K. Hayashi, T. Imamura, H. Nakayama and M. Fujimoto, Bull. Chem. Soc. Jpn., 45 (1972) 1417.
10 D. C. Olson and D. W. Margerum, Anal. Chem., 34 (1962) 1299.
11 K. Vytřas, J. Vytřasová and S. Kotrlý, Chem. Listy, 70 (1976) 234.
12 K. Eckschlager, Errors, Measurements and Results in Chemical Analysis, Van Nostrand, London, 1969, p. 142.
13 K. Vytřas, unpublished work.
14 T. Yoshino, S. Murakami and M. Kagawa, Talanta, 21 (1974) 199.
15 M. Murakami, T. Yoshino and S. Harasawa, Talanta, 14 (1967) 1293.
16 H. Flaschka, Talanta, 7 (1960) 90.

Analytica Chimica Acta, 94 (1977) 435—441

AN EXAMINATION OF CHLORPROMAZINE HYDROCHLORIDE AS INDICATOR AND SPECTROPHOTOMETRIC REAGENT FOR THE DETERMINATION OF MOLYBDENUM(V)

H. PUZANOWSKA-TARASIEWICZ, A. GRUDNIEWSKA and M. TARASIEWICZ

Department of Chemistry, Warsaw University Division, Białystok (Poland)

(Received 30th May 1977)

SUMMARY

Chlorpromazine hydrochloride (CPA) has been tested as indicator in the titration of molybdenum(V) with cerium(IV) sulphate at room temperature in sulphuric acid medium. It gives a sharp, reversible colour change from colourless to dark-red at the equivalence point. Chlorpromazine hydrochloride also reacts in acidic media with thiocyanato-molybdenum(V) complexes forming an orange compound with the formula (CPA · H) $[MoO(SCN)_4]$. This reaction provides a sensitive method for spectrophotometric determination of molybdenum(V). Molybdenum(VI) is reduced with ascorbic acid in hydrochloric acid solution, and complexed with thiocyanate, and the complex formed is extracted with chlorpromazine hydrochloride in chloroform. The molar absorptivity is 1.6×10^4 l mol^{-1} cm^{-1} at 465 nm. Beer's law is obeyed in the range 0.5—5.0 μg Mo ml^{-1}.

Chlorpromazine hydrochloride forms red oxidation products with a number of oxidants (e.g. Ce(IV), VO_3^-, $Cr_2O_7^{2-}$, BrO_3^-, IO_3^-, IO_4^-, NO_2^-, etc.) in acidic media [1]. This reaction is reversible, but the coloured oxidation product (free radical) is further oxidized irreversibly by strong oxidizing agents to a colourless sulphoxide [2, 3]. The reaction may be represented as follows:

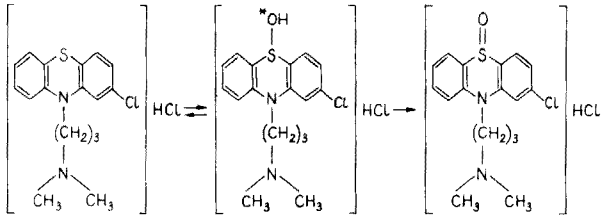

This property enables chlorpromazine hydrochloride and some analogous compounds to be used as indicators in various redox titrations [3—6]. In the present work, which is a continuation of previous studies [4—6] the behaviour of chlorpromazine hydrochloride in titrations with cerium(IV) was examined.

It was also found that chlorpromazine hydrochloride reacts in acidic media with thiocyanato—molybdenum(V) complexes, forming an orange compound with the formula (CPA · H) $[MoO(SCN)_4]$, where CPA denotes chlorpromazine. This compound is insoluble in water but can be quantitatively extracted into chloroform. Molybdenum can therefore be determined spectrophotometrically directly in the organic phase.

Many methods have been suggested for the spectrophotometric determination of molybdenum. Probably the oldest and most widely used reagent for molybdenum is thiocyanate [7—11]. In these determinations, interference by various metals, stability, and reproducibility of measurements have been the main problems. The stability of the molybdenum thiocyanate complex can be enhanced by adding a second ligand to form a new mixed complex which can be extracted into an organic solvent; several such methods have been reported [8, 12—14]. Since molybdenum(V) gives a more intense colour with thiocyanate than molybdenum(VI), various reducing agents for molybdenum(VI) have been studied.

The method described here involves ascorbic acid as the reducing agent. The molybdenum—thiocyanate complex formed is extracted with chlorpromazine hydrochloride in chloroform. The method is rapid and reproducible and the colour of the complex is stable for at least 48 h.

EXPERIMENTAL

Reagents and apparatus

Ammonium molybdate solution (0.01 M) was standardized gravimetrically with 8-hydroxyquinoline [15]. Working solutions of molybdenum were prepared by dilution. Cerium(IV) sulphate (0.01 M) solution in 0.5 M sulphuric acid was standardized against sodium oxalate [16].

Chlorpromazine hydrochloride (2-chloro-10-(3-dimethylaminopropyl)-phenothiazine hydrochloride; EGYT, Budapest) was used as aqueous 0.01 M and 0.1% solutions. The material was standardized gravimetrically with tungstosilicic acid [17]. Chlorpromazine hydrochloride was also used as a 0.02 M solution in chloroform.

All chemicals used were of analytical purity.

Unicam SP800 and Spekol (Carl Zeiss, Jena) spectrophotometers were used with 1-cm cells.

AN EXAMINATION OF CHLORPROMAZINE HYDROCHLORIDE AS REDOX INDICATOR IN TITRATION OF MOLYBDENUM(V) WITH CERIUM(IV)

The optimal conditions for the formation of the red oxidation product of chlorpromazine hydrochloride with $Ce(SO_4)_2$ in acidic medium were examined. The absorption spectra of the coloured oxidation product of chlorpromazine hydrochloride with $Ce(SO_4)_2$ in aqueous solutions containing varying concentrations of sulphuric acid, hydrochloric acid and nitric acid were recorded.

The spectra obtained for chlorpromazine hydrochloride oxidized in 0.2—6.0 N solutions of sulphuric or hydrochloric acid showed that the absorption of the solution is maximal at acidities of 1.5—4.0 N. Nitric acid cannot be used because above a concentration of 0.1 M it oxidizes chlorpromazine hydrochloride to form coloured products.

The absorption curves obtained for the chlorpromazine hydrochloride—$Ce(SO_4)_2$ system in 1 M sulphuric acid showed that maximum absorption was obtained at a CPA: $Ce(SO_4)_2$ molar ratio of 1:1.

Figure 1 shows the ultraviolet and visible spectra of the non-oxidized and oxidized forms of chlorpromazine hydrochloride. The spectrum of the CPA free radical shows a bathochromic shift, whereas the sulphoxide shows a hypsochromic shift relative to the non-oxidized form of CPA in the range 225—285 nm. Table 1 summarises the results of these experiments.

Titration of molybdenum(V) with cerium(IV) sulphate

Diphenylamine, diphenylbenzidine, diphenylaminesulphonic acid, *N*-phenylanthranilic acid [18], ferroin [16], copper phthalocyaninesulphonic acid [19], nickel phthalocyaninesulphonic acid [20] and β-colubrine [21] have been used as indicators for this titration. Chlorpromazine hydrochloride is a satisfactory reversible indicator at room temperature in sulphuric acid medium. The transition potential of chlorpromazine hydrochloride in 0.5 M H_2SO_4 at 20°C is 0.76 V [3, 4].

Recommended procedure

Reduce molybdenum(VI) to the pentavalent state quantitatively in 2 M hydrochloric acid with mercury [16]. Wash the mercury and mercury(I)

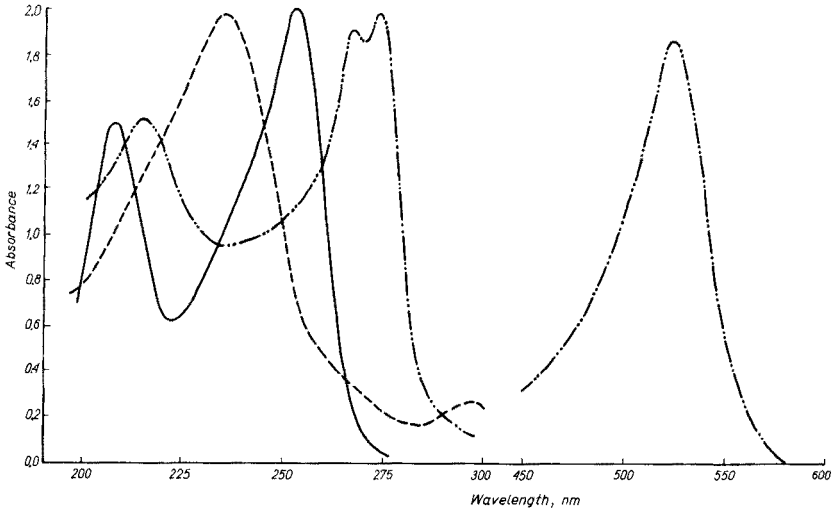

Fig. 1. Absorption spectra of aqueous solutions of chlorpromazine hydrochloride (CPA). Non-oxidized form ——; free radical —— ·· ——; sulphoxide ·····. [CPA] (u.v.) = 6×10^{-5} M, 10^{-2} M HCl; [CPA] (vis.) = 3.5×10^{-4} M, 2 M HCl. Mole ratio CPA: Ce^{4+} = 1:1.

TABLE 1

Values of λ_{max} and ϵ of non-oxidized and oxidized forms of CPA

Form of CPA	Ultraviolet region		Visible region	
	λ_{max}	ϵ	λ_{max}	ϵ
Non-oxidized	207	25000		
	256	34000		
	309	4000		
Free radical	215	25000		
	268	32000	525	7700
	274	33000		
Sulphoxide	235	33000		
	295	4200		

chloride five times with 20-ml portions of (1 + 5) hydrochloric acid, shaking well for a few seconds each time, and decanting through the filter. To the filtrate, add 10—20 ml of (1 + 1) sulphuric acid and 3 ml of syrupy phosphoric acid, to catalyze the reduction of the oxidized form of CPA by molybdenum(V). Add 1 ml of 0.1% solution of chlorpromazine hydrochloride for a titration volume of 100 ml, and titrate with 0.01 M cerium(IV) sulphate to the end-point. The colour of the test solution changes from colourless to dark-red.

Table 2 shows some results for the titration of molybdenum(V). The indicator blank never exceeded 0.05 ml of 0.01 M cerium(IV) sulphate. Chlorpromazine hydrochloride gave sharper end-points than diphenylamine or *N*-phenylanthranilic acid in these titrations. Interferences were found from Fe^{2+}, Sn^{2+}, VO_3^-, $Cr_2O_7^{2-}$ and HNO_3.

SPECTROPHOTOMETRIC EXAMINATION OF THE EXTRACTION OF THIOCYANATO–MOLYBDENUM(V) COMPLEXES WITH CHLORPROMAZINE HYDROCHLORIDE

The coloured molybdenum complex formed with thiocyanate in hydrochloric or sulphuric acid can be extracted by chlorpromazine hydrochloride in chloroform, in the presence of ascorbic acid as a reducing agent. The intensity of the colour depends on the reducing agent. Figure 2 shows that the ascorbic acid is a more reliable reductant than tin(II); a 2% concentration of ascorbic acid was selected for further work.

TABLE 2

Titration of molybdenum(V) with 0.01 M cerium(IV) sulphate

Mo(V) taken (mmol)	0.1586	0.2234	0.2664	0.3249
Mo(V) found (mmol)	0.1584	0.2232	0.2659	0.3254

The effects of concentration of mineral acids, potassium thiocyanate and chlorpromazine hydrochloride were studied. The results showed that the optimal concentrations for the determination were 2 M hydrochloric or sulphuric acid (the absorbances remained constant over the range 1—3 M), 9% (w/v) potassium thiocyanate (the absorbances remained constant over the range 4—20%) and 0.01 M chlorpromazine hydrochloride dissolved in chloroform (the absorbances remained constant over the range 0.005—0.05 M). Under these conditions it was possible to determine 0.5—5.0 μg Mo ml^{-1}. The absorbance of the complex at 465 nm obeys Beer's law over this range. The reproducibility of the measurements, expressed as standard deviation, is 0.3—2%, depending on the molybdenum concentration.

The molybdenum thiocyanate complex with chlorpromazine hydrochloride in the organic phase shows maximum absorbance at 465 nm (Fig. 3), at which wavelength the absorbances were measured. The molar absorptivity is 1.6×10^4 l mol^{-1} cm^{-1}. The photometric sensitivity, as defined by Sandell [7] is 0.0062 μg Mo cm^{-2}. The absorbance of chloroform solutions of the complex is stable for at least 48 h.

Nitric acid can be used for acidification at a concentration below 2 M; at greater concentrations the chloroform extracts are cloudy.

Procedure

In a separatory funnel, place a solution containing 5—50 μg of molybdenum, add 2 ml of 10 M hydrochloric acid or sulphuric acid, 3 ml of 30% potassium thiocyanate solution and 2 ml of 10% ascorbic acid solution and water to bring the total volume to about 10 ml. Leave the reaction mixture at room temperature for 20 min. Add 5 ml of 0.02 M CPA in chloroform and shake

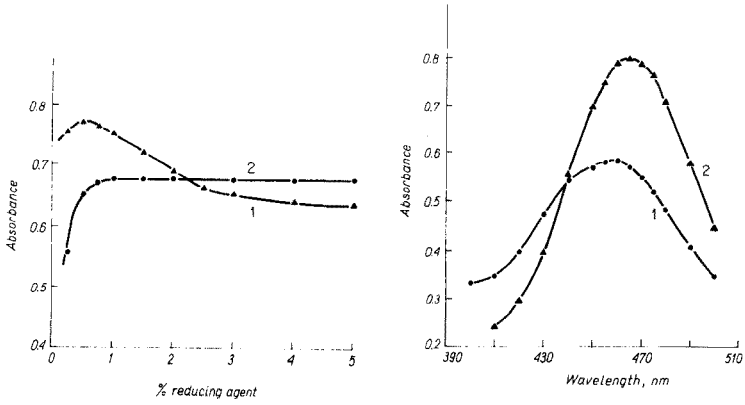

Fig. 2. Dependence of absorbance of the molybdenum complex on reducing agent. (1) $SnCl_2$ varied; (2) ascorbic acid varied. 2 M HCl, 9% KSCN, 5×10^{-5} M Mo, 10^{-2} M CPA in $CHCl_3$ in all tests.

Fig. 3. Absorption spectra. (1) Aqueous solution of thiocyanate molybdenum(V) complex. (2) Its compound with CPA in $CHCl_3$. 5×10^{-5} M Mo, 2% ascorbic acid, 2 M HCl, 10^{-2} M CPA.

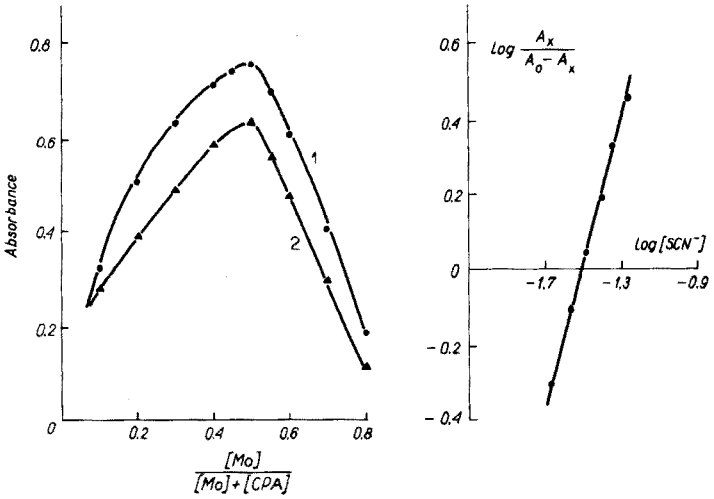

Fig. 4. Application of Job's method for the extracted complex. (1) λ = 465 nm. (2) λ = 450 nm. [Mo] + [CPA] = 1 × 10^{-4} M, 2% ascorbic acid, 2 M HCl, 9% KSCN.

Fig. 5. Dependence log $A_x/A_0 + A_x$) vs. log [SCN^-], where A_0 is the absorbance of the solution after complexation of all Mo(V), and A_x is the increasing absorbance before complete molybdenum complexation. KSCN varied from 10^{-2} to 10^{-1} M. 5 × 10^{-5} M Mo, 2% ascorbic acid, 2 M HCl, 10^{-2} M CPA.

for 2 min. Transfer the chloroform layer to a 10-ml volumetric flask and extract the aqueous solution twice with 2-ml portions of chloroform. Combine the chloroform extracts in the volumetric flask and dilute to the mark with chloroform. Measure the absorbance at 465 nm against a reagent blank.

Effect of foreign ions

The influence of foreign ions was ascertained by the general procedure. The metal ions Na^+, K^+, Mg^{2+}, Ca^{2+}, Ba^{2+}, Zn^{2+}, Pb^{2+}, Ni^{2+}, Mn^{2+}, Cd^{2+}, Al^{3+}, Cr^{3+} and anions such as Cl^-, NO_3^-, SO_4^{2-}, ClO_4^- do not interfere in 50-fold amounts. Cations which react with thiocyanate ions to form coloured compounds (e.g. Co^{2+}, Cu^{2+}, Fe^{3+}, Bi^{3+}, Ti^{4+}, W^{5+}, UO_2^{2+}) interfere with the determination of molybdenum.

Composition of extractable molybdenum complex

The composition of the extractable molybdenum complex with CPA was studied spectrophotometrically by Job's method and the equilibrium shift method. The results obtained (Figs. 4 and 5) indicate that the molar ratio of Mo to CPA is 1:1 and of Mo to SCN^- is 1:4. On the basis of the results obtained, it can be presumed that the composition of the extracted thiocyanato—molybdenum(V) complex with CPA is (CPA · H) $[MoO(SCN)_4]$.

REFERENCES

1 H. Basińska, H. Puzanowska-Tarasiewicz and M. Tarasiewicz, Chem. Anal. (Warsaw), 15 (1970) 317.
2 J. S. Forrest, F. M. Forrest and M. Berger, Biochim. Biophys. Acta, 29 (1958) 441.
3 H. Sanke Gowda and R. Shakunthala, Talanta, 13 (1966) 1375.
4 R. Belcher, H. Puzanowska-Tarasiewicz and W. I. Stephen, Rev. Roum. Chim., 22 (1977) 531.
5 H. Basińska, H. Puzanowska-Tarasiewicz and M. Tarasiewicz, Chem. Anal. (Warsaw), 14 (1969) 883.
6 H. Puzanowska-Tarasiewicz, Chem. Anal. (Warsaw), 15 (1970) 939; 18 (1973) 753; Mikrochim. Acta, (1972) 876; Acta Polon. Pharm., 30 (1973) 67.
7 E. B. Sandell, Colorimetric Determination of Traces of Metals, 3rd edn., Interscience, New York, 1959.
8 G. P. Savariar, M. K. Arunchalam and T. R. Hariharan, Anal. Chim. Acta, 69 (1974) 305.
9 E. G. Lillie and L. P. Greenland, Anal. Chim. Acta, 69 (1974) 313.
10 C. Rózycki, Chem. Anal. (Warsaw), 11 (1966) 447.
11 Z. Kh. Sultanowa, L. K. Chuchalin, B. Z. Jofa and Y. A. Zolotov, Zh. Anal. Khim., 28 (1973) 413.
12 B. Tamhina, M. J. Herak and V. Jagodič, Anal. Chim. Acta, 76 (1975) 417.
13 O. G. Koch and G. A. Koch-Dedic, Handbuch der Spurenanalyse, Springer-Verlag, Berlin, 1974, p. 835.
14 B. Tamhina and M. J. Herak, Mikrochim. Acta, (1976) 553.
15 A. I. Vogel, A Text book of Quantitative Inorganic Analysis, Longmans, London, 3rd edn., 1961, p. 508.
16 W. Böttger, Newer Methods of Volumetric Chemical Analysis, Butterworths, London, 1956.
17 Polish Pharmacopoeia, Vol. 1, Warsaw, 1965.
18 S. J. Lyle, Talanta, 2 (1959) 293.
19 G. Gopala Rao, Z. Anal. Chem., 163 (1958) 1; 167 (1959) 1.
20 G. Gopala Rao and N. Venkateswara Rao, Z. Anal. Chem., 190 (1962) 213.
21 T. P. Sastry, P. S. Sastry, E. L. R. Dyanand and K. A. N. Reddy, Chem. Anal., 56 (1967) 66.

Analytica Chimica Acta, 94 (1977) 443—447

Short Communication

ANALYTICAL STUDY OF A NEW PICRATE-SELECTIVE MEMBRANE ELECTRODE

T. P. HADJIIOANNOU and E. P. DIAMANDIS

Laboratory of Analytical Chemistry, University of Athens, Athens (Greece)

(Received 4th May 1977)

Since the introduction of a liquid-membrane electrode selective for calcium in 1967 [1], many new electrodes of this type for different ions have become available. The use of liquid ion-exchangers has significantly extended the number of ions which can be determined. Salts of bulky quaternary ammonium ions with various anions have been widely used for constructing anion-selective liquid-membrane electrodes. Tetrahexylammonium picrate in methylene chloride has been used as the liquid ion-exchanger in an electrode which was used for several ions but not for picrate ions [2].

The communication reports the use of the water-insoluble tetrapentylammonium picrate, dissolved in 2-nitrotoluene, as the active electrode substance in a picrate-selective membrane electrode. This picrate-selective electrode has been used successfully in direct potentiometry and in the potentiometric titration of silver in the presence of thiourea with picrate.

Experimental

Apparatus. The picrate-selective electrode was used as the indicator electrode, with a double-junction silver—silver chloride electrode, Orion Model 90-02-00, as the reference electrode. The outer chamber of the reference electrode was filled weekly with a 10% (w/v) KNO_3 solution. The electrode potential was measured with an Orion Ionanalyzer (Model 801A digital pH/pIon meter). The cell potential was recorded with a Heath-Schlumberger system, which consisted of a pH/pIon electrometer (EU-200-30), a potentiometric amplifier (EU-200-01), a d.c. offset module (EU-200-02) and a strip-chart recorder (EU-205-11). The titrant was added with a multi-speed constant-rate burette (Sargent-Welch Model S-111 20-12). pH values were measured with a Metrohm pH meter (Model E350B). Test solutions were placed in 50-ml cells thermostated at 25.0°C and stirred magnetically.

Reagents. All solutions were prepared with deionized twice-distilled water and reagent-grade substances, except where stated.

Sodium picrate (0.1000 M) was prepared by neutralizing a suitable picric acid solution with NaOH to a pH of about 6. More dilute standard solutions were prepared by serial dilution. All picrate solutions were stored in amber

bottles. The picric acid used (Fluka, purum) was standardized against sodium hydroxide solution.

Tetrapentylammonium bromide (Eastman Organic Chemical Co.) was used without purification.

Preparation of the liquid ion-exchanger. Tetrapentylammonium picrate was precipitated by mixing equimolar (0.1 M) aqueous solutions of tetrapentylammonium bromide and sodium picrate. The salt is readily soluble in 2-nitrotoluene, which was therefore used for its extraction; the nitrotoluene solution was washed twice with double-distilled water to remove any traces of the bromide salt (and NaBr). The organic phase was dried thoroughly with anhydrous sodium sulfate.

Construction of the electrode. The body of an Orion 92 electrode equipped with Orion 92 membranes (e.g. 92-81-04 perchlorate membrane) was used as the liquid membrane electrode. The electrode was assembled as described in the manufacturer's instructions, and the internal reference and liquid ion-exchanger solutions were injected into the appropriate ports in the electrode body. The internal reference solution was 0.01 M sodium picrate—0.1 M NaCl. The liquid-ion exchanger solution was a 0.01 M solution of tetrapentylammonium picrate in 2-nitrotoluene.

The measuring cell was:

Ag/AgCl	reference solution (Na picrate—NaCl)	membrane ($(C_5H_{11})_4NC_6H_2N_3O_7$)	test solution	KNO_3 salt bridge	AgCl/Ag

The picrate electrode was conditioned by soaking in a 0.01 M sodium picrate solution for 48 h before use, and was also stored in this solution when not in use. The operative life of the electrode was about 40 days.

Results and discussion

The tetraalkylammonium salts tested for preparing the picrate ion-exchanger were: trimethylphenylammonium bromide, tetrahexylammonium bromide, tetrapentylammonium bromide, tetraheptylammonium bromide, tetrapropylammonium bromide, tetrabutylammonium bromide, dimethyldioctadecylammonium chloride, didodecyldimethylammonium bromide, and tetraphenylarsonium bromide. The solvents tested were: 2-nitrotoluene, dibenzyl ether, dichloroethane, 1-decanol, chlorobenzene, and phthalic dibutylester. The shorter the chain length, the greater the solubility of the picrate in water. The tetrapentylammonium picrate was the most suitable sensor and 2-nitrotoluene was the best solvent.

Linear response range. A typical calibration graph for the electrode in stirred sodium picrate solutions (Fig. 1) shows that the response is linear in the 10^{-2}—10^{-5} M range; the graph has a slope of 58 mV/decade change in activity at 25°C. All concentrations were converted to activities by the expression: $\log f = -0.511\ [\mu^{\frac{1}{2}}/(1+\mu^{\frac{1}{2}})]$, where f is the activity coefficient ($z_{pic} = -1$). After 8 days there was a decrease in the calibration graph slope in the 10^{-4}—10^{-5} M range.

Effect of pH. To check the pH-dependence of the potential of the picrate-selective electrode, potential—pH curves at various picrate concentrations were constructed. The pH of the initial solution was altered by addition of very small volumes (less than 0.1 ml per 20 ml of test solution) of NaOH or H_2SO_4 solutions. The plots (Fig. 2) show that between pH 3 and 10 the potential is practically independent of pH. At higher pH the potential increases slowly, probably because of complex formation between picrate and hydroxide ions [3]. During the operative life of the electrode, no discernible change in the potential—pH behavior was observed.

Dynamic response of the electrode. The dynamic response was tested for 10^{-2}—10^{-5} M sodium picrate solutions; the sequence of measurements was from low concentrations to high concentrations and back. The response times were quite short (less than 4 s, including the mixing and recorder time) and depended on the concentration change, the stirring rate and efficiency of solution mixing. It should therefore be possible to employ the picrate electrode in titrations with continuous addition of titrant and for the continuous monitoring of changing systems.

Potentiometric selectivity coefficients. The interference of various anions was studied by the graphical mixed solution method [4]. The concentration of the tested anion was kept constant, while the picrate concentration was varied in the range 10^{-2}—10^{-5} M. Selectivity coefficients are presented in Table 1. The electrode has a very high selectivity for picrate compared to the following ions: Cl^-, F^-, NO_3^-, HCO_3^-, CH_3COO^-, IO_3^-. At constant ionic strength, variations in the concentrations of these anions did not affect the electrode potential.

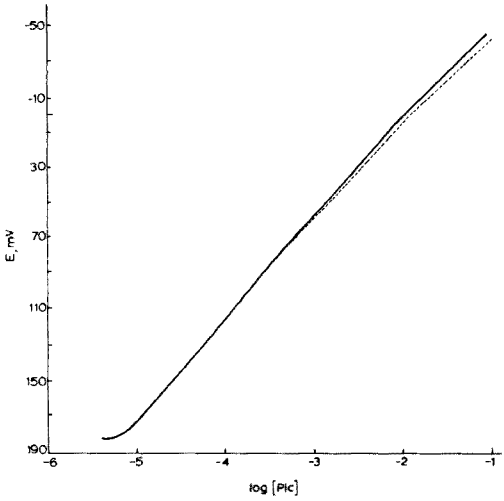

Fig. 1. Calibration curve for the picrate-selective membrane electrode. —— Activity. ---------- Concentration.

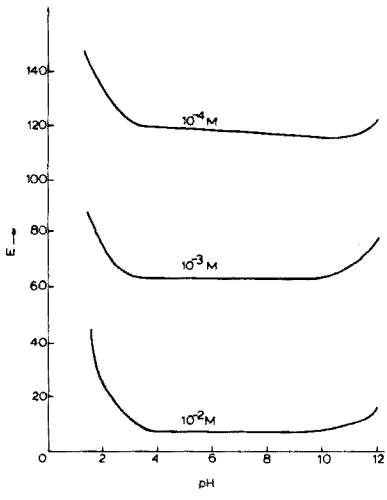

Fig. 2. Effect of pH on the potential of picrate-selective electrode at the different concentrations of sodium picrate marked.

TABLE 1

Potentiometric selectivity coefficients for interfering univalent anions

Interferent, j	$[j]$	$K^{pot}_{pic,j}$
2-Nitrophenol	1.0×10^{-2}	1.5×10^{-2}
2,4-Dinitrophenol	1.0×10^{-2}	6.5×10^{-2}
Phthalate	1.0×10^{-2}	3.3×10^{-3}
Benzoate	2.5×10^{-2}	1.4×10^{-3}
Iodate	1.0×10^{-2}	3.7×10^{-2}
Perchlorate	2.0×10^{-2}	3.0×10^{-2}

Analytical application

The picrate-selective electrode can be used practically for the determination of picrate either by direct potentiometry, or by potentiometric titration. The electrode can also be used as an indicator electrode in potentiometric precipitation titrations of cations forming insoluble picrates. As an example, titration of silver(I) was examined, based on the formation of the insoluble picrate of the silver—thiourea complex [5, 6]

$$2S = C\begin{<}{}^{NH_2}_{NH_2} + Ag^+ + C_6H_2N_3O_7^- \rightarrow [Ag(SCN_2H_4)_2]\,[C_6H_2N_3O_7] \qquad (1)$$

For the titration, a 20.00-ml aliquot of the sample and 5 ml of 0.2 M thiourea solution were pipetted into a 50-ml beaker and the mixture was titrated with standard 0.0250 M sodium picrate solution. The sharp potential change (ca. 80 mV) near the equivalence point allows precise location of the end-point.

Silver in aqueous solutions of known concentrations (2.2—18.4 mg) was determined with an average error of 1.1%; the absolute error varied from —1.9% at the 2-mg level to +1.2% at the 18-mg level. The relative standard deviation was 1.1% for a sample containing 12 mg of silver ($n = 6$). There was no interference from the following ions when present in amounts 10 times that of silver: Pb^{2+}, Zn^{2+}, Ni^{2+}, Co^{2+}, Ca^{2+}, Sr^{2+}, Ba^{2+}, Mg^{2+}, and Cd^{2+}. Hg(I), Hg(II) and Cu(II) ions interfered seriously.

Work in progress indicates that thiourea can be determined by potentiometric precipitation titration with standard silver nitrate solution on the basis of reaction(1) with the picrate-selective electrode. It has also been found that creatinine can be determined by a kinetic method based on the Jaffé reaction [3]. This work and other analytical possibilities of the picrate-selective electrode will be reported later.

The authors are grateful to M. Koupparis for valuable advice. This research was supported in part by a research grant from the Greek National Institute of Research.

REFERENCES

1 J. W. Ross, Science, 156 (1967) 1387.
2 S. G. Back, Anal. Lett., 4 (1971) 793.
3 R. S. Henry, Clinical Chemistry, Principles and Techniques, New York, Harper and Row, 1964, p. 287.
4 G. J. Moody and J. D. R. Thomas, Selective Ion Sensitive Electrodes, Merrow, Watford, 1971, p. 14.
5 P. Spacu and M. Gafiteanu, Analele Univ, Bucuresti, Ser. Stiint. Nat., 11 (1956) 123 C.A. 52, 19723h.
6 P. Spacu and M. Gafiteanu, Analele Univ., Bucuresti, Ser. Stiint. Nat., 14 (1957) 77 C.A. 53, 6888.

Analytica Chimica Acta, 94 (1977) 449—451

Short Communication

THE DETERMINATION OF SULPHATE IN PHOSPHORIC ACID WITH A SILVER/SILVER SULPHIDE ION-SELECTIVE ELECTRODE

S. R. PORTER and A. P. RUNNACLES

Fisons Limited — Fertilizer Division, Levington Research Station, Levington, Ipswich IP10 0LU (Gt. Britain)

(Received 16th June 1977)

The percentage by weight of sulphate in the filtered reactor slurry is an important control parameter in the wet process manufacture of phosphoric acid [1]. A convenient method of following sulphate trends in the reactor solution is by barium chloride titration with sodium rhodizonate as an external indicator [2] or sulphonazo III internally [3]. However, it is well known that barium chloride titrations are subject to coprecipitation errors, particularly from phosphate. A reference method, which overcomes this problem but is too lengthy for process control, involves reduction of sulphate to hydrogen sulphide which is then determined colorimetrically [4], by iodimetric titration [5], or by titration with mercury(II) or cadmium salts and dithizone indicator [6].

The present communication reports a method which eliminates the necessity for a titration. The hydrogen sulphide from reduction of sulphate is detected by an Orion silver/silver sulphide ion-selective electrode. The reducing agent — a mixture of hypophosphorous and hydriodic acids — is similar to that of Luke [5]. St. Lorant [7] and Johnson and Nishita [8] prepared reducing agents from red phosphorus, hydriodic and formic acids. Modifications to Luke's original apparatus enable the analysis to be completed in about 15 min.

Experimental

Equipment. A diagram and description of the apparatus is given in Figure 1.

White Spot Nitrogen was used to sweep hydrogen sulphide out of the reaction vessel into the detector cell, which consisted of a 100-ml Pyrex glass beaker, a rubber bung and a Pyrex ground-glass tap. The outer chamber of the double-junction reference electrode was filled with 25% Sulphide Antioxidation Buffer (SAOB) to minimize the junction potential between the electrode and the absorbing solution.

Reduction mixture. Reflux a mixture of 200 ml of hydriodic acid (55%, d. 1.7), 100 ml of hydriodic acid (66%, d. 1.9), 83 ml of hypophosphorous acid (30%) and 200 ml of concentrated hydrochloric acid for 1.5 h with a

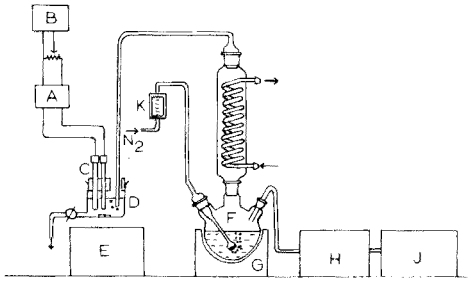

Fig. 1. Apparatus for the determination of sulphate in wet process phosphoric acid reactor solution. A, Vibret laboratory pH meter. B, Servoscribe RE 516.20 chart recorder. C, Orion model 94.16 silver/silver sulphide ion-selective electrode and an Orion model 90.02 double junction reference electrode. D, Detector cell. E, Magnetic stirrer. F, Reduction vessel containing 250 ml reduction mixture. G, Heating mantle. H, Carlo Erba model 1515/20 proportioning pump. J, Carlo Erba distributor SD3 model 1512 sample changer. K, Nitrogen flowmeter.

stream of White Spot Nitrogen blowing through it. Store in a dark glass bottle until required.

Sulphide antioxidation buffer (SAOB). Dissolve 80 g of analytical-grade sodium hydroxide and 320 g of reagent-grade sodium salicylate in about 500 ml of deionized water in a 1-l volumetric flask, then add 72 g of ascorbic acid, and make up to the mark. Store in a screw-cap plastic bottle. Prepare 25% SAOB as required by dilution (1 + 3) with deionized water.

Sulphate standards. Dissolve 73.9324 g of dried analytical-grade sodium sulphate in water and make up to 500 ml. This stock solution contains 10% (w/v) sulphate. Prepare standards containing 1% to 3.5% sulphate by dilution of suitable aliquots to 100 ml.

Procedure. Reflux the reduction mixture continuously with nitrogen purging it. Pipette a 50-ml aliquot of 25% SAOB into the measurement cell through the hole in the rubber bung. Pipette 1 ml of sample or standard into a plastic sampling cup and pump this completely into the reaction vessel. (Pump deionized water from a second cup to ensure complete transfer of sample to the reaction vessel.) To calculate the % (w/w) sulphate concentration, it is necessary to weigh (to 0.1 mg) the amount of sample pumped into the reaction vessel.

After about 5 min, there is sufficient sulphide in the measurement cell to produce a signal on the chart recorder. This increases, and then flattens to a plateau when no further hydrogen sulphide is being produced in the reaction vessel.

Empty the measurement cell by suction through a tap at the bottom and to one side of the beaker. Rinse out the cell with 50 ml of 25% SAOB before admitting a further 50 ml ready for the next sample. The total time for this sequence is about 15 min.

Results and discussion

The potential of the sulphide-selective electrode is given by the equation: E = constant + $(2.303RT \log a_{S^{2-}})/2F$, where the constant includes the potential of the internal electrode, the potential of the reference electrode and its junction potentials.

Calibration graphs were plotted on semi-logarithmic graph paper, log (weight of sulphate) vs. signal height, so that the % (w/w) sulphate could be calculated from the weight of sample taken from the sample cup.

The calibration graph obtained for six standards containing between 1.0% and 3.5% sulphate was a straight line with the equation: $y = 69.85 + 134.97x$, where y is the chart deflection in mm and x is log(concentration of sulphate). The line had a correlation coefficient of 0.994.

Table 1 compares results obtained from the reference reduction method [5] involving absorption of the hydrogen sulphide in ammoniacal cadmium acetate solution, addition of a standard potassium iodate/iodide solution, acidification with hydrochloric acid to generate hydrogen sulphide and iodine in situ and titration of the excess of iodine with sodium thiosulphate.

Conclusion

The method described gives results in agreement with those obtained by the reference method [5]. It is quicker than others based on reduction, since a titration is not required. The reduction reaction and transfer of H_2S from the reaction vessel to the absorption cell is hastened by the overwhelming excess of reduction mixture over the sulphate in the sample.

TABLE 1

Comparison of results obtained by the present method and the reference method

Sample No.	% (w/w) Sulphate	
	Present method	Reference method
1	1.67	1.75
2	2.44	2.50
3	2.98	2.74
4	2.05	2.03
5	3.20	3.19

REFERENCES

1 A. V. Slack, in Kirk-Othmer Encyclopaedia of Chemical Technology, Vol. 9, Interscience, New York, 1968, p. 91.
2 R. Strebinger and L. V. Zombory, Z. anal. Chem., 105 (1936) 346.
3 B. Budesinsky and D. Vrzalora, Z. anal. Chem., 210 (1965) 161.
4 L. Gustafsson, Talanta, 4 (1960) 227.
5 C. L. Luke, Ind. Eng. Chem., Anal. Ed., 15 (1943) 602.
6 E. E. Archer, Analyst, 81 (1956) 181.
7 I. St. Lorant, Z. physiol. Chem., 185 (1929) 252.
8 C. M. Johnson and H. Nishita, Anal. Chem., 24 (1952) 736.

Analytica Chimica Acta, 94 (1977) 453—456

Short Communication

DETERMINATION OF OXYPHENBUTAZONE AND PHENYLBUTAZONE BY DIFFERENTIAL PULSE POLAROGRAPHY AFTER DERIVATIZATION

A. G. FOGG* and Y. Z. AHMED

Chemistry Department, Loughborough University of Technology, Loughborough, Leics. (England)

(Received 11th May 1977)

Differential pulse polarography (d.p.p.) has become popular for the determination of low levels of drug substances either by direct determination or after derivatization. If derivatization produces a coloured product, both polarographic and colorimetric methods can be developed; the d.p.p. method usually proves to be the more sensitive. The most sensitive colorimetric methods can be applied at the 10^{-6} M level whereas d.p.p. can be used at the 10^{-7} M, and in some cases even at the 10^{-8} M level. Thus, d.p.p. can be used to extend the sensitivity of suitable colorimetric procedures. Recently, for example, a d.p.p. method has been described for the determination of sulphonamides at the 10^{-7} M level after diazotization and coupling with 1-naphthol [1].

The present communication is concerned with the determination of the anti-inflammatory drugs, oxyphenbutazone (4-butyl-2-(4-hydroxyphenyl)-1-phenylpyrazolidine-3,5-dione monohydrate) and phenylbutazone (4-butyl-1,2-diphenylpyrazolidine-3,5-dione); the colorimetric test for oxyphenbutazone in the British Pharmacopoeia [2] has been adapted. In this test, oxyphenbutazone is hydrolysed by a mixture of acetic and hydrochloric acids to 4-hydroxyazobenzene, which rearranges to give a benzidine derivative; this is then diazotized and coupled with 2-naphthol. This reaction has now been made quantitative for both oxyphenbutazone and phenylbutazone, and the azo dye formed has been determined by d.p.p. 1-Naphthol was used in place of 2-naphthol because it gives improved blank polarograms [1].

Very little difficulty was met in adapting the B.P. test to the d.p.p. determination of oxyphenbutazone. After diazotization it was important to add the 1-naphthol before the pH was increased to a value at which the coupling reaction occurred. For solutions containing more than 10^{-6} M oxyphenbutazone, polarographic measurements were made at pH 9—9.5; precipitation of the azo dye occurred at lower pH values. At levels below 10^{-6} M, the most satisfactory polarograms were obtained at pH 7.0; at these low concentrations precipitation did not occur and a better blank

was obtained. Reagent amounts were cut to one-tenth for less than 10^{-6} M oxyphenbutazone. Piperidine gave lower blanks than sodium hydroxide at these low levels. The peak current was independent of pH above pH 9.0.

The development of a satisfactory d.p.p. determination of phenylbutazone proved to be more difficult, partly because the azo derivative has no ionizable hydroxyl group, which causes solubility problems. This was overcome by the addition of methanol after coupling. With phenylbutazone, low peak currents were obtained at pH 9.5 and it was necessary to raise the pH to 11—11.5 at concentrations greater than 10^{-6} M (pH 9.5 was used for concentrations below 10^{-6} M). The use of 30% (v/v) methanol gives the best polarograms at levels below 10^{-6} M, and this concentration of methanol was used for all levels of phenylbutazone. In contrast to oxyphenbutazone, low levels of phenylbutazone gave better polarograms when sodium hydroxide solution was used.

Experimental

Equipment. D.p.p. measurements were made with a PAR 174A polarographic analyser (Princeton Applied Research). The forced drop time was 2 s, the pulse height 50 mV and the scan rate 2 mV s^{-1}. Two-electrode operation was used with a large surface calomel electrode as anode. The pH was adjusted with the aid of a combined glass electrode connected to an EIL 7050 pH meter.

Benzidine derivatives are formed as intermediates in these reactions and appropriate precautions should be taken. Reactions should be carried out in a fume cupboard and gloves worn when handling tubes and when disposing of the solutions.

Standard oxyphenbutazone and phenylbutazone solutions in methanol. The stock solutions were 5×10^{-3} M. Working standards were prepared by suitable dilution.

Calibration for the determination of oxyphenbutazone. Transfer an exact aliquot (0—0.9 ml) of the appropriate standard solution to a 40-ml boiling tube and add 1 ml of glacial acetic acid and 2 ml of concentrated hydrochloric acid. Heat the mixture for 1.5 h at 90—95°C in a water bath without allowing the contents of the tube to evaporate completely. (If the tube is allowed to become completely dry, low results are obtained. Additional acid can be added if this is done before the tube becomes completely dry.) Cool the tube and add 5—10 ml of distilled water.

Add 0.2 ml of 0.1 M sodium nitrite solution, mix and allow the solution to stand for 5 min. Add 1.0 ml of 0.1 M sulphamic acid solution and mix. After 1 min, add 0.1 ml of 0.1 M 1-naphthol solution in methanol, and add piperidine dropwise (ca. 1—2 ml are required) to give pH $\geqslant$ 10. At oxyphenbutazone levels above 10^{-6} M, sodium hydroxide solution can be used if preferred. Leave the solution for 30 min to allow complete formation of the azo dye. Adjust the pH to 9—9.5, and dilute the solution to 25 ml in a volumetric flask. (For oxyphenbutazone levels below 10^{-6} M, adjust the pH to 7.0 with

hydrochloric acid solution, and dilute to 25 ml. Reduce the reagent concentrations ten-fold by using 0.01 M sodium nitrite, sulphamic acid and 1-naphthol solutions.)

Deoxygenate the solution by passing nitrogen and record the polarogram between —0.4 and —0.8 V. Measure the height of the peak at —0.56 V. For oxyphenbutazone levels below 10^{-6} M, record the polarogram between —0.3 and —0.6 V and measure the peak height at —0.45 V.

Calibration for the determination of phenylbutazone. Carry out the procedure for oxyphenbutazone except for the following points. For phenylbutazone levels above 10^{-6} M, after adding 1-naphthol, add sodium hydroxide solution to give pH ⩾12. Allow the solution to stand for 30 min, add 7.5 ml of methanol, mix and adjust the apparent pH of the solution to 11.5.

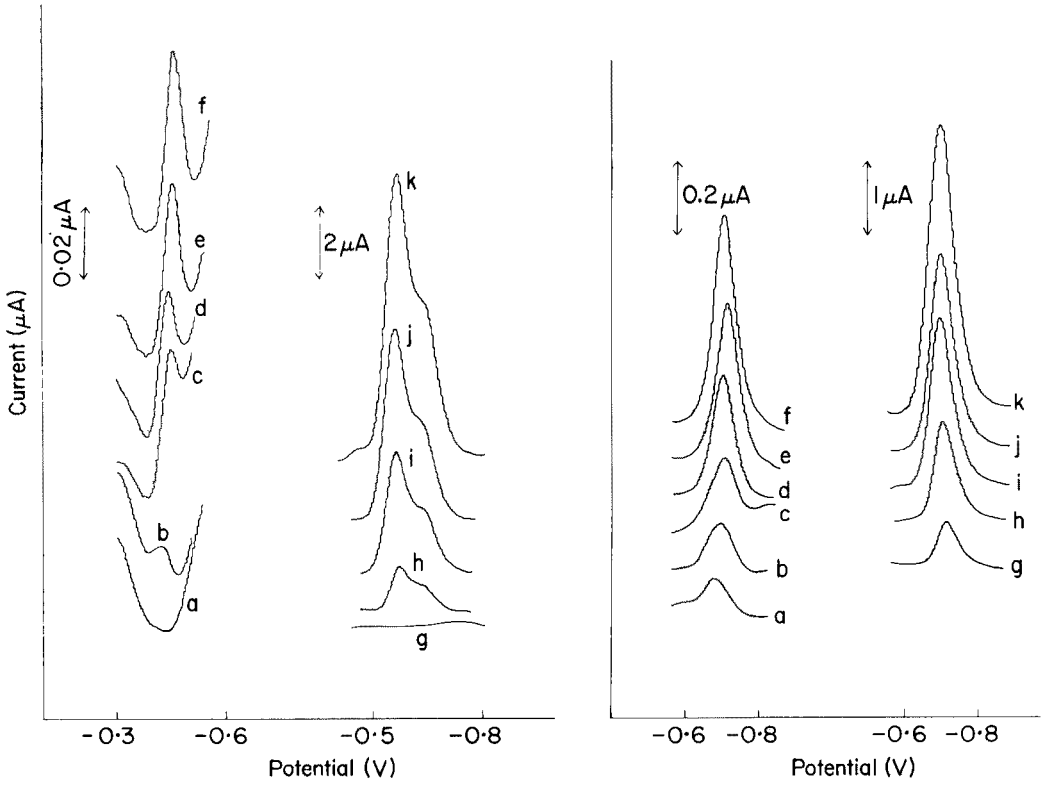

Fig. 1. Differential pulse polarograms for the oxyphenbutazone derivative. Oxyphenbutazone equivalent in measured solutions: (a) 0, (b) 1, (c) 3, (d) 5, (e) 7 and (f) 9 × 10^{-7} M at pH 7.0; (g) 0, (h) 1, (i) 3, (j) 5, and (k) 7 × 10^{-5} M at pH 9.1.

Fig. 2. Differential pulse polarograms obtained with derivatized phenylbutazone. Phenylbutazone equivalent in measured solutions: (a) 0, (b) 1, (c) 3, (d) 5, (e),7 and (f) 9 × 10^{-6} M at pH 11.7; (g) 1, (h) 3, (i) 5, (j) 7 and (k) 9 × 10^{-5} M at pH 11.7.

For phenylbutazone levels below 10^{-6} M, adjust the pH for coupling to pH 10 with sodium hydroxide solution and then after 30 min, add 7.5 ml of methanol and adjust the apparent pH to 9.5.

Results and discussion

Typical polarograms obtained for oxyphenbutazone and phenylbutazone are shown in Figs. 1 and 2. The calibration curves are rectilinear, and typically a standard deviation of 3% is obtained at the 5×10^{-6} M level for oxyphenbutazone. Unfortunately, for low levels of phenylbutazone ($<10^{-6}$ M) the blank value caused by 1-naphthol, or an impurity in the 1-naphthol, is appreciable (see Fig. 2) and must be taken into account.

In the calibration procedure, no attempt is made to evaporate the methanol before addition of acetic and hydrochloric acids. The same result is obtained, however, if the methanol is first evaporated. The procedure should therefore be applicable to the determination of oxyphenbutazone and phenylbutazone in organic extracts from plasma samples. Unfortunately, the procedure is not suitable for distinguishing between the two compounds.

The colorimetric determination of oxyphenbutazone and phenylbutazone by means of the diazotization and coupling reactions is under study. Preliminary results indicate that the absorbance depends on pH and that the optimum solution conditions for measurement are 30% methanol solutions at an apparent pH of 11.5. These studies will be reported separately together with the application of these reactions to the determination of the drugs in plasma.

The authors thank Ciba-Geigy for providing the samples and Dr. L. A. Gifford for advice.

REFERENCES

1 A. G. Fogg and Y. Z. Ahmed, Anal. Chim. Acta, 70 (1974) 241.
2 British Pharmacopoeia 1973, HMSO, 1973.

Analytica Chimica Acta, 94 (1977) 457—459

Short Communication

THE DESIGN OF HANGING MERCURY DROP ELECTRODES

P. SAGBERG and W. LUND*

Department of Chemistry, University of Oslo, Box 1033, Blindern, Oslo 3 (Norway)

(Received 7th June 1977)

The hanging mercury drop electrode (h.m.d.e.) is widely used as a working electrode in anodic stripping voltammetry. It was one of the first electrodes to be developed for this purpose, and it is still often considered to be the electrode of choice. The sensitivity of the h.m.d.e. is somewhat poorer than that of thin mercury film electrodes, particularly when linear sweep stripping is employed. However, when the more sensitive differential pulse technique is used for stripping a h.m.d.e., it is normally non-instrumental factors, e.g. the magnitude of the blank value or the degree of positive or negative contamination of the sample, which determine the practical limit of detection [1].

In modern versions of the h.m.d.e., the mercury drop is formed at the end of a glass capillary. The mercury is extruded from an internal reservoir by means of a micrometer screw. The functioning of the h.m.d.e. is of vital importance for the precision and accuracy of anodic stripping voltammetric analysis; therefore the filling procedure and other handling hints normally given by the manufacturer, should be followed strictly. However, while some electrodes rarely cause trouble, other electrodes frequently give irreproducible results. This malfunctioning of the latter electrodes was traced to incorrect dimensions of the top of the capillary reservoir relative to the micrometer head.

Experimental

The h.m.d.e. examined was the Metrohm type E 410, which is identical with the Princeton Applied Research model 9323. The anodic stripping voltammetric experiments were carried out with a differential pulse polarograph (Princeton Applied Research model 174). A detail of the electrode, illustrating the fitting of the capillary to the micrometer head, is shown in Fig. 1. To the right in this Figure are indicated the profiles of "quad-style O-rings", which may be used instead of the normal O-rings.

Discussion

The construction of only one particular type of h.m.d.e. is discussed here, but this type is one of the most frequently used in anodic stripping

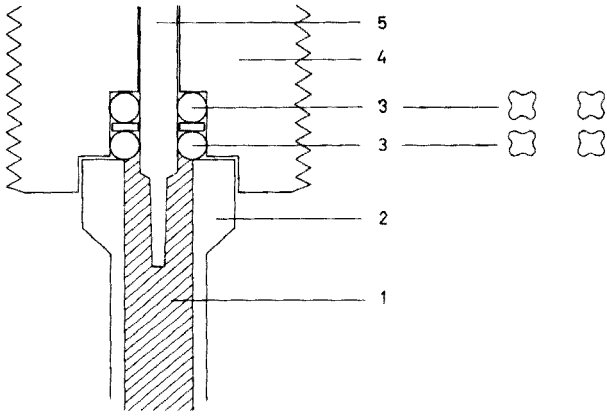

Fig. 1. Detail of the hanging mercury drop electrode. 1, Mercury reservoir; 2, upper end of glass capillary; 3, ordinary O-rings (left) and "quad-style O-rings" (right); 4, lower part of micrometer head; 5, stainless steel piston.

voltammetry. For satisfactory performance of this electrode, air must not be trapped within the electrode during the filling operation. However, irreproducible results were frequently observed for certain electrodes even when the filling was done very carefully. In these cases, the crucial point was not the filling procedure as such, but rather the dimensions and shape of the particular glass capillary used. The most satisfactory capillaries were those having the narrowest inner diameter of the mercury reservoir (cf. Fig. 1). Furthermore, the upper ground end of the glass capillary must be flat and perpendicular to the capillary axis. Only then is a tight fit of the capillary to the micrometer head ensured with a minimum of air trapped inside the assembly.

Generally, the inner diameter of the reservoir was too large. Thus, for 20 capillaries the reservoir diameter varied from 2.5 to 3.6 mm, with only three capillaries below 2.7 mm, which was found to be the upper limit for optimal electrode performance. The lower limit of the reservoir diameter is probably about 2.3 mm, because the stainless steel piston of the micrometer head (see Fig. 1) has a diameter of 2.0 mm.

It has been suggested [2] that better electrode performance may be obtained if the normal O-rings in the micrometer head are replaced by "quad-style O-rings" (see Fig. 1). However, no significant improvement was observed with such rings.

Presumably it is the air trapped between the mercury-filled reservoir and the micrometer head which causes the malfunctioning of certain electrodes. A successful electrode filling can be checked by holding the electrode vertically with the capillary tip pointing upwards; the mercury thread in the capillary should withdraw no more than 1—2 mm, once a mercury drop is removed.

Although there is a correlation between the inner diameter of the capillary reservoir and the functioning of the electrode, it should be stressed that even capillaries with a relatively large diameter will occasionally give reproducible results. Furthermore, other factors also influence the performance of the h.m.d.e. Thus, proper cleaning and silicone treatment of the capillary is of great importance for satisfactory performance; a dirty capillary tip will give noisy or irreproducible stripping curves, and the mercury drop will easily fall off. Similar experimental difficulties may also arise from chemical reactions at the electrode surface during the electrolysis and stripping steps. Finally, the drop extrusion capacity of the h.m.d.e. should be noted. Normally, a single filling will give ca. 100 medium-size mercury drops. As it is sound practice to extrude a few extra drops between each stripping experiment, the electrode must be refilled after ca. 5 h when in continuous use. In certain types of experiment, e.g. automated stripping voltammetric analysis, a higher drop capacity may be desirable. In these cases, the newly developed pressurized "universal mercury electrode" [3] may be the electrode of choice. This electrode has a drop extrusion capacity of ca. 600 medium-size drops per filling.

REFERENCES

1 W. Lund and D. Onshus, Anal. Chim. Acta, 86 (1976) 109.
2 H. Siegerman, personal communication.
3 A. M. Bond and B. S. Grabarić, Anal. Chim. Acta, 88 (1977) 227.

Analytica Chimica Acta, 94 (1977) 461—465

Short Communication

THE POLAROGRAPHIC DETERMINATION OF NITROVIN

ASTRI ROGSTAD*

Department of Food Hygiene, Veterinary College of Norway, P.O. Box 8146, Oslo-Dep. Oslo 1 (Norway)

KNUT HØGBERG

Department of Chemistry, University of Oslo, Blindern, Oslo 3 (Norway)

(Received 20th December 1976; in revised form 16th June 1977)

The feed additive nitrovin [1,5-di(5-nitro-2-furyl)-1,4-pentadiene-3-one aminohydrazone hydrochloride] has been introduced as a growth-promoting agent for poultry and pigs [1, 2]. The compound is added to the feed as a powdered carrier substance containing ca. 2.2% of the growth promoter to give a final nitrovin concentration of 10 mg per kg of feed. Presently, nitrovin is used in several countries all over the world.

The residue of nitrovin in the tissues and the food products from animals given nitrovin-containing feed can be determined by a spectrophotometric method after separation from the biological material by several steps of liquid—liquid extraction [3]. Recently, nitrovin residues in tissues from broiler chickens were studied in this laboratory [4]. The extraction procedure was found to be very time-consuming with poor recovery, and the sensitivity of the method was limited to 0.1 ppm. In an attempt to eliminate these disadvantages of the spectrophotometric method, the applicability of a direct differential pulse polarographic technique was investigated for both residues in broiler tissue and control analyses of the broiler feed. Polarographic methods are rapid, less susceptible to interferences and of high sensitivity when differential pulse polarography is used. The electro-reduction of nitrovin was therefore studied in detail, and for comparison the spectrophotometric method [4] was also applied to the feed.

Experimental

Instrumental. A PAR polarographic analyzer model 174 was used in the differential pulse and d.c. modes. An Ag/AgCl/saturated KCl electrode served as reference electrode. All experiments were performed at room temperature. Dissolved air was removed from the solutions by bubbling oxygen-free nitrogen or argon through the cell for 10 min and passing it over the solution during the electrolysis.

Chemicals. Nitrovin (97.3% purity; American Cyanamid Co.) and a carrier material containing 2.2% nitrovin (Marvell Hauge Farmasøytisk A/S, Norway)

were used. The feeds examined were broiler pellets type I, with nitrovin, and type III, without nitrovin (Felleskjøpet, Oslo, Norway).

The solubility of nitrovin in most organic solvents is rather poor. The same solvents as in the spectrophotometric residue analysis [3], i.e. methanol and a 10% solution of triethanolamine (TEA) in methanol, were therefore used. All solvents were of analytical grade. Stock solutions (ca. 0.2×10^{-3} M) were prepared by dissolving the appropriate amount of nitrovin. Solutions of the 2.2% nitrovin-containing substance were prepared by dissolving 40—600 mg in 500 ml of 10% TEA in methanol. All solutions were stored at 5°C because of their instability at room temperature [4].

Procedures. For direct polarography of nitrovin in the carrier material, the sample was dissolved in 10% TEA solution and an appropriate volume was pipetted into a 100-ml volumetric flask; 25 ml of acetate buffer pH 4.6 and 25 ml of distilled water were added, and the solution was diluted to the mark with the TEA solution. A suitable volume of the solution was transferred to the polarographic cell and deaerated with pure nitrogen or argon, and the differential pulse polarogram was recorded in the potential range 0 to −0.6 V.

The isolation of nitrofurazone from feed has been described by Sindelářová et al. [5]. This method was slightly modified and applied for extraction of nitrovin from the feed. The broiler pellets were ground in a mortar, and a 2-g sample was extracted with 25 ml of 10% TEA solution by shaking continuously for 15 min. The solution was filtered into a 100-ml volumetric flask. The extraction was repeated twice with 5-ml portions of TEA for 5 min, and the extracts were combined. After buffer addition and dilution as above, the sample was analysed by differential pulse polarography. A precipitate appeared in the solution after the addition of water and electrolyte, but this did not interfere with the polarographic measurements.

The recovery studies of nitrovin from feed were carried out by addition of the nitrovin-carrier material to broiler pellet type III in the concentration range 1.0—0.1 mg of nitrovin per 100 g of feed. After thorough mixing, the feed was extracted and analysed.

For the spectrophotometric analysis, the feed was extracted with 10% TEA as above. Nitrovin was separated from the biological components by several steps of liquid—liquid extraction [3].

Residue and recovery studies of nitrovin in chicken tissue were done after homogenization in 10% TEA solution. After centrifugation, the supernatant liquid was transferred to a 100-ml volumetric flask, diluted and analysed as described above.

Results and discussion

Preliminary experiments showed that 0.05×10^{-3} M nitrovin gave a well-defined polarographic wave when acetate buffer (0.1 M) was used as supporting electrolyte. Figure 1 shows the differential pulse and d.c. polarograms of nitrovin.

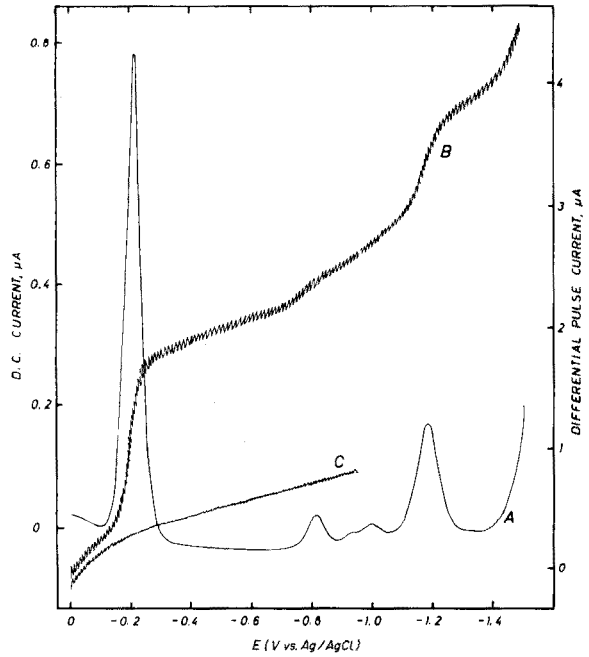

Fig. 1. Differential pulse (A) and d.c. (B) polarograms of 8.6×10^{-6} M nitrovin in acetate buffer. Curve C is the d.c. polarogram of the solvent methanol in acetate buffer. For differential pulse polarography, the conditions were: modulation amplitude, 50 mV; scan rate, 5 mV s^{-1}; drop time, 0.5 s.

The effect of pH on the polarographic wave was investigated by recording the d.c. and differential pulse polarograms of 8.6×10^{-6} M nitrovin in various supporting electrolytes. The results showed that the best-defined differential pulse polarograms and the highest peak currents (Table 1) were obtained for solutions containing acetate buffer as supporting electrolyte. Acetate buffer was therefore used in further work. The differential pulse polarograms showed small peaks at lower potentials (Fig. 1). In the pH range 3.85—6.15, a second reduction wave ($E_{\frac{1}{2}}$ ca. —1.2 V) was observed.

TABLE 1

Polarographic data for 8.6×10^{-6} M nitrovin in methanol with various supporting electrolytes

Supporting electrolyte	pH	i_d (μA)	$-E_{\frac{1}{2}}$ (V)	i_p (μA)
H_2SO_4	1.40	0.258	—0.07	3.95
Citrate	3.85	0.299	0.10	3.67
Acetate	5.65	0.237	0.20	3.94
Citrate	6.15	0.254	0.22	3.49
Phosphate	8.35	0.267	0.37	3.15
NH_3	11.10	0.211	0.48	2.72

The effect of drop time was investigated by recording d.c. polarographic curves of 8.6×10^{-6} M nitrovin solution at various heights of the mercury column. The value $ih^{-\frac{1}{2}}$, where h is the height of the column after correction for the "back-pressure", was constant (0.261), indicating that the current is diffusion-controlled.

Differential pulse polarograms recorded for acetate buffer with various amounts of nitrovin present, showed that the current increased linearly with concentration over a useful range. For the range 4.9×10^{-5}—1.96×10^{-7} M, the mean i_d/c value was $4.036 \times 10^5 \pm 0.141 \times 10^5$ μA M^{-1} ($n = 10$). The limit of determination was about 7×10^{-8} M (27 ppb) for which i_d/c was about 2.90×10^5 μA M^{-1}, which indicates the sensitivity of the method.

From the polarographic measurements, the number of hydrogen ions (Z) consumed in the electrode reaction and the number of electrons in the rate-determining step (n_a) were calculated [6]; the values found were $Z = 1.86$ and $\alpha n_a = 1.76$ (where α is the transfer coefficient). The results indicated that two hydrogen ions participate in the rate-determining step. Obviously, the nitro groups are reduced electrochemically, in accordance with the well known reaction mechanism for nitro group reduction [6, 7].

Analysis of the carrier material gave a nitrovin content of 2.9% and 2.8% by the polarographic and spectrophotometric methods, respectively. The manufacturer specifies a nitrovin content of 2.2%. The amount of nitrovin was determined from standard curves prepared by the same procedures.

In recovery studies, 95—98% of nitrovin added to the feed was found by the polarographic method ($\bar{x} = 96.8 \pm 1.4\%$) and 81—87% by the spectrophotometric method ($\bar{x} = 84.2 \pm 2.6\%$). The results are listed in Table 2. Analyses of the broiler pellets type I showed a nitrovin content of 8.5 mg kg^{-1} of feed ($s_r = \pm 0.30$) by polarography and 7.7 mg kg^{-1} ($s_r = \pm 0.19$) by spectrophotometry. The advantage of the polarographic procedure is evident. The method is faster as the measurements can be performed immediately after extraction of the additive, and the tedious clean-up procedure is unnecessary. Possible losses of nitrovin during the liquid—liquid extractions are also avoided. Significantly higher recoveries were obtained by electroanalysis.

TABLE 2

Recoveries of nitrovin from feed by the polarographic and spectrophotometric methods

Amount added to feed (mg/100 g)	Polarography		Spectrophotometry	
	Found (mg/100 g)	Recovery (%)	Found (mg/100 g)	Recovery (%)
1.304	1.265	97.0	1.120	85.8
1.151	1.098	95.4	1.005	87.3
1.024	1.005	98.2	0.838_5	81.9
0.951_0	0.905_2	95.2	0.771_5	81.1
0.316_8	0.312_1	98.5	0.273_8	86.4
0.139_0	0.134_0	96.4	0.115_1	82.8

The differential pulse polarographic measurements on extracts from chicken tissues showed an interfering peak at ca. −0.25 V. Because of the narrow band width, the peak cannot be an adsorption peak of proteins, which would exhibit a broad band in the region 0.0 to −1.0 V. Several attempts were made to separate the nitrovin peak from the interfering peak by varying the supporting electrolyte, and simple extraction procedures were also applied, but with no success. It was evident that more tedious clean-up procedures such as that reported by Borgatti et al. [3, 4] must be used.

We are grateful to Kari Holte for technical assistance. Financial support to A. R. from the Norwegian Research Council for Agricultural Science is gratefully acknowledged.

REFERENCES

1 K. Nakamura, Sogo Igaku (General Medicine), 9 (1952) 37.
2 L. M. Koster, The Synthetic Growth Stimulant Nitrovin, Orphahell B.V., Amsterdam, 1973.
3 A. R. Borgatti, F. Tarozzi, G. Crisetig and A. Brusco, La Nuovo Veterinaria, 46 (1970) 6.
4 A. Rogstad and H. K. Dahle, Norsk Vet.-tidsskr., 87 (1975) 242.
5 L. Sindelářová, M. Březina and V. Neuman, Vet. Med. (Prague), 5 (1960) 875.
6 K. Fossdal and E. Jacobsen, Anal. Chim. Acta, 56 (1971) 105.
7 C. L. Perrin, Mechanisms of Organic Polarography, in Organic Polarography, Wiley, N.Y., 1969.

Analytica Chimica Acta, 94 (1977) 467—469

Short Communication

POTENTIOMETRIC TITRATION OF OXALATE WITH LANTHANUM(III)

ANDERS CEDERGREN* and GÖSTA SUNDIN

Department of Analytical Chemistry, University of Umeå, S-901 87 Umeå (Sweden)

(Received 2nd June 1977)

Among the various titrants used for the determination of oxalate (Table 1), lanthanum(III) seems to be the most suitable for low concentrations. Thus, Curran and Fletcher [7] reported turbidimetric titrations with lanthanum(III) down to 0.3 mM of oxalate with a precision and accuracy in the 1—2% range (negative errors). According to the solubility product, bismuth(III) should be a better titrant than lanthanum(III), since log K_{s_0} ($Bi_2(C_2O_4)_3$ (s)) = −35.4, compared to −25.0 for $La_2(C_2O_4)_3$ (s). Nevertheless, preliminary experiments with bismuth(III) showed that the equilibrium reaction $2Bi^{3+} + 3C_2O_4^{2-} \Leftrightarrow Bi_2(C_2O_4)_3$ (s) was too slow to be of analytical use. Further studies of the conditions for the lanthanum(III) titration showed that much lower levels of oxalate could be determined with a lanthanum fluoride electrode in an ethanol—water titration medium (see Table 1).

Experimental

Pro analysis chemicals were used. The sodium oxalate was dried at 105°C for 12 h. An Orion fluoride-selective electrode was used in combination with an Orion double-liquid-junction reference electrode (10% KNO_3). The titrations were performed in a Metrohm titration vessel (30 ml) and the titrant was added with an Agla micrometer syringe (1—500 μl). Potentials were measured with a digital voltage meter (HP type 3460B). Sensitivity was improved by repolishing the fluoride ion-selective electrode with alundum (1 μm) after every ten titrations.

Results and discussion

At pH 5.5 about 90% of the oxalate is in the form of $C_2O_4^{2-}$ (pK_2 = 4.27), which means that the pH will decrease during the titration as hydrogen ions are liberated. The lanthanum precipitation reaction is usable down to pH 3; thus there was no need to buffer the titration solution provided that its initial pH was about 5.5 and the concentration of oxalate was less than 10^{-2} M.

The best sensitivity (titration curve slope) was obtained in (3 + 1) ethanol—water medium (Table 2). Higher levels of ethanol gave unstable potential readings.

TABLE 1

Survey of titrimetric methods for the determination of oxalate

Titrant	Indication	Range (mM)	Relative error (%)	Interferences	Ref.
Pb^{2+}	Bromopyrogallol red	50—100	0.2	—[a]	1
Pb^{2+}	(4-(2-Pyridylazo)-resorcinol	2.75—10.0	1	—[a]	2
Pb^{2+}	Pb^{2+}-selective electrode	0.65—1.60	1	acetate citrate	3
		≈100	—	—[a]	4
Ca^{2+}	Ca^{2+}-selective electrode	>100	2—6	—[a]	5
$^{45}Ca^{2+}$	Activity after equiv. point	10—100	0.5—1.0	—[a]	6
La^{3+}	Turbidimetric	>0.3	−2	Na^+, K^+	7
La^{3+}	LaF_3-electrode	10—0.025	0.8—4	—[b]	This work

[a]Not reported. [b]See text.

TABLE 2

Slopes of the titration curves ($\Delta E = E$ (4 ml) − E (2 ml); $v_{e.p.}$ = 3.3 ml) obtained for various partially non-aqueous solvents
(5 μmol of oxalate in 20 ml of solvent was titrated with 1.00×10^{-3} M lanthanum(III).)

Solvent	ΔE (mV)	Solvent	ΔE (mV)
50% dioxan	5.5	75% ethanol	90
75% dioxan	8.5	50% acetone	52
50% ethanol	50	50% isopropanol	54

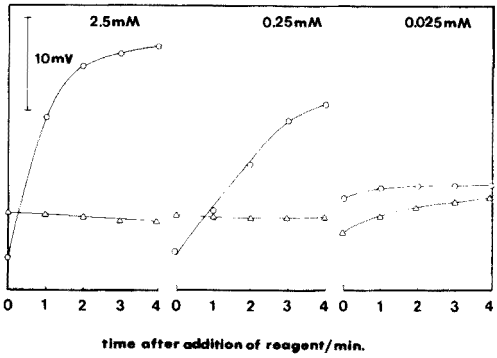

Fig. 1. The stability of the indicating electrode system for various concentrations of oxalate titrated with lanthanum(III). (○) potential readings before and (△) after the equivalence point.

The stability of the indicating electrode system is shown in Fig. 1 for various amounts of oxalate being titrated. As can be seen, the equilibrium is attained very slowly before the end-point is reached. After the end-point

TABLE 3

Results obtained for various oxalate concentrations
(Titrations in 20 ml of 75% (v/v) ethanol/water.)

Taken (mM)	Found mean value (mM)	S.d. (mM)
2.50	2.52	0.01_8
0.250	0.252	0.005_8
0.0250	0.0263	0.0003_3

TABLE 4

Maximum allowable concentration of diverse ions in the titration of 0.25 mM oxalate

Ion	Ca^{2+}	Na^+	K^+	Cl^-	SO_4^{2-}	$S_2O_3^{2-}$	SO_3^{2-}
Allowable conc. (mM)[a]	0.01	1.00	0.10	2.50	2.50	2.50	0.25

[a]Concentration giving a negative error of 10%.

the drift of the system is about 0.1 mV min^{-1}. A convenient procedure was to read the potential value at a fixed time, 3 min, after each addition of titrant. The end-point was evaluated by means of the second derivative method. The results obtained (Table 3) were always somewhat high, probably because the time required for equilibrium is longer than 3 min around the equivalence point. However, this error can be compensated since the reproducibility of the potential measurements is good. Table 3 shows that levels of oxalate about one tenth of the previously reported values (Table 1) may be determined with a relative standard deviation of about 1% and with a relative error of 0.8—4% depending on the concentration.

A survey of some interfering species is given in Table 4. Bismuth(III) causes a severe positive interference. The strong negative interference from calcium is probably due to an initial precipitation of calcium oxalate. The interferences caused by sodium and potassium are due [8] to the formation of double salts of the type $La_2(C_2O_4)_3 \cdot (Na \text{ or } K)_2C_2O_4$.

The authors thank Dr. J. D. R. Thomas for valuable discussions.

REFERENCES

1 P. S. Dubey and K. N. Tandon, Talanta, 13 (1966) 765.
2 M. C. Eshwar and S. G. Nagarkar, Science and Culture, July, 1969.
3 W. Selig, Microchem. J., 15 (1970) 452.
4 M. Mascini and A. Liberti, Anal. Chim. Acta, 60 (1972) 405.
5 A. K. Mukherji, Anal. Chim. Acta, 40 (1968) 354.
6 Cs. Ömböly, Radiochem. Radioanal. Lett., 1 (1969) 149.
7 D. J. Curran and K. S. Fletcher III, Anal. Chem., 40 (1968) 1809.
8 J. J. Lingane, Anal. Chem., 39 (1967) 881.

Analytica Chimica Acta, 94 (1977) 471—473

Short Communication

A PRACTICAL APPROACH TO QUANTITATIVE ANALYSIS FOR OXYGEN WITH AN ELECTRON MICROPROBE

M. HECQ* et C. LABART

Université de l'Etat à Mons, Faculté des Sciences, Laboratoire de Chimie Inorganique, 23, Avenue Maistriau, B-7000 Mons (Belgique)

(Received 31st May 1977)

Quantitative analysis with an x-ray microprobe, gives a precision of about 3% for most elements. For light elements, the problem is more complex. First, the mass absorption coefficients are not accurately known and are very large, so that only x-rays originating from near the surface are detected; therefore, the shape of the ionization function ($\phi(\rho z)$) in this region is important, and the simplified Philibert formula where it is assumed that $\phi(\rho z)$ at the surface ($\phi(0)$) is zero is incorrect. Secondly, the overvoltage ratio U ($U = E_0/E_c$ where E_0 is the incident electron energy, and E_c the critical excitation energy) is usually high, e.g. 47 for the oxygen K_α line and E_0 = 25 keV. The variation of the ionization cross-section (Q) with U, which is omitted in the full Philibert expression, is therefore significant for light elements. Thirdly, it is generally assumed in electron probe micro-analysis that the electron transmission follows Lenard's law [$n(\rho z) = n_0 e^{-\sigma \rho z}$, where $n(\rho z)$ is the number of electron at thickness ρz; σ has been adjusted to $4.5 \times 10^{-5}/(E_0^{1.67} - E_c^{1.67})$]. However, the interaction of electrons with matter depends on the target material. These difficulties help to explain the relatively poor results obtained by Love et al. [1] in the application of the Andersen—Wittry, Bishop or the simple or full Philibert expression to the determination of oxygen.

This communication reports the development from the experimental results of Love et al. [1], of a practical, simple approach to the determination of oxygen by electron probe analysis. This method is based on Reuter's function [2], which is a modification of the Philibert equation, where ϕ and the variation of Q with U are incorporated.

$$\phi(\rho z) = R(\rho z) \cdot n(\rho z) \cdot Q_{A,\rho z}/Q_{A,0}$$

where $R(\rho z) = R_\infty - (R_\infty - R_0) \exp - (b\rho z)$

$R_\infty = 3 + 4.05 \times 10^{-10} Z^2$

$R_0 = \phi(0) = 1 + 2.8(1 - 0.9/U_0)\eta$

$\eta = -0.0254 + 0.016 Z - 0.000186 Z^2 + 8.3 \times 10^{-7} Z^3$

$b = 6.27 \times 10^4 Z^{3/2}/E_0 A$

The ionization cross-section is assumed to depend on U by the relation: $Q = U^{-0.7} \ln U$. For the electron transmission, Reuter [2] proposed the linear expression $n(\rho z) = n_0(1 - 4 \cdot 10^4 Z^{0.5} z/E_0^{1.7})$ for the first part of the curve; the rest of the curve followed Lenard's law.

Fitting the ionization function to the experimental data shows that $Z^{0.5}$ should be replaced by $Z \exp(-0.28 \ln Z + 0.34)$. Mass absorption coefficients can also be optimized by using the expression [1]

$$\mu/\rho \ (A/Z) = a\lambda^3 Z^4 + bZ^2$$

where λ is the x-ray wavelength and a and b are constants between particular absorption edges. Best values for a and b are 3.65×10^{-5} and 1.47 for Z values between 8 and 21; for Z values between 24 and 42, the best values are, respectively, 1.02×10^{-6} and 2.33. Calculated mass absorption coefficients for the oxygen K_α are given in Table 1; these coefficients are compatible with the data of Henke and Ebisu [3].

Finally, in order to avoid the logarithmic integral function in the calculation of E as a function of ρz, the adsorbed electron energy can be expressed as

$$\Delta E = 7.85 \times 10^4 \frac{1}{E_1} \frac{Z}{A} \ln\left(\frac{1.166 E_1}{j}\right) \rho \Delta z$$

where $E_1 = (2E_0 + Ec)/3$, [4], and j is the mean excitation energy taken from Reed [4]. For compounds

$$Z = \sum_i c_i Z_i, \quad A = \sum_i c_i A_i, \quad \text{and} \quad j = \sum_i c_i j_i$$

where c_i is the mass concentration of A in the sample.

The x-ray intensity (I_A) is proportional to

$$C_A \int_0^\infty \phi(\rho z) \exp(-\chi \rho z) \, d\rho z$$

TABLE 1

Calculated mass absorption coefficients

Element	Z	μ/ρ (calculated)	μ/ρ (Lit. [3])
O	8	1.030	1.200
Mg	12	5.022	5.174
Al	13	6.731	6.715
Si	14	9.342	8.790
Cr	24	2.673	3.140
Fe	26	3.586	4.001
Ni	28	4.802	5.245
Zn	40	16.687	16.140
Mo	42	20.065	18.660

TABLE 2

Calculated and experimental intensity ratios
(Al_2O_3 is the standard; the take-off angle is 35°.)

Oxide formula	Probe voltage					
	5	10	15	20	25	30
MgO	1.07	1.05	1.07	1.04	1.03	1.04
SiO_2	1.04	0.99	0.97	1.00	0.98	0.98
Cr_2O_3	1.00	1.02	1.09	0.90	1.02	1.02
Fe_2O_3	0.98	1.03	0.94	1.05	1.07	1.09
NiO	1.03	1.03	1.01	1.02	0.95	0.98
ZrO_2	1.01	0.98	1.00	1.02	1.06	1.11
MoO_3	0.97	1.03	1.00	0.98	0.96	0.97

where $\chi = \mu \mathrm{cosec}\theta$, θ = take off angle, and μ = mass absorption coefficient $= \Sigma_i c_i \mu_i$. This integral is easily calculated by numerical evaluation with a minicomputer.

Experimentally, the x-ray intensity ratio is measured: $K = I(\text{specimen})/I(\text{standard})$. Generally Al_2O_3 is the standard.

Calculated and experimental intensity ratios (K'/K) are reported in Table 2. The root mean square for all compounds is 4.45% and the mean is 1.01. Considering that the reproducibility is ±3% and that the best absorption correction model (full Philibert) study gives a r.m.s. error of 6% [1], this method is an improvement for electron probe microanalysis based on oxygen x-rays.

REFERENCES

1 G. Love, M. G. C. Cox and V. D. Scott, J. Phys. D, 7 (1974) 2131, 2142.
2 W. Reuter, in G. Shinoda, K. Kohra and T. Ishinokawa (Eds.), X-Ray Optics and Microanalysis, Tokyo UP (1972) 121.
3 B. L. Henke and E. S. Ebisu, Advances in X-Ray Analysis, 17 (1973) 150.
4 S. J. B. Reed, Electron microprobe analysis, Cambridge U.P., 1975.

Analytica Chimica Acta, 94 (1977) 475—478

Short Communication

A KINETIC METHOD FOR THE MICRODETERMINATION OF PERBROMATE

L. A. LAZAROU, P. A. SISKOS, M. A. KOUPPARIS and T. P. HADJIIOANNOU*
Laboratory of Analytical Chemistry, University of Athens, Athens (Greece)
E. H. APPELMAN
Argonne National Laboratory, Argonne, Illinois 60439 (U.S.A.)
(Received 2nd May 1977)

The recent successful preparation of perbromates [1] and the discovery of perbromate in radiolyzed crystalline $KBrO_3$ and $CsBrO_3$ [2] have created the need for a sensitive, rapid and accurate method for the determination of perbromate in its compounds and in the presence of much larger concentrations of bromate. Various titrimetric [1] and spectrophotometric [3] methods are accurate but time-consuming, the titrimetric methods requiring preliminary steps for the determination of perbromate in the presence of bromate. Polarographic [4] and potentiometric [5] methods are relatively fast and accurate but not very sensitive. A simple and accurate iodometric method reported recently [6] permits the determination of perbromate in the presence of bromate, but its sensitivity is very low. Chromatographic methods have been reported for the detection of perbromate [7, 8].

This communication describes a new spectrophotometric reaction-rate method for the microdetermination of perbromate, based on the perbromate—iodide reaction in neutral aqueous solution [6]

$$BrO_4^- + 3I^- + 2H^+ \rightarrow BrO_3^- + I_3^- + H_2O \qquad (1)$$

The reaction curves (change of triiodide absorbance versus time) are recorded for about 60 s and the slopes, $\Delta A/\Delta t$, are related directly to the perbromate concentration. Speed, precision, simplicity and very high sensitivity are the distinctive advantages of this method. Microamounts of perbromate in the 0.3—3 μg range (10^{-6}—10^{-5} M) can be determined with relative errors and a precision of about 1%.

Experimental

Apparatus. A Beckman DK-1 double-beam spectrophotometer with the Beckman No. 92527 thermostated cell holder was used with 2 matched 1.000-cm quartz cells. The absorbance of triiodide was recorded at its absorption maximum, 353 nm.

Reagents. All solutions were prepared with deionized twice-distilled water and reagent-grade substances. The saturated (at 20°C) solution of potassium iodide was prepared freshly when needed. A 4 M potassium iodide solution was used to prepare more solutions by dilution as required.

Potassium perbromate solutions. For the 0.001000 M stock solution, dissolve 0.1830 g of $KBrO_4$ in water and dilute to 1 l. Prepare working standards (1.000×10^{-5}, 5.00×10^{-5}, and 1.000×10^{-4} M) by dilution. All perbromate solutions were stored at 4°C.

During measurements all solutions were thermostated at 26°C.

Procedure. Use the hydrogen lamp and set the wavelength at 353 nm. Pipet 2.00 ml of perbromate standard or sample solution into the sample cell, inject 1.00 ml of saturated potassium iodide solution with a 1-ml syringe and turn on the recorder immediately. Record the reaction curve for about 30–60 s and calculate the slope of the reaction curve.

Results and discussion

The reaction rate depends not only on the perbromate concentration but also on pH, temperature, and iodide concentration. By choosing the proper conditions, the reaction can be made pseudo-first order with respect to perbromate. In the recommended method, triiodide is used as its own indicator because of its intense absorbance maximum at 353 nm (ϵ_{353} = 26400 l mol^{-1} cm^{-1}). There is a linear relationship between reaction rate and iodide concentration (Fig. 1). A saturated potassium iodide solution was chosen in order to obtain the maximum reaction rate. The reaction rate is independent of pH in the 2—10 range, hence all measurements were made in unbuffered aqueous solutions. This confirms reported data [4].

Linear working curves $(\Delta A/\Delta t) = f[BrO_4^-]$ were obtained in the 21—37°C temperature range. The reaction rate has temperature variation of about

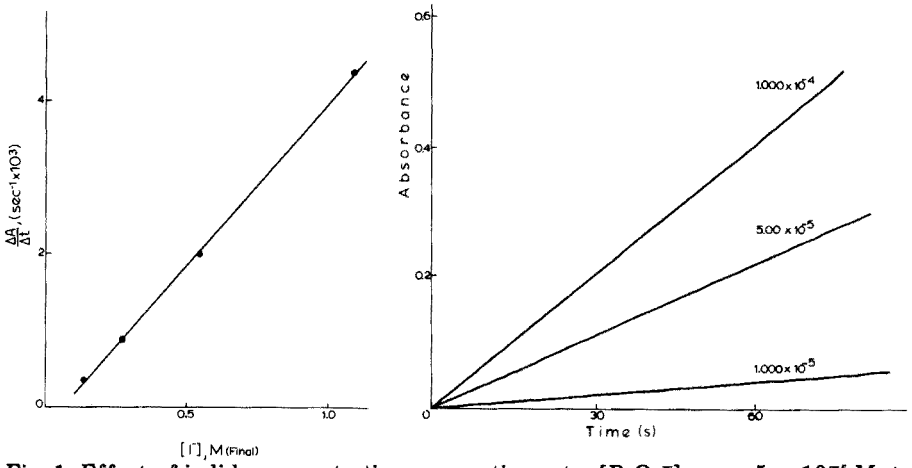

Fig. 1. Effect of iodide concentration on reaction rate, $[BrO_4^-]_{final} = 5 \times 10^{-5}$ M, t = 26°.

Fig. 2. Recorded curves of absorbance versus time for the perbromate—iodide reaction at 26°.

5.0% per degree at 30 ± 5°C. From Arrhenius plots of ln k_{obs} versus reciprocal of absolute temperature, the activation energy was calculated to be 9.0 kcal mol^{-1}.

Kinetics. The initial reaction rate can be expressed as:

$$dA/dt = k[H^+]^a\ [I^-]^b\ [BrO_4^-]^c \qquad (2)$$

where dA/dt is the rate of change of absorbance. Under the recommended conditions, the reaction rate is independent of pH ($a = 0$), and directly proportional to iodide and perbromate concentrations ($b = c = 1$). Therefore $dA/dt = k[I^-]\ [BrO_4^-]$. Since the iodide is in enormous excess over the perbromate, the reaction can be considered pseudo-first order with respect to perbromate. Thus $dA/dt = k_{obs}[BrO_4^-]$. Since the rate of change of absorbance at 353 nm is constant during the measurement time,

$$\Delta A/\Delta t = K_{obs}[BrO_4^-] \qquad (3)$$

The term $\Delta A/\Delta t$, i.e. the slope of the absorbance vs. time curve, is proportional to the perbromate concentration, and thus a calibration curve (slope vs. perbromate concentration) can be obtained with standards. A calibration curve obtained from the recorded curves (Fig. 2) was a straight line.

Analytical data. Results for the determination of perbromate in pure aqueous potassium perbromate solutions are given in Table 1. The data indicate that perbromate in the 0.3—3-μg range can be determined with relative errors of about 1%. Five replicate determinations were made at the level of 1.4 μg of perbromate, by the recommended procedure; the relative standard deviation was 1.5%.

Effect of bromate. Practically the same results were obtained for the determination of 20 nmol of perbromate in a 2-ml sample in the absence of bromate and in the presence of a large excess of bromate (up to a 5000-fold excess) (Table 2). In strongly acidic solutions, bromate reacts slowly with iodide; therefore, the determination of perbromate in the presence of very large amounts of bromate should be made at pH > 5.

TABLE 1

Results for aqueous perbromate solutions

Slope, $\Delta A/\Delta t$ ($s^{-1} \times 10^3$)	Perbromate in 2-ml sample (ng)		Error (%)
	Taken	Found[a]	
0.55	288	287	−0.3
1.89	863	839	−2.8
3.32	1439	1428	−0.8
4.86	2015	2062	+2.3
6.86	2878	2886	+0.3
		Av.	1.3

[a]From straight-line working curve; single runs.

TABLE 2

Results for the determination of perbromate in the presence of bromate

Bromate added (nmol)	Perbromate found[a, b] (nmol)	Error (%)	Perbromate found[a, c] (nmol)	Error (%)
0	20.1	+0.5	101.1	+1.1
10	19.6	−2.0	98.8	−1.2
100	19.8	−1.0	99.6	−0.4
1000	19.7	−1.5	98.8	−1.2
10000	20.2	+1.0	100.0	—
100000	19.8	−1.0	100.8	+0.8

[a]From straight-line working curve; single runs.
[b]20.0 nmol of perbromate taken.
[c]100.0 nmol of perbromate taken.

The authors thank D. Katakis and C. E. Efstathiou for stimulating discussions. This research was supported partly by a research grant from the Greek National Institute of Research and partly by the United States Energy Research and Development Administration.

REFERENCES

1 E. H. Appelman, J. Am. Chem. Soc., 90 (1968) 1900; Inorg. Chem., 8 (1969) 223.
2 L. C. Brown, G. M. Begun and G. E. Boyd, J. Am. Chem. Soc., 91 (1969) 2250.
3 L. C. Brown and G. E. Boyd, Anal. Chem., 42 (1970) 291.
4 B. Jaselskis and J. L. Huston, Anal. Chem., 43 (1971) 581.
5 J. R. Brand and M. L. Smith, Anal. Chem., 43 (1971) 1105.
6 R. Keil, Z. Anal. Chem., 281 (1976) 123.
7 M. Lederer and M. Sinibaldi, J. Chromatogr., 60 (1971) 275.
8 L. Ossicini and M. Balsoni, J. Chromatogr., 79 (1973) 311.

Analytica Chimica Acta, 94 (1977) 479—483

Short Communication

KINETIC DETERMINATION OF BINARY MIXTURES OF PHENOLS WITH A STOPPED-FLOW TECHNIQUE

EZIO PELIZZETTI, GIANFRANCO GIRAUDI and EDOARDO MENTASTI*
Istituto di Chimica Analitica, Università di Torino, Via P. Giuria, 5. 10125 Torino (Italy)
(Received 13th June 1977)

Many papers deal with methods for determining phenols in aqueous samples. Phenols are present in many pollutants, derived from organic contamination, and can cause an unpleasant taste in potable waters that have been chlorinated (many pesticides generate phenols). The most widely used methods are colorimetric [1] and few methods concern the simultaneous determination of phenol mixtures: little work on kinetic methods of analysis has been done [2]. The present communication reports the kinetic determination of binary mixtures of phenols, by oxidative coupling with *N,N*-diethyl-*p*-phenylenediamine in the presence of hexacyanoferrate(III).

Coupling reactions

The oxidative coupling reactions of phenols (P) with *p*-phenylenediamine and *N,N*-dialkyl-*p*-phenylenediamines (PPD) has been investigated extensively [3—5]. At pH 8, PPD are oxidized to the corresponding benzoquinonedimines (QDI) which react with phenols to give leucodyes which are finally oxidized to indoaniline dyes which have high molar absorptivities.

The difference in reactivity (see Table 1) suggests a possible application of indoaniline dye formation to the kinetic analysis of binary mixtures of phenols. The analysis of mixtures of *o*-cresol and *m*-cresol (which show one of the more unfavourable reactivity ratios) with *N,N*-diethyl-*p*-phenylenediamine as reactant has therefore been investigated.

The following kinetic scheme holds for a binary mixture of phenols

$$P_A + QDI \xrightarrow{k_1^A} D_A$$

$$P_B + QDI \xrightarrow{k_1^B} D_B$$

By operating with a large excess of QDI, the reactions follow a simple pseudo-first order kinetic law, and it is possible to set $k_A = k_1^A [QDI]_0$ and $k_B = k_1^B [QDI]_0$. Then, the absorbance of the mixture after the reaction time t (A_t) and the final absorbance (A_∞) are given by

$$A_t = \epsilon_{D_A} b(1 - e^{-k_A t}) [P_A]_0 + \epsilon_{DB} b(1 - e^{-k_B t}) [P_B]_0 \qquad (1)$$

TABLE 1

Relative rates[a] of oxidative coupling of monosubstituted (R) phenols with *N,N*-dialkyl-*p*-phenylenediamines [5]

R	Relative rate constants[b]	R	Relative rate constants[b]
H	1	*m*-Cl	0.19
o-CH_3	37	*m*-NO_2	0.0019
o-Cl	0.30	*m*-$COCH_3$	0.063
o-Ph	8.1	*p*-Cl	0.030
o-NO_2	0.0037	*p*-OCH_3	3.7
m-CH_3	7.4		

[a]These data concern the reaction of phenols with 4-amino-3-methyl-*N*-ethyl-*N*-(1-methylsulphonamido-ethyl)aniline.
[b]This ratio refers to specific rate constants [3—5].

$$A_\infty = \epsilon_{D_A} b [P_A]_0 + \epsilon_{D_B} b [P_B]_0 \quad (2)$$

where ϵ represents the molar absorptivities and b the cell pathlength.

Method A. For a binary mixture undergoing simple first-order reactions, the method of Lee and Kolthoff [6] was revised to take into account the formation of two different final products. If the total concentration of the mixture can be determined separately, from eqns. (1) and (2), eqn. (3) can be derived

$$\frac{A_\infty - A_t}{([P_A]_0 + [P_B]_0)\,\epsilon_{D_A} b} = \left(e^{-k_A t} - \frac{\epsilon_{D_B}}{\epsilon_{D_A}} e^{-k_B t}\right)\frac{[P_A]_0}{[P_A]_0 + [P_B]_0} + \frac{\epsilon_{D_B}}{\epsilon_{D_A}} e^{-k_B t} \quad (3)$$

and by plotting the left-hand side of eqn. (3) vs. the initial molar fraction of P_A, a straight line is obtained.

The optimum time, t^*, was chosen as described by Lee and Kolthoff [6], and a calibration plot can be drawn if the first-order rate constants (k_A and k_B) and the molar absorptivities of the products (ϵ_{D_A} and ϵ_{D_B}) are known.

Alternatively, by subtracting eqn. (1) from eqn. (2) and dividing by A_∞, eqn. 4 is obtained

$$(A_\infty - A_t)/A_\infty = (e^{-k_A t} - e^{-k_B t})\,\rho_A + e^{-k_B t} \quad (4)$$

where ρ_A represents the absorbance fraction of D_A, defined as

$$\rho_A = \epsilon_{D_A} [P_A]_0 / (\epsilon_{D_A} [P_A]_0 + \epsilon_{D_B} [P_B]_0) \quad (5)$$

and is related to the molar fraction of the components by

$$x_A = \epsilon_{D_B} \rho_A / \{\epsilon_{D_A} + (\epsilon_{D_B} - \epsilon_{D_A})\,\rho_A\} \quad (6)$$

Equations (3) and/or (4) can be used for evaluating the composition of the mixture when the total concentration is known.

Method B. When the total concentration of the mixture is not available, an expression for the direct evaluation of the concentration of each component can be derived by a simple rearrangement of eqns. (1) and (2). By dividing eqn. (1) by $(1 - \exp(-k_i t))$, then subtracting from eqn. (2) and rearranging, the concentration of P_i can be calculated from

$$[P_i]_0 = \{A_\infty (1 - e^{-k_j t}) - A_t\}/\{b\, \epsilon_{D_i} (e^{-k_i t} - e^{-k_j t})\} \quad (7)$$

The same optimum time of reaction, t^*, was chosen, as described above.

Experimental

Reagents. All the reagents were analytical-grade chemicals (Erba, Merck). The solutions of cresols and *N,N*-diethyl-*p*-phenylenediamine were prepared immediately before use. Two equivalents of hexacyanoferrate(III) were added for each mole of PPD. Buffer solutions were prepared by mixing 0.05 M borax with 0.1 M NaOH to give pH 9.50. The pH of the reacting mixture was constant within 0.05 units.

Apparatus. Absorption spectra were recorded with an Hitachi Perkin-Elmer EPS 3t spectrophotometer. The kinetic measurements were performed with a Durrum—Gibson stopped-flow spectrophotometer (2.00-cm cell) and the reaction traces, stored on a Tektronix 564 oscilloscope, were photographed. The pH was measured with a Metrohm E 388 potentiometer.

Procedure. The progress of the reaction at 25.0 ± 0.1°C was followed at the proper wavelength by mixing a solution of phenols (2×10^{-6} M total concentration) and $K_3Fe(CN)_6$ (1.2×10^{-4} M) with a solution of PPD (6×10^{-5} M), both at pH 9.50. The species monitored on the storage oscilloscope screen were the indoaniline dyes.

Evaluation of the rate constants. Because of the small difference in reactivity between *o*- and *m*-cresol, the rate constants k_A and k_B were evaluated under strictly identical experimental kinetic conditions. The method proposed by Connors [7] for the analysis of a binary mixture of components with close pseudo-first order rates was adapted for the evaluation of reaction rates of components of a binary mixture of known composition.

Hence, subtraction of eqn. (2) from eqn. (1) gives eqn. (8)

$$\frac{A_\infty - A_t}{[P_A]_0\, \epsilon_{D_A}\, b} = e^{-k_A t} + \frac{[P_B]_0\, \epsilon_{D_B}}{[P_A]_0\, \epsilon_{D_A}}\, e^{-k_B t} \quad (8)$$

and this expression can be used for calculating k_A and k_B by plotting the left-hand side of eqn. (8) vs. $([P_B]_0\, \epsilon_{D_B})/([P_A]_0\, \epsilon_{D_A})$ at various compositions of the mixture.

According to the methods of mixture analysis, the optimum time to be employed in eqn. (8) was chosen, by iteration, to be consistent with t^*. At this time, the rate constants show the minimum standard deviation, as calculated from the regression line of the plot of eqn. (8). In the present case the side-reactions affecting QDI (i.e. deamination giving benzoquinone

monoimines [8]) can be neglected [3, 5]; these side-reactions would introduce a common factor in the estimated rate constants which would not affect the validity of the method.

Results

The formation of indoaniline dyes was followed at 650 nm (λ_{max} for the dye corresponding to *o*-cresol [5]). The values of ϵ_i at 650 nm for the indoaniline dyes corresponding to *o*- and *m*-cresol were $(2.45 \pm 0.03) \times 10^4$ and $(1.88 \pm 0.03) \times 10^4$ l mol^{-1} cm^{-1}, respectively. The first-order rate constants, $k = 1.115 \pm 0.048$ (for *o*-cresol) and $k = 0.724 \pm 0.062$ s^{-1} (for *m*-cresol) were obtained from three independent sets of kinetic runs at a total cresols concentration of 2×10^{-6} M and 11 different molar fractions of each component from 0.05 to 0.95. These values are close to those determined for each pure compound [5].

Method A. The optimum reaction period, computed [6] with the first-order rate constants reported above, is 1.104 s. The equation of the calibration straight line is $Y = 0.3450 - 0.0530\ X$, where Y represents the left-hand side of eqn. (3) and X the molar fraction of *o*-cresol. Table 2 shows the recoveries at different molar fractions, averaged for two different sets.

Method B. The working equations for the evaluation of the mixture composition found for time t^* are $[o\text{-cresol}]_0 = (A_t - 0.5504\ A_\infty)/3.862 \times 10^3$ and $[m\text{-cresol}]_0 = (0.7080\ A_\infty - A_t)/\ 5.928 \times 10^3$.

Table 2 shows the average data for the kinetic runs performed by method B. The results show that the kinetic method resolves a binary mixture of phenols, even with an unfavourable reactivity ratio such as 1.54, with satisfactory accuracy in spite of the very low concentrations involved. This method allows a fast evaluation of a binary mixture of isomers to be made,

TABLE 2

Kinetic determination of *o*-cresol and *m*-cresol in their mixtures (Total concentration, 2×10^{-6} M.)

Method A		Method B			
Molar fraction of *o*-cresol (%)		*o*-Cresol ($\times 10^{-6}$ M)		*m*-Cresol ($\times 10^{-6}$ M)	
Taken	Found	Taken	Found	Taken	Found
10	8.5	0.20	0.12	1.80	2.01
20	20.5	0.40	0.33	1.60	1.86
30	32	0.60	0.64	1.40	1.35
40	43.5	0.80	0.67	1.20	1.29
50	50	1.00	0.88	1.00	1.11
60	65	1.20	1.08	0.80	0.88
70	68	1.40	1.47	0.60	0.52
80	78	1.60	1.72	0.40	0.28
90	96	1.80	1.83	0.20	0.15

Analytica Chimica Acta, 94 (1977) 485—488

Short Communication

SPECTROPHOTOMETRIC DETERMINATION OF MICROAMOUNTS OF SULPHATE IN RIVER WATERS WITH 6-(*p*-ACETYLPHENYLAZO)-2-AMINOPERIMIDINE

KYOJI TÔEI*, HARUO MIYATA and YOSHIO YAMAWAKI

Department of Chemistry, Faculty of Science, Okayama University, Tsushima-naka 3-1-1, Okayama-shi 700 (Japan)

(Received 21st June 1977)

The determination of small amounts of the sulphate ion in aqueous solution is important in many fields of applied analysis. Stephen [1] described an excellent precipitant, 2-aminoperimidine hydrochloride, for sulphate and the reagent was applied to the nephelometric determination of 0.1—5 ppm of sulphate ion. If a coloured precipitant for sulphate were available, this type of reagent would be utilized more widely. In attempts to establish such a reagent, 2-aminoperimidine was coupled with diazotized aniline derivatives such as chloro-, nitro-, methoxy-, methyl- and acetyl-aniline or naphthylamine derivatives. Of these compounds, 2-aminoperimidine coupled with diazotized *p*-aminoacetophenone, 6-(*p*-acetylphenylazo)-2-aminoperimidine was best. Its ethanolic solution formed precipitates quantitatively with sulphate, and the supernatant liquid was clear brownish-orange.

Experimental

Apparatus. A Hitachi Perkin-Elmer Model 139 spectrophotometer with 0.5-cm glass cells was used for absorbance measurements and a Hitachi Model EPS-3T recording spectrophotometer for the spectra. A Hitachi-Horiba Model M-5 pH meter, an Iwaki KM shaker, and a Marusan superior centrifuge were also used.

Synthesis of 6-(p-acetylphenylazo)-2-aminoperimidine. 2-Aminoperimidine was prepared by the McClure method [2]. The reagent, 6-(*p*-acetylphenylazo)-2-aminoperimidine, was obtained by coupling 2-aminoperimidine with the diazonium salt of *p*-aminoacetophenone, and the product was recrystallized from glacial acetic acid and obtained in the form of greenish needles. The position of the phenylazo group of this reagent has not yet been confirmed, but it seems reasonable to assume that the azo group is attached at the 6-position of 2-aminoperimidine.

Solutions. The reagent was used as a 7×10^{-4} M solution in ethanol. The standard sulphate solution (1000 ppm) was prepared by dissolving 1.815 g of K_2SO_4 in 1 l of distilled water. Buffer solution pH 3.8 was prepared by mixing 1 M acetic acid and 1 M sodium acetate solutions.

Standard procedure. To 5 ml of water containing sulphate ion (0—10 ppm) in a 10-ml stoppered centrifuge tube, add 2 ml of the reagent solution and 3 ml of the buffer solution. Shake for 5 min in a mechanical shaker, and leave for 10 min. Centrifuge the precipitate for 10 min at 1500 rpm, and pour the clean supernatant liquid into a 0.5-cm cell. Measure the absorbance at 480 nm against water in the reference cell.

Results and discussion

Figure 1 shows the absorption spectra of solutions containing 0, 5 and 10 ppm sulphate by the standard procedure. The wavelength at the maximum absorption of each spectrum occurs at 480 nm.

A study of the effect of pH showed that a constant maximum absorbance was obtained between pH 3.4 and 4.1. A pH value of 3.8 was chosen for further studies.

The effects of shaking and centrifuging times on the absorbance were also studied. The absorbance remained unchanged for shaking periods of 5—60 min or for centrifuging times of 5—60 min. Accordingly, a shaking time of 5 min, and a centrifuging time of 10 min at 1500 rpm was selected for further work.

Calibration curves. The absorbance was measured by the standard method and the absorption differences between blank and known amounts of sulphate were plotted against the sulphate concentration. The calibration curve was linear, passing through the origin, in the range 0—10 ppm of sulphate. The slope was 0.080 absorbance unit per 1 ppm of sulphate.

Effect of diverse ions. The ions normally present in river waters do not interfere. As shown in Table 1, Na^+ (CH_3COONa), K^+ (KCl), NH_4^+ (NH_4Cl), Mg^{2+} ($Mg(NO_3)_2 \cdot 6H_2O$), Ca^{2+} ($Ca(NO_3)_2 \cdot 4H_2O$), NO_3^- ($NaNO_3$) and SiO_3^{2-} (Na_2SiO_3) do not interfere when present in amounts 100-times the normal contents of the ion in Japanese river waters. There is no interference from even tenfold amounts of Fe^{3+} ($Fe(NO_3)_3 \cdot 9H_2O$), Cl^- (NaCl) and $H_2PO_4^-$ (KH_2PO_4).

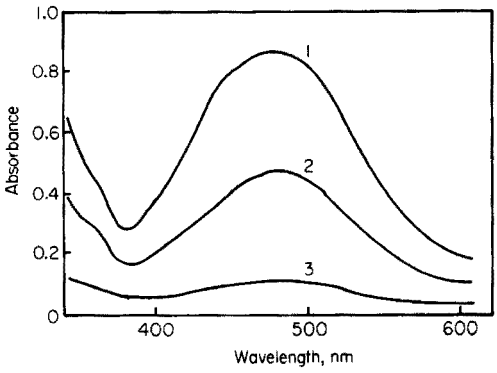

Fig. 1. Absorption spectra of the reagent. 1, Reagent blank. 2, Sulphate ion 5 ppm. 3, Sulphate ion 10 ppm. pH 3.4—4.1.

TABLE 1

Effect of foreign ions

Foreign ion [X]	Normal content[a] ($mg\ l^{-1}$)	$\frac{[X]}{[M.A.]}$	Absorbance
none			0.482
Fe^{3+}	0.24	10	0.483
Mg^{2+}	1.9	100	0.484
Ca^{2+}	8.8	100	0.479
Na^{+}	6.7	100	0.480
K^{+}	1.2	100	0.490
NH_4^{+}	0.05	100	0.482
SiO_3^{2-}	19.0	100	0.483
Cl^{-}	5.8	10	0.484
$H_2PO_4^{-}$	0.02	10	0.491
NO_3^{-}	0.26	100	0.476

[a]Mean amount (M.A.) of the ion in Japanese river waters.

TABLE 2

Determination of sulphate in river waters

Sample No.[a]	Absorbance[b]	SO_4^{2-} (ppm)	Recovery of added SO_4^{2-} [c] (%)
A1	0.340 ± 0.006	4.3	
A2	0.358 ± 0.006	4.5	
A3	0.402 ± 0.003	5.1	
A4	0.360 ± 0.008	4.6	98
A5	0.447 ± 0.002	5.7	
A6	0.461 ± 0.002	5.9	97
A7	0.496 ± 0.003	6.3	
Y1	0.286 ± 0.006	3.6	
Y2	0.420 ± 0.005	5.3	103
Y3	0.430 ± 0.004	5.5	
Y4	0.585 ± 0.002	7.5	
Y5	0.585 ± 0.005	7.5	
Y6	0.972 ± 0.003	12.4	97
Y7	1.084 ± 0.002	13.8	
T1	0.194 ± 0.004	2.4	98
T2	0.442 ± 0.002	5.6	101
T3	0.481 ± 0.005	6.1	
T4	0.539 ± 0.001	6.9	
T5	0.580 ± 0.004	7.4	

[a]Samples A, Y and T were taken on 13th, 19th and 24th January, 1977, respectively.
[b]Absorbance difference from the reagent blank, the mean value of five determinations.
[c]10 μg of sulphate was added in all cases.

Application to river waters

The proposed method was applied to the determination of sulphate in waters from the Asahi (142 km), the Yoshii (133 km) and the Takahashi (111 km) Rivers in Okayama Prefecture, Japan. Samples from the rivers were filtered through a membrane filter (pore size, 0.45 μm) before the determination. All samples were clear. They were numbered from the upper to the lower reaches of the rivers. Analyses were done without any pretreatment within several hours of sampling.

The results are shown in Table 2. The sulphate content increases gradually towards the lower reaches. The amount in the lower reaches in the Yoshii River is higher than that in the other two rivers. This seems to be due to contamination by waste water from a pyrite region and clay factories in the middle reaches.

Recovery tests indicated that this method is not affected by the various ions existing in the river waters.

One of the authors (K. T.) is very grateful to Professor R. Belcher and Dr. W. I. Stephen, because the idea of this compound arose from discussions with them in Birmingham during December 1975.

REFERENCES

1 W. I. Stephen, Anal. Chim. Acta, 50 (1970) 413.
2 G. L. McClure, Anal. Chim. Acta, 64 (1973) 289.

Analytica Chimica Acta, 94 (1977) 489—491

Short Communication

LIQUID—LIQUID EXTRACTION OF TITANIUM THIOCYANATE WITH HEXAMETHYLPHOSPHORAMIDE AND DIRECT SPECTROPHOTOMETRIC DETERMINATION IN THE ORGANIC PHASE

MONIDIPA MITRA and B. K. MITRA

Department of Chemistry, Jadavpur University, Calcutta 700 032 (India)

(Received 16th February 1977)

Traces of titanium are often determined spectrophotometrically. Among the standard methods [1], hydrogen peroxide, tiron, chromotropic acid and ascorbic acid have been widely used. But most of these methods suffer either from lack of sensitivity or from interferences from other elements generally associated with titanium. Various studies have been made with *N*-benzoyl-*N*-phenylhydroxylamine (BPHA) and its derivatives [2]; the most sensitive methods use thiocyanate and BPHA [3], but again the selectivity is low.

Busev and Solov'eva [4] examined the extraction—photometric determination of Ti(III, IV), using tribromopyrogallol in the presence of fourteen different antipyrine derivatives. The molar absorptivities are fairly high ($1—2 \times 10^4$) but the serious interferences of Mo(V, VI), Fe(III), Cr(VI), V(IV, V), Nb(V), fluoride, EDTA and oxalic acid limit the uses of the method. A method based on bromopyrogallol red and diantipyrylmethane [5] has high sensitivity ($\epsilon_{620\,nm} = 4.77 \times 10^4$ l mol^{-1} cm^{-1}); the main drawback is that the Ti(IV) complex is not extracted by common solvents, and that it is stable for only 10—15 min.

In the method described here, a new reagent, hexamethylphosphoramide, is proposed as a spectrophotometric reagent for titanium, together with ammonium thiocyanate. The molar absorptivity is high, i.e., 28 740 l mol^{-1} cm^{-1} at 420 nm. The process is simple and rapid; interferences are few and can be removed very easily. The method has been successfully used for the determination of Ti(IV) in the ferro-titanium alloy and also for traces of Ti(IV) in synthetic mixtures containing Fe(III), Cr(III), Mn(II) and Ni(II).

Experimental

Apparatus. A Hilger Uvispek spectrophotometer with 10-mm glass cells, and an Elico (Hyderabad, India) model LI-10 pH meter, were used.

Reagents. Hexamethylphosphoramide ($[(CH_3)_2N]_3PO$; Fluka) was used as received. Other chemicals were of reagent grade (Merck). Titanium sulphate solution was prepared by digesting potassium titanyl oxalate with concentrated sulphuric acid and diluting suitably. This was standardized by

precipitating as hydrated TiO_2 igniting and finally weighing as TiO_2. The standard solution was subsequently diluted to give a 10 μg Ti ml^{-1} solution.

General procedure

Mix an aliquot of titanium solution containing sufficient titanium to give 0.25—1.7 ppm Ti in the final extract, with about 500 mg of ammonium thiocyanate in a 100-ml beaker. Adjust the acidity to 1.5 M in hydrochloric acid. Add about 1 ml of hexamethylphosphoramide and heat on a boiling water bath for about 15 min. After cooling, transfer to a separatory funnel and extract with an equal volume of chloroform. Repeat the extraction twice, and dilute to 25 ml with chloroform. Measure the absorbance at 420 nm against a reagent blank prepared under identical conditions.

Results and discussion

The absorbance of the extracted complex measured against a reagent blank shows a maximum at 420 nm (Fig. 1). The system obeys Beer's law over the range 0.1—2 ppm of titanium. The optimum concentration range [6] is 0.25—1.7 ppm. The sensitivity calculated (for $\log I_0/I = 0.001$) is 0.00166 μg cm^{-2}. The molar absorptivity is 28 740 l mol^{-1} cm^{-1}. The photometric error [7] is 2.7%. For ten different measurements, made with 0.5 ppm of titanium at 420 nm, the average absorbance was 0.305 with a relative standard deviation of 2.9%.

Optimal reaction conditions. When the reaction mixture is warmed for at least 15 min, the absorbance of the final extract attains its maximum and remains constant for at least 5 h. The complex is not formed at pH 6. Complex formation appears to start at pH 4. The absorbance of the extract reaches a maximum when the initial acidity of the aqueous layer is 1—2 M HCl, and decreases again at higher acidity. A 1.5 M HCl solution was therefore chosen.

With 50 mg of ammonium thiocyanate, there is only a very faint colouration. As the concentration of ammonium thiocyanate is increased, the absorbance increases; a plateau region is reached with 300 mg of ammonium thiocyanate; 500 mg was selected for the general procedure. There was very little difference

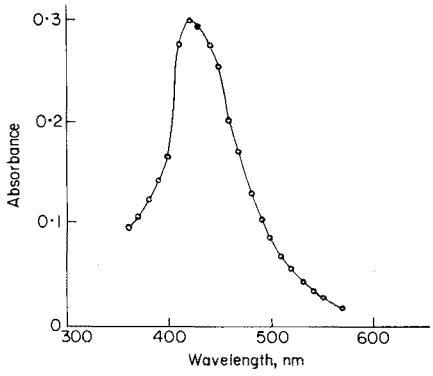

Fig. 1. Absorbance spectrum for 0.5 ppm Ti.

in the absorbance of the Ti(IV) complex when 0.5—2 ml of the phosphoramide was added.

Effect of diverse ions. There is no interference from 10—20-fold amounts of U(VI), Zr, V(V), V(IV), W(VI) or Ta. Iron interferes, but iron(III) can be removed by extraction from 6 M HCl medium with diethyl ether or di-isopropyl ether [8]. Copper(II) can be masked with thiourea to give the colourless copper(I) complex. Moderate amounts of tartaric acid, citric acid, ascorbic acid, EDTA and hydroxylammonium chloride are also tolerated.

Analysis of ferrotitanium alloy. The alloy (250 mg) was digested with 5 ml of concentrated sulphuric acid for 1 h. The mixture was cooled, and then boiled with 1 ml of the acid for another 30 min. After boiling with about 50 ml of water, the mixture was filtered into a 250-ml volumetric flask. The filter was washed thoroughly with distilled water, and the solution was diluted to 250 ml. An aliquot (2 ml) was diluted to 25 ml; this solution contained 0.08 mg ml^{-1} of alloy. A 1-ml aliquot was treated with a few drops of (1:1) nitric acid, and 3 ml of concentrated hydrochloric acid and 1 ml of water were added. Iron(III) was then extracted with three 5-ml portions of diethyl ether [8]. The aqueous layer was treated with 5—10 mg of thiourea to mask Cu(II), and water was added so that the solution contained 1—2 M HCl after addition of 2 ml 25% (w/v) ammonium thiocyanate solution and 1 ml of hexamethylphosphoramide. The general procedure was then applied.

Analysis of BCS ferrotitanium (243/2) gave a result of 41.00 ± 0.2% Ti (certified value, 40.95%).

Determination of Ti(IV) in a synthetic mixture. Because no suitable standard material containing minor amounts of titanium was available, a synthetic mixture containing 98% Fe, 0.5% Ti, 0.4% Mn, 0.75% Cr and 0.35% Ni was analysed; sulphates were used to prepare the mixture and these percentages are given in terms of the total metal content. A 1-g sample of the mixture was prepared; after suitable dilution, the solution analysed contained 2 μg Ti ml^{-1}. An aliquot (10 ml) of this solution was evaporated and then the procedure used for ferrotitanium was applied. The actual amount of titanium in this sample was 0.513 mg; the amount found was 0.514 ± 0.005 mg (average of 3 determinations).

The financial help of CSIR (India) through a Scholarship to one of us (M. M.) is gratefully acknowledged.

REFERENCES

1 E. B. Sandell, Colorimetric determination of traces of metals, 3rd edn., Interscience, New York, 1959.
2 A. K. Majumdar, *N*-Benzoylphenylhydroxylamine and its Analogues, Pergamon Press, Oxford, 1972.
3 B. K. Afghan, R. G. Marryatt and D. E. Ryan, Anal. Chim. Acta, 41 (1968) 131.
4 A. I. Busev and N. G. Solov'eva, Zh. Anal. Khim., 27 (1972) 131.
5 L. A. Zharnovskaya and L. I. Ganogo, Zh. Anal. Khim, 28(5) (1973) 933.
6 A. Ringbom, Z. Anal. Chem., 115 (1938/39) 332.
7 G. H. Ayres, Anal. Chem., 21 (1949) 652.
8 A. I. Vogel, A Text Book of Quantitative Inorganic Analysis including Elementary Instrumental Analysis, 3rd edn., Longmans, London, 1961.

Analytica Chimica Acta, 94 (1977) 493—495

Book Reviews

T. F. Yen (Ed.), *Chemistry of Marine Sediments*, Ann Arbor Science, Ann Arbor, Michigan, 1977, vi + 265 pp., price U.S. $22.00, £13.40.

This book is not by any means as all-embracing as its title would imply, being composed, for the most part, of revamped and updated versions of papers given at an American Chemical Society Symposium of the same name. The papers in it vary in nature from review articles (some of which are very sketchy) to papers describing the results of original research. The balance of the chapters is more or less evenly distributed between trace metals and organic compounds, the discussion of the latter being weighted particularly towards the genesis of petroleum. All but one of the chapters are concerned with continental shelf or coastal sediments, which, although obviously of greater economic significance, represent, on an areal basis, less than 10% of marine sediments. This lop-sided presentation is to be regretted since the picture of organic geochemistry being revealed as a result of the Deep Sea Drilling Program is a fascinating one and has thrown much light on the diagenesis of sedimentary organic matter.

The book falls far short of being the comprehensive and detailed overview of the subject claimed on the dust cover by the publisher's blurb; indeed the latter is rather dishonest in that it makes no mention of the fact that the book is merely based on a symposium. Although there are a few good chapters in it (e.g. those by Kaplan et al., and by Baker and Smith) the remainder are a rather mediocre hotchpotch of the sort of papers which many people unfortunately give as a justification for going to conferences!

J. P. Riley

R. L. Pecsok, L. D. Shields, T. Cairns and I. G. McWilliam, *Modern Methods of Chemical Analysis*, 2nd edn., J. Wiley, New York, 1976, xviii + 573 pp., price £13.50, U.S. $21.50.

The preface to this book mentions that "perhaps the only constant feature of science is that of change", and so it is not inappropriate that the contents of the first edition (1968) of this now well-known text have been revised considerably. The effect in general has been to curtail, even more severely, the more classical topics included, e.g. acid—base equilibria, so as to make way for a revised — and improved — treatment of absorption spectra, and new sections dealing with complex ion equilibria, methods of data handling, and automatic and process analyzers. Answers are now given to the problems set at the end of most chapters.

The text is clear and free from trivial errors; there are many helpful illustrations, tables of data, and model spectra etc. The primary objective of the authors — to write a textbook for students to use and enjoy — has

probably been achieved — at least for those students who use text-books sufficiently to give themselves a chance to be able to come to enjoy some of them. Another objective of this book was to reach the middle level of compromise between an elementary survey and a sophisticated treatment in depth, but there seems little doubt that it tends towards the former rather than the latter. Yet another objective, however — to present a variety of principles and concepts which underlie most of the instruments and techniques in current use in analytical chemistry — is clearly achieved. This is a good book; it should be on the list recommended to all first or second year students.

E. Heftmann, *Chromatography of Steroids*, Elsevier, Amsterdam, 1976, xiii + 203 pp., price Dfl 90, U.S. $34.75.

This is volume 8 of the Journal of Chromatography Library. It was largely written whilst the author was at the Federal Institute for Lipid Research in Munster under the terms of a U.S. Senior Scientist Award by the Humboldt Foundation. His objective was to organise for his own benefit, as well as that of his readers, a collection of over 2000 reprints (1196 are cited here) on the chromatography of steroids that had been acquired since 1964. A comprehensive review of this subject has not been published since Neher's Steroid Chromatography (1964).

Dr. Heftmann is a prolific author, well-known for his publications in the fields of steroids and chromatography. This book will enhance his reputation. The contents are arranged according to the techniques used as well as the steroids studied: the aim has been to produce an effective laboratory handbook. The references and the subject index take up almost one-third of this book, and, in terms of the amount of information conveyed in the remaining pages, this book must be regarded as a model of its kind; it is clear, critical, and concise.

A. Frigerio (Ed.), *Advances in Mass Spectrometry in Biochemistry and Medicine*, Volume 2, Spectrum Publications, distributed by Halstead Press (J. Wiley), New York, 1977, xviii + 609 pp., price £35.00, U.S. $60.00.

This volume presents the proceedings of the Third International Symposium of Mass Spectrometry in Biochemistry and Medicine, held in Milan in June 1976. The pattern and scope of the first volume in this series, which dealt with the second of these Symposia, held in 1974, is therefore being maintained; the price becomes even more daunting (increased from £27.20).

The texts of 48 papers are presented; the Symposium was clearly a truly international occasion, with 14 countries represented. As in Volume 1, many different compound classes are involved, and a wide range of techniques in mass spectroscopy — and of m.s. used conjointly with other techniques — are described. Consultation of this volume is advisable for all those who were

unable to attend the Symposium but are active analytically in the fields of biochemistry, pharmacology, and the life sciences generally. All aspects of the production of this volume are satisfactory; the editor has carried out his task competently.

D. M. W. Anderson

Announcements

XXI COLLOQUIUM SPECTROSCOPICUM INTERNATIONALE
8th International Conference on Atomic Spectroscopy

The University of Cambridge, 1—6th July 1979

The Conference will reflect the current level of interest in all branches of spectroscopy with a particular emphasis on the general theme of Analytical Spectroscopy. Specific 1-, 2- and 3-day Symposia on selected techniques of spectroscopy will be arranged to feature advances in the following topics: Molecular Spectroscopy; X-ray Spectroscopy; Optical Emission Spectroscopy; Atomic Absorption Spectroscopy; Gamma-Ray and Neutron Activation Techniques; Mass Spectrometry; Auger, Esca, and Photoelectron Spectroscopy.

In addition, Symposia concerned with the application of the techniques of spectroscopy will be arranged to include: Trace Analysis; Environmental Analysis; Solution Analysis; Surface Analysis; Determination of Major Components; Polymer Analysis; Spectroscopy in plant and on-line processes.

The Conference is sponsored by the Association of British Spectroscopists, and is held under the auspices of The Royal Society, The Chemical Society and The Institute of Physics.

There will be an instrument exhibition, and a full social and Ladies' programme. Residential accommodation will be available in the Colleges of the University. Further information can be obtained from the Conference Secretariat, P.O. Box 109, Cambridge CB1 2HY, Great Britain.

31st Chemists Conference—British Independent Steel Producers Association

Scarborough, Great Britain, June 14—15th 1978

The 31st Chemists Conference will be held on June 14/15th, 1978 at the Royal Hotel, Scarborough, Great Britain. Further information can be obtained from the British Independent Steel Producers Association, 5 Cromwell Road, London SW7 2HX.

ERRATUM

G. B. Cox, C. R. Lascombe and K. Sugden, Some applications of bonded phase high performance liquid chromatography to the analysis of pharmaceutical formulations, *Anal. Chim. Acta*, 92 (1977) 345—352.

Page 346 was omitted during printing. The page is as follows.

Materials

LiChrosorb SI 60 (5 μm average particle size, BDH Chemicals Ltd, Poole) and Spherisorb S5W (Phase Separations Ltd, Queensferry, Clwyd) silica gels were used. Spherisorb S5-ODS (Phase Separations Ltd) was used for reverse phase separations. Organotrichlorosilanes were used as purchased (Pfaltz and Bauer, and Silar Inc.). Dioxan (analytical-reagent grade) was dried over a 3A molecular sieve before use.

Strong cation exchanger (SCX). This was prepared with Spherisorb S5W silica gel [2].

Weak cation exchanger (WCX). Acid-washed silica gel [2] (5 g) was heated under reflux with bis-(3-chloropropyl)dichlorosilane (1.5 g) in dioxan (50 ml) for 4 h. The product was filtered, washed with dioxan and acetone and dried; it was then heated under reflux with 3-aminopropionic acid (1.5 g) in 50% (v/v) aqueous ethanol for 4 h. The product was filtered, washed, and dried.

Determination of ion-exchange capacity

The weak cation-exchange material (0.5 g) was treated with an excess of 0.01 M sodium hydroxide in 0.5 M sodium chloride. The ion-exchanger was filtered and washed and the combined filtrates were titrated against 0.01 M hydrochloric acid with methyl red as indicator.

Sample preparation and chromatographic conditions

These are summarised in Table 1.

RESULTS AND DISCUSSION

The advantages of carrying out liquid chromatographic separations on microparticulate column packings (i.e. materials of approximately 5-μm diameter) have been well documented; separations of compounds of pharmaceutical interest (albeit as pure standards rather than formulations) on columns packed with microparticulate silica gel have been reported [5]. Silica gel has some limitations as a separation medium. Problems arise in the chromatography of both non-polar and highly polar compounds; the former category displays retention times strongly dependent upon trace concentrations of water or polar components in the mobile phase, whilst the latter may not elute at all. Both of these problems may be avoided by the use of partition or ion-exchange chromatography; these procedures, having different criteria for separation, are probably more useful for the analysis of pharmaceutical formulations because of the wide range of polarity of the components present. The problems besetting partition chromatography (e.g. long equilibration times and solubility of stationary phase in the mobile phase) and ion-exchange chromatography with resin-based materials (low efficiencies and swelling of the resin with changes of ionic strength) can in turn be eliminated by bonding the partitioning or ion-exchanging moiety to a rigid silica gel support. A major advantage in the use of bonded-phase

ANALYTICA CHIMICA ACTA, VOL. 94 (1977)

AUTHOR INDEX

ANALYTICA CHIMICA ACTA, VOL. 94 (1977)

SUBJECT INDEX

(continued from page 4 of cover)

VOL. 94 NO. 2 ANALYTICA CHIMICA ACTA DECEMBER 1, 1977

CONTENTS

(continued on inside page of the cover)